A STUDY OF SOLVENT AND pH EFFECTS ON ABSORPTION AND FLUORESCENCE CHARACTERISTICS OF SELECTED ORGANIC COMPOUNDS

A Thesis Submitted
in Partial Fulfilment of the Requirements
for the Degree of

DOCTOR OF PHILOSOPHY

by

M. SWAMINATHAN

to the

DEPARTMENT OF CHEMISTRY

INDIAN INSTITUTE OF TECHNOLOGY KANPUR
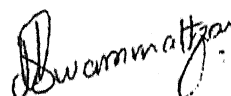
MAY, 1982
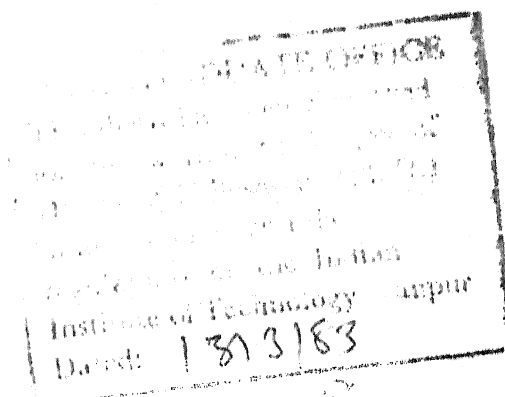
Dedicated

to my parents

STATEMENT

I hereby declare that the work embodied in this thesis entitled, "A STUDY OF SOLVENT and pH EFFECTS ON ABSORPTION AND FLUORESCENCE CHARACTERISTICS OF SELECTED ORGANIC COMPOUNDS" has been carried out by me under the supervision of Dr. S.K. Dogra.

In keeping with scientific tradition, whereever work done by others has been utilized, due acknowledgement has been made.
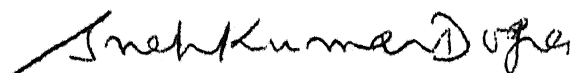
M. Swaminathan

CERTIFICATE I

Certified that the work presented in this thesis entitled, "A STUDY OF SOLVENT AND pH EFFECTS ON ABSORPTION AND FLUORESCENCE CHARACTERISTICS OF SELECTED ORGANIC COMPOUNDS" by Mr. M. Swaminathan, has been carried out under my supervision and not submitted elsewhere for a degree.

Dr. S.K. Dogra
Department of Chemistry
I.I.T. Kanpur-16

May, 1982.

DEPARTMENT OF CHEMISTRY

INDIAN INSTITUTE OF TECHNOLOGY, KANPUR

CERTIFICATE II

This is to certify that Mr. M. Swaminathan has satisfactorily completed all the courses required for the Ph.D. degree programme. These courses include:

Chm 521 Chemical Binding
Chm 523 Chemical Thermodynamics
Chm 524 Modern Physical Methods in Chemistry
Chm 534 Electronics for Chemists
Chm 622 Chemical Kinetics
Chm 800 General Seminar
Chm 801 Graduate Seminar
Chm 900 Post-Graduate Research

Mr. M. Swaminathan was admitted to the candidacy of the Ph.D. degree programme in March 1980 after he successfully completed the written and oral qualifying examinations.

(U.C. Agarwala)
Professor and Head
Department of Chemistry
I.I.T. Kanpur

(N. Sathyamurthy)
Convener,
Departmental Post-Graduate
Committee, I.I.T., Kanpur.

CONTENTS

* * * * * *

ACKNOWLEDGEMENTS

I would like to place on record my deep sense of gratitude to Professor S.K. Dogra for guidance, stimulating discussions and constant encouragement throughout this work and for his interest in my welfare.

Besides I am grateful to –

Prof. N. Sathyamurthy for his valuable suggestions to improve the language of the thesis and for the personal care he took for the last three years;

Prof. Ragunathan and Prof. Chandrasekaran for their encouragement and kind interest in my progress;

Prof. Shanker Mukherjee for allowing me to use his lab facility;

Prof. Pinaki Gupta-Bhaya for the interest he took in the maintenance of cary 17D spectrophotometer, which was most useful to me;

Mr. Ashok Kumar Mishra, my lab-mate for his cooperation and for his valuable help at all stages in the preparation of the thesis;

All my friends particularly to Drs. Rakesh, P.B.K. Sharma, R. Ragunathan and Messers Arulsamy, Ramasamy, Govindaraj, Dinesh, Pratibha, S.K. Srivastava, Brij Bhushan, Kesavan, Sandip Sur, Kumar, Murali,Trinadha Rao, Noor, Muthu and Venkatramani for their help during my stay at I.I.T., Kanpur;

<u>SYNOPSIS</u>

There has been a considerable interest in recent years on the study of photochemical properties of systems in excited states. The information on the acid-base properties of molecules in the excited states and their relation to structure is of primary importance in the mechanistic elucidation of photochemical reactions. For reactions proceeding through excited singlet or triplet state and dependent on acidity of the system, the information on the excited state pK_a values is necessary to optimize the reaction conditions. In this thesis, an attempt is made to determine the excited state acidity constants mainly in the singlet states of selected organic compounds (pyrazoles, imidazoles, phenanthrenes and 5-aminoindazole) and to study the effect of solvents on absorption and fluorescence characteristics of these compounds. The solvent dependence of absorption and fluorescence provides information about the ground and excited state geometries and the site of proton exchange in few compounds studied by us.

Chapter 1 reviews the literature on the excited state acid-base properties as well as solvent effect on absorption and fluorescence of organic molecules having acidic or basic functional groups. A brief account of present investigation is also given.

Chapter 2 contains the instrumentation part of the work. The details of spectrofluorimeter which has been fabricated using quantum photometer and other accessories are given. The cell compartment is designed to accommodate the low temperature fluorescence and phosphorescence accessory. A modification in the cell to increase the fluorescence intensity is described. Excitation and emission spectra correction curves, determined for the instrument, are presented. Chapter 3 gives the experimental part of the work.

In chapters 4 and 5, a study of solvent effect on the absorption and fluorescence spectra of the molecules is presented. The abnormal shifts in the absorption maxima in certain pyrazoles and 4,5-diphenylimidazole are explained in terms of steric effects due to solute-solvent interaction. In other compounds, the behaviour is different and the solvent shifts in absorption show that the hydrogen donor/acceptor interactions are more prominent in the ground state.

A comparison of absorption and fluorescence spectra of 3,5-diphenylpyrazole in cyclohexane indicates a change in nuclear conformation from the ground to the excited state. This conclusion is further supported by other spectroscopic parameters. Analysis of solvent shifts on absorption and fluorescence shows a change in site of hydrogen bonding from ground to excited state in 9-aminophenanthrene and 5-aminoindazol

The increase in the fluorescence intensity of cations of
1,3,5-triphenylpyrazole and 4,5-diphenylimidazole with the
increase in irradiation time is explained on the basis of
reversible and irreversible excited state reactions respectively.
The specific quenching of 3-methyl,5-phenylpyrazole cation by
chloride ion is also analysed. /

Chapter 6 contains the study of pH effects on absorption
and fluorescence spectra. The ground state pK_a values, determined
spectrophotometrically, are reported. From the pH effects on
fluorescence, an attempt is made to measure excited state
acidity constants (pK_a^*) for all equilibria present in each
compound. There are four methods for the determination of pK_a^*
values. The results obtained are compared and assumptions
made for each method are discussed in order to determine the
best way by which excited state acidity constants may be
obtained. Unlike the behaviour in pyridine, pyrazole etc., the
pyridinic nitrogen atom at position 3 in 9,10-phenanthroimidazole
becomes less basic in the excited state. This is explained on
the basis of excited state charge transfer interaction. The
fluorescence titration plots of 9-hydroxyphenanthrene are
stretched sigmoid curves covering both ground and excited state
pK_a regions, implying that the variations of quantum yields of
fluorescence of conjugate acid-base pair with pH is governed by

the kinetics of the excited state prototropic reaction. The excited state kinetics is analysed to account for the shape of the curve observed.

An interesting behaviour, quite different from ground state, is observed in the excited state of 5-aminoindazole. In the ground state the first protonation occurs at the amino group and deprotonation at the pyrrole type nitrogen atom at position 1 of the ring, whereas in the excited state the pyridinic nitrogen atom at position 2 of the ring gets protonated first and amino group gets deprotonated. This conclusion is also supported by the room temperature and low temperature (77K) fluorescence spectra of indazolammonium chloride and 5-amino-indazole anion. A scheme of excited state equilibrium is proposed. The indazolammonium ion at pH 1.4 undergoes inter-molecular phototautomerism which is assisted by solvent.

For compounds, whose pK_a^* values lie in the mid pH region, if the   excited state equilibrium is not attained due to low concentration of protons, the equilibrium can be achieved with high buffer concentration. Chapter 7 presents the effects of varying concentration of buffers on the equilibria of benzimidazole, indazole and 9,10-phenanthroimidazole and it is found that the equilibrium in excited state is displaced towards the expected direction in all compounds.

The thesis has a brief description of the vibrational analysis of low temperature fluorescence and phosphorescence spectra of few compounds. The triplet state acidity constants determined from phosphorescence spectral shifts are also reported.

A summary of work done and the future work planned are given in the last chapter.

LIST OF FIGURES

Fig.

Fig.

LIST OF TABLES

Table

CHAPTER - 1

GENERAL INTRODUCTION

A chemical compound has certain characteristic chemical and physical properties which are determined, to a large extent, by its electronic charge distribution. Therefore it is reasonable to consider a molecule in one of its electronically excited states, as a different compound. A study of the effect of factors like solvent polarity and pH of the solution on absorption and fluorescence spectra of a compound provides valuable information about its ground and excited states.

In this chapter we present a brief survey of solvent effects on absorption and fluorescence spectra relevant to our study, and excited state pK_a along with their applications, followed by a description of the scope of the present work.

1.1 Solvent effects on absorption and fluorescence spectra

The first general treatment of solvent effects on absorption spectra was given by Bayliss and McRae[1] in 1954.

They pointed out that interactions of solvent and solute molecules are predominantly electrostatic, and may be of the induced dipole-induced dipole, dipole-induced dipole, dipole-dipole or the hydrogen bonding types. Later the solvent effects were discussed by several authors.[2-5] A consolidated account of these effects in terms of different kinds of electronic interactions depending upon the nature of solvent, solute and the electronic transition has been given by Jaffe and Orchin[6] and Suzuki.[7] The results of these effects have been used to assign the nature of electronic transition[6] and to calculate the dipole moment of the molecule.[3,8-10] Schulman et al.,[12,26-28] studied the solvent effects on the absorption spectra of different isomeric aminoquinolines and from the shifts of the absorption maxima (λ_{max}) they concluded that in ethanol, the hydrogen bonding was at the heterocyclic nitrogen atom whereas in water it was at the exocyclic amino group. In contrast, in 3-aminoquinoline[13] the shifts were attributed to the dispersive, hydrogen bond interactions. From the absorption and emission data in different solvents, a study of dipole moments and geometries of the aromatic esters in the excited singlet state have been carried out recently.[14]

The environmental effects on the fluorescence spectra of aromatic compounds in solution were first reviewed by Pringsheim[15] and then by Förster.[16] In 1963 Von Duuren[17] reviewed this subject giving a detailed account of the solvent effects for

various types of aromatic compounds and their derivatives. He discussed the λ_{max} shifts and the quenching of fluorescence in addition to the viscosity effect caused by the solvents. The λ_{max} shifts were explained using the Franck-Condon principle. Accordingly, the fluorescence is always red shifted to absorption in the same solvent and the shift increases with increase in the solvent polarity for the $\pi - \pi*$ transitions.

The effect of hydrogen bonding on fluorescence spectra was studied extensively by Mataga and Coworkers.[18-20] They pointed out that the hydrogen bonding can cause either a red shift or a blue shift in fluorescence in naphthylamines depending upon the nature of the hydrogen bonding interactions with the solvent. They demonstrated the use of fluorescence spectrometry in calculating equilibrium constants for hydrogen bonding in excited states of organic compounds.[18]

From a comparison of the solvent effects on the absorption and fluorescence spectra, one may derive information regarding the nature of the electronically excited state in contrast to the ground state and also the nature of the interactions between the solute and the solvent molecules in the excited as well as the ground state. This comparison, together with a theoretical interpretation of the characteristics of the spectra of α -and β -naphthylamines has shown that the lowest excited singlet state in the light absorption is $^{1}L_{b}$, and the fluorescent state is $^{1}L_{a}$ in the case of α -isomer, while $^{1}L_{b}$ is the relevant excited

state for both light absorption and fluorescence in the case of
β -Naphthylamine. This level reversal has been attributed to
the change in the structure of the amino group during the life
time of the excited state.[21]

From the solvent and protonation effects on photoisomeri-
sation and luminescence of styrylpyridines, Bartocci et al.,[23]
have concluded that the singlet mechanism prevails in the photo-
isomerisation for the unsubstituted styrylpyridines.

Werner and Hercules[22] have studied the environmental
effects on the fluorescence spectra of 9-anthroic acid and its
esters. They found the large Stokes shift in the emission of
9-anthroic acid,to be a consequence of the excited-state rotation
of the carboxyl group into the plane of the anthracene ring.
This rotation, which can result in an excited state six membered
ring formation through intramolecular hydrogen bonding, is
shown to be dependent upon temperature and the solvent matrix.
In a study of solvent dependence of absorption and fluorescence
of aminoquinolines, Schulman et al.,[26-28] reasoned that the
opposite trend observed in the fluorescence shifts when compared
to the absorption shifts in the same series of solvents is due
to the change in the site of hydrogen bonding from the ground
to the excited state. That is, in the excited state, the
hydrogen bonding is at the ring nitrogen atom while in the
ground state it depends on the nature of the solvent (see above).

Berlman[24] obtained an empirical correlation between nuclear conformation and certain fluorescence and absorbance characteristics of aromatic ring and ring-chain systems from a study of solvent effects on the absorption and fluorescence spectra. He classified these compounds into five categories in assigning the conformation of the molecule in both states.

The absorption and fluorescence spectra shifts of o-Phenanthroline and its cation in different solvents were used to explain the discrepancies in the Förster cycle[34] pK_a^* values.[25]

Further information regarding the intramolecular photo-tautomerism[29,30], nature of hydrogen bonding[31], chemical structure,[32] geometry and dipole moment[14] in the ground and excited states can also be obtained from a study of the effect of solvent on absorption and fluorescence characteristics of a compound.

1.2 Excited state pK_a studies

Weber[33] was the first to report the "abnormal" fluorescence due to protolytic dissociation of 1-naphthylamine-4 sulphonate in 1931. He noticed the change of blue-violet fluorescence of neutral solutions of this compound to green in strongly alkaline solutions, although there was no change in the absorption spectrum. Later in 1950, Förster[34] showed this effect to arise from the protolytic dissociation in solutions containing hydroxy- and

aminopyrene sulphonates in their first excited singlet states. Similar results were observed with hydroxy and other naphthalene derivatives.[35,36] In the study of the protonation equilibrium of β-naphthylamine, very strongly acidic solutions (characterized by negative pH value[11]) were used. In these compounds the appearance of fluorescence due to the formation of the protonated and the deprotonated species occurred in a pH region different from that corresponding to the ground state pK_a value. Förster[34,35] suggested a method to determine the excited state pK_a (pK_a^*) value from the electronic transition energy (ΔE) between the ground and the electronically excited states. This energy can be obtained either from the difference in the long wavelength absorption maxima or from the difference in the short wavelength fluorescence maxima of the conjugate acid-base pair. This method is based on the thermodynamic equivalence of all routes from the ground state of the acid to the excited state of the conjugate base and it is commonly known as Förster cycle. In this scheme, entropy changes for the protonation and deprotonation are assumed to be equal in both states.

As a criterion for the establishment of the acid-base equilibrium in the excited state, the change from one fluorescent form to another should take place within a narrow pH range; that is from 1% to 99% of each form within 4 pH units.

Weller[37] developed another method to find out the pK_a^* by using fluorescence intensity as a function of pH of the system. This method, known as fluorimetric titration, is free from the assumptions made in the Förster cycle calculations. The pK_a^* values determined by the former method are found to be in accord with the latter for α -and β -naphthols.

Bartok et al.,[38] estimated the pK_a^* values of some p-substituted phenols from spectroscopic data. Apart from a large increase in pK_a as a result of excitation, the variation of the pK_a^* values with substitution, as obtained by different methods, could not be accounted for. Hence it was suggested that pK_a^* calculated by using the average of absorption and fluorescence maxima could be more accurate than the pK_a^* values obtained by either absorption or emission data.

Haylock et al.,[39] estimated the excited state dissociation constants of some substituted quinolines from spectroscopic data and from the change in the fluorescence intensity with pH. A critical examination of the methods used, revealed that the assumption of equal entropy changes for the corresponding prototropic equilibria in the ground and excited states of a conjugated acid-base pair may not be justified as the solvation energies in both states, in general, are not identical due to the difference in the electronic charge distribution.

Again from a study of substituted quinolines Mason et al.,[40] found that the pK_a^* values obtained by different methods for the same compound differed from each other. This is apparently due to the fact that ΔE value of the Förster cycle refers solely to the electronic energy difference between the ground and excited states of the molecule. But the absorption and emission maxima of the species studied.measure the associated vibrational energy difference also between the two states. As a result, pK_a^* values obtained from the absorption and emission data may differ from each other by as much as six units and both may diverge substantially from the pK_a^* value obtained from the fluorimetric titration.

Jaffe and Jones[41], in 1964, reviewed and carefully examined the assumptions involved in the Förster cycle method.[34] In azobenzene and azoxybenzene, Jaffe et al.,[42] calculated five different excited state pK_a values for each compound from the absorption maxima of five different bands present in these compounds. The pK_a^* values reported for each compound varied from 0 to 19.7. The tautomeric equilibria in substituted amino-azobenzenes and the uncertainty in using the Förster cycle calculations for these compounds were determined by Ellerhost et al.,[43].

Wehry and Rogers[44] determined the protolytic dissociation constants of phenols and monosubstituted phenols in the lowest

triplet (T_1) and the first excited singlet (S_1) states by using Förster cycle. They found the resonance effects to be more important than inductive effects in the excited state.

The pK_a^* values of different isomers of quinolinol and their derivatives were reported by several authors.[45-47] Schulman et al.,[47] explained the differences in the pK_a^* values obtained for halogenated 8-quinolinol in terms of the assumptions made in Förster cycle. But the large difference in the pK_a^* values, obtained by different methods for 5-isoquinolinol could not be explained.

Goldman and Wehry[48] attributed the quenching of 8-quinolinol fluorescence to hydrogen bonding by hydroxylic solvents. However Schulman[49] interpreted the results to be primarily due to proto-tropic equilibria in the S_1 state of the various prototropic species derived from 8-quinolinol.

Vander Donckt[50] reviewed the acid base properties of the excited states, wherein he discussed the effect of excited state geometrical relaxation on the Förster cycle calculations. Subsequently more pK_a^* data have accumulated and the subject has been reviewed by several authors.[52-54] The review by Ireland and Wyatt[53] contains extensive reference tables of experimental results available in the literature upto 1974. Most of the pK_a^* values were determined by the Förster cycle[34] method and yet there were unexplained discrepancies in those values.

Schulman et al.,[29,31,55-59] determined pK_a^* values of many organic compounds of biological and medicinal importance. His recent review[86] and a book[95] provide a complete picture of the acid-base chemistry of S_1 state. The shapes of fluorimetric titration curves are analysed on the basis of the kinetics of the S_1 state proton transfer and the discrepancies in the Förster cycle pK_a^*s are explained using solvent dependence and low temperature studies.[25,55] Schulman and Capomacchia[59] proposed a modified cycle and have derived equations similar to those of the Förster cycle. In this approach effects of vibration, solvent and geometrical relaxations in the ground as well as the excited states are taken into account.

A comparison of pK_a^* values obtained by fluorimetric titration with those obtained by the three Förster cycle methods (see above) shows which of the three methods is accurate.[86] From an analysis of the discrepancies in these values, useful information about various factors like solvent relaxation, geometry change and complex formation in the excited state is obtained.

The effect of high concentration of buffers on the excited state equilibrium was first studied by Weller[5], using steady state kinetics. Schulman and Capomacchia[56] extended this study and modified the kinetic equations to incorporate the pH conditions.

The excited triplet state acidity constants (pK_T^*) were determined mainly by using Förster cycle[34] and phosphorescence spectra at 77K. The energy changes, determined directly from the short wavelength limit of phosphorescence spectra were used in the Forster cycle calculations. Jackson and Porter[60] used flash spectroscopy and determined pK_T^* from T-T absorption measurements. Fitch[61] determined the pK_T^* values for substituted anthraquinones and fluorenes by both methods. It has been found that pK_T^* values generally lie in between pK_a^* and pK_a, and often closer to the latter.

1.3 Applications of excited state acidity constants

A knowledge of acid-base properties of molecules in their excited states is of importance in unravelling the mechanism of photochemical reactions. This was first recognised by Godfrey et al.,[62] while determining the course and yield of photochemical reduction of aromatic ketones by hydrogen abstraction from the solvent. Photoreduction results of 4-hydroxybenzophenone[63], methylene blue[64] and phenazine[65] have been interpreted similarly. The yields in photoisomerisation reactions of 3-styrylpyridines, in the pH range (0-14), are related to the acid-base equilibria in the ground and S_1 states.[23] Hine and Childs[66] found that the complex photoisomerisation of eucarvone appears to proceed in acid media via a protonated triplet species.

Vinylcations are known for their high reactivity but their stability only at high acid conditions precludes the use of delicate functional groups in the substituent. The possibility of existence of these ions under mild acid conditions in the excited state was examined by Woolridge and Roberts.[67] The presence of vinyl cation intermediate was suggested in the photohydration of phenylacetylene in dilute acid solutions. From the formation of this intermediate they were able to explain the earlier reports concerning the photoaddition of methanol and acetic acid to diphenylacetylene.[68]

Plots[69] of photohydration rates as a function of pH for uracil and cytosine derivatives showed inflection points near the pK_a^* values of these compounds. They concluded that neutral excited species are the most reactive with water. Further evidence for the participation of the S_1 state in the reaction is provided by the negative temperature coefficients for photohydration and fluorescence intensity. For a similar reaction, the photo-induced alcoholysis of 3,4-dihydroxycoumarins, the variation of quantum yield of the product with pH correlates reasonably well with the pK_a^* values.[70]

The molecules which can undergo intramolecular proton transfer in the excited state have been found to be unusually photo-stable.[71] Williams and Heller[72] reported the photochemical stability of crystalline 2-(2'hydroxyphenyl)-benzothiazole and

its derivatives. In these compounds a proton is transferred in the excited state from oxygen to a nitrogen atom and the photochemical stability of the compound is greatly improved relative to the N-methylated derivatives in which no hydrogen transfer can take place.

The excited state acid-base behaviour of molecules has direct implications in the field of analytical fluorimetry and phosphorimetry. An increase in the sensitivity and selectivity of analytical procedures due to change in the emitting species with pH has been discussed by several authors.[73-76]

In biochemistry, excited state protolytic behaviour is increasingly used both to interpret results and to act as a probe.[77-81] In recent years the potential application of excited state proton transfer to the studies of biological molecules is increasing. As rate constants are generally dependent upon the solvent and on the character of any possible proton donor and acceptor present in solution, Loken et al.,[82] have suggested that the rate of excited state proton transfer should give a quantitative measure of the environment of a probe molecule. De Luca et al.,[83] and Bowie et al.,[84] have demonstrated the importance of excited state proton transfer for investigating the active sites of enzymes. For example, the mechanism of the action of firefly luciferase was explained using excited state proton transfer.[85]

As the ground state pK_a data have been used to draw inference concerning the structure, electronic charge distribution and chemical reactivity of molecules in the ground state, pK_a^*s can be used to get similar inferences for the molecules in the S_1 state. Schulman[86,87] has discussed the use of pK_a^* as an index of chemical reactivity and structure in the S_1 state. Thus for example an anomalously low pK_a^* value for the S_1 state equilibrium between the cation and the zwitter ion derived from 8-mercaptoquinoline, and an anomalously short emission wavelength of 8-mercaptoquinoline cation relative to that of 8-hydroxyquinoline can be explained by valence shell expansion of the sulphur atom of the protonated 8-mercaptoquinoline in the S_1 state.[88] Moreover, since the shifts in absorption spectra of 8-mercaptoquinoline on protonation are similar to the shifts in the absorption spectra of 8-hydroxyquinoline on protonation, valence shell expansion might be occurring following excitation.

1.4 Scope of the present work

The discussion in the previous section shows the widening scope of the applications of the excited state pK_a values. In the past, most of the pK_a^* values were determined only by Förster cycle methods, even though there was a possibility of determining pK_a^* values by fluorimetric titration for some of the compounds. Furthermore, except in some of the recent papers, no explanation

was given for the different pK_a^* values obtained for the same compound by Förster cycle methods.

We have started this work (a) to compare the pK_a^* values obtained by Förster cycle and fluorimetric titration, (b) to find out the best pK_a^* value, (c) to interpret any discrepancies in the Förster cycle pK_a^* by solvent dependence and low temperature studies and (d) to get information about the geometry change, charge transfer interaction and complex formation in the excited state using the error involved in the Förster cycle calculation as a guide.

In this thesis, most of the compounds studied are five membered heterocyclics having two nitrogen atoms, one of pyridine type and the other of pyrrole type. It had been reported earlier that pyrrole type nitrogen becomes more acidic[89-94] and pyridine type nitrogen becomes more basic[5] in the excited state. Reasons for choosing the heterocyclic compounds with two nitrogen atoms are (i) to find the effect of solvents on the spectral behaviour,as little systematic work is available on the emission characteristics of pyrazoles except for the qualitative work done by Russian workers.[96] , (ii) to find out their excited state acid-base properties (a) when they are in the same ring and adjacent to each other (as in pyrazoles and indazole) and (b) when they are apart (4,5-diphenylimidazole and 9,10-phenanthroimidazole).

Since excited state equilibrium was not attained in pyrazoles due to their short life times, amino-and hydroxy-phenanthrenes were also included in this study. Solvent dependence and low temperature studies were started mainly to account for the discrepancies in the Förster cycle pK_a^* values. In addition, we were able to get information on the vibrational structure of the ground state.

Chapter 2 describes the instrumentation part of the work. Although many commercial instruments are available with accessories, we have fabricated the instrument with changable lamp sources and gratings to suit our needs. Chapter 3 gives the details of the experiments. Results from a study of solvent effects on absorption and fluorescence spectra are presented in chapters 4 and 5. In the latter, an analysis of the fluorescence spectra of cations of 1,3,5-triphenylpyrazole, 1,5-diphenyl-3-methyl-pyrazole and 4,5-diphenylimidazole is followed by a brief account of vibrational analysis of low temperature emission spectra of some of the compounds. Chapter 6 gives pK_a values for all the compounds in their S_1 states and for a few compounds in their T_1 states. The effect of high buffer concentration on excited state equilibrium of a few compounds is discussed in chapter 7.

CHAPTER - 2

INSTRUMENTATION

2.1. Spectrofluorimeter

Fluorescence and phosphorescence spectra were recorded on a scanning spectrofluorimeter, fabricated in our laboratory. The block diagrams of the spectrofluorimeter and the arrangement to take spectrum at low temperature are given in figs. 2.1 and 2.2 respectively. A brief description of each part is given below.

A stabilized power supply for the lamp (LPS 251 HR) and the lamp housing (LH 150) were procured from Schoeffel Instruments. They can accommodate 150 W Xe lamp, 200 W Xe-Hg lamp and 200 W Hg lamp.

Two Jarrell-Ash 0.25 m and f/3.5 Ebert grating monochromators (82-410 and 82-415) were used. The monochromator (M_1) with one grating, blazed at 300 nm (1180 grooves/mm with a reciprocal linear dispersion of 3.3 nm/mm), was used for

Fig. 2.1 Block diagram of the Spectroflourimeter

Liq. N₂

Quartz cell

Quartz wind⸗

Liq. N₂

Air inlet

Motor
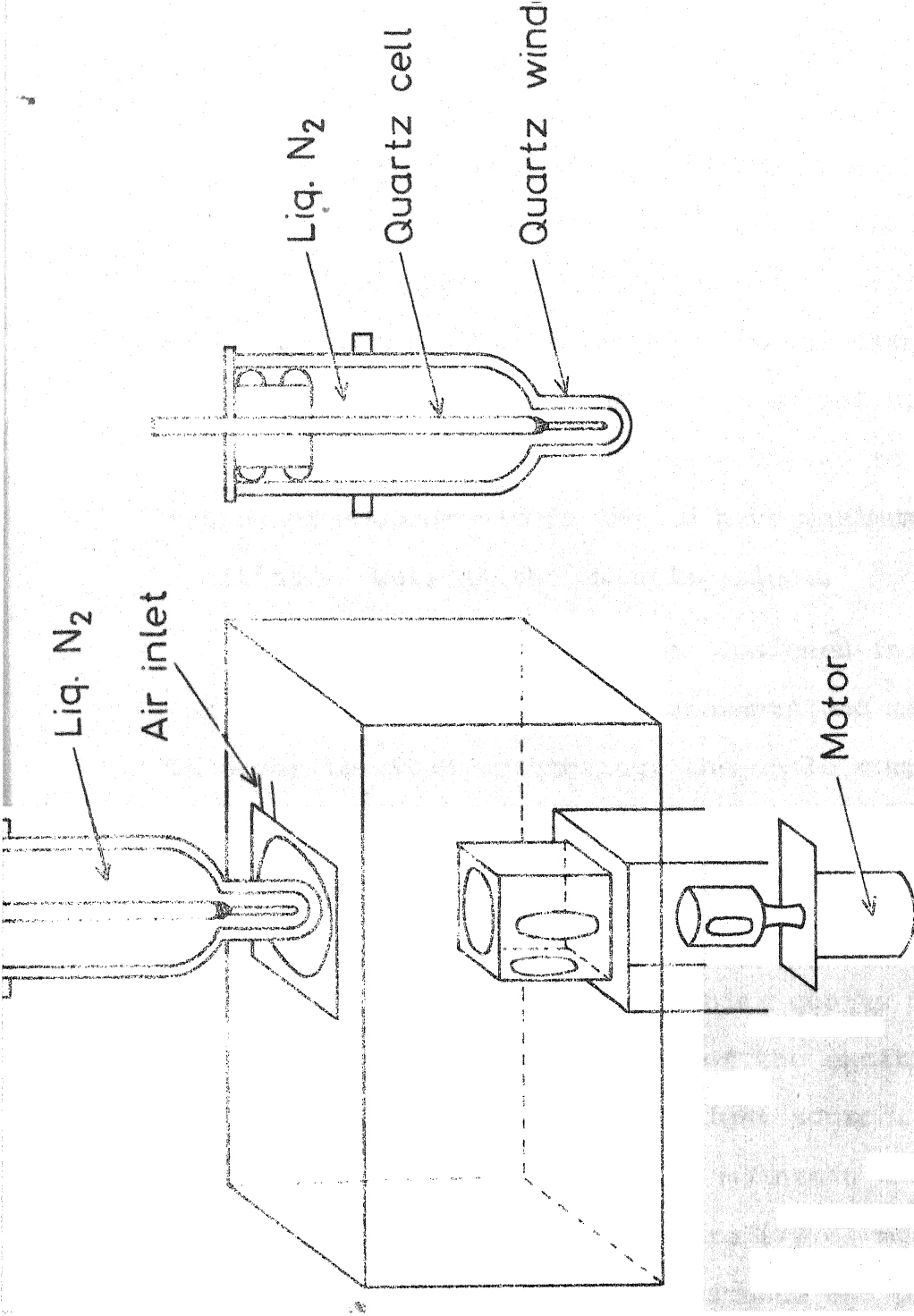
Fig. 2·2   Diagram of low temperature set up for fluorescence and phosphorescence.

selecting the excitation wavelength. The monochromator (M_2) with two gratings, one blazed at 300 nm (2360 grooves/mm with reciprocal linear dispersion 1.65 nm/mm) and the other at 500 nm (1180 grooves/mm with reciprocal linear dispersion of 3.3 nm/mm), was used for the resolution of the emission. The focal lengths of the quartz lenses (L_1-L_5) were chosen to suit the aperture ratios of monochromators and to have maximum collection of the exciting as well as the emitting light.

The cell compartment was designed for both room temperature and low temperature measurements and made in our workshop. In order to avoid scattering, the whole compartment and the lens holders were blackened by anodizing them. The cell compartment houses a beam splitter and two double walled cell holders C_1 and C_2 to accommodate the sample and reference cells respectively. The beam splitter B is a 1 mm thick quartz plate and it is placed at an angle of 45° in the path of the exciting light to reflect 10% of it for calibrating the light source. The purpose of the double walled cell holder is to maintain a constant temperature of the cell. For low temperature (77 K) measurements, Aminco-Bowman's low temperature fluorescence and phosphorescence accessory was fitted in the cell compartment by replacing the normal cell holder C_1 as shown in fig.2.2. A motor with a shutter drum was fitted at the bottom of the cell holder, only for phosphorescence measurements. Provision was also made for

passing dry air to remove the condensed moisture from the walls of the dewar flask.

Princeton Applied Research Quantum Photometer console (model 1140 A) was used for detection and amplification of emission. It consists of a detector assembly, an amplifier/ discriminator, an electrometer, a detector voltage supply and a log and a linear rate meter. The detector assembly with a 1P 28 photomultiplier tube (Hammatsu, Japan) was fixed at the exit slit of the M_2. The Quantum photometer has two modes of measurements: (i) photoncounting and (ii) current measuring. The photon counting mode is sensitive enough to measure very weak signals. The detected and amplified signal was read from the rate meter in the front panel. A multi range (1-12.5 mv) millivolt recorder (Sargent model SR) was used to record the signal out-put from the Quantum photometer.

Another set of detector-amplifier was attached at the other side of the cell compartment facing the exit of C_2 for calibrating the excitation light source and to check its constant intensity. The high voltage required for the photomultiplier tube was supplied from a stabilized DC power supply, fabricated in the Electrical Engineering Department, IIT, Kanpur. The detected signal was fed into an electrometer amplifier (EA) (Electronic Corporation of India Ltd model EA 815) and read.

Occasionally it was also recorded on a chart recorder. A constant speed motor was used for driving both excitation and emission monochromators and it was coupled with the chart recorder motor while scanning.

2.2. Experimental procedure

A sample in the quartz cell was placed in the thermostatted cell holder maintained at $25 \pm 1^{\circ}C$. The light of excitation wavelength selected by M_1 was focussed on the sample and the emission from the sample at a right angle was directed to M_2. The emission intensities at wavelengths selected by M_2 were measured from the Quantum photometer display. The complete emission spectrum was recorded by scanning M_2. While scanning, the intensity of the excitation light source was checked often.

To check the intensity of the excitation source, a solution of Rhodamine B in ethyleneglycol (3 gm/litre) was taken in a quartz cell of size 1 cm x 0.5 cm and was placed in C_2 at an angle of 45°. The emission was viewed from the back of the cell (Fig 2.1). The advantage of this arrangement,[97] is that if the incident radiation contains a small portion of "impure wavelengths" not absorbed by the quantum counter (Rhodamine B solution), they are not registered by the detector (D_2). The signal, detected by D_2, was amplified by the electrometer amplifier. The constant reading in EA shows the constancy in the intensity of excitation

source. The intensity of the excitation source was always found to be constant during the time of scanning.

For a low temperature run, the cell compartment was fitted with a low temperature accessory. The sample in the proper cell was placed in liquid nitrogen kept in dewar flask for some time till the bubbling of nitrogen gets reduced. Then, after removing the moisture condensed, the dewar flask with the sample was placed in the cell compartment. During scanning, dry air was passed to remove any moisture condensed. In the same set up, phosphorescence spectrum was obtained after fitting the chopper motor around the cell holder.

The fluorescence excitation spectrum at room temperature can also be obtained by setting M_2 at the fluorescence maximum and by scanning M_1. Similarly the low temperature excitation spectrum can be obtained for fluorescence or phosphorescence after fitting the necessary accessories.

The excitation and emission spectra thus obtained were uncorrected. The corrected spectra in the frequency scale ($\bar{\nu}$) were obtained wherever necessary. The observed emission intensities at different frequencies when divided by the correction factors determined (2.3) for those frequencies, yield the corrected emission intensities. The corrected spectra were obtained by plotting corrected emission intensities as a function of $\bar{\nu}$. Automatic recording of the corrected excitation spectra,

linear in wavelength is possible in this instrument if the
signal from the sample cell and the signal from the reference
cell are fed into a recorder which can record the ratio of the
two signals (Ratio recorder). This part is indicated by dotted
lines in the block diagram (Fig. 2.1).

2.3. Correction Factors Determination

In a spectrofluorimeter, the intensity of the lamp,
efficiency of the monochromator and the response of the photo-
multiplier tube are wavelength dependent. So all spectro-
fluorimeters record only an "apparent emission spectrum" and those
which do not have automatic excitation correction accessory,
record only an "apparent excitation spectrum". Such spectra, in
some regions are grossly distorted versions of the true spectra.
Even though the uncorrected emission spectra can be used for
some experiments like fluorimetric titrations which are done
at a particular wavelength, they are not useful in calculating
quantum efficiencies and for reporting the fluorescence spectra
of new compounds. Several methods have been described and used
for the determination of correction factors by several
authors.[74,98-102] All calibration procedures were done with
150 W Xe lamp.

2.3.1. Correction factors for the light source (150 W Xe lamp)--Excitation Monochromator combination

The principle of Melhuish's[100] method was used for the calculation of correction factors Q (λ), since it is accurate and also convenient.

A concentrated solution of Rhodamine-B, as described earlier, was used as a fluorescent screen. The emission was passed through a narrow band metal interference filter placed before D_2. It has a maximum transmission at 620 nm with a band width of 10 nm. The intensity of the fluorescence signal at 620 nm is proportional to the intensity of the excitation light. This signal amplified by the electrometer amplifier, was recorded by scanning the M_1 from 230 to 600 nm during which the slits of M_1 were kept at 1 mm (11 nm band width). The spectrum recorded is called the excitation system calibration curve and it is shown in fig. 2.3. This curve gives the relative intensities of the excitation light emerging from M_1 at all wavelengths. These are the correction factors at different wavelengths i.e. Q (λ). This Q (λ) was used for the calibration of emission system.

2.3.2. Correction factors for the Emission Monochromator-1P 28 photomultiplier tube combination

The calibration factors for M_2 were calculated from 230 to 450 nm for the low blaze grating and 350 to 550 nm for the high blaze grating as described by Chen.[101]
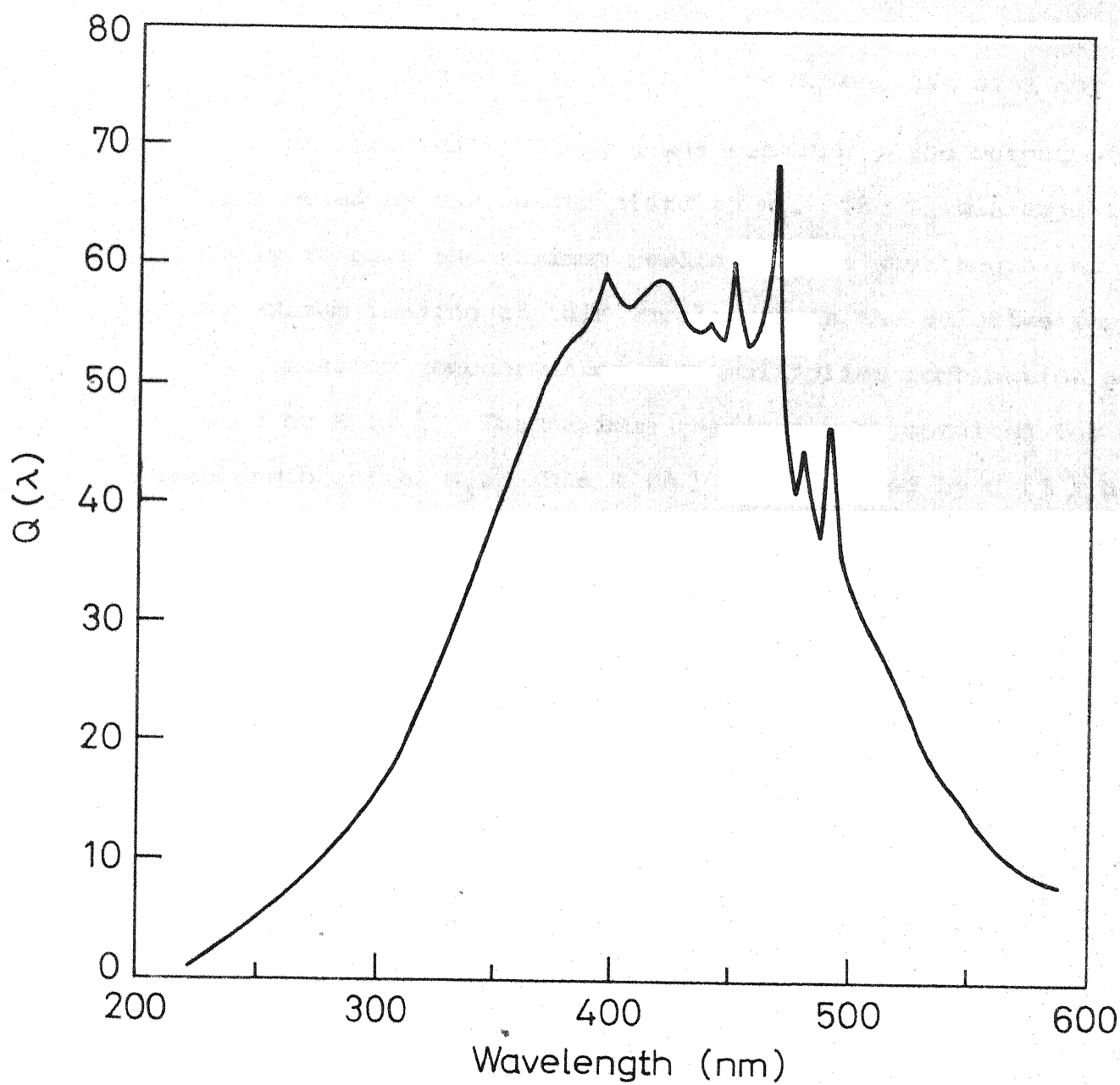
Fig. 2·3   Relative intensity distribution of excitation source.

A quartz plate at 45° to the incident light was placed in C_1. The intensity of the incident light was reduced by adjusting the slit of M_1. The slit of M_2 was set at 1 mm.

One selected wavelength was set at M_1, the output of which was reflected by the quartz plate to M_2. The M_2 was adjusted manually to give the maximum reading at the wavelength set in M_1. This maximum reading at this wavelength is the relative response of the emission monochromator-photomultiplier combination and is denoted by R (λ). The maximum readings were obtained for each wavelength set at M_1. This R (λ) when divided by Q (λ) determined earlier, gave S (λ), the emission correction factor at λ. A plot of S (λ)Vs λ gives the emission spectral sensitivity curve or the correction curve as shown in fig.2.4 for the low blaze and the high blaze gratings. A flat region in the high blaze grating spectral curve shows that emission spectra with their maxima in this region do not need any correction. Since the corrected spectrum is generally plotted in the frequency scale, the correction factors for frequencies corresponding to the wavelengths were determined by

$$S(\bar{\nu}) = \frac{S(\lambda)}{\lambda^2} \qquad \cdots \cdots \; 2.1$$

These correction factors were used to correct the fluorescence spectrum of anthracene (5 x 10^{-6}M in ethanol), recorded using the low blaze grating and quinine sulphate
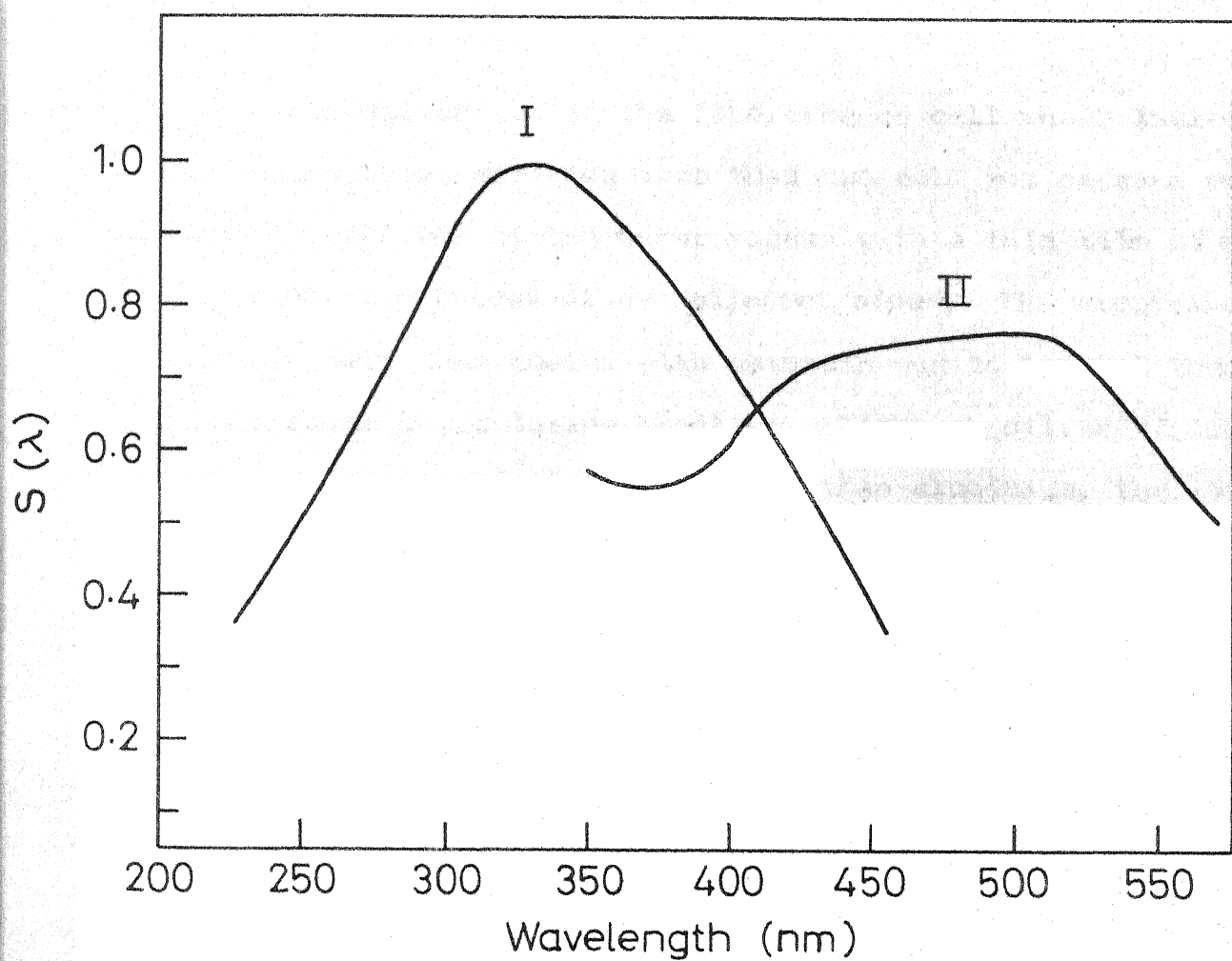
Fig. 2·4   Emission calibration curves : I 300 nm blaze grating
II 500 nm blaze grating.

$(2 \times 10^{-6}M$ in $1N$ H_2SO_4) recorded using high blaze grating. The corrected spectra thus obtained are shown in figs 2.5 and 2.6. They match exactly with the spectra reported in the literature.[100]

2.4. Cell modification

A modification of the fluorescence cell which increased the intensity of emission more than two fold was carried out. A quartz cell was coated under vacuum with a thin film of aluminium on the outer surfaces of two adjacent sides. The mirrorised surfaces were then coated with paraffin wax to prevent the removal of the metal layer during handling. Although silver[104] is a better reflecting material (88-93%) than aluminium, the latter is preferred as it is not easily corroded.

The mirrorised cell has certain advantages over a simple cell which are as follows:

(a) The excitation light is made to pass through the solution twice by the reflection of the mirror surface.

(b) In addition to the observed emission at 90°, the emission in the opposite side is also reflected. This increases the detection angle for emission.

Uncorrected fluorescence spectra of anthracene taken in mirrorised as well as non-mirrorised cells are shown in fig 2.7. The fluorescence intensity has increased by more than a factor of two in mirrorised cell without any change in the shape of any
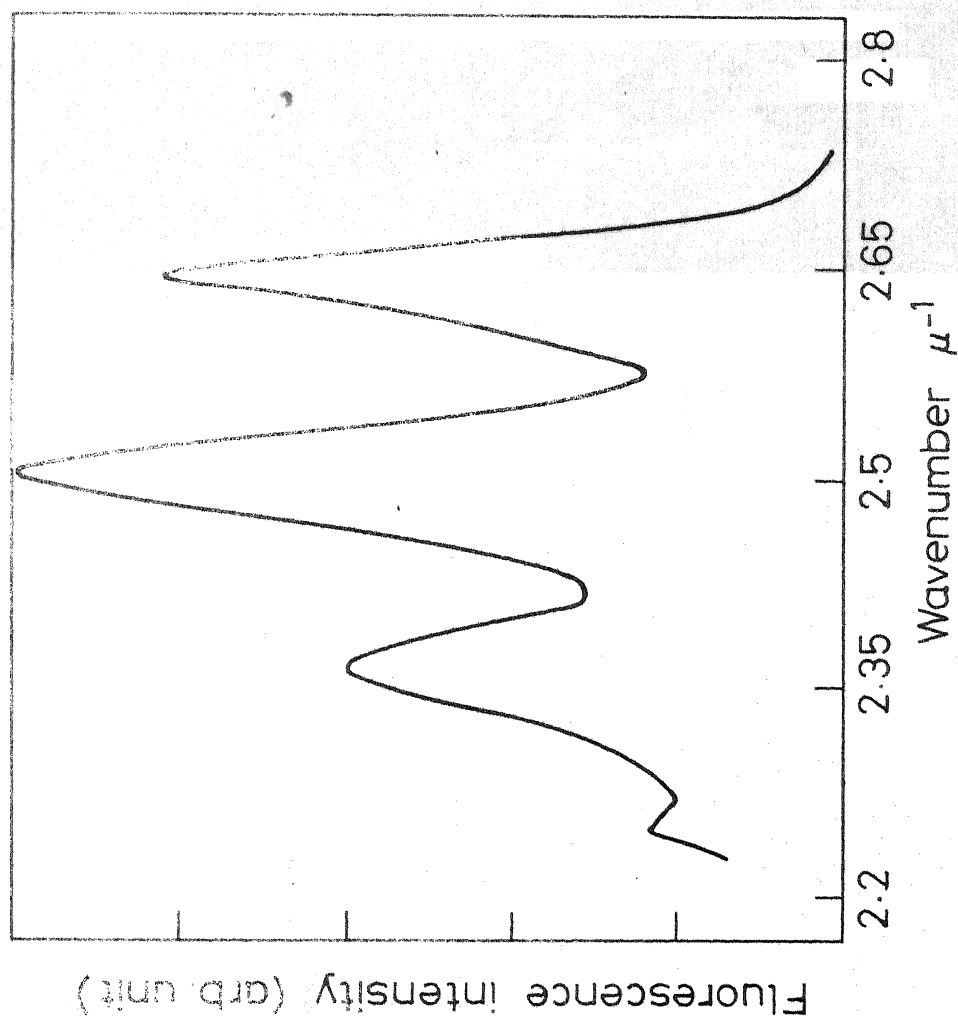
Fig. 2.5 Corrected Fluorescence spectrum of Anthracene (5×10^{-6} M in ethanol)
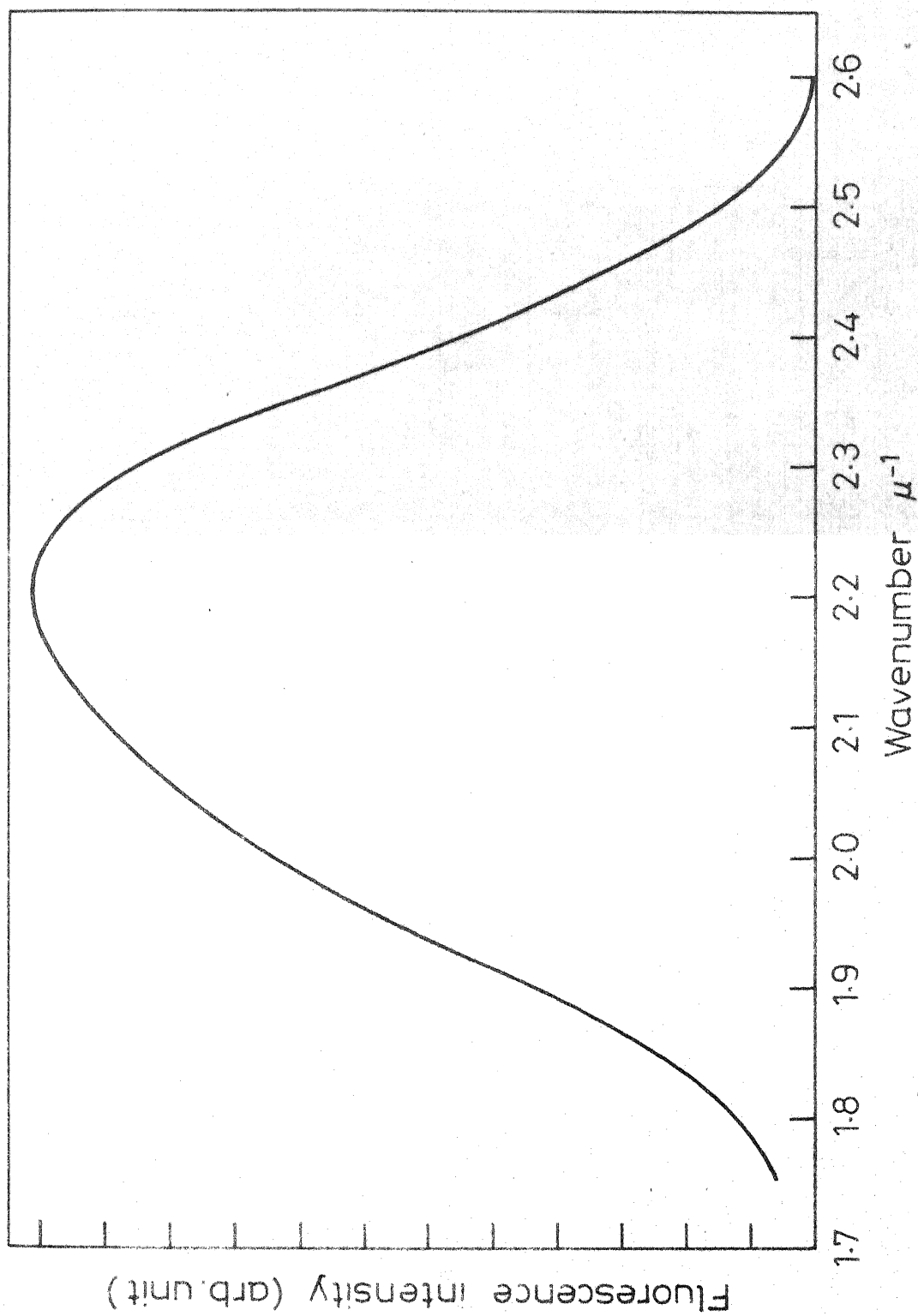
Fig. 2.6   Corrected Fluorescence spectrum of Quinine Sulphate
(2×10^{-6} M in 1N H_2SO_4)

Fig. 2·7 Fluorescence spectra of Anthracene in Cyclohexane
(a) With Mirrorised cell (b) With simple cell.
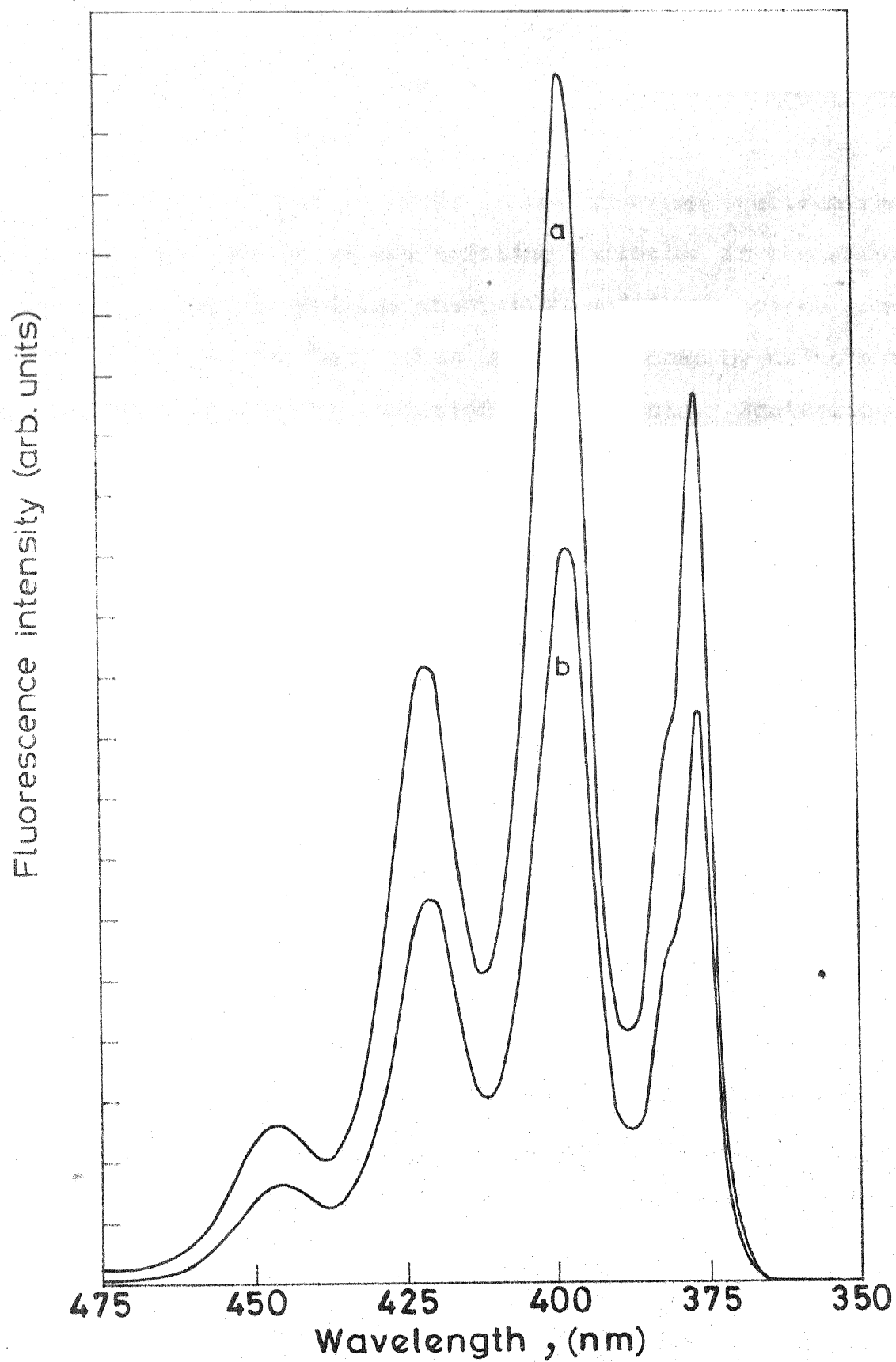
of the bands. Signal can also be increased by using concave

mirrors with a different cell compartment design[103], but our

modification is much simpler and can be easily incorporated in

any spectrofluorimeter.

There could be an error in the observed spectrum resulting

from self absorption of the emitting radiation if the sample is

highly fluorescent and the absorption and fluorescence spectra

overlap with each other. This can be overcome by using a very

dilute solution for the emission measurements. Scattering of

light is not very much different from that in the ordinary cell

except at the wavelength of excitation which does not affect the

emission spectrum significantly. This scattering can also be

avoided by placing filters in front of M_2.

This cell is much more useful for the less absorbing and

less fluorescent samples. It also gives a very high sensitivity

for highly fluorescent compounds by making their fluorescence

measurable at very low concentrations.

2.5. Other Instruments

All absorption spectra were recorded in a Cary 17D

spectrophotometer. Absorption measurements used for the deter-

mination of the ground state pK_a values were made in Beckman

DU/Toshniwal Spectrophotometers. Hydrogen ion concentrations (pH)

of various solutions employed were measured using a Toshniwal

pH meter model CL 44A. Standard buffer solutions were used
for the calibration of the pH meter.

CHAPTER - 3

MATERIALS AND METHODS

3.1. Materials

Pyrazole was obtained from Koch-Light laboratories.
9-Aminophenanthrene, 5-aminoindazole, 9-hydroxyphenanthrene and
Rhodamine-B were obtained from Aldrich Chemical Company. These
compounds were purified by repeated crystallisation from suitable
solvents. AnalaR grade sodium hydroxide, sulphuric acid,
perchloric acid, hydrochloric acid, acetic acid, phosphoric acid,
and sodium acetate were used as such. The following compounds
were synthesised in the laboratory as per the procedure given in
the literature.

__3,5-Dimethylpyrazole__[105] Equimolar quantities of acetylacetone
and hydrazine hydrate in ethanol were mixed and stirred at room
temperature. The mixture was heated and refluxed for half an hour.
The cooled solution was poured into a saturated brine solution
and the yellow oily liquid was extracted with ether. The dried

ether extract on evaporation gave the desired product which on crystallisation from petroleum-ether (60°C) gave pure 3,5-dimethylpyrazole as colourless plates, with a m.p. 106°C.

1-Phenyl 3,5-dimethylpyrazole[106] was prepared by treating equimolar quantities of acetylacetone and phenylhydrazine and refluxing the mixture for an hour. The resulting compound was separated by collecting the fraction between 157-161°C under a pressure of 24 mm. The compound was further purified by low pressure distillation and was kept in refrigerator.

1,3,5-Triphenylpyrazole[107] was prepared from chalcone (benzalacetophenone). A solution of chalcone (8.32 gm in 80 ml methanol) was treated with 12 ml of 15% H_2O_2 and 5 ml of 2M NaOH. The mixture was stirred in a water bath maintained below 30°C. After a short time colourless crystals of chalcone epoxide were formed. 4.8 gms of dried chalcone epoxide was treated with 2.8 ml of phenylhydrazine in glacial acetic acid. The solution was warmed to 60°C, stirred for half an hour and kept at room temperature. Yellow crystals of 1,3,5-triphenylpyrazole appeared after 6 hours. This compound was purified by recrystallisation from 1:4 mixture of benzene and isooctane; m.p. 137°C.

3-Methyl - 5-phenylpyrazole[108] : Benzoylacetone and hydrazine hydrate were treated in equimolar quantities in benzene and stirred for one hour at room temperature. Crystals of 3-methyl-

5-phenylpyrazole separated. The compound,on recrystallisation from benzene-petroleum-ether mixture,melted at 121-122°C.

1,5-Diphenyl-3-methylpyrazole[108]: Benzoylacetone in benzene was treated with 1.5 times phenylhydrazine at 30-45°C. The mixture was stirred for half an hour at 50°C. The solvent was evaporated and cooled to get crystals which on recrystallisation from benzene-petroleum-ether mixture, melted at 63°C.

9,10-Phenanthroimidazole[109] was prepared by a general imidazole synthesis. A mixture of phenanthroquinone (4.1 gm), hexamine (0.52 gm) and ammonium acetate (12 gm) in glacial acetic acid was heated under reflux for one hour. The resulting solution was added to water, and basified with a concentrated ammonia solution. The precipitated product was separated and purified by recrystallisation from pyridine-water; m.p. 299°C.

Benzimidazole[109] was prepared by the same method as described for 9,10-phenanthroimidazole from benzil, hexamine and ammonium acetate. It was purified by recrystallisation from water m.p. 169°C.

Other compounds such as 3,5-diphenylpyrazole,[110] indazole[111] and 4,5-diphenylimidazole[111] were obtained from organic laboratories and purified by recrystallisation from suitable solvents.

The solvents were purified by the methods described below.[112]

B.D.H. laboratory reagent <u>hexane</u> was treated two times with an equal volume of nitrating mixture (58% weight conc. H_2SO_4, 25% weight conc. HNO_3 and 17% weight water) and shaken machanically for 8 hours. The separated hydrocarbon layer was washed with conc. H_2SO_4, then with water and dried with sodium hydroxide. After drying again with sodium wire it was distilled and kept over sodium wire.

B.D.H. <u>cyclohexane</u> was passed through a 11 mm diameter 50 ml burette filled with 40 g silica gel to remove benzene, paraffinic hydrocarbons and carbonyl compounds. This was fractionally distilled over sodium at $80^{\circ}C$.

Spectrograde methanol, and chloroform (BDH) were used as such. AnalaR grade acetonitrile (E-Merck) was further purified by fractional distillation over P_2O_5 at $81.5^{\circ}C$.

3.2. <u>Purity of Materials</u>

All the compounds were checked for their purity by thin layer chromatography and ultraviolet spectra, in addition to their sharp melting points which were in agreement with the reported values. The fluorescent compounds were further tested by their same emission maxima with different excitation wavelengths. The purity and the transparency of all solvents

were checked by their ultraviolet spectra taken by using triple distilled water as the reference.

3.3. Adjustment of pH, and the Acidity or Basicity scale

The pH of various solutions were adjusted by adding either H_2SO_4 or NaOH. The low and high concentrated buffer solutions at required pH were prepared by using acetate or phosphate buffers. Selection of buffers was made according to the required pH range and to their maximum transparency in the analytical wavelength.

Hammett's acidity scale (H_o) was used for the solutions with pH below 1. To measure the strength of very weak bases, Hammett[11] used a succession of strongly acidic solvents, such as mixtures of hydrochloric, nitric, perchloric or sulphuric acids with water and developed a H_o scale, determined by using a series of indicators. This scale has been reviewed by Paul et al.,[113]. Later this has been modified for H_2SO_4-H_2O mixture by Jorgenson and Hartter[114] with a good selection of indicators. We have used this modified H_o scale in this study.

Similarly with indole derivatives (very weak organic acids) as indicators, Yagil[115] constructed a H_- scale for aqueous sodium, potassium and lithium hydroxide solutions by using Hammett's indicator acid concept. With this scale he determined the pK_a of very weak organic acids like pyrrole,

pyrazole and imidazole etc. We have used the sodium hydroxide H_- scale for the compounds whose pK_a and pK_a^* are above 13.

3.4. Ground state Acidity constant

Absorption spectra of an acid and its conjugate base were different enough that clear isosbestic points could be obtained in each equilibria except that of the deprotonation of 9-phenanthrylamine. Two sets of wavelengths on either side of the isosbestic points were selected and absorbances at these λ's were measured. Calculation for different set of λ's were also done separately. The concentration of each species at a different pH was calculated from the following equation

$$C_1 = \frac{A(\lambda_1)\,\epsilon_2(\lambda_2) - A(\lambda_2)\,\epsilon_2(\lambda_1)}{\epsilon_1(\lambda_1)\,\epsilon_2(\lambda_2) - \epsilon_1(\lambda_2)\,\epsilon_2(\lambda_1)} \qquad \text{... 3.1}$$

$$C_2 = C_T - C_1 \qquad \text{... 3.2}$$

where C_T is the total concentration of the compound in both forms and $\epsilon_1(\lambda_1)$, $\epsilon_1(\lambda_2)$, $\epsilon_2(\lambda_1)$ and $\epsilon_2(\lambda_2)$ are the molar extinction coefficients of species 1 and 2 at wavelengths λ_1 and λ_2 respectively. The latter were determined from the absorbances at a pH $\gg pK_a \pm 2$ where only one species is present. The pK_a for the equilibrium

$$BH \rightleftharpoons B^- + H^+$$
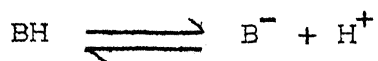
BH - species 1

B - species 2

was calculated by using the equation

$$pK_a = pH + \log \frac{C_1}{C_2}$$

$$\text{or } pH = pK_a + \log \frac{C_2}{C_1} \qquad \ldots 3.3$$

The intercept of the plot between pH and log $\frac{C_2}{C_1}$ gives pK_a.

3.5. Excited state Acidity constants

For the determination of pK_a of a singlet excited state, four methods are available and theyhave been discussed by several authors.[34-39,41,116] All these four methods have been used in this work depending upon their suitability to the compounds. They are described below briefly.

3.5.1. Fluorimetric titration

In this method fluorescence of a given sample is measured at a chosen λ as a function of pH. If both species involved in the equilibrium are fluorescent and if they are excited at isosbestic wavelength, fluorescence becomes a valuable tool for the measurement of the concentration of each species and its variation with acidity. Thus the relative fluorescence intensities (I/I_o) at the analytical wavelength can be determined as a function of $pH/H_o/H_-$. If the prototropic equilibrium is established within the lifetime of S_1 state, a plot of I/I_o

against solution acidity will give a sigmoid curve whose point of inflection is a measure of the dissociation constant in the excited state. If on the other hand, the prototropic equilibrium is not established in the excited state before the emission takes place, i.e. if the rate of fluorescence is relatively too fast, the sigmoid curve represents only the ground state acid-base equilibrium. Generally this occurs if the lifetime of the excited species is short and/or if the pK_a^* falls in the mid pH region. In the latter case, even if the rate constant for the proton transfer is very large, the rate of the reaction will be slow due to the less concentration of protons. The rate of proton transfer in the excited state can be increased by the addition of buffers. The effect of buffers has been analysed in detail[5,116] and it has been shown that concentrated buffers help in achieving the excited state equilibrium provided buffer ions do not quench the fluorescence of the excited species. We have used different concentrations of phosphate buffers to study their effect on the excited state equilibrium of a few compounds (Chapter 7).

3.5.2. Förster Cycle

Förster[34] developed a thermodynamic cycle which is based upon the thermodynamic equivalence of all routes from the ground state of the acid to the thermally equilibrated S_1 state of the

conjugate base. For the equilibrium

$$BH \rightleftharpoons B^- + H^+$$
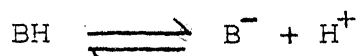
the energy level diagram is shown below
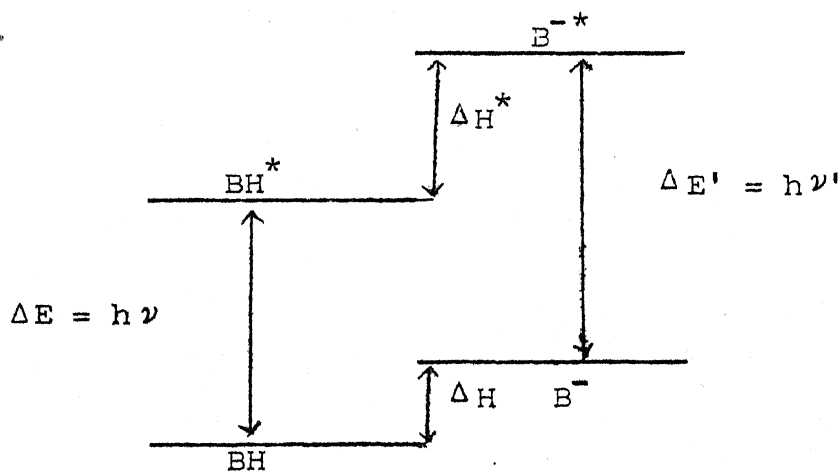
From the figure it is clear that there are two mechanistically different but energetically equivalent path ways from the ground state acid BH to the excited state base B^{-*}. So it follows that

$$\Delta E + \Delta H^* = \Delta E' + \Delta H \qquad \ldots 3.4$$

where ΔE and $\Delta E'$ are the energy changes depicted in the figure. Enthalpies of acid ionization in the ground and excited states are, respectively, ΔH and ΔH^*. Their difference can be expressed as

$$\Delta H - \Delta H^* = (\Delta G + T\Delta S) - (\Delta G^* + T\Delta S^*) \qquad \ldots 3.5$$

where ΔG and ΔS are the free energy and entropy changes respectively (excited state values are denoted by asterisks). Assuming $\Delta S = \Delta S^*$, it follows from

$$\Delta G^O - \Delta G^* = - RT(\ln K_a - \ln K_a^*) \qquad \ldots 3.6$$

that

$$- RT(\ln K_a - \ln K_a^*) = \Delta E - \Delta E'$$

$$pK_a - pK_a^* = \frac{\Delta E - \Delta E'}{2.303 \ RT}$$

$$= \frac{Nhc}{2.303 \ RT} (\bar{\nu} - \bar{\nu}') \qquad \ldots 3.7$$

At 25^OC it becomes

$$pK_a - pK_a^* = 2.1 \times 10^{-3} (\bar{\nu} - \bar{\nu}') \qquad \ldots 3.8$$

where $\bar{\nu}$ and $\bar{\nu}'$ are the wavenumbers of 0-0 transition from BH to BH^* and B^- to B^{-*} respectively. These wavenumbers can be determined from either absorption or emission spectra. Knowing $\bar{\nu}$ and $\bar{\nu}'$ and pK_a, pK_a^* can be calculated.

(a) Averaging the absorption and fluorescence

The Förster cycle is a priori applicable only to the 0-0 vibrational bands of either absorption or emission spectra. If the absorption and emission spectra are structured for both BH

and B^- forms then $\bar{\nu}$ and $\bar{\nu}'$ can be determined to a fair accuracy from the long wavelength absorption and short wavelength fluorescence maxima. But generally the absorption and emission spectra of both forms are not structured, and the position of the 0-0 band is unknown. In order to overcome this difficulty, an average of the absorption and the fluorescence maxima can be used to obtain 0-0 transition energy, assuming a mirror image similarity between absorption and fluorescence spectra and equal displacements of absorption and fluorescence maxima from the 0-0 band. Thus eq. (3.8) becomes

$$pK_a - pK_a^* = 2.10 \times 10^{-3} \left(\bar{\nu}_{ave} - \bar{\nu}'_{ave} \right) \qquad \ldots 3.9$$

where
$$\bar{\nu}_{ave} = \frac{\bar{\nu}_{ab} + \bar{\nu}_{flu}}{2}$$

$$\bar{\nu}'_{ave} = \frac{\bar{\nu}'_{ab} + \bar{\nu}'_{flu}}{2}$$

(b) Absorption only

This method presumes that the maxima of the absorption bands of the acid and its conjugate base occur at an equal amount above the 0-0 transition. If this is true, absorption spectra alone can be used in the Förster cycle to determine pK_a^* and the eq. (3.8) becomes

$$pK_a - pK_a^* = 2.10 \times 10^{-3} \left(\bar{\nu}_{abs} - \bar{\nu}'_{abs} \right) \qquad \ldots 3.10$$

(c)   Fluorescence only

This method makes the same assumption concerning the maxima of the fluorescence bands of acid and its conjugate base. Thus

$$pK_a - pK_a^* = 2.1 \times 10^{-3} (\bar{\nu}_{flu} - \bar{\nu}'_{flu}) \qquad \text{... 3.11}$$

The accuracy of the pK_a^* obtained by the three different Förster cycle methods depends upon the validity of the assumptions made. These assumptions and their validity have been discussed in great detail.[41,116]

3.6. Triplet State Acidity Constants

Triplet state acidity constants can be determined in much the same way as described for the S_1 state. Energies of the triplet states of both acidic and basic forms of the molecule above the ground state must be determined from phosphorescence because in most of the cases the $S_0 \longrightarrow T_1$ absorption spectra can not be observed as it is spin forbidden. Since phosphorescence is generally observed at 77K, the spectrum is mostly structured. This helps in locating the 0-0 band as the shortest wavelength peak. If pK_a is known pK_T^* can be calculated from the equation

$$pK_a - pK_T^* = \frac{Nhc}{2.303 \ RT} (\bar{\nu}_{phos} - \bar{\nu}'_{phos}) \qquad \text{... 3.12}$$

CHAPTER - 4

SOLVENT EFFECTS ON ABSORPTION SPECTRA

4.1. Introduction

Absorption spectra of organic molecules in solution can
be different from their spectra in vapour phase, since in the
latter they behave nearly as isolated molecules, especially
at low pressures. The spectra in a non-polar solvent in which
the intermolecular interactions are minimal, approximate the
vapour phase spectra. Depending upon the nature and the extent
of solute - solvent interactions the spectral shape, maxima and
intensity change :[1,2-5,7,95]

Solute-solvent interactions are of two types,
(a) dispersive and (b) hydrogen bonding. In the former the
lowering of energy is produced by electrostatic interaction of
permanent/induced dipole of solvent with ground/excited state
dipole of solute. The effect of this interaction on the
absorption depends upon whether the solute becomes more or less

polar as a result of excitation. If the solute molecule becomes more polar, as in most $\pi - \pi^*$ transitions, the dipole-dipole interaction lowers the energy of the Franck-Condon (FC) excited state relative to the ground state and the effect is a red shift in the absorption spectrum, increasing with solvent polarity. The converse is true if the polarity of the solute decreases upon excitation.

Hydrogen bonding interactions can be further classified as hydrogen donor and hydrogen acceptor interactions. In the hydrogen donor interaction lowering of energy is produced by the electrostatic interaction of positively polarised hydrogen of the solvent with the lone pair of electrons on a basic atom of the solute in the ground or excited state. If during excitation, the electron density migrates away from the basic atom, (eg. n- π^* transition), formation of hydrogen bond opposes this migration. As a result, the energy separation between FC excited and ground states increases and a blue shift is observed with an increase in the hydrogen donor capacity of the solvent. On the other hand if the charge migration occurs towards the basic atom upon excitation, (eg. $\pi - \pi^*$ transition), energy of the .FC excited state is lowered and a red shift is noticed with increasing hydrogen donor capacity of the solvent.

In the hydrogen acceptor interaction, chemical energy is produced by the electrostatic interaction between the lone pair

of the solvent with the positively polarised hydrogen atom of the solute molecule. The effects would be opposite to what have been discussed for the hydrogen donor interaction. Hydrogen bond acceptor solvents cause red shift when solvating solutes at atomic sites which lose electron density in the FC excited state, and cause blue shift when solvating solutes at atomic sites which gain electron density in the FC excited state. If only hydrogen bonding interactions are present, shifts in the λ_{max} with change from a non-polar to a hydrogen bonding solvent are related to the strength of the hydrogen bond in the ground state.[118]

The dispersive and hydrogen bonding interactions may alter the geometry of a molecule. The change in the geometry of the molecule due to interaction with the solvent in the ground state would also be reflected in the absorption spectra. Generally a combination of these effects is present but some times one may overweigh the other.

In this chapter an analysis of the shape and the shifts in the absorption spectra of a set of twelve compounds, consisting of seven pyrazoles, two imidazoles, two phenanthrenes and 5-aminoindazole are presented. Poor solubility of many of these compounds in certain solvents restricted the analysis of the changes in their molar absorptivities. The nonpolar solvents used were hexane and cyclohexane and the polar solvents used

were (hydrogen bonding solvents) acetonitrile, methanol and water. This investigation of solvent effect was undertaken to (a) study the steric effect caused by the solvent interaction with pyrazoles and 4,5-diphenylimidazole,

(b) explain the discrepancies in the pK_a^* calculated by the Förster cycle method using the absorption data (see chapter 6),

(c) study the shifts in the λ_{max} during protonation or deprotonation since these processes are the extremes of hydrogen bonding,

(d) compare the solvent effect on absorption and fluorescence and find out the difference (see chapter 5). The differences can give information on the nature of solute-solvent interactions and geometries of the solute molecules in the excited as well as the ground states.

4.2. Results and discussion

4.2.1. Pyrazoles and 4,5-diphenylimidazole

Absorption spectra of seven pyrazoles and 4,5-diphenylimidazole in solvents of different polarity are shown in figs. 4.1 - 4.8. The λ_{max} values are given in Table 4.1 along with the values for the corresponding cations and/or anions. A red shift is observed for pyrazole and its 3,5-dimethyl derivative while a blue shift is observed for other pyrazoles and 4,5-diphenylimidazole with increasing polarity and hydrogen bonding ability of solvents.

Conc. 4×10^{-4} M

- - - - - Hexane
.... Acetonitrile
- · - · - · Methanol
——— Water
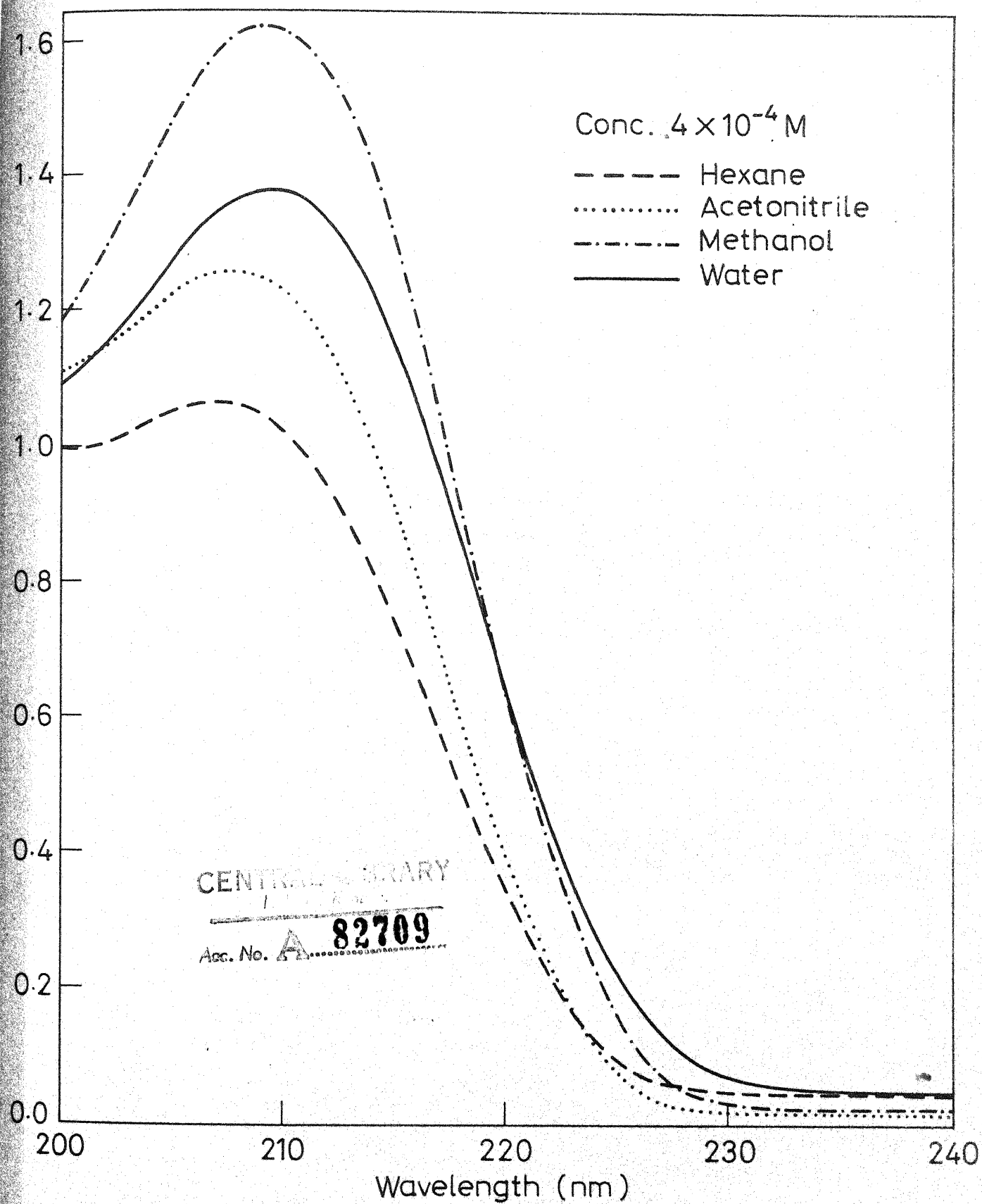
Fig. 4.1 Absorption spectra of Pyrazole in different solvents.
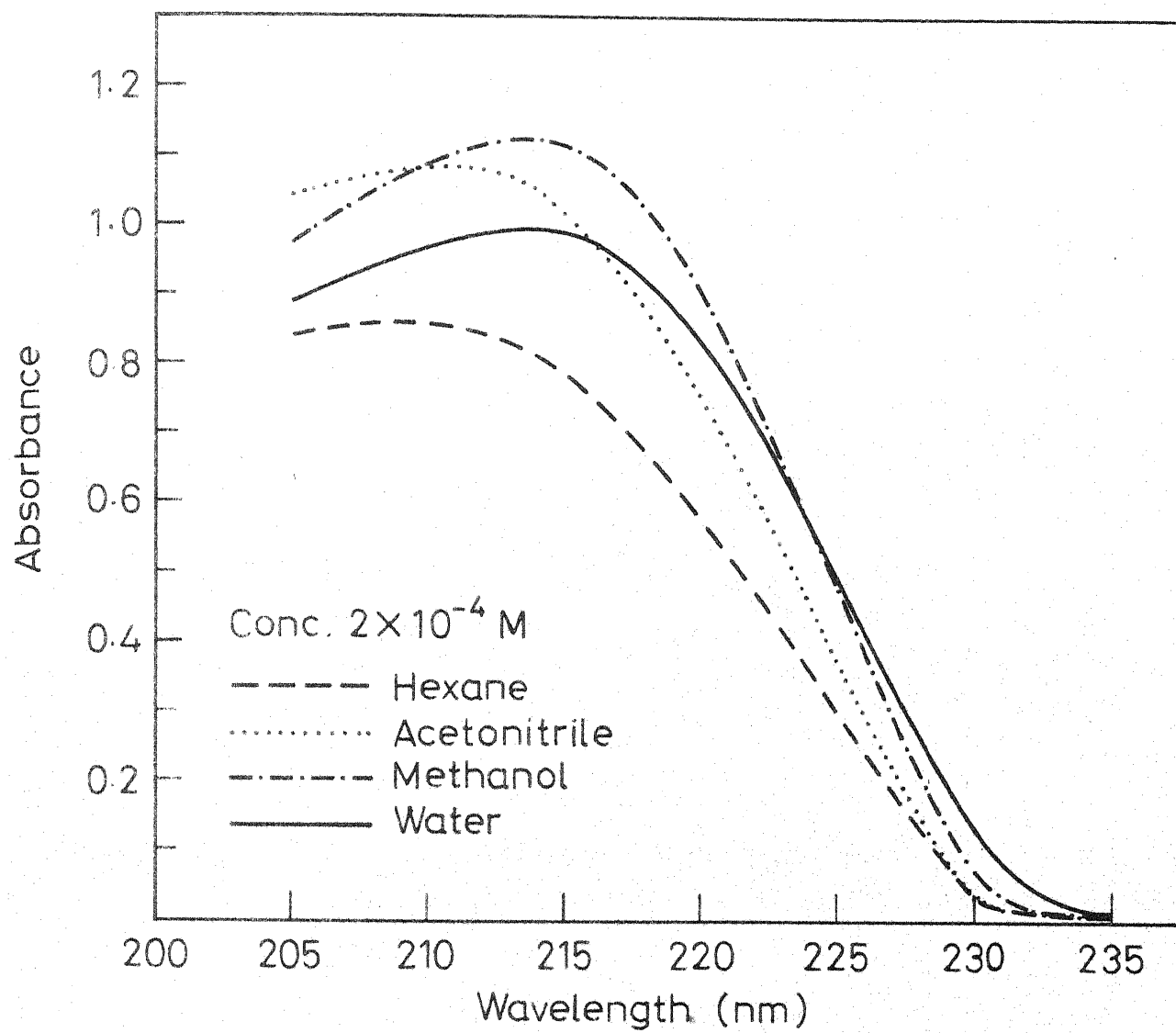
Fig. 4·2 Absorption spectra of 3,5-Dimethylpyrazole in different solvents.
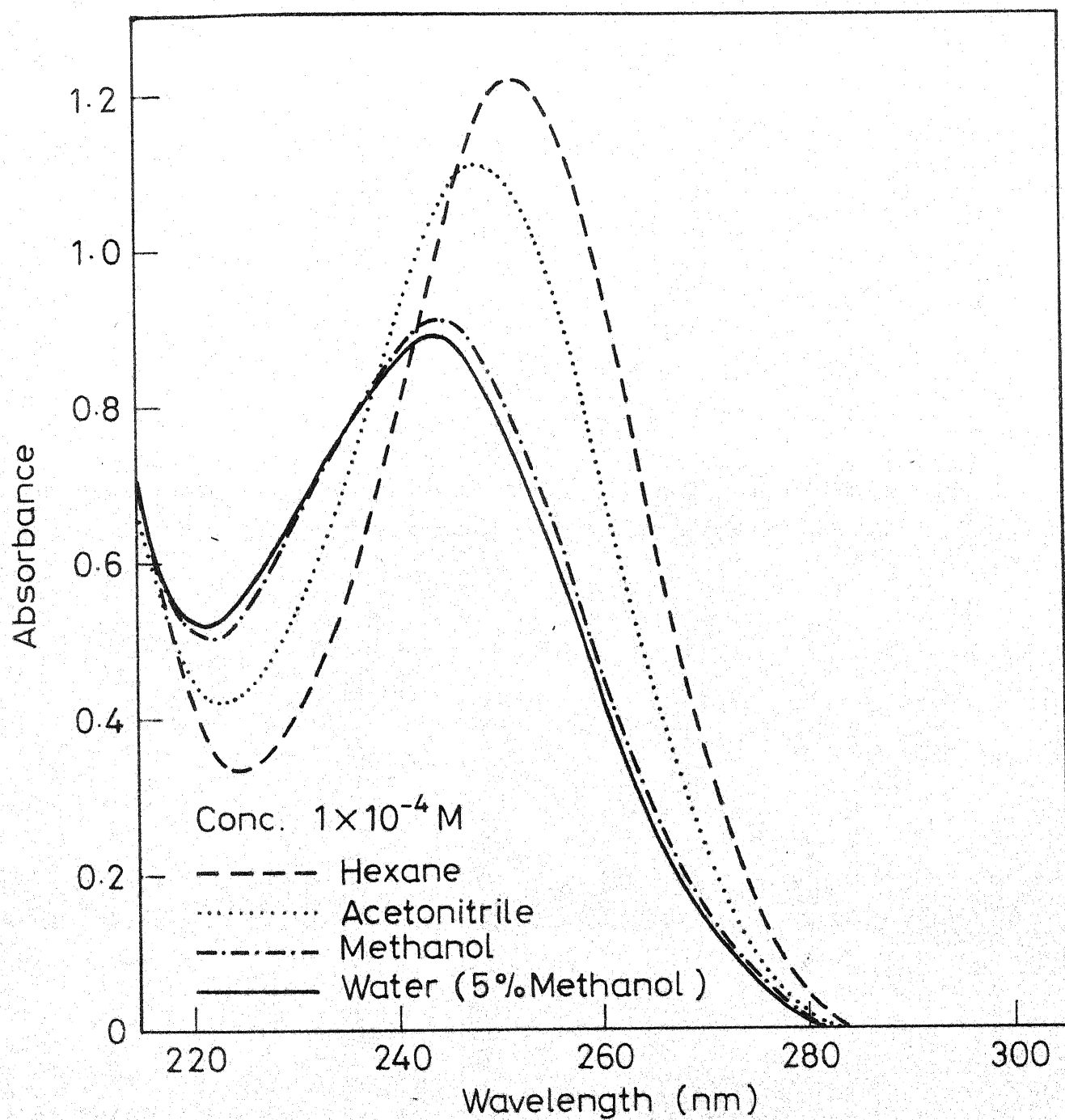
Fig. 4·3 Absorption spectra of 1-Phenyl-3,5-dimethylpyrazole in different solvents.
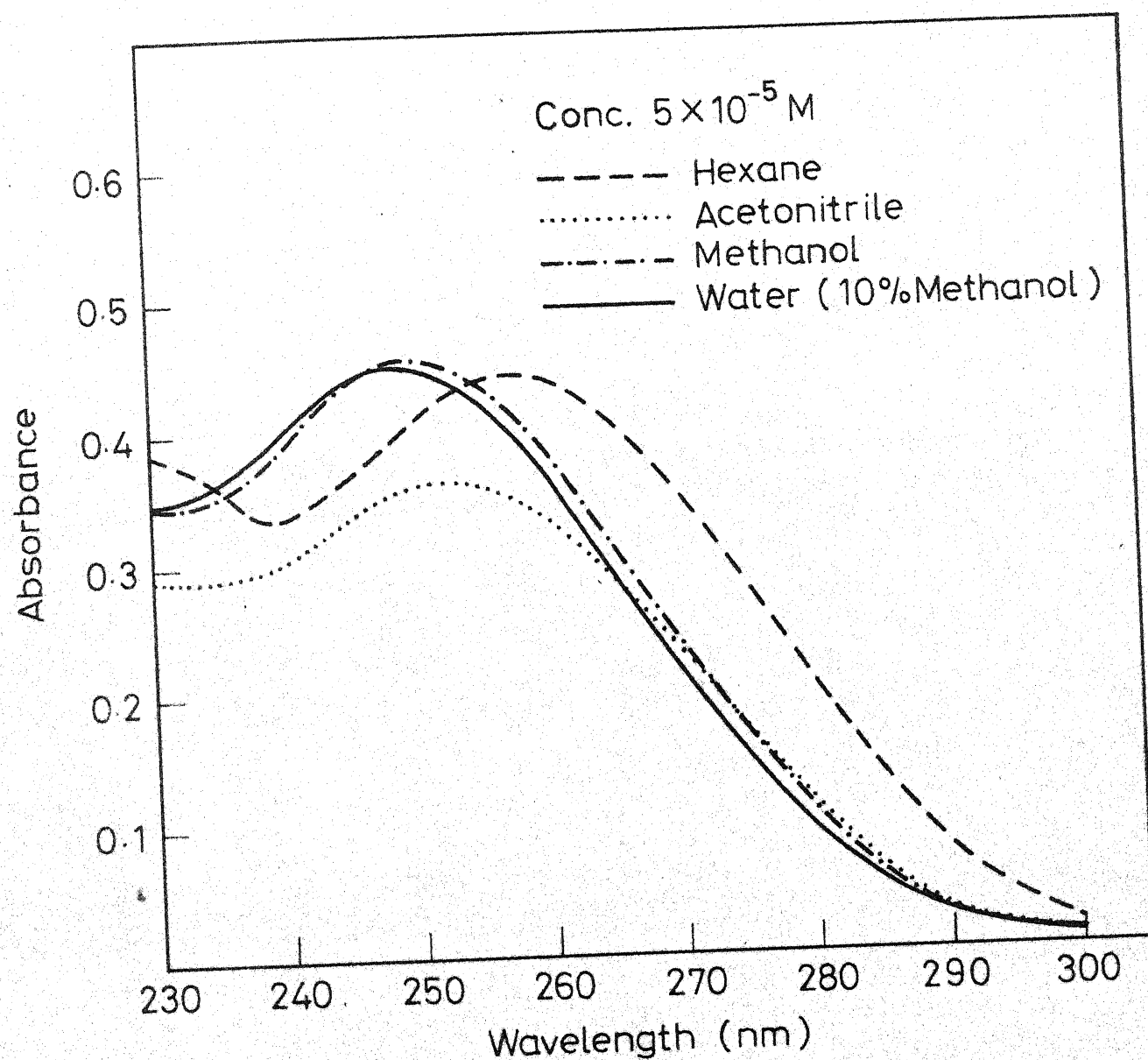
Fig. 4.4 Absorption spectra of 1,5-Diphenyl-3-methylpyrazole in different solvents.
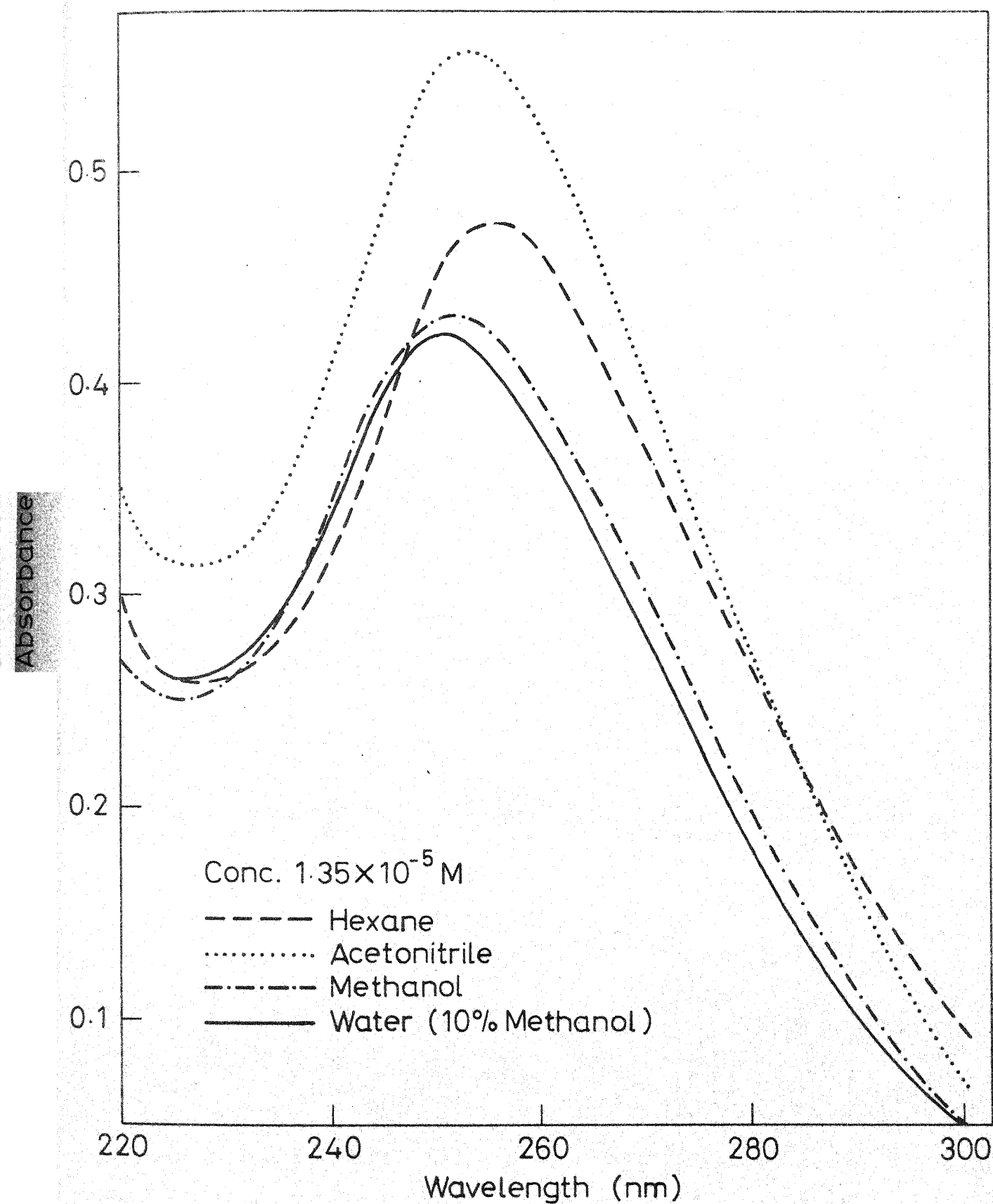
Fig. 4.5 Absorption spectra of 1,3,5-Triphenylpyrazole in different solvents.
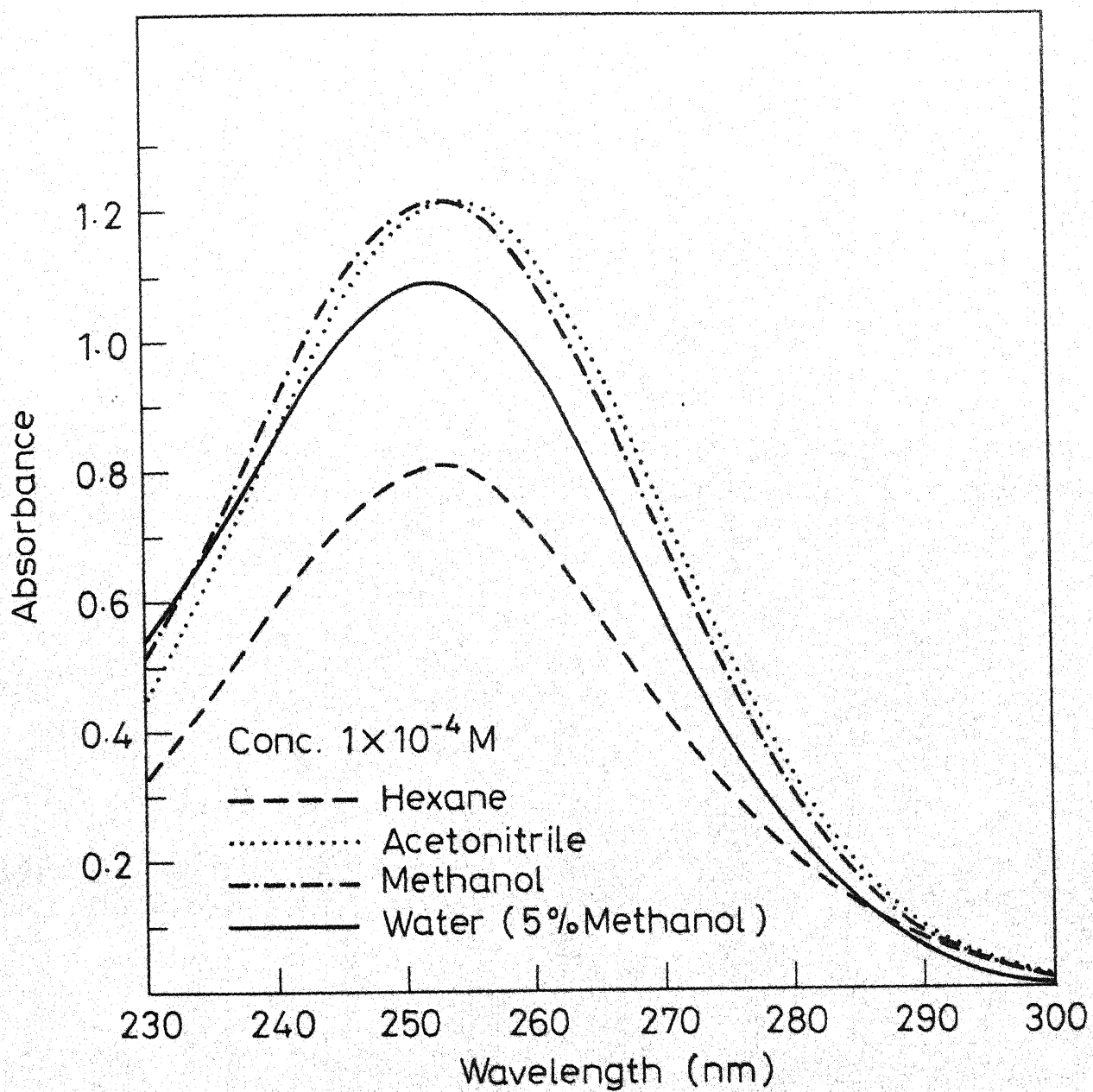
Fig. 4·6 Absorption spectra of 3,5-Diphenylpyrazole in different solvents.
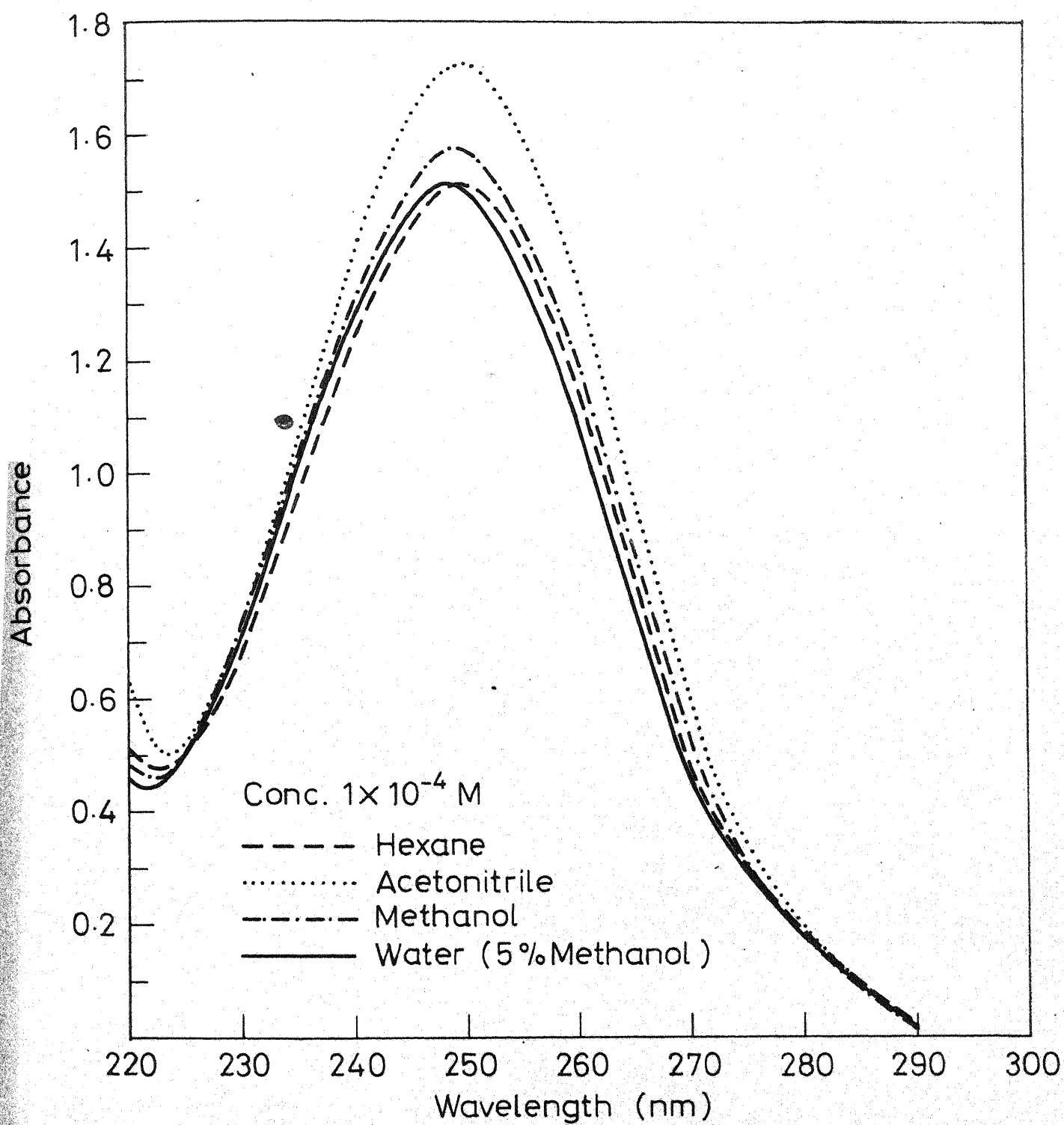
Fig. 4·7 Absorption spectra of 3-Methyl-5-phenylpyrazole in different solvents.
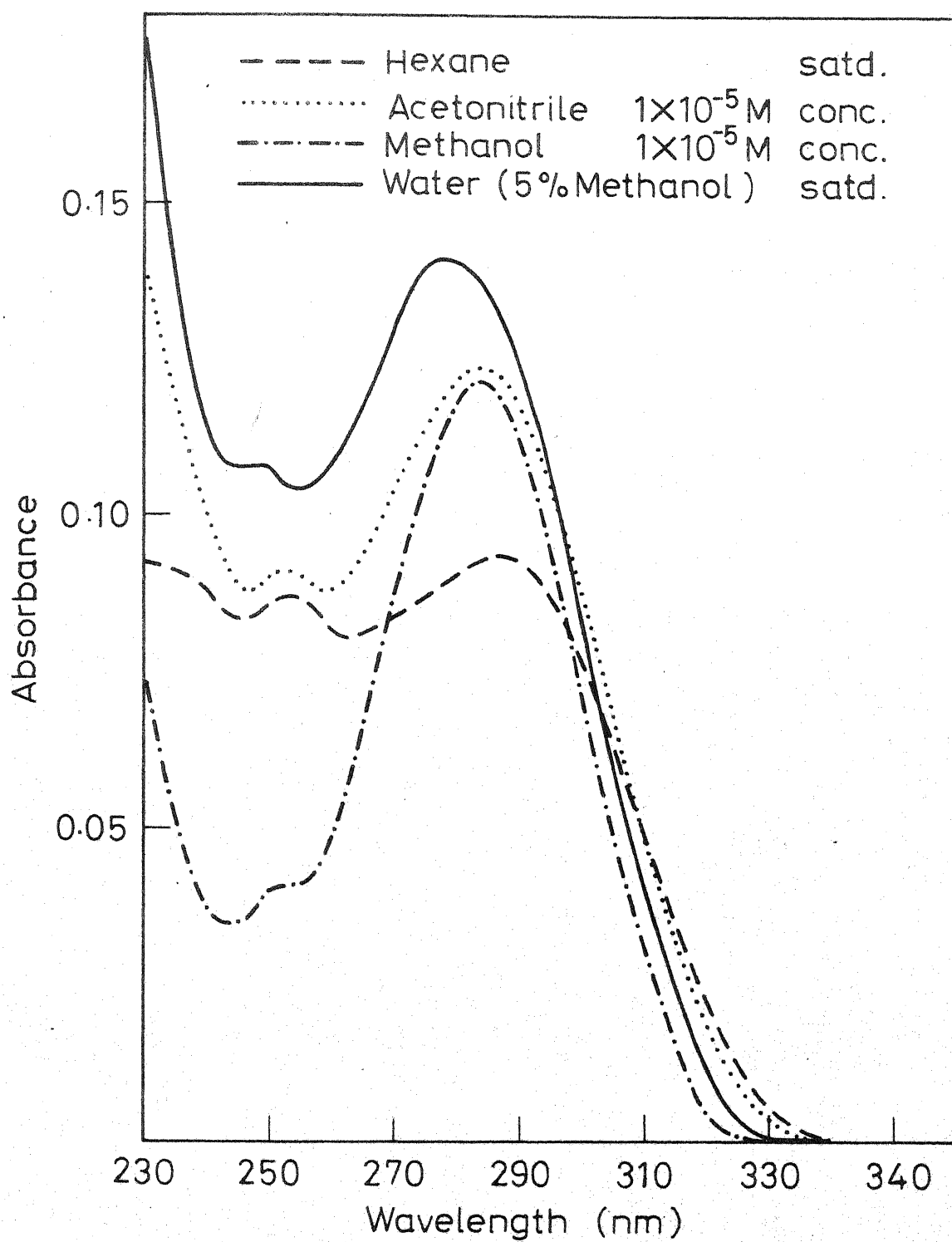
Fig. 4·8 Absorption spectra of 4,5-Diphenylimidazole in different solvents.

Table - 4.1

Absorption maxima (cm^{-1}) of pyrazoles and 4,5-diphenylimidazole in different solvents

Compound	Hexane	Acetonitrile	Methanol	Water	Acid medium (cation)	Alkaline medium (anion)
Pyrazole	48543	48192	47846	47619	46728	
3,5-Dimethylpyrazole	47846	47393	46838	46512	45662	
1-Phenyl-3,5-dimethylpyrazole	39682	40322	40816	40816	42735	
1,5-Diphenyl-3-methylpyrazole	38910	39603	40080	40160	40322	
1,3,5-Triphenylpyrazole	39062	39603	39682	39840	36496	
3,5-Diphenylpyrazole	39370	39370	39525	39603	37313	37879
3-Methyl-5-phenylpyrazole	40000	40000	40160	40322	39370	37593
4,5-Diphenylimidazole	34722	35335	35211	36101[a]	39840	33333

a) Solution at pH 8.

The red shift mentioned above is in accordance with the shift observed in $\pi - \pi^*$ transition. Theoretical calculations[119] on pyrazole and the experimental data on 3-aminopyrazole[120] and other pyrazoles[122-125] have shown that the lowest energy band in pyrazole and alkyl and phenyl substituted pyrazoles is due to $\pi - \pi^*$ transition. The blue shift for the other compounds can be explained by the steric effect caused by the solvents. In 1-phenyl-3,5-dimethylpyrazole, 1,5-diphenyl-3-methylpyrazole and 1,3,5-triphenylpyrazole, the solvent interacts with the lone pair of the ring nitrogen atom at the 2-position and this interaction is similar to the formation of a partial bond. The phenyl group attached to the nitrogen atom at the 1-position thus experiences an ortho effect[126], as observed in biphenyl and other related compounds.[6] Consequently phenyl group undergoes a rotation through the single bond and it is no longer in the same plane as the pyrazole ring. As a result, the π-conjugation of the phenyl group with the pyrazole ring is lost and a blue shift results. The blue shift with increasing solvent polarity is maximum for 1-phenyl-3,5-dimethylpyrazole but decreases with an increase in the number of phenyl groups attached to the pyrazole ring. As the number of phenyl substituents increases, some of them are in conjugation and the effect of solvent is not large.

In the three pyrazoles mentioned above, the steric effect already present[126] due to adjacent groups is further enhanced by solvent interaction. But in 3,5-diphenylpyrazole and 3-methyl-5-phenylpyrazole, the substituents are so far away from each other that the steric effect is created only by solvent interaction. Also the solvent molecules can interact with the nitrogen atom either at 1-position or at 2-position. In these molecules hydrogen bonding interactions at both position lead to red shift whereas steric effect caused by solvent interactions lead to blue shift. The small blue shift observed for both pyrazoles mentioned above shows that steric effect overweighs the hydrogen bonding effect. The blue shift in acetonitrile solution is less than that in methanol, though the dielectric constant of the former is greater than the latter. This is because the linearly structured acetonitrile cause less steric hindrance. This again shows that steric effect is relatively more important in these compounds.

In 4,5-diphenylimidazole both phenyl groups are present at adjacent positions, and the molecule gets more crowded by the solvent interaction resulting in a significant blue shift.

4.2.2. 9,10-Phenanthroimidazole (PI)

Due to poor solubility of this compound in solvents like hexane and water, the longer wavelength peaks were absent in hexane and their resolution was poor in water. Absorption

spectra of PI at two different concentrations (1×10^{-4}M and 1×10^{-5}M) in different solvents were recorded (Fig. 4.9). The λ_{max} are given in Table 4.2. As the molecule is rigid, the structure is not lost even in polar solvents. All absorption bands except those at 252.5 nm and below are blue shifted. This blue shift can not be attributed to the steric hindrance by the solvent molecule. It can not be due to n- π^* transition either because of the following reasons. (i) The extinction coefficient of all the bands are large. (ii) At room temperature, fluorescence is generally observed if the transition is $\pi - \pi^*$ and phosphorescence is observed if the lowest transition is n- π^*[121]. The observed emission spectra (chapter 5) indicate that the longest wavelength bands as well as others are due to $\pi - \pi^*$ transition.

Hence the blue shift observed in PI is explained as follows. The lone pair on one of the imidazole nitrogen atom of PI is perturbing the π -cloud of the phenanthrene moiety resulting in a charge migration from the imidazole ring during excitation as in aminophenanthrene.[129] Since this process is opposed by the hydrogen donor interaction of methanol and water with the lone pair on the nitrogen atom, absorption spectra in these solvents are blue shifted relative to acetonitrile which is a weak hydrogen acceptor solvent. The absorption spectrum of the protonated phenanthroimidazole is further blue shifted and
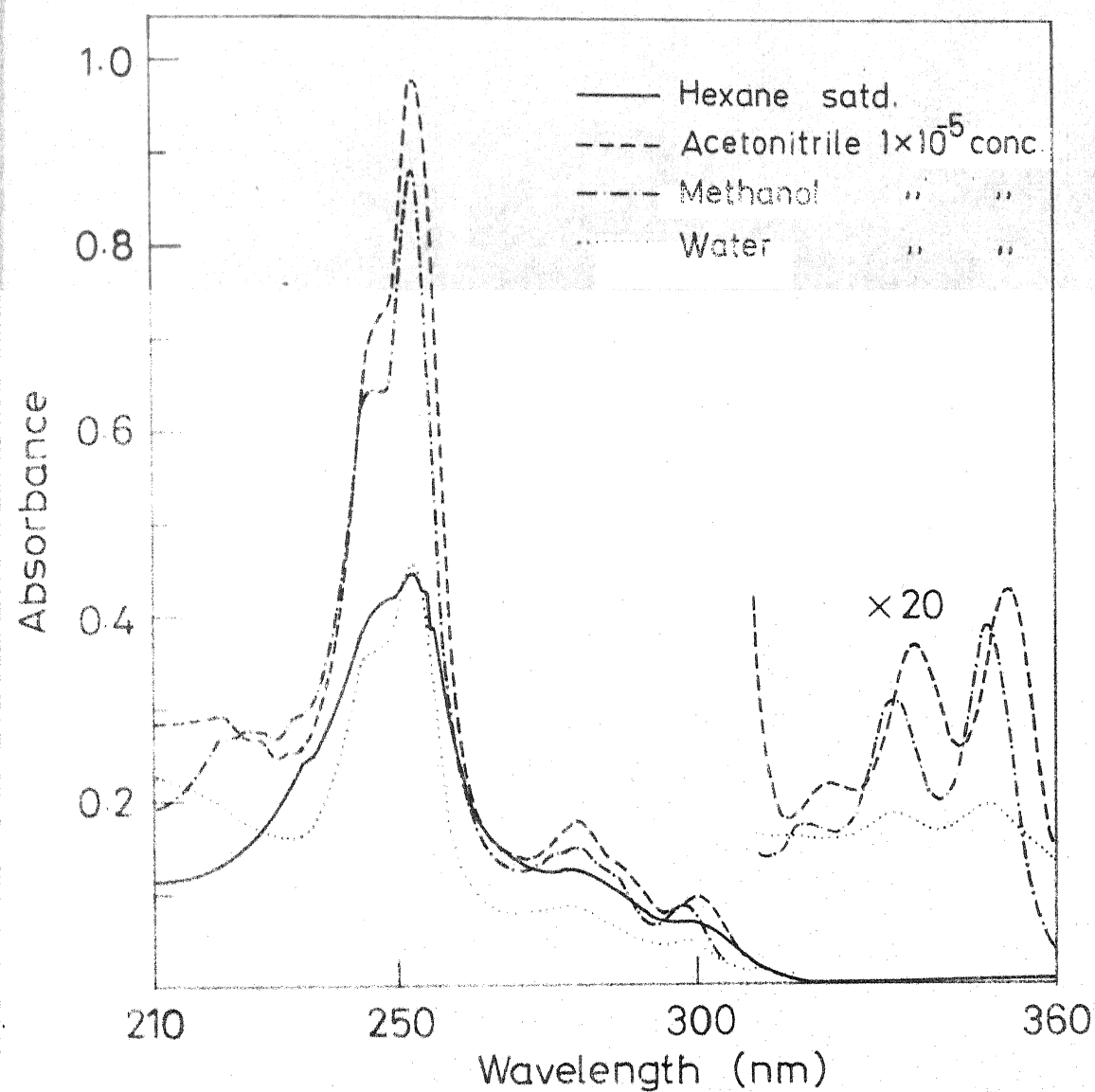
Fig. 4.9 Absorption spectra of 9,10-Phenanthroimidazole in different solvents.

Table – 4.2

Absorption maxima (cm^{-1}) of PI, AMP, HP, AI and Indazole in different solvents

Compound	Hexane	Acetonitrile	Methanol	Water	Cation	Anion
9,10-Phenanthroimidazole	40816	40650	40816	40816	41152	40160
	39603	39525	39603	39603	39920	39062
	35714	35714	35842	35842	36900	35087
	33333	33333	33557	33613	35842	32679
		31007	31446		34423	28169
		29717	30030	30075	30978	27322
		28409	28667	28735	29585	
9-Aminophenanthrene	45248	39761	39920	40080		
	40080					
	38834					
	36832					
	35398	35335	32206	32733		
	32051	31746				
9-Hydroxyphenanthrene	39840	39682	39525	39840		
	36769	36697	36429	36764		
	33990	33670	33500	33898		
	32840	29673	32679			
	29761		29411	29629		
	28288	28169	28011	28248		
5-Aminoindazole	30769	30911	30627	31250	39840	30864
					38910	
					35211	
					34722	
					33898	

Table 4.2 (contd.

Table 4.2 (contd.)

Compound	Hexane	Acetonitrile	Methanol	Water	Cation	Anion
Indazole	40160	40160	40160	40160		
	39062	39062	39062	39062		
	36231	36101	35971	35971		
	35460	35398	35273	35273		
	34843	34782	34662	34662		
	34071	34013	33840	33840		

resembles that of phenanthrene.[127] This confirms the above explanation.

4.2.3. 9-Aminophenanthrene

Absorption spectra of this compound in different solvents are displayed in fig. 4.10 and the λ_{max} are reported in Table 4. Solvent interaction with this compound is interesting. Amino group attached to the phenanthrene moiety can interact with a hydrogen donor solvent through its lone pair or it can interact with a hydrogen acceptor solvent through its hydrogen atom. A blue shift in the former and a red shift in the latter relativ to the maxima in hexane are expected. From the spectra in figure 4.10 it is clear that band at 249.5 and 312 nm in hexane are blue shifted in methanol and water indicating that hydrogen donating tendency of these solvents overweighs their hydrogen accepting nature. The red shift observed in acetonitrile must be due to its hydrogen accepting nature. Since the longer wavelengths band was not observed in some solvents due to poor solubility of the compound, the shift in that band could not be ascertained. Absorption spectrum of the protonated form is significantly blue shifted and resembles that of phenanthrene,[12] reiterating our conclusion about solute-solvent interactions.
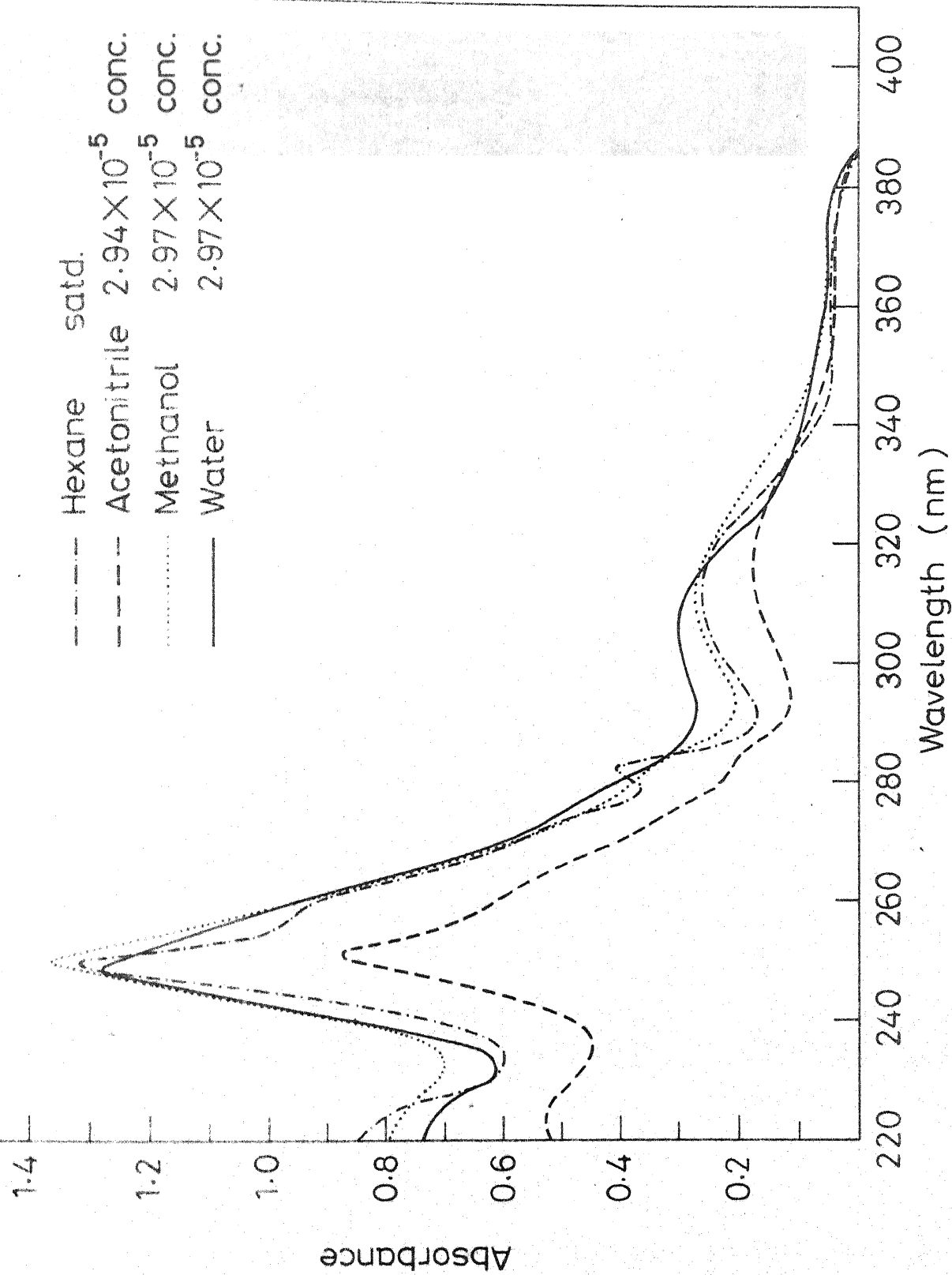
Fig. 4.10 Absorption spectra of 9-Aminophenanthrene in different solvents.

Legend (within figure):

Hexane — satd.
Acetonitrile — 2.94×10^{-5} conc.
Methanol — 2.97×10^{-5} conc.
Water — 2.97×10^{-5} conc.

X-axis: Wavelength (nm)
Y-axis: Absorbance

4.2.4. 9-Hydroxyphenanthrene

Due to the presence of many absorption bands with different ϵ_{max} for this compound, the λ_{max} in each solvent could be located only by recording spectra at different scales with 10^{-5}M solutions. As it is difficult to represent spectra in all solvents with all maxima, only the absorption spectrum in hexane is shown in fig. 4.11 and the λ_{max} in each solvent are listed in Table 4.2. When compared to the values in hexane, λ_{max} in other solvents are red shifted, but the shift is not regular either with polarity or hydrogen bonding ability of the solvents. The red shift in methanol is more than in acetonitrile showing that hydrogen bonding interactions are more dominant than dispersive interactions. But in water a blue shift is observed relative to the maxima in methanol.

As in 9-aminophenanthrene, the solvent can interact either with the lone pair on oxygen or with the hydrogen atom of the hydroxyl group, resulting in a blue or a red shift respectively. In hydroxyphenanthrene the charge transfer interaction of the hydroxyl group is less as is clear from its structured absorption spectrum in comparison to that of 9-aminophenanthrene. Moreover due to the high polarity of O-H bond the solvent interaction with the hydrogen atom of the solute must be more than the solvent interaction with the lone pair. This would explain the red shift observed in acetonitrile and methanol.
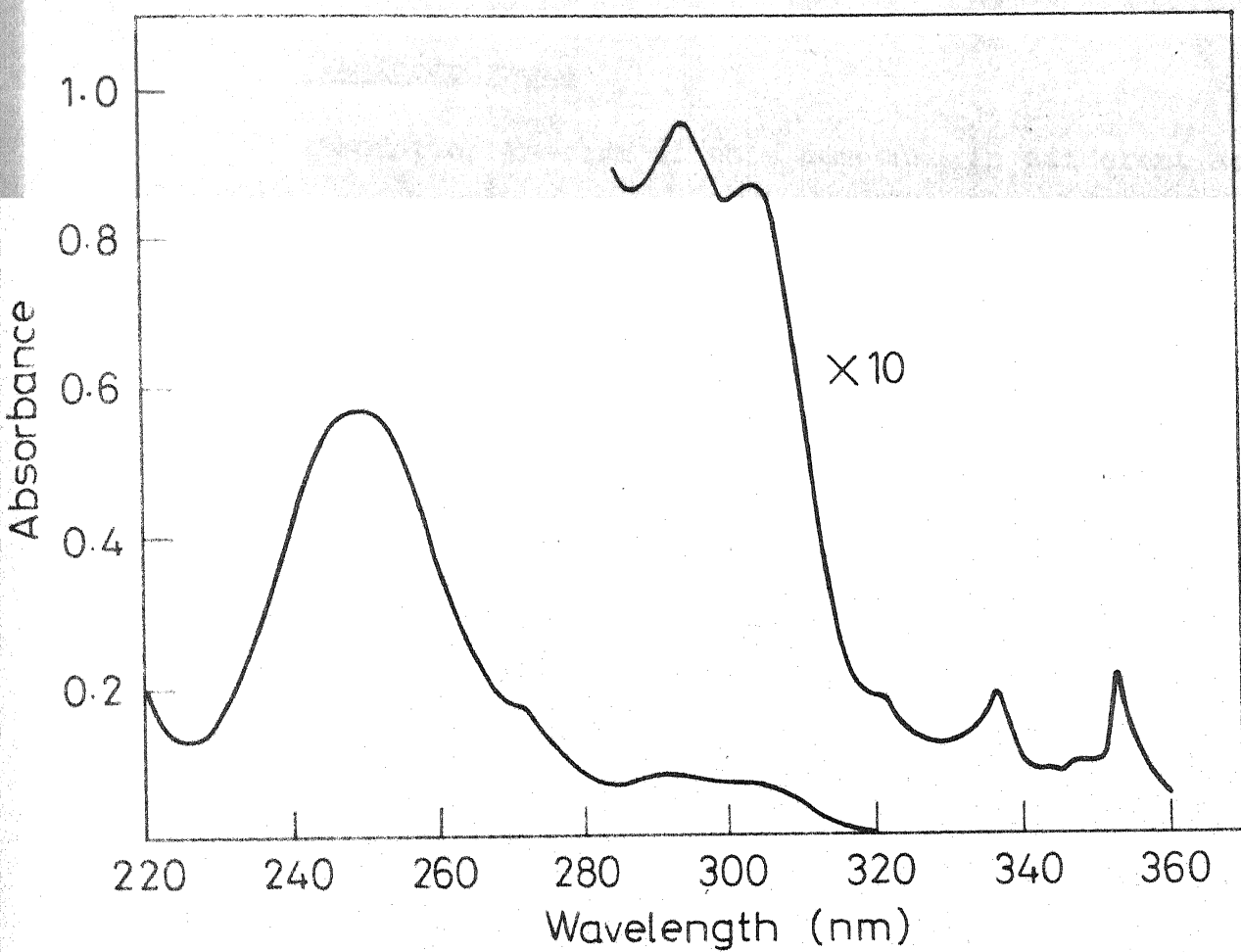
Fig. 4·11 Absorption spectra of 9-Hydroxyphenanthrene in hexane, conc. 3×10^{-5} M

When compared to methanol, a blue shift is observed in water indicating the hydrogen donor interaction due to its greater hydrogen donating capability than methanol.

4.2.5. 5-Aminoindazole

Absorption spectra of this compound in different solvents are shown in fig. 4.12. The λ_{max} are given in Table 4.2 along with the corresponding values for indazole for comparison. The amino group interacts with the π cloud of indazole ring and as a result , vibrational structure of the spectrum is lost. The broadness and the red shift of the absorption spectrum relative to the indazole spectrum suggest charge transfer from the aminogroup to the ring as in 9-aminophenanthrene. In indazole,[128] the small red shift with the solvent polarity is due to the usual effect on π - π* transition. But aminoindazol undergoes a blue shift in methanol and water (hydrogen donor solvents) and a red shift in acetonitrile (a hydrogen acceptor solvent) relative to hexane. This shows that the solvent interaction in the ground state is only at the amino group. In the extreme case of hydrogen donation i.e. protonation of the amino group, the absorption spectrum is blue shifted relative to aminoindazole and resembles the spectrum of indazole (Fig. 6.13) This adds to the further confirmation that the site of solvent interaction is at the aminogroup in the ground state.
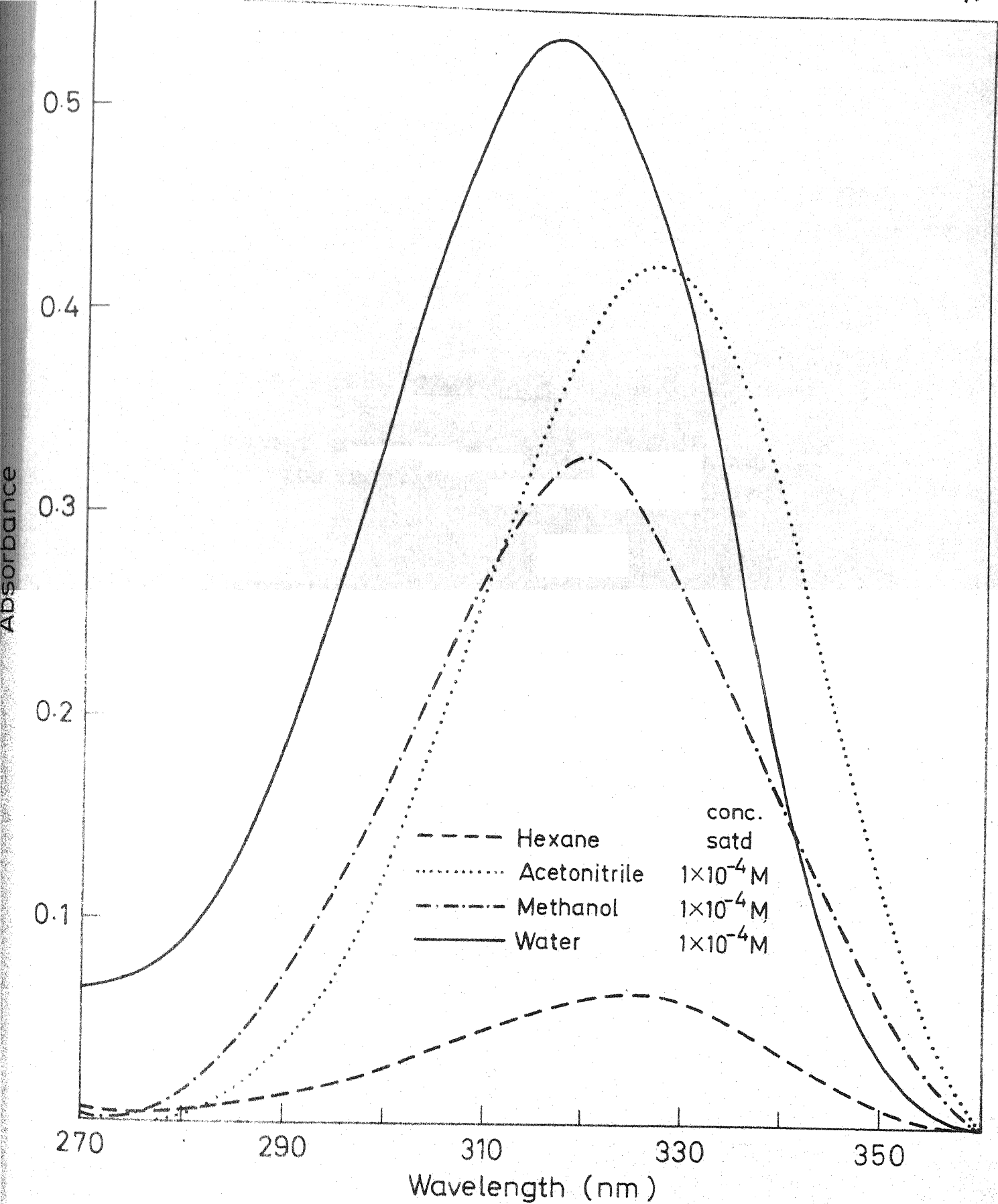
g.4.12 Absorption spectra of 5-Aminoindazole in different solvents.

CHAPTER - 5

SOLVENT EFFECTS ON FLUORESCENCE SPECTRA AND
LOW TEMPERATURE EMISSION STUDIES

5.1. Introduction

Fluorescence spectra of organic molecules in solution depend upon the nature of solvents. Shifts in the λ_{max}, shapes of the bands and the relative intensities of absorption and fluorescence spectra in solvents of different polarity and hydrogen bonding ability, provide a clue on the nature of interactions with the solvents, nature of the excited state and the change in geometry of the molecule upon excitation. The solvent effect has been reviewed by several authors in detail.[15-22,26,28,54,95,103,130] Therefore, only a brief summary is given below.

The influence of a solvent upon fluorescence or phosphorescence of a compound can be quite different from that observed for the UV absorption spectrum of the same compound. This can

be explained on the basis of the Franck-Condon principle.
Representative energy level diagrams, along with the implications
of this principle are shown in fig. 5.1 (a and b). These
figures illustrate the relative magnitudes of different kinds
of relaxations in the ground and electronically excited states in
(a) a molecule in which dipole moment increases (fig. 5.1. a)
(b) a molecule in which dipole moment decreases (fig. 5.1. b),
upon excitation.
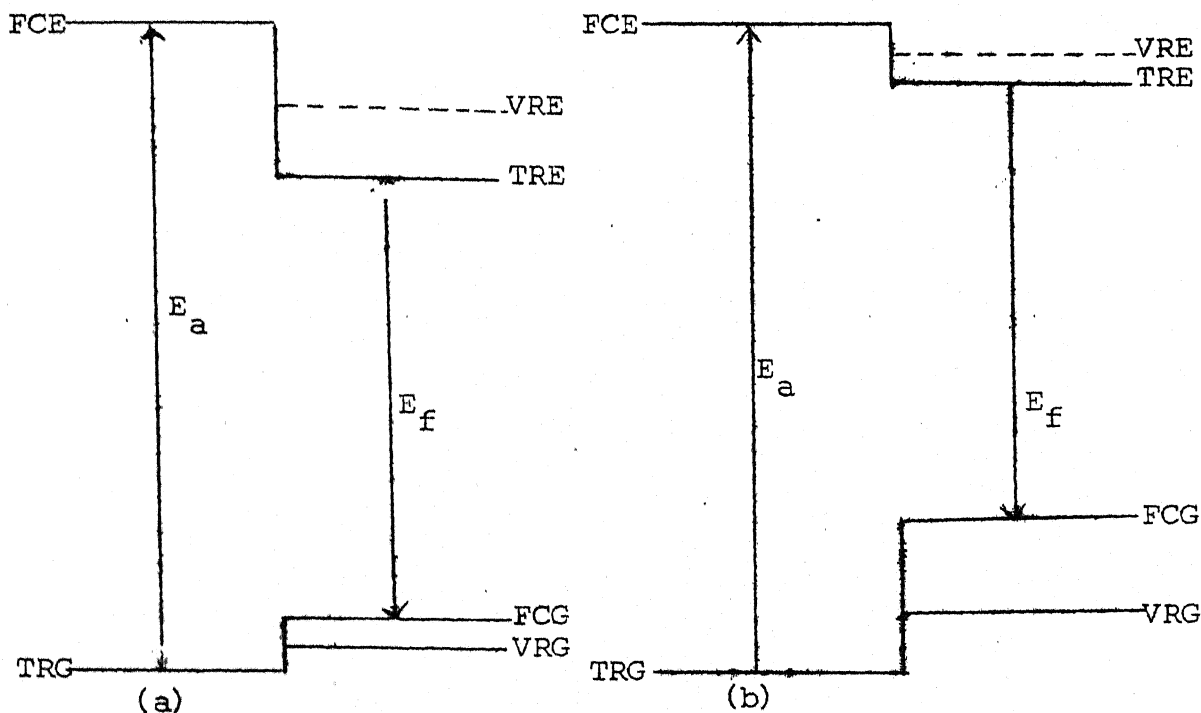
Fig. 5.1. Energy level diagram

E_a and E_f are the spectral absorption and fluorescence energies.
FCE and TRE are the energies of Franck-Condon and thermally
relaxed excited states respectively. FCG and TRG are the

corresponding energies for the ground states. VRE and VRG are the energies of thermally relaxed excited state and the FC ground state when vibrational relaxation is the only thermal relaxation mechanism (i.e., if the fluorescence was measured in a rigid matrix so that solvent relaxation was impossible in ground or excited state).

Fig. 5.1.a closely resembles the behaviour of the compounds selected for our study because in all our compounds $\pi - \pi^*$ is the lowest energy transition which is accompanied by a large increase in dipole moment.

When a molecule is electronically excited, it ends up in FCE, in which the solute molecule is still in the environment of the ground state. Subsequently, due to change in electronic charge distribution in the solute molecule, reorientation of solvent cage or making and breaking of hydrogen bonds take place. Since this is similar to the vibrational motions, this act is complete within a period of $10^{-14} - 10^{-12}$ sec and the molecule attains TRE within the life time of the excited state ($\sim 10^{-8}$ sec). Consequently fluorescence originates from TRE which is lower in energy than FCE and VRE. When fluorescence occurs, it terminates in the FCG in which the solute molecule is still in the excited state environment, due to the rapidity of the electronic transition. Rapid solvent relaxation then occurs and the solute molecule ends up in the ground state solvent cage (TRG). The

FCE is higher in energy than the TRE, and TRG is lower than FCG. Therefore fluorescence occurs often at considerably longer wavelengths than expected purely on the basis of vibrational relaxation in polar solvents. As a result, the 0-0 bands of absorption and fluorescence do not coincide.

Thermal relaxation in the excited state includes vibrational, solvent and geometry relaxation. At a given temperature fluorescence spectrum depends upon these relaxations. All these processes influence the fluorescence maxima simultaneously and thus a study of their effect individually becomes difficult. Yet a careful analysis of the spectrum can provide valuable information regarding these processes.

Vibrational relaxation would be present in all kinds of solutes and solvents. But the magnitude of this relaxation depends upon of the structure of the solute molecule. In the absence of hydrogen bonding, polarity of the solvent affects the fluorescence spectrum. In a $\pi - \pi^*$ transition, in which dipole moment increases upon excitation (Fig. 5.1. a), solvent relaxation in the excited state increases with an increase in the polarity of the solvent. Therefore the fluorescence spectrum of the molecule tends to show a greater wavelength dependence on solvent polarity than the absorption spectrum. Fluorescence maximum in such a case is usually red shifted with increase in solvent polarity.

Effects of hydrogen bonding of solvent on fluorescence spectra are more involved than that of solvent polarity. From an extensive study of hydrogen bonding effect, it was shown that hydrogen bonding can affect the intensity and λ_{max} of fluorescence in several ways.[18,95,102,103,130,137] For example, in case of aromatic compounds containing electron-donor substituents like -OH and -NH$_2$ groups, hydrogen donor solvents partially inhibit the lone pair on these substituents from participating in the excited state charge transfer interaction with the ring. As a result, fluorescence maxima get shifted to higher frequencies when compared to the maxima in non-polar solvents. In hydrogen acceptor solvents on the other hand, fluorescence maxima of the solute molecules are red shifted relative to the maxima in non-polar solvents due to the increased charge transfer interaction of the lone pair with the ring. Effects of hydrogen donor/ acceptor solvents on the fluorescence of the aromatic molecules containing electron withdrawing groups such as $>C=O$ are opposite to those in the compounds containing electron-donating groups. In general, the effects are similar on absorption and fluorescence spectra. But in some cases, like aromatic amines, the solvent shifts in absorption and fluorescence maxima are opposite to each other for the same series of solvents. This is found to be due to the difference in site of hydrogen bonding interaction in the excited state from the ground state.[28,13]

In addition to the solvent relaxation, if a molecule undergoes a change in its geometry, the shape and λ_{max} of the fluorescence spectra are affected.[132] Berlman[24] has discussed the empirical correlations that exist between spectroscopic properties (solvent effects on absorption and fluorescence, Stokes shift, mirror-image similarity etc.) and the planarity of a molecule in a given electronic state. He has classified the aromatic ring-ring chain compounds into five categories depending upon their conformations in the ground and excited states. From a study of their spectroscopic properties, it is possible to detect the differences in the ground and excited state geometries and to assign a molecule to one of the five categories.

Luminescence spectra have been studied at low temperature (77K) and such studies, due to the rigidity of the medium help (i) in obtaining the fluorescence spectra of a molecule which otherwise is not possible due to some excited state processes (photo reaction, solute-solvent complex formation etc.)[139] (ii) in analysing the molecular vibrational frequencies.[138,140]

In this chapter we analyse the fluorescence spectra of five pyrazoles, 4,5-diphenylimidazole (DPI), 9-hydroxyphenanthrene(HP), 9-aminophenanthrene (AMP) and 5-aminoindazole (AI) in different solvents, at different pHs, where a cation or anion is exclusively present, and at temperatures 298K and 77K.

5.2. Results and discussion

5.2.1. Pyrazoles and 4,5-diphenylimidazole

Fluorescence spectra of 1-phenyl-3,5-dimethylpyrazole (PDP), 1,5-diphenyl-3-methylpyrazole (DPMP), 1,3,5-triphenyl-pyrazole (TPP), 3,5-diphenylpyrazole (DPP), 3-methyl-5-phenyl-pyrazole (MPP) and 4,5-diphenylimidazole (DPI) were studied in different solvents and pHs at 298K. The spectra are shown in figs. 5.2 - 5.7. The concentrations of most of the compounds were kept equal in all solvents except for some compounds whose solubility is poor in certain solvents. The fluorescence maxima of all the compounds in different solvents are listed in Table 5.1. Except for DPMP, TPP and DPI, the $\lambda_{max}(f)$ of the cations and/or of anions of the compounds are also included in Table 5.1.

An analysis of the fluorescence spectra of these compounds show that there is a regular red shift and a decrease in relative fluorescence intensity with an increase in the solvent polarity except for MPP. Fluorescence spectra of DPP and MPP exhibit vibrational structure in cyclohexane/hexane but not in polar solvents. Fluorescence of DPP$^+$ and MPP$^+$ are quite intense while that of PDP$^+$ is very weak. Fluorescence of DPMP$^+$ could not be detected. Cations of TPP, DPMP and DPI seem to behave strangely on excitation and are discussed separately. A quenching of MPP$^+$ fluorescence by chloride ion (Cl$^-$) has been observed and is analysed further (5.2.1.d).
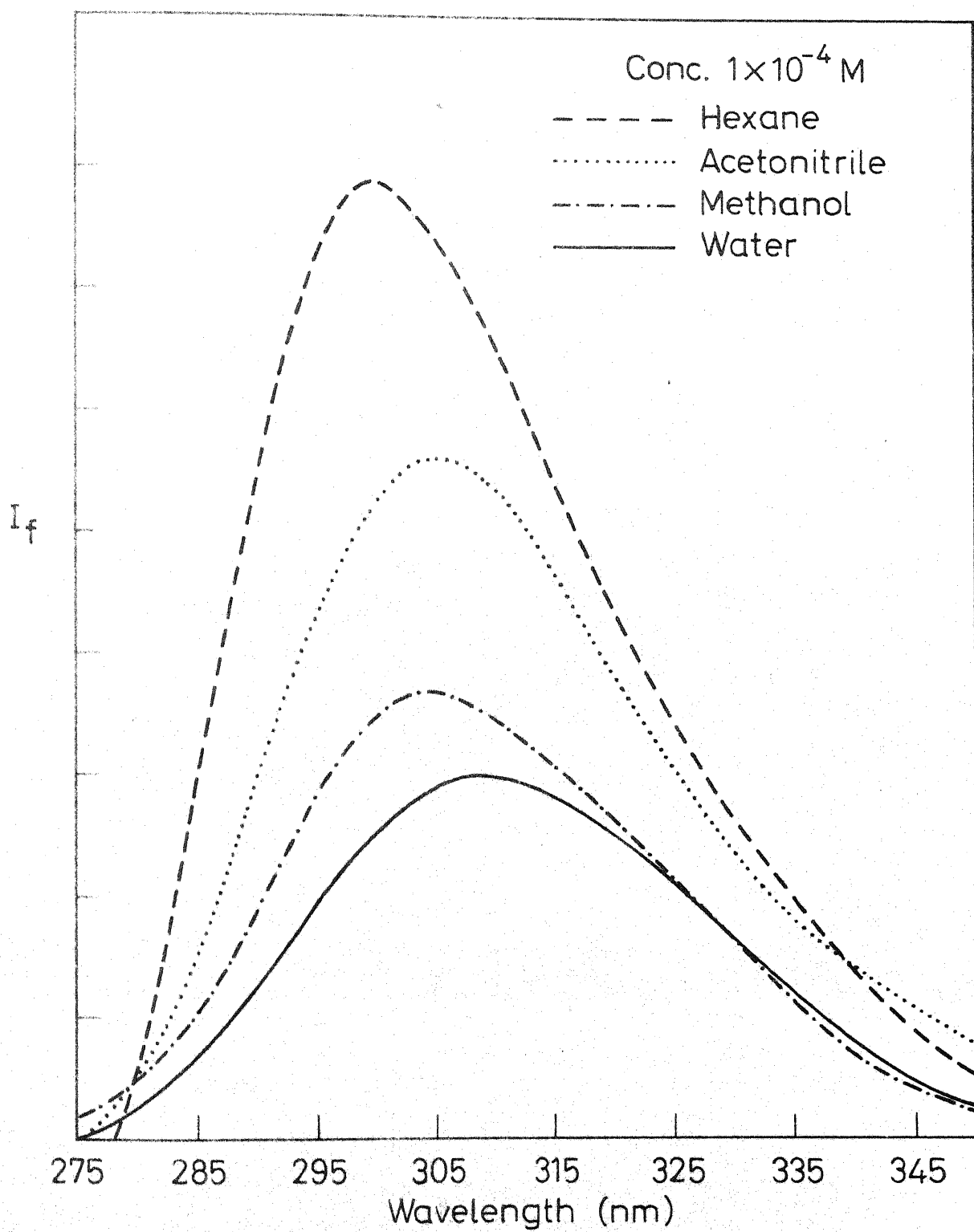
Fig. 5·2 Fluorescence spectra of 1-Phenyl-3,5-dimethylpyrazole
in different solvents.

Conc. 5×10^{-5} M

----- Hexane
··········· Acetonitrile
-·-·-·- Methanol
——— Water
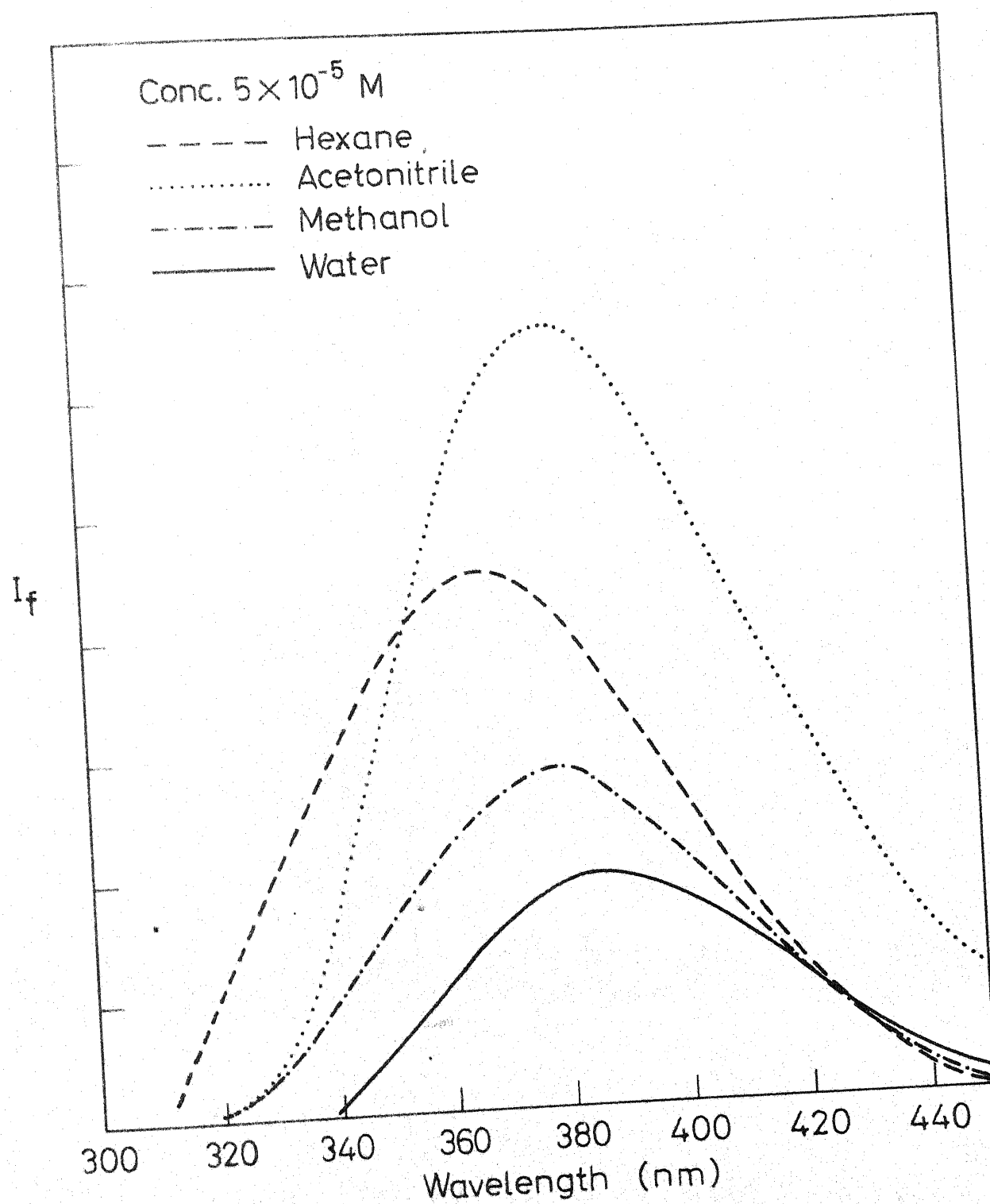
Fig. 5.3 Fluorescence spectra of 1,5-Diphenyl-3-methylpyrazole in different solvents.
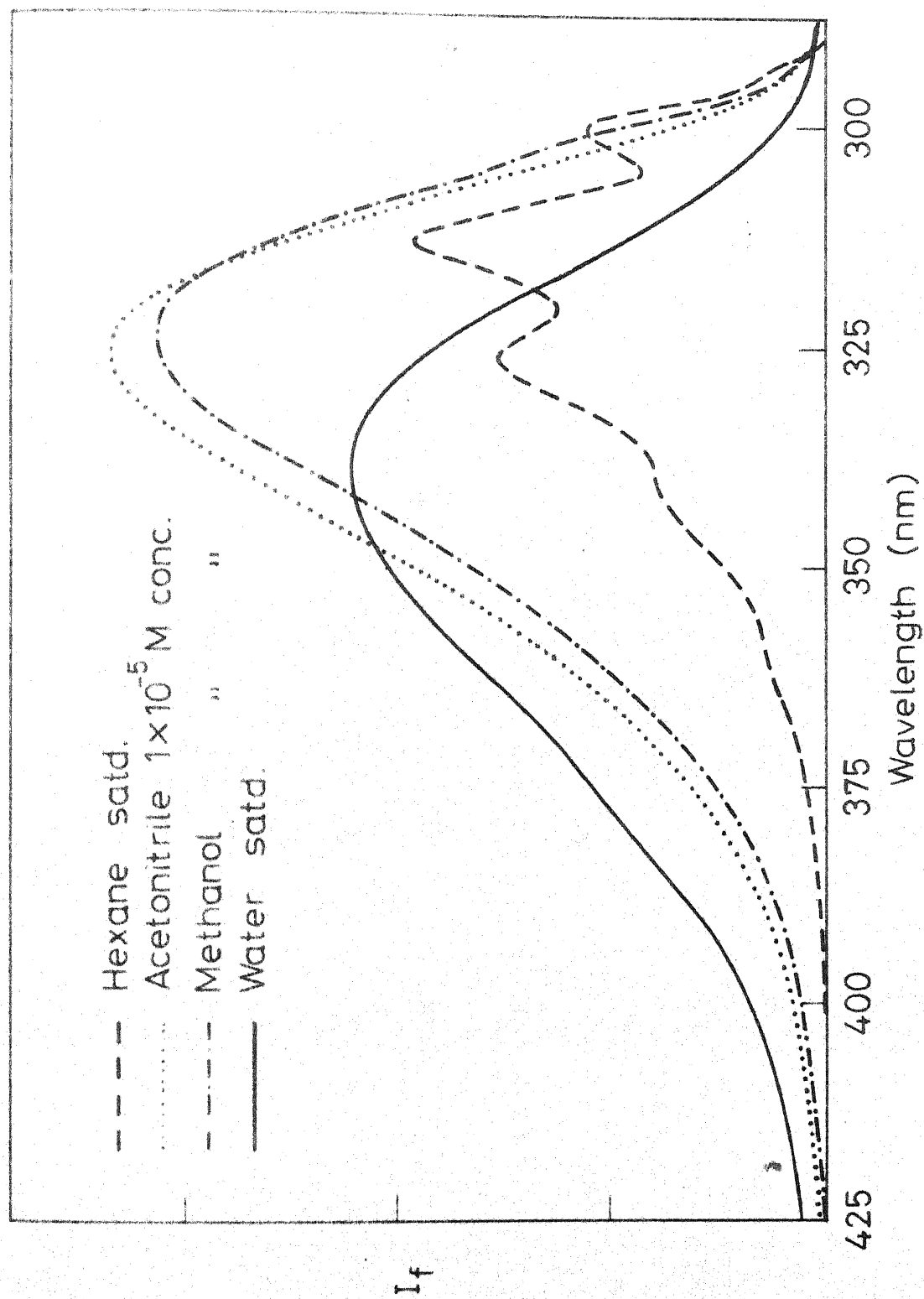
Fig. 5.5 Fluorescence spectra of 3,5-Diphenylpyrazole in different solvents.
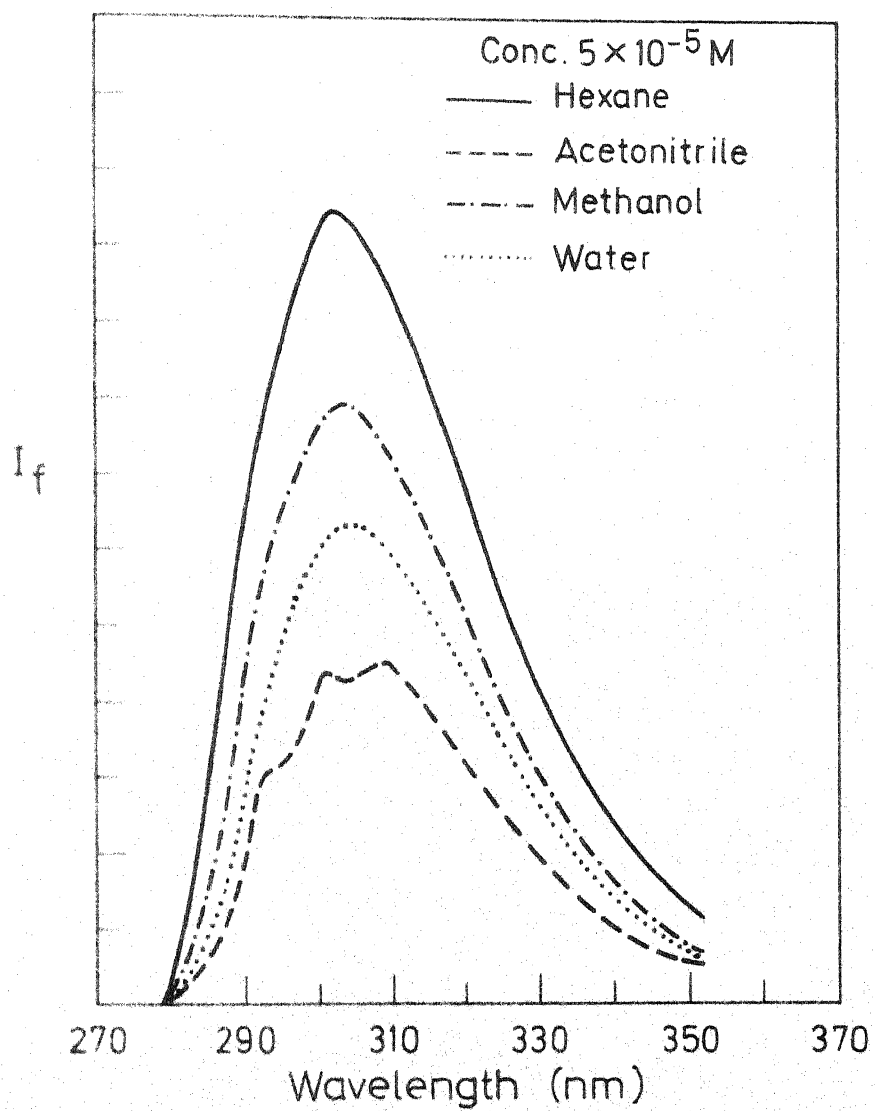
Fig. 5.6 Fluorescence spectra of 3-Methyl-5-phenyl-
pyrazole in different solvents.
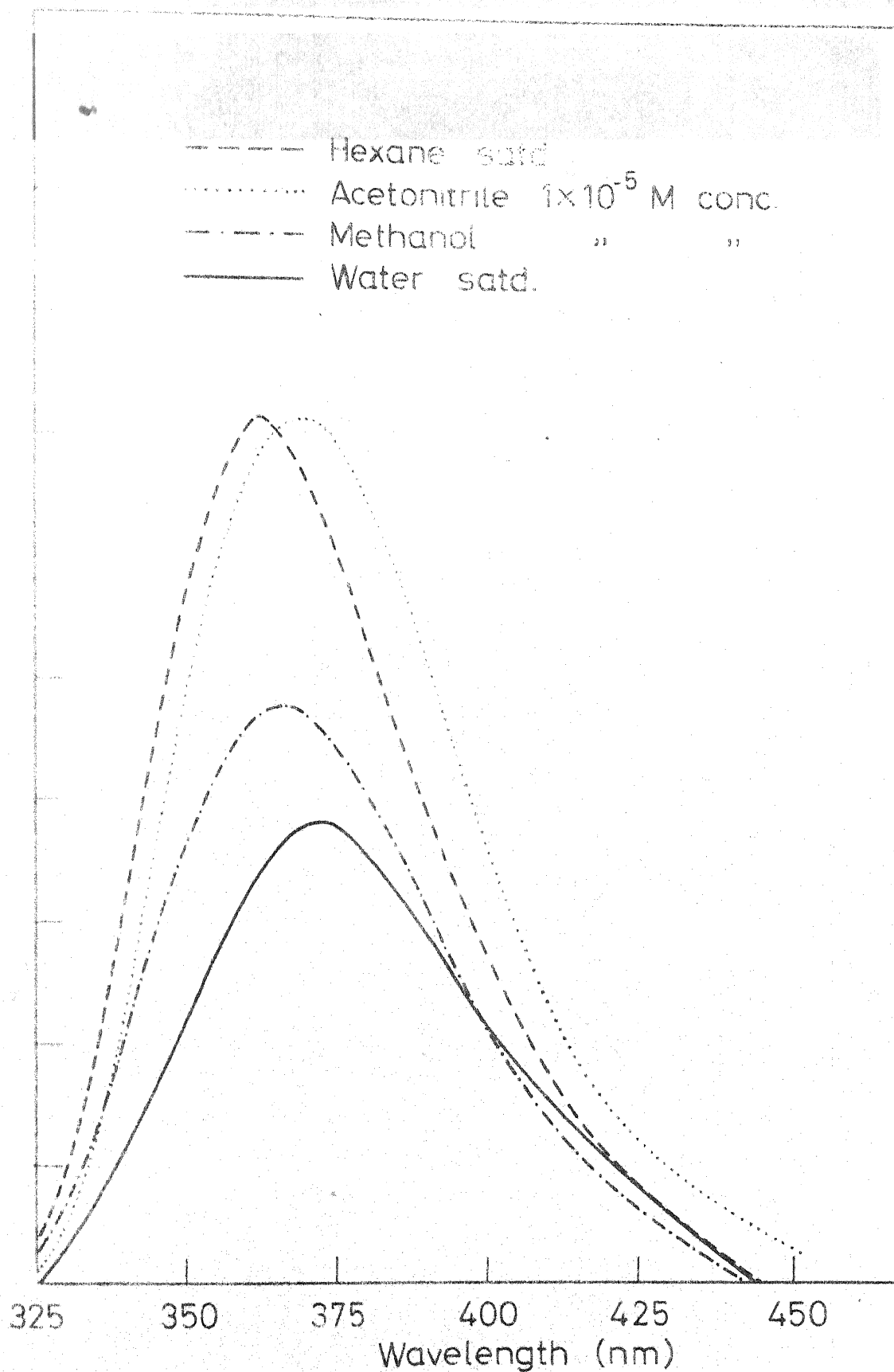
Fig. 5.7 Fluorescence spectra of 4,5-Diphenylimidazole in different solvents.

Table - 5.1

Fluorescence maxima (cm^{-1}) of Pyrazoles and 4,5-Diphenyl-imidazole in different solvents

Compound	Hexane	Acetonitrile	Methanol	Water	Acid medium (cation)	Alkaline medium (anion)
PDP	33388	32786	32786	32414	32051	
DPMP	27173	26315	26315	25806		
TPP	27397	27000	27100	26882		
DPP	33167 31796(m) 30581 29325(s)	30534	30864	29498	28901	27027
MPP	34188(s) 33250 32414(m)	32840	33003	33057	32051	27027
DPI	27510	27210	27247	26881		24813

Fluorescence from pyrazoles and 4,5-diphenylimidazole was observed in all solvents at room temperature. According to Kasha's rule[121], at room temperature the fluorescence is generally observed if $\pi - \pi*$ is the lowest excited singlet state and phosphorescence is the main emission if $n - \pi*$ is the lowest excited singlet state in aromatic compounds. The difference in energy observed between the first excited singlet and triplet states are quite large, i.e., $E_S - E_T$ 9000 cm^{-1}. This difference is much larger than for $n - \pi*$ transitions for which the difference is of the order of 3000-4000 cm^{-1}. These results and earlier results in chapter 4 show that the lowest emitting state in all these solvents is $\pi - \pi*$ singlet.

The $\pi - \pi*$ transition is followed by an increase in dipole moment of the molecule. This increases the electron density at the pyridine nitrogen atom and decreases the electron density at the pyrrolic nitrogen atom. So the solvent interactions at both nitrogen atoms will be strong and will lead to a red shift which is observed for most of our compounds. For MPP the solvent effect is less which is confirmed from its pK_a^* values obtained by the Förster cycle method (Chapter 6). The reason for the blue shift, <u>albeit</u> small in this case is not clear. Furthermore the protonation and deprotonation of MPP lead to only a red shift indicating that hydrogen bonding interactions should also result in a red shift.

a. Fluorescence analysis of TPP[+]

Excited TPP[+] exhibits a very interesting behaviour at 298K. It does not emit in the beginning but starts fluoresçing with a λ_{max} around 403 nm, after the sample is irradiated for a few minutes. The fluorescence intensity increases with irradiation time. Fig. 5.8 shows the change in the fluoresence intensities for different periods of irradiation time. When the light is shut off for a few minutes and again if the solution is irradiated, then a similar behaviour, described above, is observed. Moreover the absorption characteristics of the sample kept under dark for some time after irradiation and those of fresh sample are found to be the same.

Above results suggest that chemical reaction is taking place in the excited state giving rise to a fluorescent product which reverts back to the reactants as soon as the light is shut off. A similar behaviour has been observed in the case of anthraquinone,[134] cis-stilbene[135] and 4,5-diphenylimidazole[136] except that the excited state reaction is irreversible.

The fluorescence maximum of 403 nm, observed at 298K, could not be due to TPP[+] as at 77K it fluoresces with a maximum at 423 nm, which is red shifted as compared to the room temperature maximum. This is contrary to the normal blue shift with lowering of temperature. The fluorescence maximum at 423 nm (which is a broad band) is close to 0-0 band (425 nm) of the phosphorescence
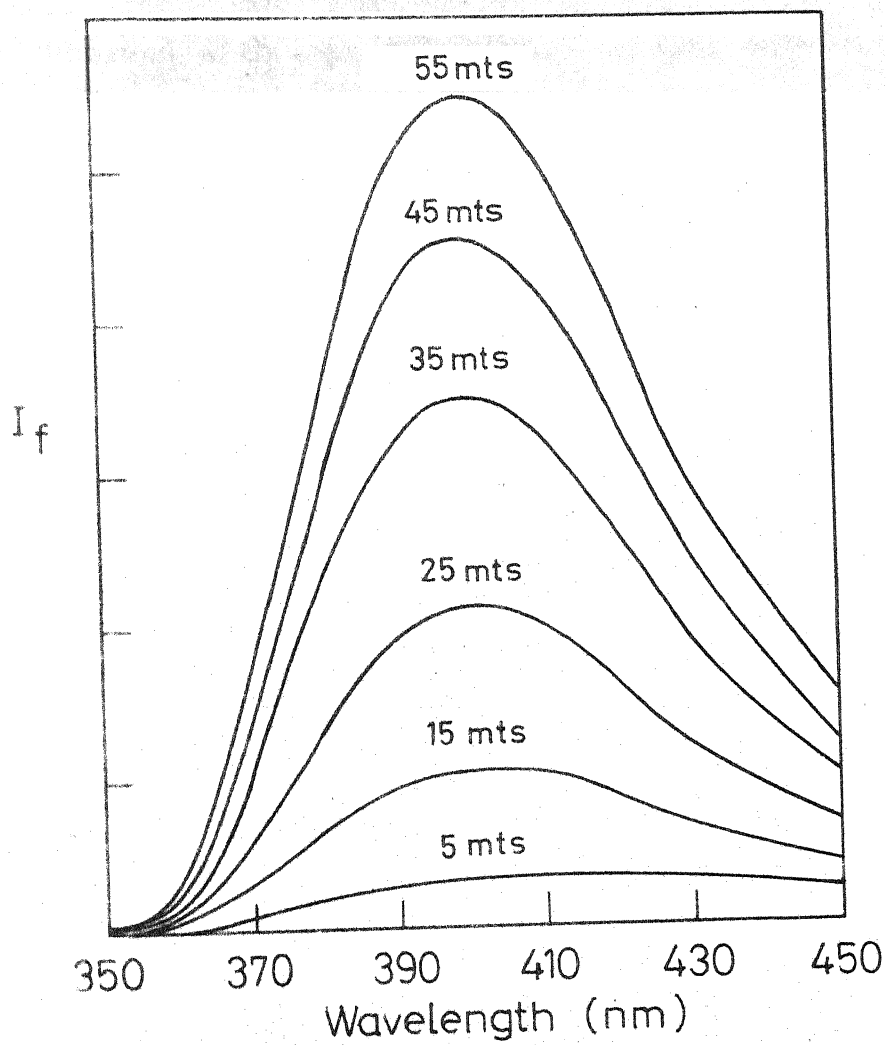
Fig. 5·8 Variation of fluorescence intensity of 1,3,5-Triphenylpyrazole cation with irradiation time.

spectrum. The other peaks of phosphorescence are at 455, 475 (maxima) and 482 nm (fig. 5.21). The λ_{max} at 423 nm is assigned to the fluorescence spectrum because the onset of emission spectra observed with a phosphoroscope starts only from 410 nm whereas the fluorescence at 77K starts from 375 nm. The near degeneracy of singlet and triplet state energy levels suggests that the stabilization of S_1 state by interaction with the solvent is almost equal to the sum of solvent stabilization and spin correlation energies of T_1 state. It is possible that in aqueous or ethanolic solutions, S_1 state is below T_1 state and therefore the fluorescence of TPP^+ could not be detected at a longer wavelength. Similar behaviour has been observed in 6-aminoquinoline[28] cation which fluoresces at 485 nm and phosphoresces at 490 nm at 77K.

b. Fluorimetric analysis of DPMP$^+$

The cation of DPMP does not fluoresce at room temperature even after irradiation for a significant length of time. But at 77K it fluoresces at 445 nm and phosphoresces at 451 nm (fig.5.20) indicating that S_1 and T_1 states are nearly degenerate for DPMP$^+$. This can be explained on the same lines as for TPP$^+$.

c. Nuclear conformation of DPP

A large red shift and loss of vibrational structure in the fluorescence of this compound from a non-polar to a polar

solvent indicates that other than solvent relaxation, the relaxation due to geometry of the molecule is also taking place in the excited state. In order to study this change, absorption and fluorescence spectra of this compound in cyclohexane were plotted in the same graph as shown in fig. 5.9. Both spectra have been normalised to their maxima. The longest wavelength absorption band is centred at 254.5 nm and is broad. The fluorescence spectrum is highly structured and the Stokes shift is substantial (3.6×10^3 cm^{-1}). A broad absorption and a structured fluorescence spectra indicate that the molecule is non-planar in the ground state and it becomes planar in the excited state. Other spectroscopic properties like a blue shift in the absorption maxima and a red shift in the fluorescence maxima with the increase in solvent polarity and a loss of mirror image relationship between the absorption and the fluorescence spectra confirm this conclusion. According to Berlman's classification[24] this molecule appears to be a class-3 molecule,similar to biphenyl.

d. <u>Fluorimetric analysis of MPP and its cation</u>

The absorption spectrum of MPP (fig. 4.7) is broad while the fluorescence spectrum (fig. 5.6) is relatively structured in hexane. In the excited state the phenyl group becomes planar but the vibrational structure observed is less when compared to the DPP molecule and could be due to the
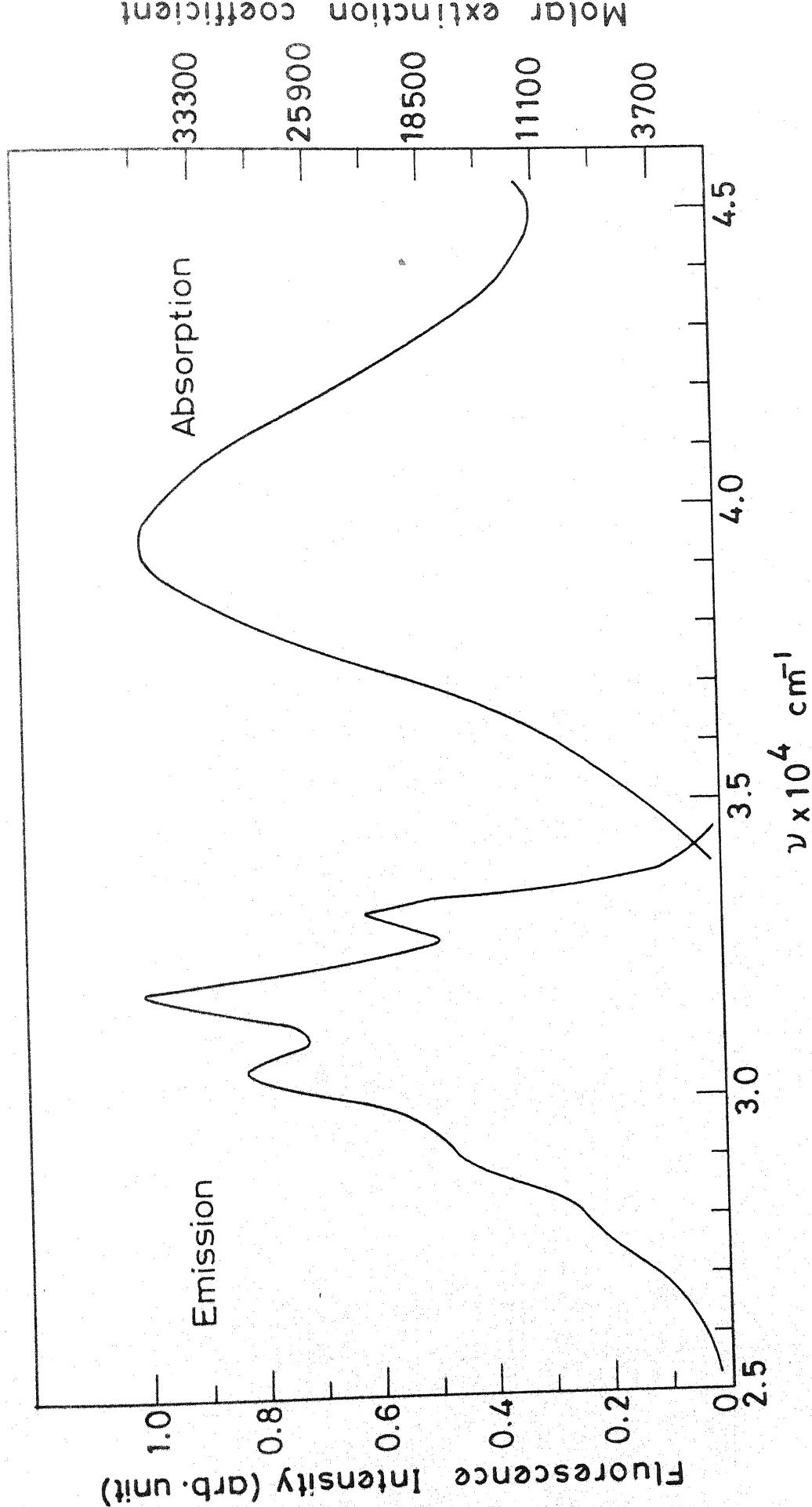
Fig.5.9 Absorption and fluorescence spectra of 3,5-Diphenylpyrazole in cyclohexane

presence of a methyl group. The broadening of fluorescence by
the introduction of a methyl group has also been noticed in
benzene[134]. Since Berlman's classification does not apply to
this kind of molecule, other spectroscopic parameters were not
analysed.

The fluorescence intensity of MPP^+ in hydrochloric acid
is found to be 100 times less than that in sulphuric acid. Also,
in the latter, addition of KCl reduces the fluorescence intensity
as seen from the spectra reported in fig. 5.10 for MPP^+ in H_2SO_4
(H_O= -0.5), HCl (H_O= -0.5) and H_2SO_4- KCl (0.15M) mixture.
However, addition of KCl does not affect the fluorescence
intensity of the neutral species, showing that the fluorescence
of the cation is specifically quenched by the chloride ion. To
ascertain whether the quenching is static or dynamic, low
temperature (77K) spectra of MPP in H_2SO_4 and in H_2SO_4 - KCl
mixture were recorded. As shown in fig. 5.11 there is no
difference in intensity and shape of the spectra for MPP^+ under
two environments mentioned above, except a zero change which was
purposely done for comparison. The absence of quenching effect
at 77K implies that the quenching occurs in the excited state
(dynamic quenching) and not in the ground state (static
quenching).

The above results can be explained on the basis of redox
potential of the anion i.e., higher the redox potential of anion,
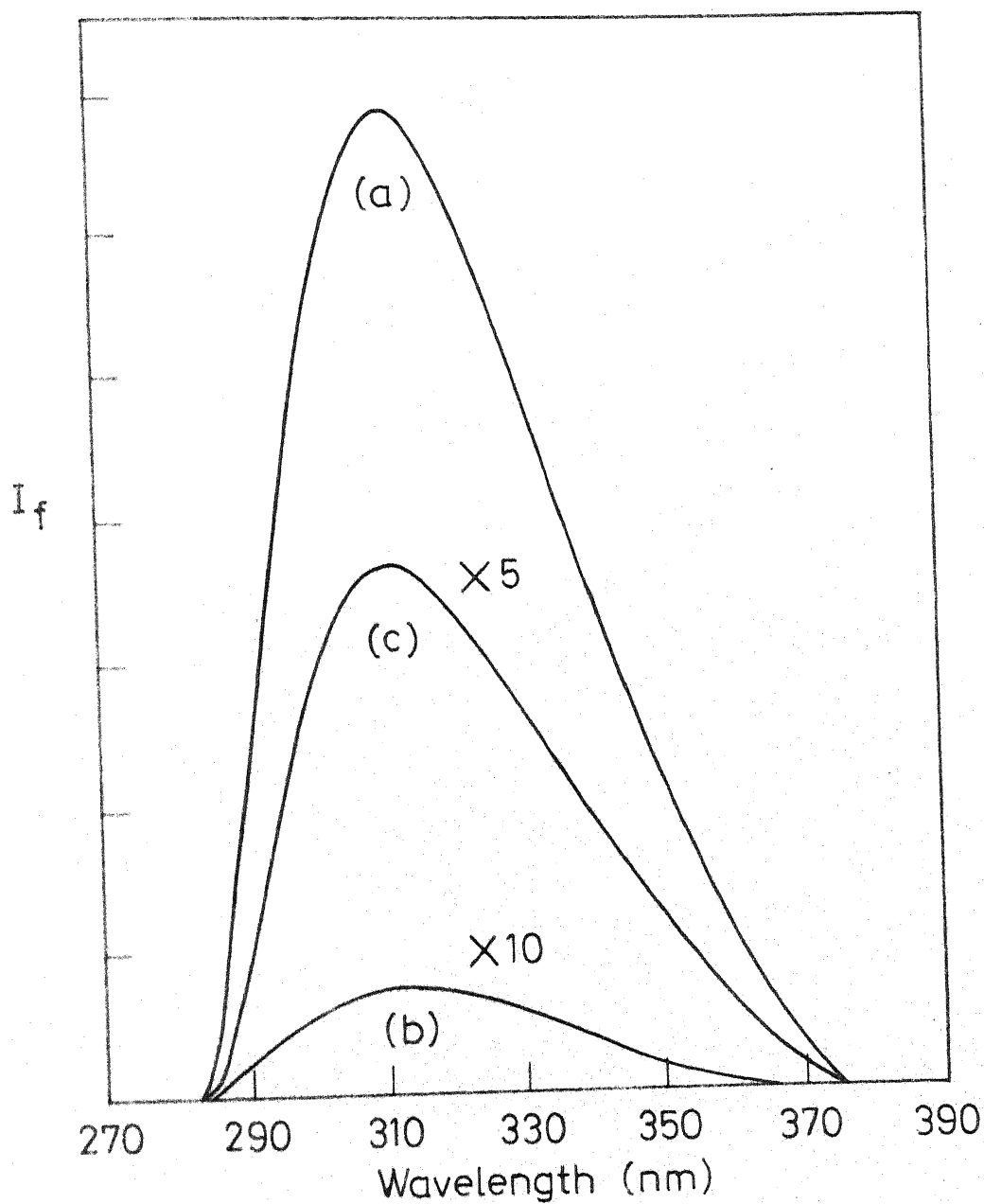
Fig. 5·10 Fluorescence spectra of 3-Methyl-5-phenylpyrazole in (a) H_2SO_4 ($H_0 -0.5$), (b) HCl ($H_0 -0.5$) (c) H_2SO_4 ($H_0 -0.5$) + KCl (0.15 M)
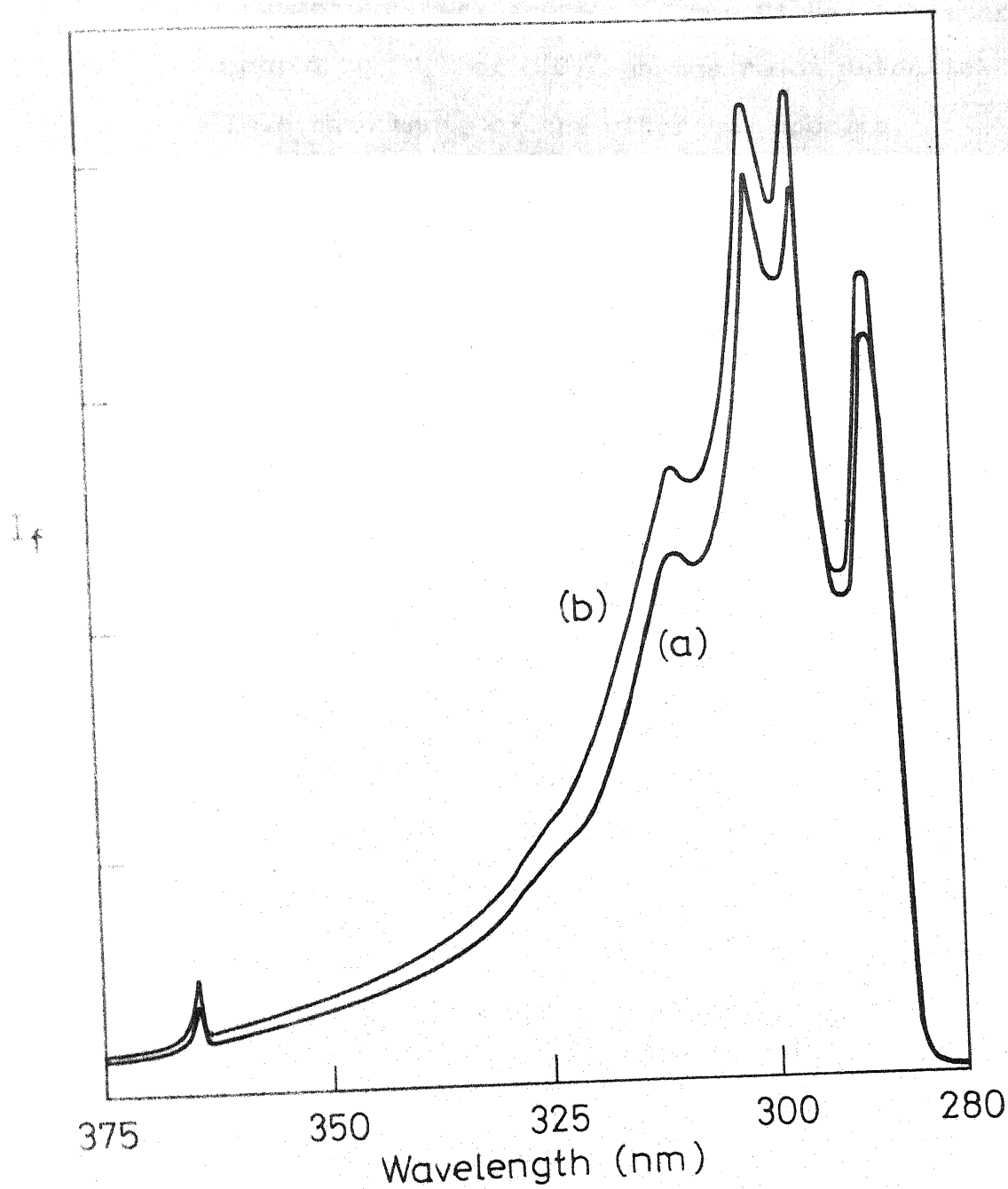
Fig. 5.11 Fluorescence spectra of 3-Methyl-5-phenyl-pyrazole in (a) H_2SO_4 (bottom) at 77 K (b) H_2SO_4 + KCl (top) "

smaller is its quenching cross section. Thus Cl^- is a better quencher as compared to SO_4^{2-} or ClO_4^- as the redox potential of the Cl^- is less than those of the other two species.[133]

e. Fluorimetric analysis of DPI and its cation

DPI on photoexcitation undergoes a reaction leading to the formation of PI in all solvents. The fluorescence of the latter, formed during the irradiation of DPI in ethanol, has one more peak at 394.5 nm in addition to the two reported[136], at 358 and 375 nm. This has been confirmed with the fluorescence spectra of an authentic sample.

The DPI^+ does not emit in the beginning at 298K, as in TPP^+, but a few seconds later DPI^+ starts fluorescing and fluorescence intensity keeps on increasing with the irradiation time as shown in fig. 5.12. The fluorescence spectrum resembles that of PI^+, which is confirmed by the fluorescence of PI in acid solution. Though the quantum yield of formation of PI from DPI in acid medium has not been measured, it appears to be higher than that in neutral medium.

The photochemistry of cis-stilbene[135] and DPI[136] suggests that two phenyl rings must be in the same plane before cyclisation takes place. This is confirmed from the present study at low temperature. At room temperature a solution of DPI fluoresces with the characteristics of DPI and PI while DPI^+ shows only the
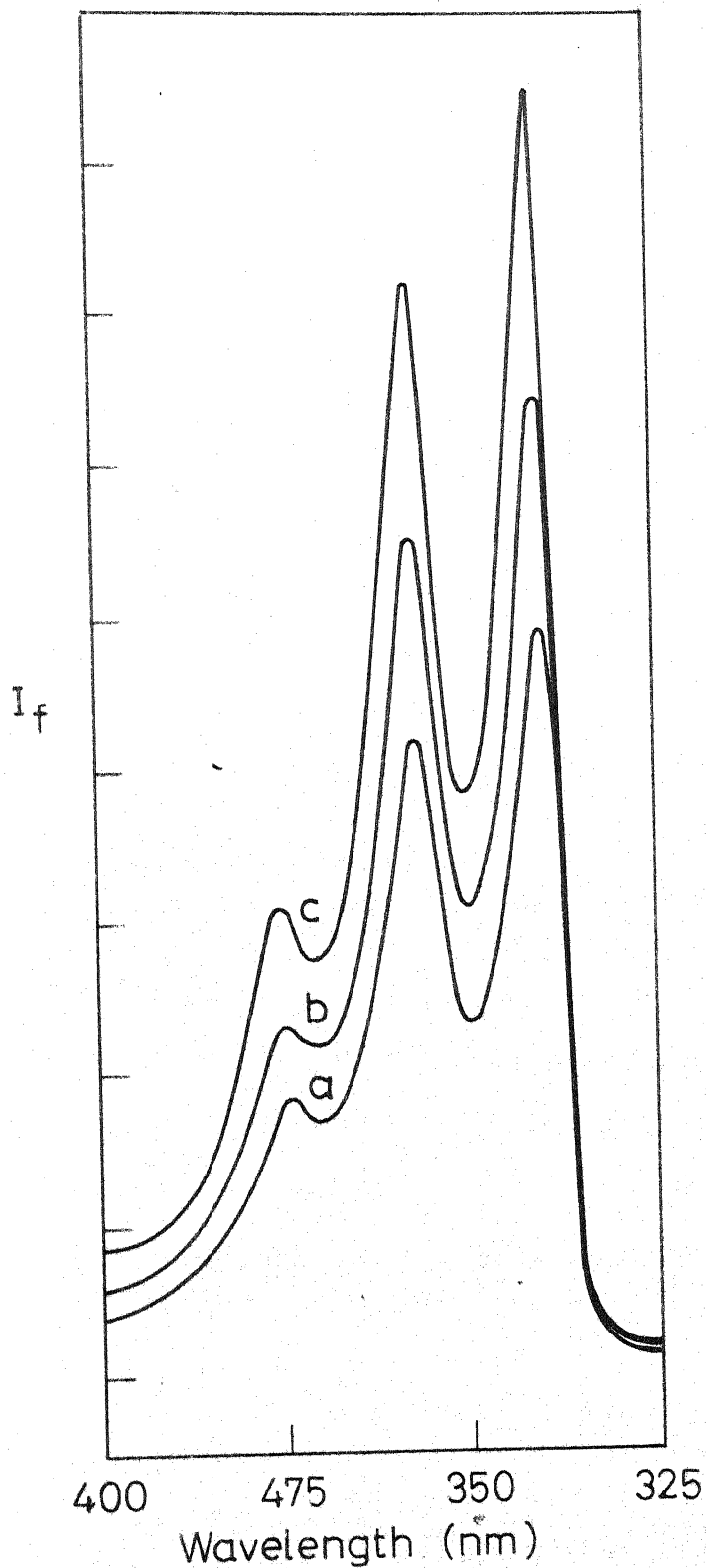
Fig. 5·12 Variation of fluorescence intensity of 4,5-Diphenylimidazole cation with irradiation time. a = 1minute, b = 6minutes, c = 11minutes

fluorescence of PI^+. At 77K, on the other hand DPI in neutral and acidic medium (i.e., DPI^+) gives the fluorescence of DPI and DPI^+ (fig. 5.13) respectively, indicating that there is no formation of PI at low temperature. These results show that at 298K the two phenyl rings in DPI and its cation attain planarity upon excitation leading to cyclisation. But at 77K, even in the excited state, the molecule is retained in the ground state configuration and so the two phenyl rings are unable to come to the same plane because of the rigidity of the medium. That is why no ring closure takes place at 77K.

5.3. Hydrogen bonding Interactions

The compounds discussed below are highly polar and therefore they behave either as hydrogen donors or acceptors in solution. Since solutions of equal concentration could not be prepared due to poor solubility of these compounds in some solvents, we discuss only the shifts in λ_{max} in terms of the nature and site of hydrogen bonding interactions.

5.3.1. 9,10-Phenanthroimidazole

The fluorescence spectra of PI in different solvents are shown in fig. 5.14. Values of λ_{max} for neutral, cationic and anionic species are listed in Table 5.2. When compared to the spectrum in hexane, spectra in other solvents are broader and the maxima are red shifted. The maxima in methanol and water

(a)

(b)

Wavelength (nm)
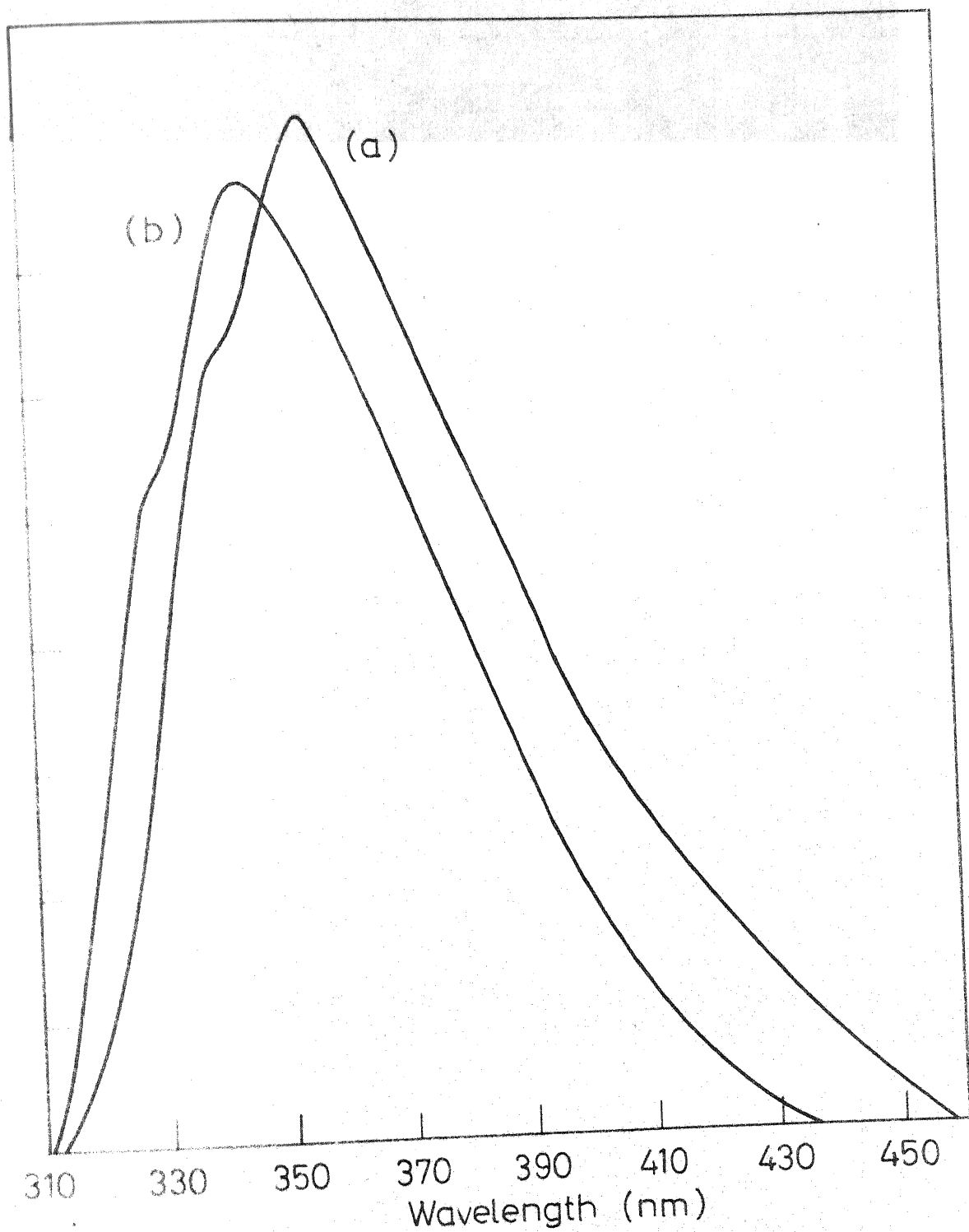
Fig. 5.13 Fluorescence spectra of 4,5-Diphenylimidazole at 77 K. (a) Neutral form (b) Cation
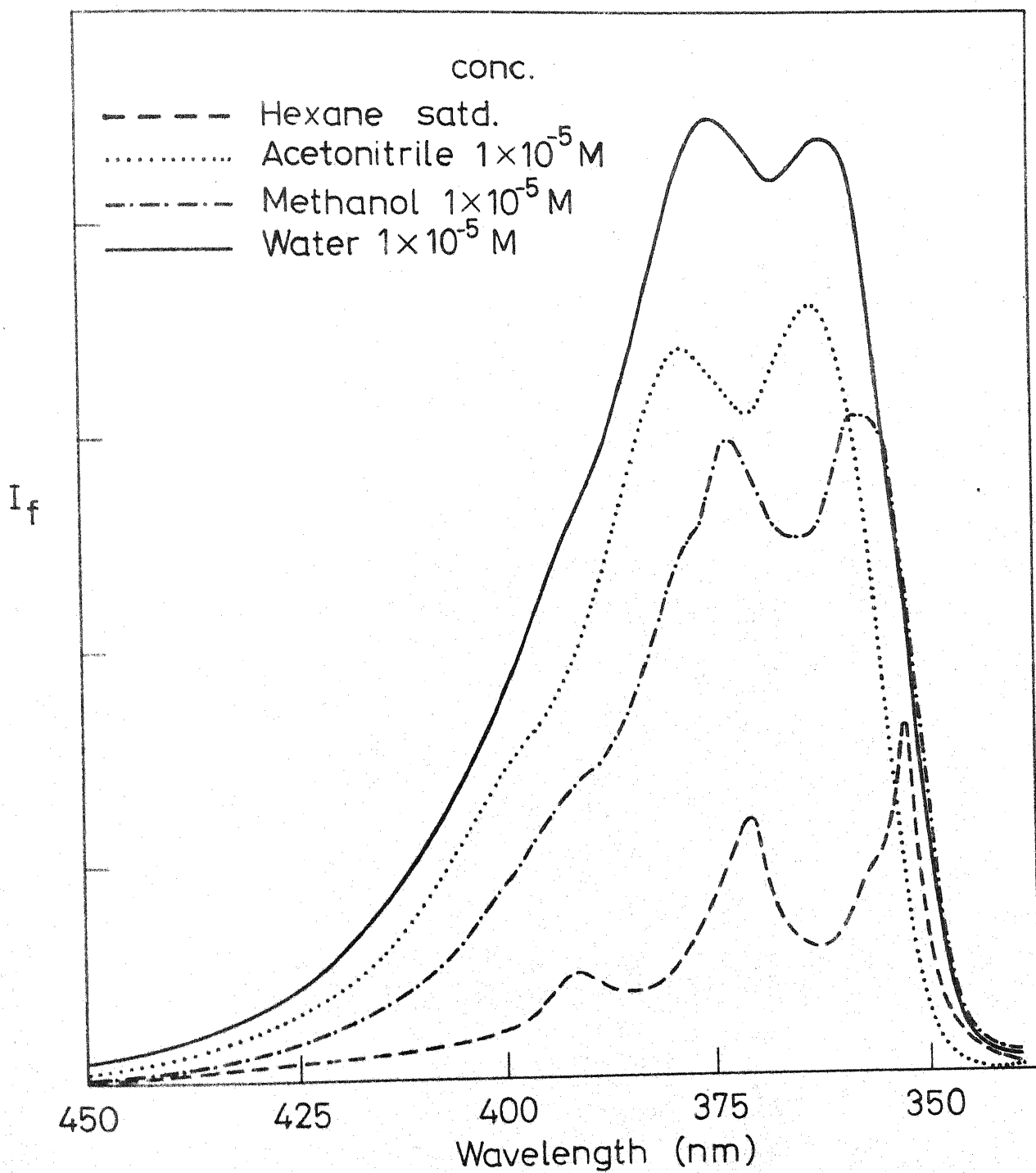
Fig. 5.14 Fluorescence spectra of 9,10-Phenanthroimidazole in different solvents.

Table - 5.2

Fluorescence maxima (cm^{-1}) of PI, AMP, HP, AI and Indazole
in different solvents

Compound	Hexane	Acetonitrile	Methanol	Water	Acid medium (Mono-cation)	Alkaline medium (anion)
PI	28368	27548	28011	27777	29455	24360
	26990	26455	26845	26667	28090	
	25510	25031	25380		26667	
AMP	25974	23201	22675	22421		
	24691					
HP	28449					
	27855	27397	27359	25974^{a}		
	27472			20833^{b}	25974^{a}	20833
					(H_o -0.5)	
	27063					
	26455(m)	26281(m)	26109			
	25000(s)					
AI	27210	25806	24937	24449	19801	
Indazole	33783	33557	33500	33333		
	32573	32414	32362	32154		
	31948	31645	31446	31397		

a) For neutral form

b) For anion

are blue shifted relative to that in acetonitrile and it is larger
in the case of methanol. The blue shift becomes maximum in
acid medium in which PI^+ is formed.

The hydrogen bonding interactions on pyrrolic nitrogen
atom always give rise to red shift and so the irregular shifts
observed can be explained by the charge transfer interaction of
the lone pair on the pyridinic nitrogen atom with the ring.
Since in this case charge migration takes place from pyridinic
nitrogen atom to phenanthrene moiety (see chapter 4),hydrogen
acceptor interaction leads to red shift and hydrogen donor
interaction leads to blue shift. The large red shift observed
in acetonitrile relative to hexane is due to dispersive intera-
ction and its hydrogen accepting nature. The red shift in
methanol and water relative to hexane and blue shift relative
to acetonitrile show that in addition to the dispersive
interaction and hydrogen acceptor tendency, they exhibit hydrogen
donating capability. The difference in the shifts for methanol
and water is due to the difference in their hydrogen donor/
acceptor ability. The magnitude of each interaction can not be
determined from our study. But qualitatively one can say that
water is acting here as poor hydrogen donor as compared to
methanol and its hydrogen acceptor interaction with pyrrolic
hydrogen atom may be stronger than that in methanol. A similar
behaviour has been observed in the absorption spectra of different

isomeric aminoquinolines on going from hexane → ethanol → water, i.e., site of hydrogen bond formation is at different atoms in different solvents. The maximum blue shift observed in an acidic medium wherein the lone pair is completely prevented from charge transfer interaction also indicates that a blue shift should be observed during hydrogen donor interaction. A similar behaviour has been observed in benzimidazole.[128]

These results clearly show that even though the lone pair is at one of the sp^2 hybrid orbitals, the π cloud of the ring is perturbed significantly by it. Indazole does not show this behaviour because the pyridinic nitrogen atom in indazole is close to another electronegative nitrogen atom and also it is separated from the ring by a carbon/nitrogen atom.

5.3.2. 9-Aminophenanthrene

A regular red shift is observed in the fluorescence spectrum of AMP as the solvent is changed from hexane to water. The spectra are shown in fig. 5.15 and the λ_{max} values are listed in Table 5.2. Our results in hexane agree with those of Tsutsumi et.al. [129]. The spectrum is structured in hexane and it becomes broad in other solvents. The red shift observed in the fluorescence spectra is contrary to the blue shift observed in the absorption spectra (see Table 4.2).

Conc. = 1×10^{-5} M

- - - - Hexane
.... Acetonitrile
-.-..-.- Methanol
——— Water

I_f

Wavelength (nm).
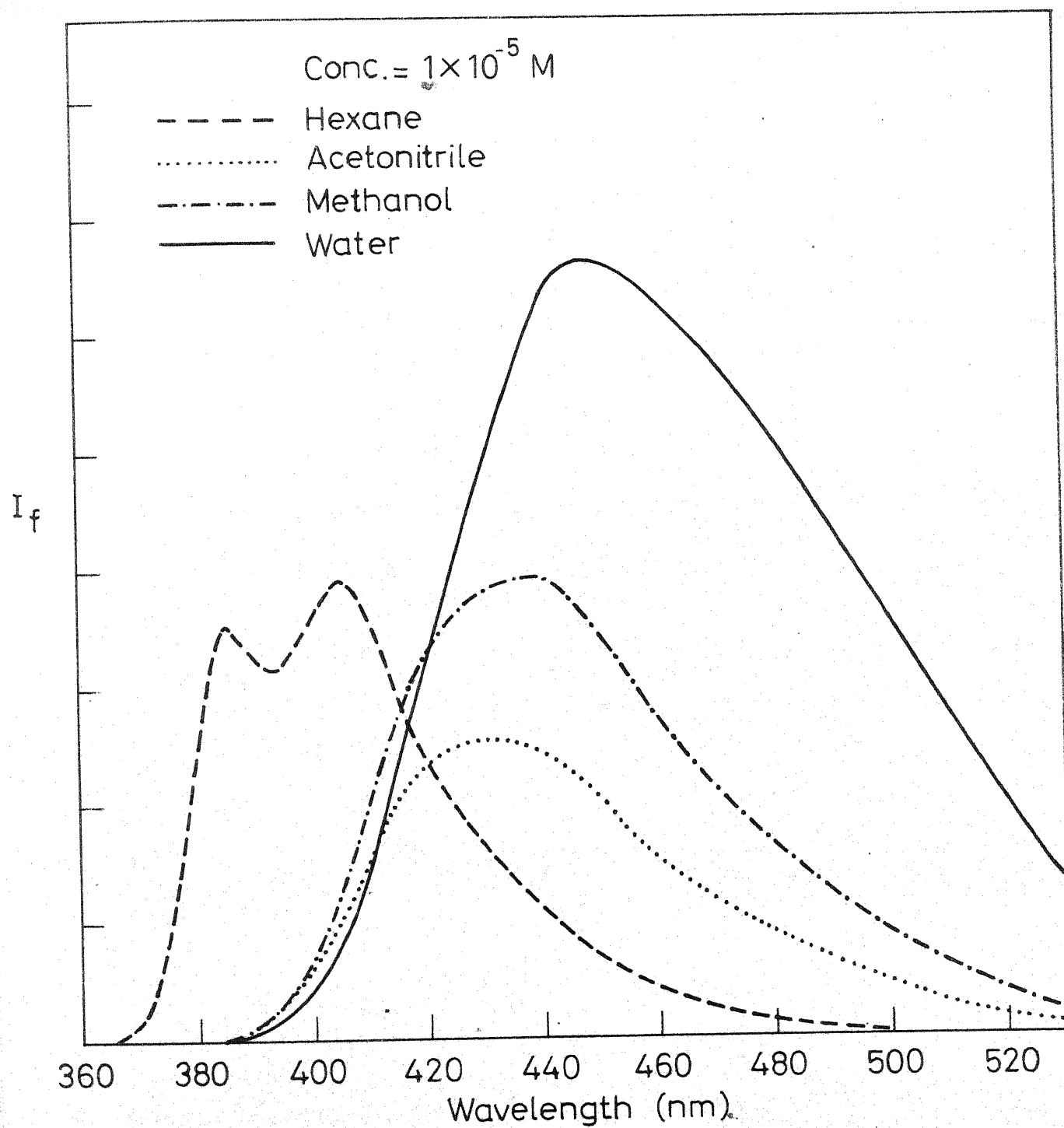
5.15 Fluorescence spectra of 9-Aminophenanthrene in different solvents.

In AMP the solvent interaction can take place either at the lone pair of the nitrogen atom or at the hydrogen atom of the amino group. The blue shift in the absorption spectra in methanol relative to hexane shows that only hydrogen donor interaction of the solvent is taking place with the lone pair on the amino nitrogen atom. Acetonitrile, being a polar and a hydrogen acceptor solvent, has no effect on the absorption spectra, indicating that hydrogen donor interaction of the solvent is predominant over the dispersive interaction in the ground state. But the red shift in the fluorescence spectrum from hexane to water, according to their hydrogen acceptor capability, shows that in the excited state, the hydrogen atom of the amino group interacts with the lone pair of the solvent. This is reasonable because in the excited state the availability of the lone pair is largely reduced by a greater charge transfer interaction of the amino group with the ring and thus reducing the charge density at the nitrogen atom of the amino group. This is also confirmed by the less basic or more acidic nature of the amino group (chapter 6).

5.3.3. 9-Hydroxyphenanthrene

This compound is an example involving hydrogen acceptor interaction between solvent and solute. Fig. 5.16 shows the fluorescence spectra of HP in different solvents and Table 5.2 reports their λ_{max}. The spectra are red shifted and become

Conc. = 1×10^{-5} M

— — — Hexane
· · · · · · · · Acetonitrile
— · — · — Methanol
———— Acid solution (H_0 -0.5)

I_f

Wavelength (nm)
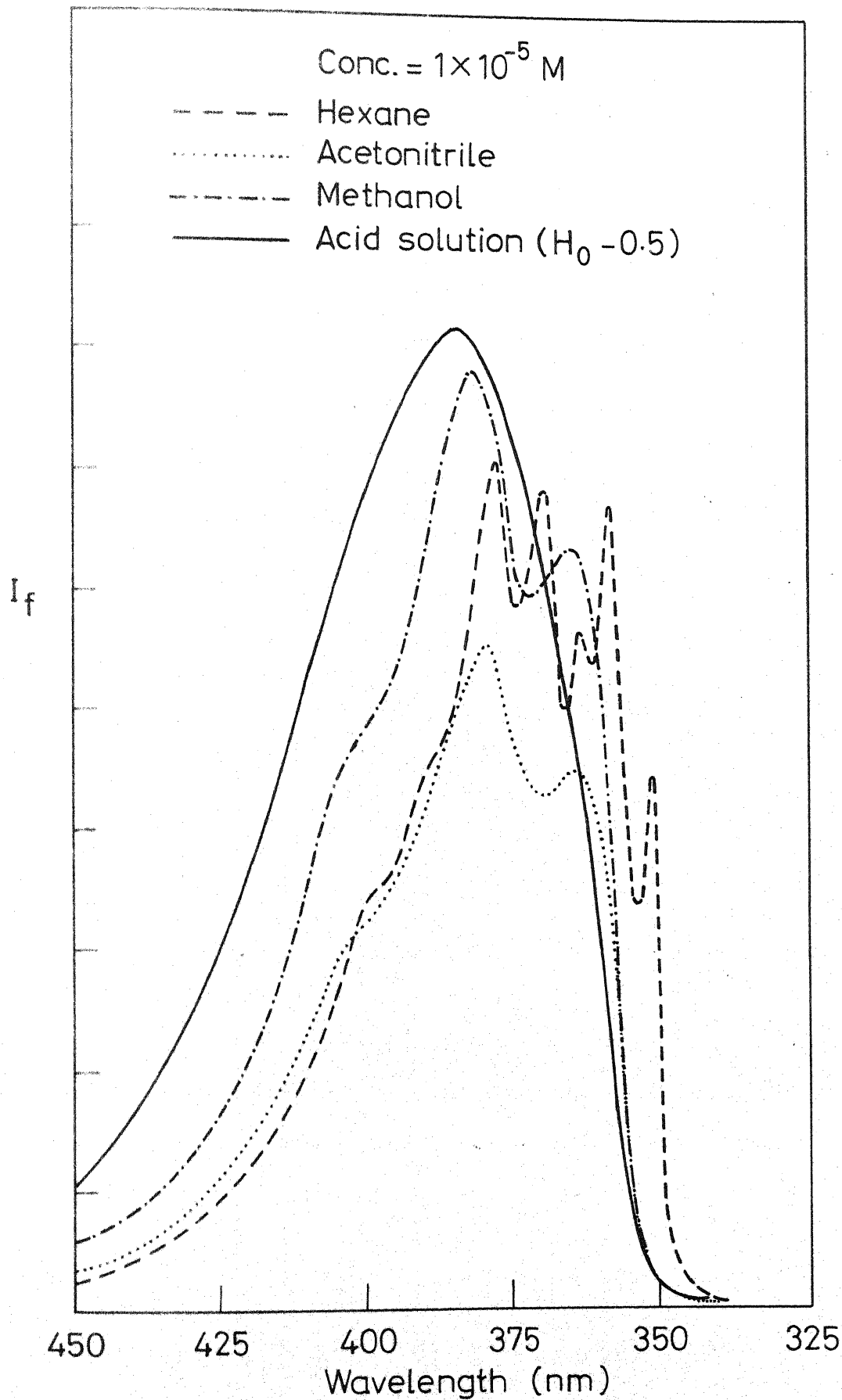
5.16 Fluorescence spectra of 9-Hydroxyphenanthrene in different solvents.

broader with an increase in the hydrogen acceptor ability of the solvent. Deprotonation results in a further red shift. This is in accordance with the solvent shift, confirming the hydrogen acceptor interaction of the solvent with the solute. In this molecule the site of interaction is found to be the same in the excited as well as the ground state.

5.3.4. 5-Aminoindazole

Fluorescence spectra of this compound in different solvents are shown in fig. 5.17 and the λ_{max} are given in Table 5.2. Similar to AMP, a blue shift in the absorption and red shift in fluorescence relative to the respective spectra in hexane are observed. Moreover the red shifts observed here are much more than the red shifts noticed in indazole. (Table 5.2).

Although AI is similar to PI and isomeric aminoquinolines in having more than one site of hydrogen bonding, the spectral behaviour of AI is different from others. Irregular shifts have been observed in PI (5.3.1) and aminoquinolines due to the change in the site of hydrogen bonding in methanol and water whereas a regular blue shift in absorption and a regular red shift in fluorescence with increasing solvent polarity are observed in AI. This clearly indicates that in both states solvent interacts only with the amino group of the solute.
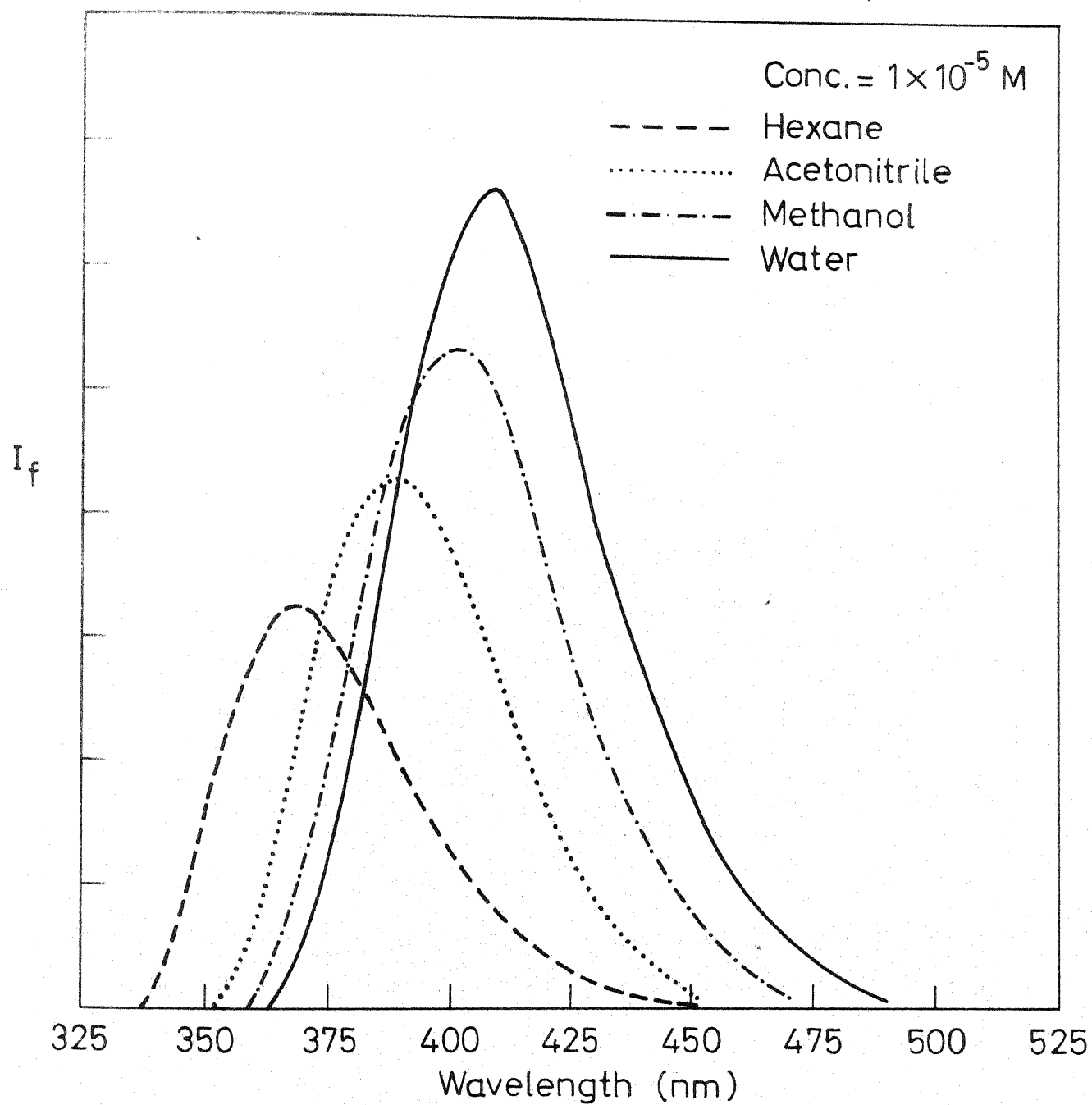
5.17 Fluorescence spectra of 5-Aminoindazole in different solvents.

Also the solvent effect has been proved to be much more useful in determining the site of protonation in the ground as well as the excited state. When pH is decreased from 7, at 5.2 protonation occurs leading to a blue shift in the absorption spectrum. Since the blue shift is characteristic of hydrogen donor interaction of the solvent <u>with lone pair on the amino nitrogen,</u> protonation should have occured at the amino nitrogen and not at the ring nitrogen atom in the ground state. On the other hand when pH is decreased below 2, fluorescence maximum gets red shifted after protonation. The red shift is characteristic of hydrogen donor interaction of the solvent <u>with the ring nitrogen atom</u> and so the red shift in fluorescence shows that protonation in the excited state might have occured at the ring nitrogen atom. The red shift noticed in indazole fluorescence on protonation also confirms this conclusion.[142]

A comparison of the fluorescence maxima in hexane and methanol shows that the red shift in methanol relative to hexane is quite large, suggesting that the hydrogen bond between the solute and the solvent is very strong and may actually result in a stoichiometric complex (exciplex) between the excited solute and the solvent molecule. To confirm this, fluorescence spectra of heptane solutions with fixed amounts of ethanol were recorded. It was found that addition of ethanol upto 3% (V/V) resulted in a red shift of 1550 cm^{-1} whereas further addition upto 100% resulted in a gradual red shift of only another 730 cm^{-1}.

The fluorescence of AI is at longer wavelength and is more intense that that of indazole. These results are similar to those observed for quinolines[54] with an amino substituent in the homocyclic ring. Quinoline with the amino substituent in the homocyclic ring showed fluorescence at longer wavelength than quinoline with the amino substituent in the heterocyclic ring. In these compounds the charge is transferred from homocyclic ring to the heterocyclic ring in the lowest excited state. Hence electron donating substituents in heterocyclic ring tend to reduce the excited state dipole,while the ones present in the homocyclic ring tend to/increase it with respect to the ground state. Though enough fluorescence data are not available for different isomers of aminoindazole, above finding would be of much help in the identification of products formed in reactions where several isomers are produced, as has been done for aminoquinoline isomers.

5.4. Low temperature fluorescence studies

The low temperature (77K) fluorescence of PDP, DPMP, TPP, DPP and MPP was recorded in hexane and aqueous methanol solution. The fluorescence maxima for the neutral as well as the cationic and anionic species at 77K are given in Table 5.3. We note the following general features :

In all the compounds the fluorescence maxima in both the solvents are blue shifted at 77K in comparison to their maxima at room temperature. But the maxima in hexane at 77K are red

shifted in comparison to the maxima in aqueous methanol. The λ_{max} for the cation is blue shifted in PDP but red shifted for other compounds. The maxima of TPP and DPMP cations are largely red shifted and are very close to their phosphorescence maxima. The reason for this was discussed in chapter 5.3. Fluorescence maxima of the anions of DPP and MPP are red shifted to the maxima of the neutral species. The fluorescence spectra of DPP and MPP are nicely structured and a vibrational analysis was carried out.

a. 3,5-Diphenylpyrazole

The low temperature fluorescence spectrum of DPP in hexane, shown in fig. 5.18, is more structured than that in 20% methanol-water mixture. The spacing between peaks are nearly constant and is represented by a simple vibrational mode of frequency 1460 cm^{-1}. The shortest wavelength band at 33613 cm^{-1} has been assigned as the 0-0 band. This frequency (1460 cm^{-1}) could be assigned to the ring streching mode of the heterocyclic ring.[143-145] The IR spectrum of DPP in KBr pellet, recorded in our laboratory[128], shows that intensity of these modes are quite large.

b. 3-Methyl-5-phenylpyrazole

Since the compound was poorly soluble in hexane the resolution of the fluorescence spectrum at 77K was very poor due
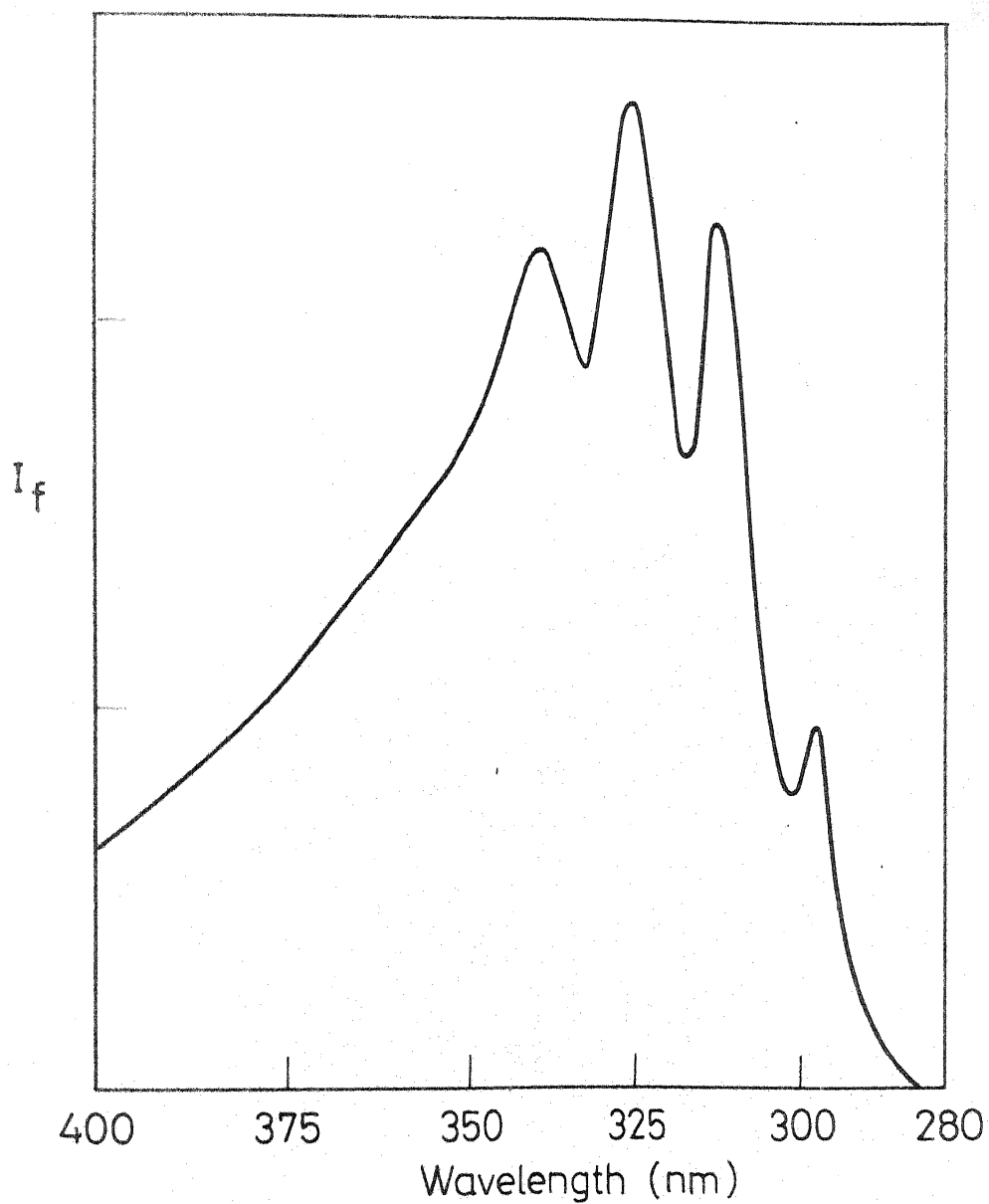
Fig. 5·18 Fluorescence spectrum of 3,5-Diphenylpyrazole in hexane at 77 K.

Table – 5.3

Low-temperature fluorescence maxima (cm^{-1}) and the results of vibrational analysis

Compound	Neutral form		$\Delta \bar{\nu}$	Assignment	Cation	Anion
	Hexane	MeOH/H_2O				
PDP	34482	35523 34364(m) 33222			35335	
DPMP	27211	28409(m) 26737			24721 22471(m)	
TPP	27586	27972			23640	
DPP	33613 32514 30769(m) 29240	34188 33003(m) 32128 30349	1459 2844 4373	1460 1460x2 = 2920 1460x3 = 4380	31746 28612(m)	32258 30769(m) 29850
MPP	32895	34904 34305 34042 33472(m) 33112 32573 32154	599 862 1432 1792 2331 2750	580 870 580+870= 1450 870x2 = 1740 870x2 + 580 = 2320 870x3 = 2610	34782 33783 33444(m) 32310	31007

to low signal to noise ratio. But a good low temperature spectrum was obtained in 20% methanol-water solution (fig. 6.8). Vibrational features of the fluorescence spectrum of MPP in aqueous methanol is more complicated than that of DPP at 77K. The main vibrational progression seems to be of 870 cm^{-1} whereas 580 cm^{-1} vibrational frequency occurs as combination bands. The shortest wavelength band at 34904 cm^{-1} is assigned as the 0-0 band.

The blue shift, observed at low temperature relative to the room temperature maxima for all the compounds, results from the fact that solvent reorientation after excitation is considerably less facile in a rigid medium than in fluid medium. This "low temperature blue shift" was reported to be an effect of viscosity, rather than temperature. This conclusion was based on the observation of very similar blue shifts (relative to solution spectra) in the room temperature fluorescence of aromatic compounds in plastic matrices.[141] At 77K the blue/red shifts observed between hexane and aqueous methanol and also between neutral and cation/anionic forms of the compounds follow exactly the same trend observed in the absorption spectra reiterating that the ground state configuration of the solvent is retained in the excited state before fluorescing.

5.5. <u>Low temperature phosphorescence studies</u>

Phosphorescence spectra of different forms of pyrazoles, DPI, PI, HP were recorded at 77K and are shown in figs. 5.19 - 5.26. For most of the compounds the spectra are structured and so a vibrational analysis was carried out for these compounds. The λ_{max} and the results of the vibrational analysis for these compounds are given in Table 5.4. All the spectra **were recorded** in aqueous methanol and all solutions were deaerated before taking the spectrum by passing oxygen-free nitrogen. The band maxima of the different forms were also used in the calculation of pK_T^* values and they are presented in the next chapter. Phosphorescence spectra for all pyrazoles in hexane were also recorded.

5.5.1. <u>Pyrazoles</u>

Phosphorescence spectrum of PDP is more structured in methanol/water mixture than in hexane at 77K (fig. 5.19). The λ_{max} in aqueous methanol is blue shifted when compared to that in hexane.

Contrary to the fluorescence spectrum the phosphorescence spectrum of DPMP at 77K in 50% aqueous methanol is structured with a maximum at 21390 cm^{-1} (fig. 5.20). The phosphorescence spectrum in hexane in less structured. It appears that in aqueous methanol 1495 cm^{-1} vibrational band forms a main

progression whereas 755 cm^{-1} band occurs as a combination band. Phosphorescence spectrum of the DPMP cation is relatively broad.

Phosphorescence spectra of TPP in hexane and 50% methanol are structured at 77K (fig. 5.21) but the spectrum in hexane does not show any regularity in the vibrational analysis. In aqueous methanol 1492 cm^{-1} vibrational mode forms a main progression whereas 505 cm^{-1} and 841 cm^{-1} occur as combination bands.

Similar to the fluorescence spectrum the phosphorescence spectrum of DPP in hexane and in 20% methanol-water mixture at 77K are structured (fig. 5.22). The peaks in aqueous methanol are somewhat sharper than those in hexane and each peak in the latter is red shifted in comparison to the peaks in the former. Vibrational analysis shows that phosphorescence spectra in both solvents can be explained with a single vibrational mode of frequency 1460 cm^{-1}. The 0-0 band in hexane and aqueous methanol are found to be 23392 cm^{-1} and 23809 cm^{-1} respectively. Peaks of phosphorescence spectrum of DPP^{+} are broader than those of the anion as well as of the neutral species but the separation of peaks in both cases can be explained with a vibrational mode of frequency 1405 cm^{-1}.

Phosphorescence spectra of MPP and its cation are more structured than that of the anion (fig. 5.23). The phosphorescence peaks of MPP in hexane are not sharp but each peak is red shifted as compared to polar solvents. The 0-0 bands of MPP, MPP cation
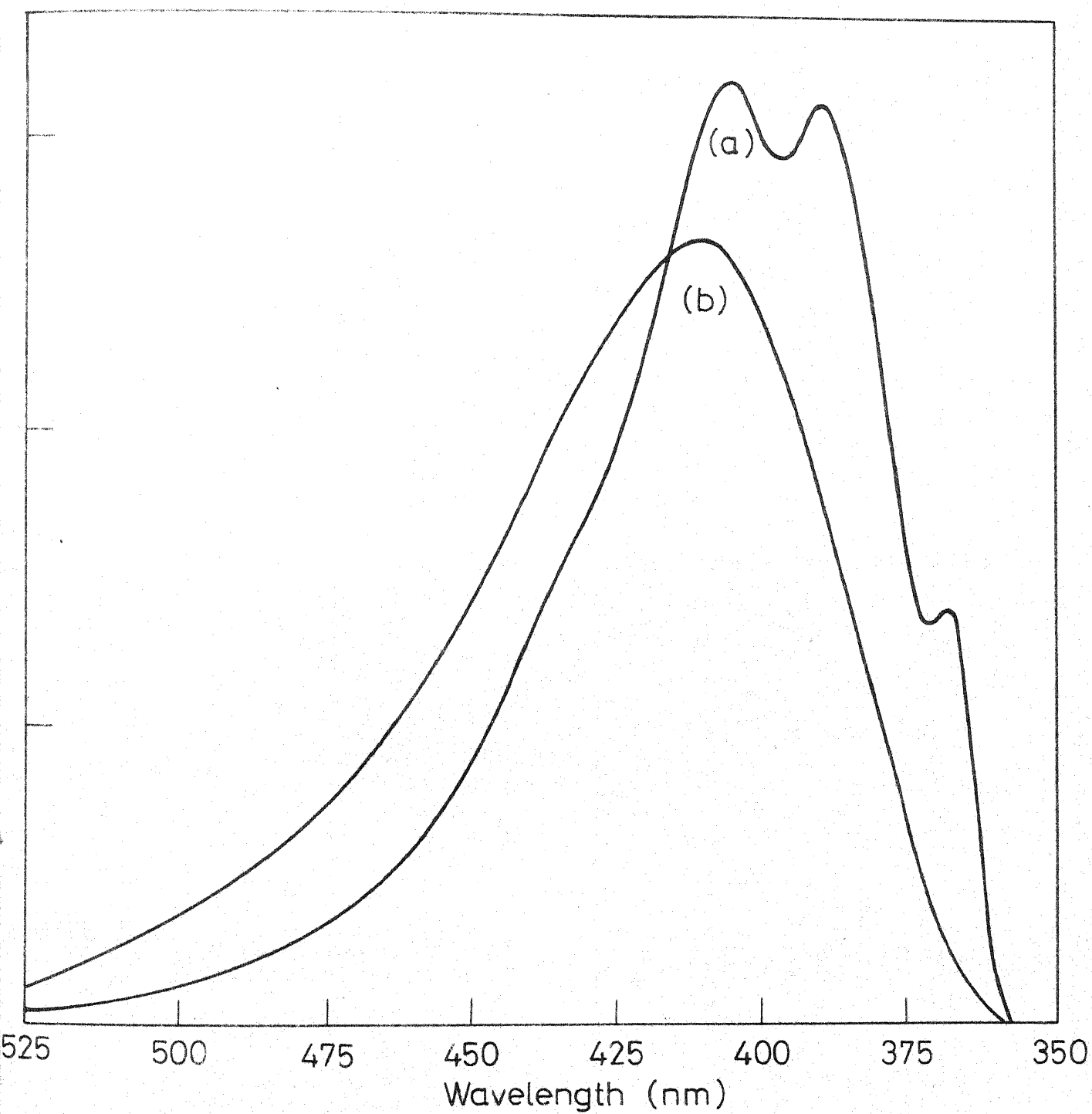
19 Phosphorescence spectra of 1-Phenyl-3,5-dimethylpyrazole at 77 K in aqueous methanol (a) Neutral form (b) Cation.
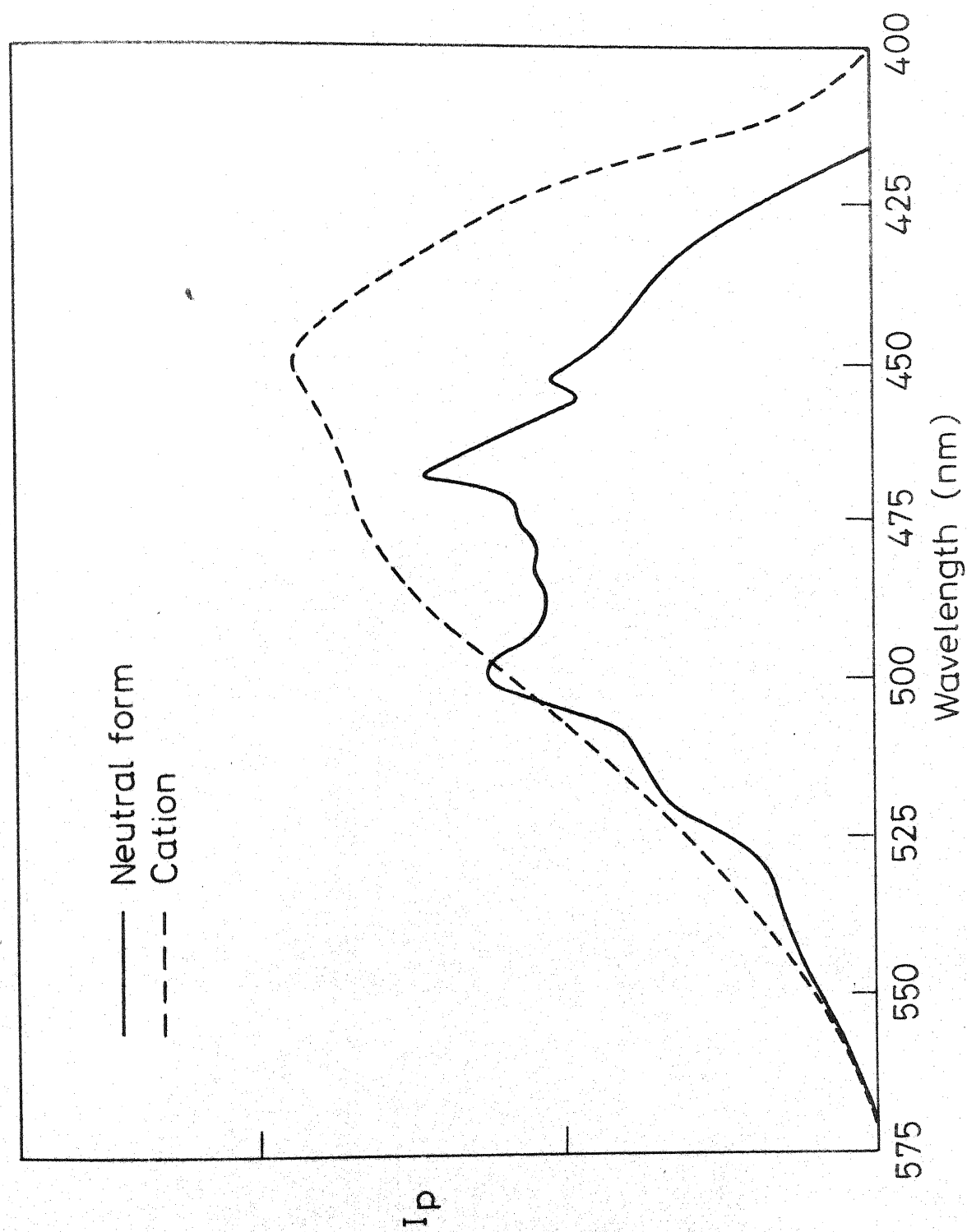
Fig. 5.20 Phosphorescence spectra of 1,5-Diphenyl-3-methylpyrazole at 77 K in aqueous methanol.
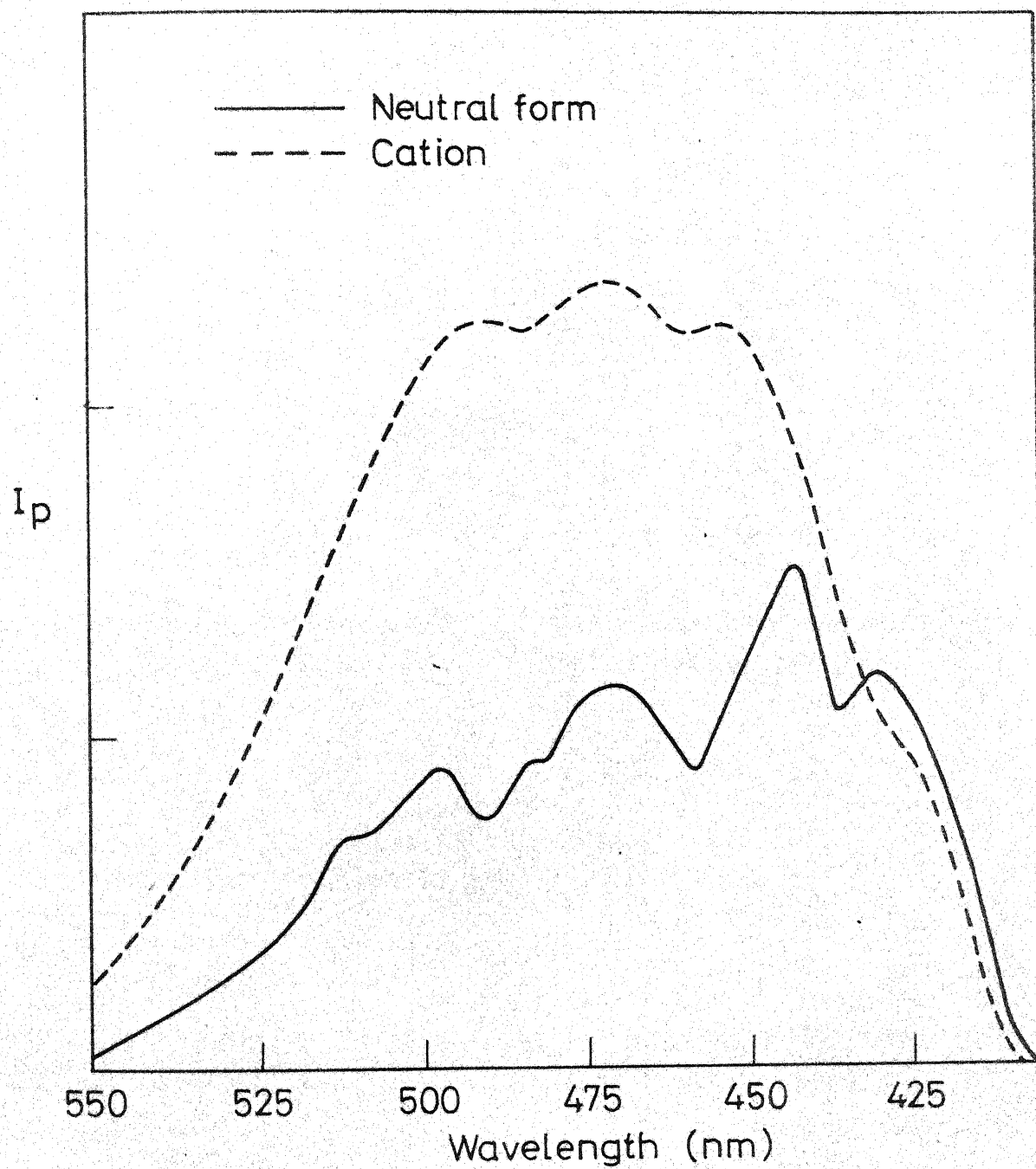
Fig. 5.21 Phosphorescence spectra of 1,3,5-Triphenylpyrazole at 77 K in aqueous methanol.

Legend (in figure):
- – – – Neutral form
- —— Anion
- —·—·— Cation

Axis labels: Ip (vertical), Wavelength (nm) (horizontal)
Horizontal axis values: 550, 500, 450, 400
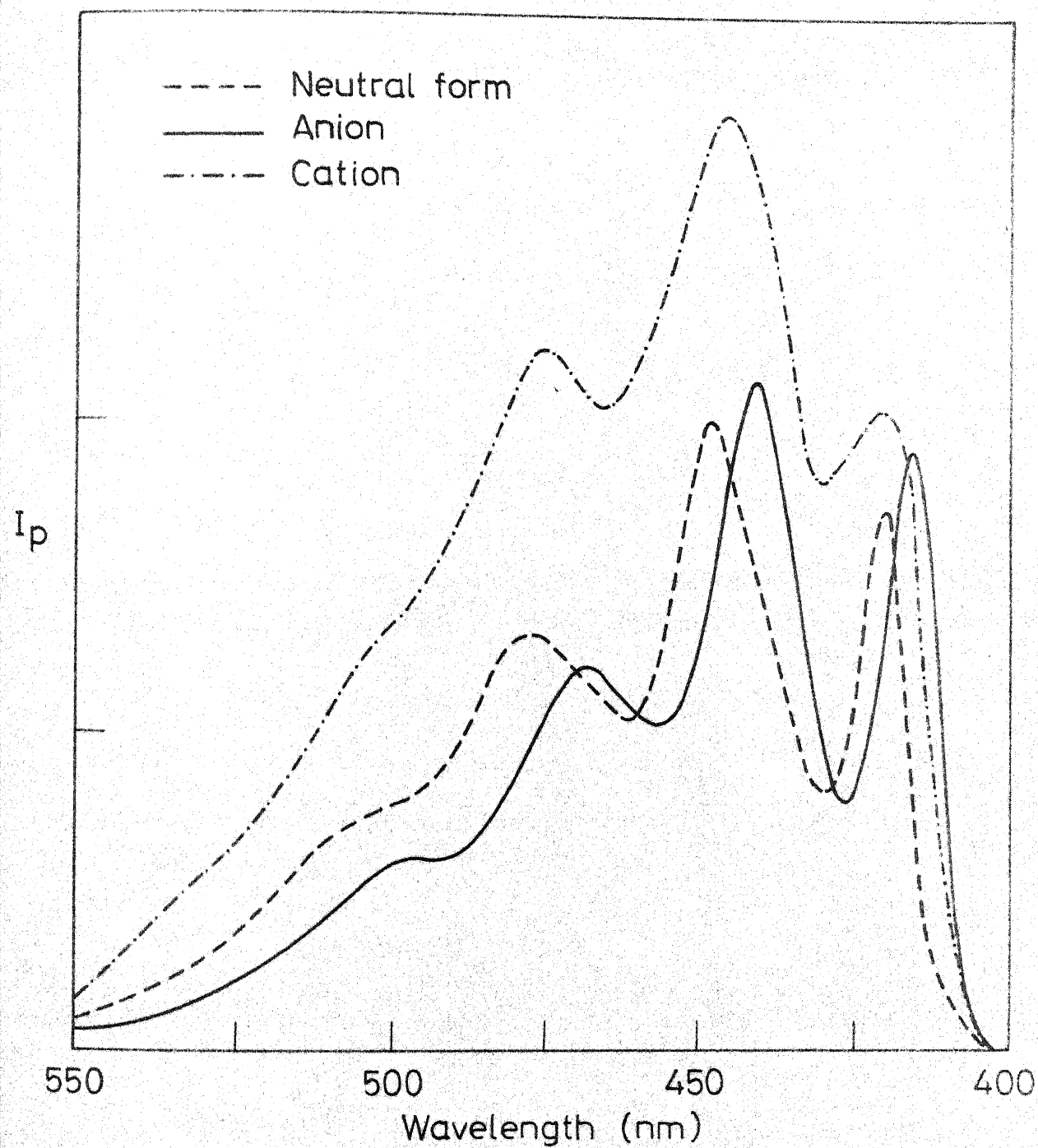
5.22 Phosphorescence spectra of 3,5-Diphenylpyrazole at 77 K in aqueous methanol.
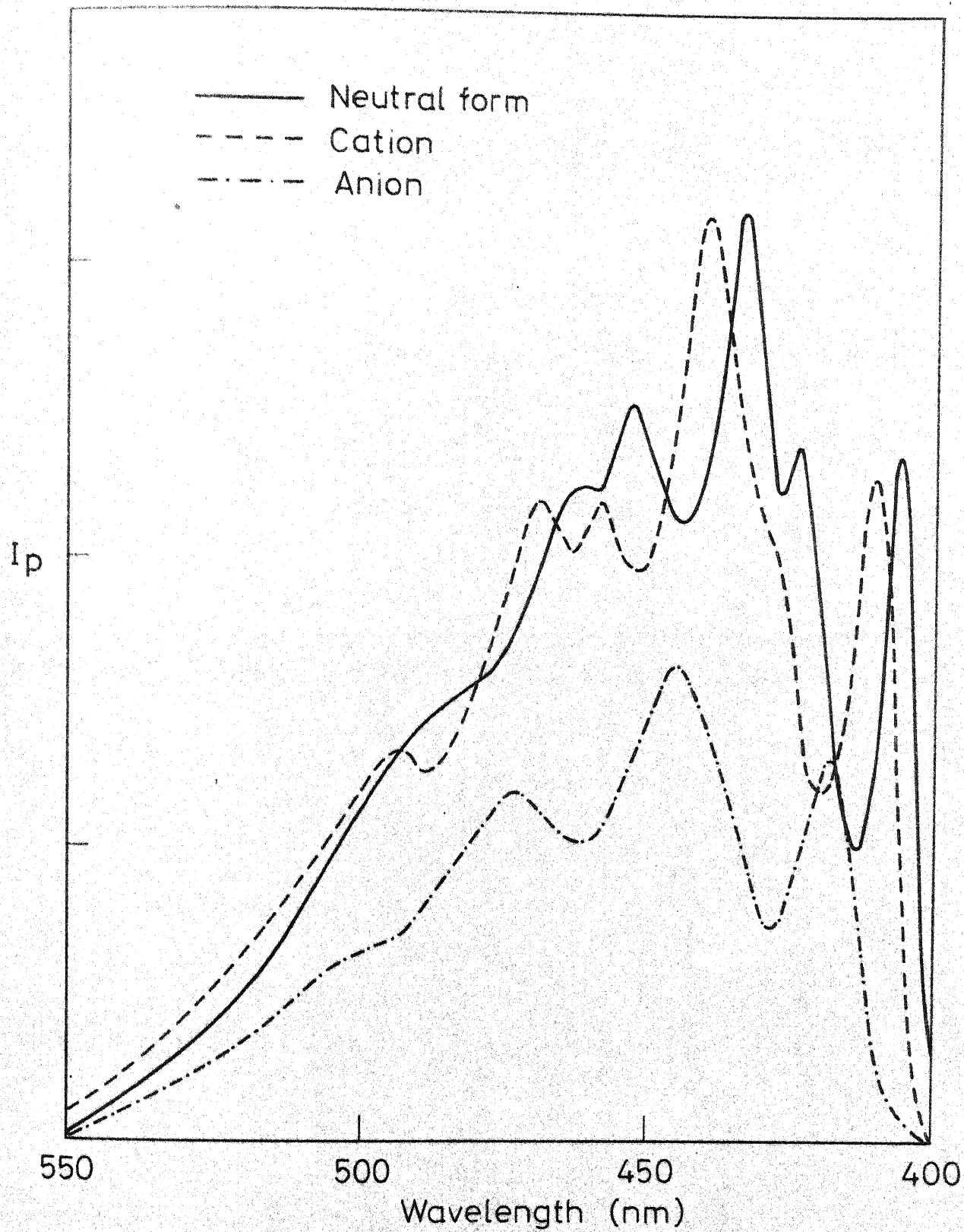
Fig. 5.23 Phosphorescence spectra of 3-Methyl-5-phenylpyrazole at 77 K in aqueous methanol.
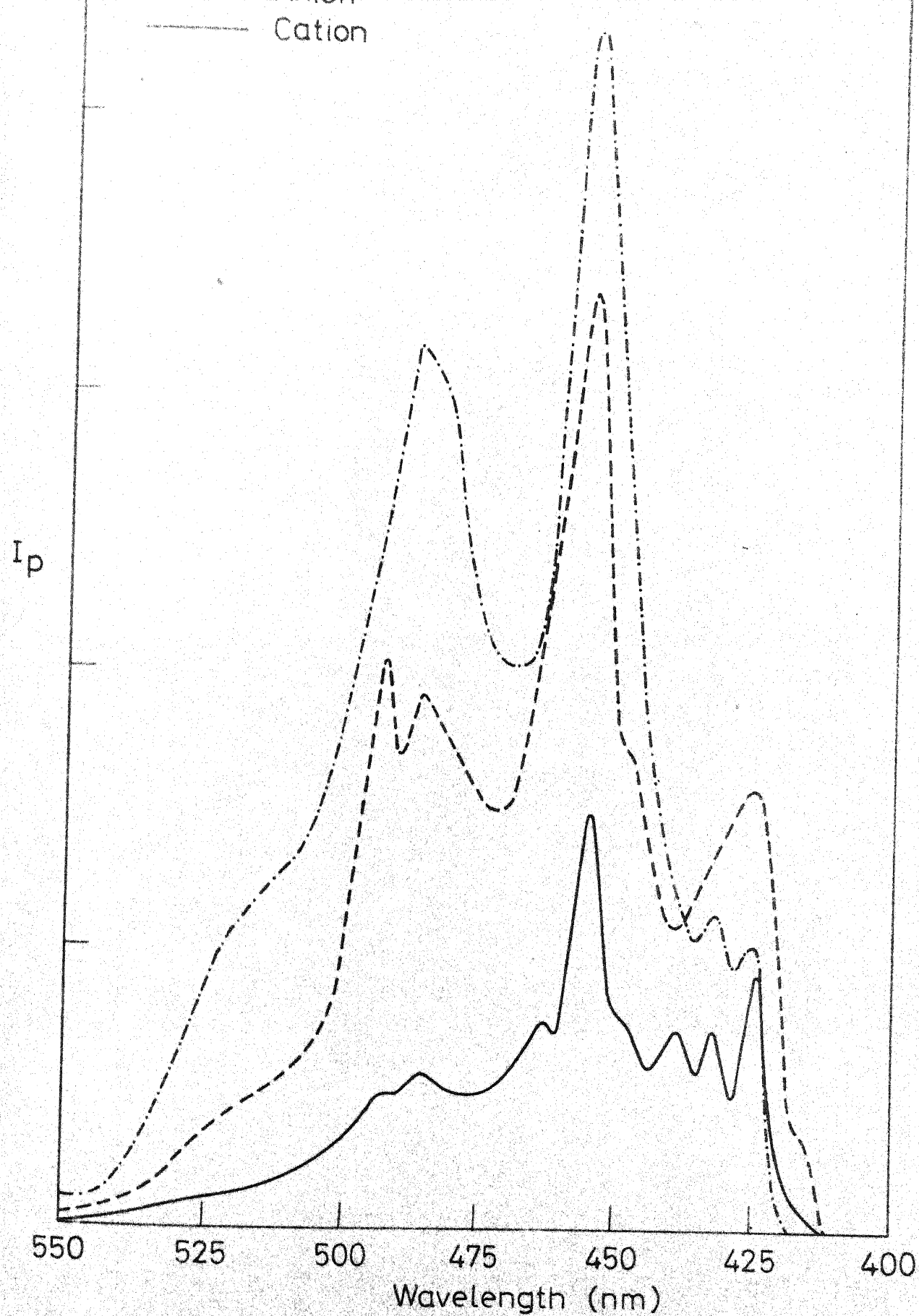
Fig 5·24 Phosphorescence spectra of 9,10-Phenanthroimidazole at 77 K in aqueous methanol.
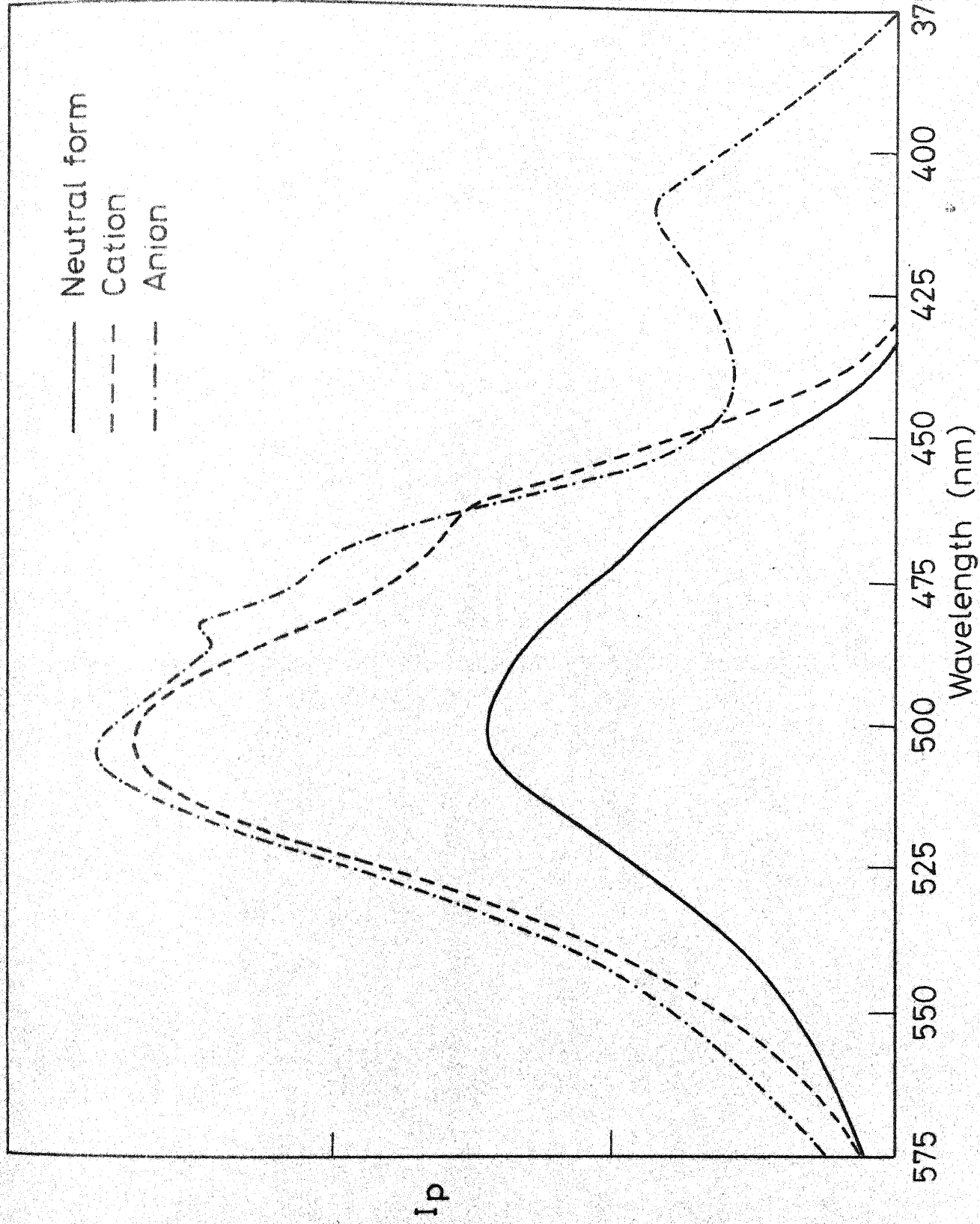
Fig. 5·25 Phosphorescence spectra of 4,5-Diphenylimidazole at 77 K in aqueous methanol.

and MPP anion in aqueous methanol are found to be 24630 cm^{-1}, 24390 cm^{-1} and 23952 cm^{-1} respectively. The 1590 cm^{-1} vibrational band forms the main progression whereas 968 cm^{-1} vibrational band appears as a combination band in the MPP neutral form. In MPP^{+}, 1590 cm^{-1} is the main vibrational progression and 1012 cm^{-1} appears as a combination band. Spectral analysis of MPP^{-} indicates only one vibrational mode of frequency 1460 cm^{-1}, present as fundamental and overtones.

5.5.2. 9,10-Phenanthroimidazole

Phosphorescence spectra of PI, its cation and the anion at 77K are structured. The peaks for the anion are very sharp, less so for the cation and broad for the neutral form (fig. 5.24). The phosphorescence spectra of all the forms exhibit one set of peaks which are sharp, intense and well separated. The other peaks occur as shoulders and are weak. In the neutral form 1570 cm^{-1} vibrational band forms the main progression whereas a vibrational frequency of 591 cm^{-1} occurs as a combination band. In the cation as well as the anion, the main progression band is the same i.e. 1570 cm^{-1}, but the combination band is 425 cm^{-1}.

Phosphorescence spectra of different forms of 4,5-diphenylimidazole and 9-hydroxyphenanthrene are not so structured (figs. 5.25 and 5.26).

Table - 5.4

Low temperature phosphorescence maxima(cm^{-1}) and the results of vibrational analysis

Compound	$\bar{\nu}$ Hexane	Neutral (methanol/H$_2$O)			Cation			Anion		
		$\bar{\nu}$	$\Delta\bar{\nu}$	Assignment	$\bar{\nu}$	$\Delta\bar{\nu}$	Assignment	$\bar{\nu}$	$\Delta\bar{\nu}$	Assignment
1	2	3	4	5	6	7	8	9	10	11
PDP	24390	27210			24390					
		25641								
		24691								
		22727								
DPMP	21978	22883		0-0						
		22099	784	755	22530					
		21390	1493	1495						
	20725	20040	2843	1495x2=2990	20833					
	19608	19230	3653	1495x2+755=3745						
TPP	23669	24096		0-0	23529		0-0			
		23255	841	841						
		22598	1498	1492	22075	1454	1450			
	21978	22099	1997	1492+520=2012						
		21141	2955	1492x2=2984	21186	2343	1450+920=2370			
	20618	20661	3435	1492x2+520=3504	20325	3204	1450+920x2=3290			
		20100	4016	1492x2+520x2=4024						
	19512	19512	4584	1492x2+520x3=4564						
DPP	23392	23809		0-0	23809		0-0	24067		0-0
	21858	22321	1488	1460	22421	1388	1405	22675	1392	1405
	20534	20920	2889	1460x2=2920	21008	2801	1405x2=2810	21321	2744	1405x2=2810
		19646	4163	1460x3=4180	19608	4201	1405x3=4215	20000	4067	1405x3=4215
		18868	4941	1460x4=5844						

1	2	3	4	5	6	7	8	9	10	11
MPP	24390	24360		0→0	24390		0→0	23951		0→0
	23392	23668	962	968	23391	999	1012	22471	1480	1460
	22599	23094	1536	1590	22805	1585	1590	21141	2810	1460x2=2920
	21930	22099	2531	1590+968=2558	21857	2533	1590+1012=2602	19940	4011	1460x3=4380
	20833	21621	3009	1590x2=3180	21276	3114	1590x2=3180			
		20618	4012	1590x2+968 =4168	20202	4184	1590x2+1012 =4182			
DPI		22020		0→0	21390		0→0	21277		0→0
		21276			19900			20725		
								19802		
PI		23529	541	0→0	23530	409	0→0	23557	409	0→0
		22988	1158	591	23121		425	23148	778	425
		22371		591x2=1182				22779	1236	425x2=850
								22321		425x3=1275
		21978	1551	1570	21978	1552	1570	21978	1579	1570
		20747	2782	1570+591x2 =2752	20619	2911	1570x2=3140	21552	2005	1570+425=1995
		20492	3037	1570x2=3140	20325	3025		20451	3106	1570x2=3140
		19471	4058	1570x2+591x2 =4322	19139	4392	1570x3=4710			
HP		20408		0→0				20513		0→0
		19608						19881		
								18975		

Phosphorescence spectra of pyrazoles at 77K are sharper
and more resolved in aqueous methanol than in hexane, possibly
due to the poor solubility of the compounds in the latter. In
all cases the λ_{max} in aqueous methanol are blue shifted in
comparison to that of the hexane solution following the same
trend as observed in the absorption spectra, illustrating that
the ground state configuration is retained in the triplet state
also at 77K. It has been further observed that spectral shift
in triplet state is less than that in singlet state. This can
be explained in terms of the much smaller differences in dipole
moment and charge transfer character between the ground and
lowest triplet state than between ground and lowest excited
singlet state.[1]

In comparison to the fluorescence, the phosphorescence
spectra of all the compounds and their cations and anions except
PDP[+] are well resolved and the 0-0 bands are identified approxi-
mately from the position of the shortest λ_{max} in phosphorescence.
The high resolution at low temperature is mostly due to the
rigidity of the medium and partly to the elimination of hot bands
resulting from the thermal population of high vibrational levels
of the ground and the excited states.

CHAPTER - 6

EFFECT OF pH ON ABSORPTION
AND FLUORESCENCE

6.1. Ground state acidity constants

Ground state acidity constants for pyrazole, DMP and DPI are available from the literature.[146] For the other compounds the ground state acidity constants (pK$_a$) were calculated spectrophotometrically by the method described in chapter 3.

All absorption spectra were run on Cary 17D spectrophotometer. The data used for the calculation of acidity constants were taken on a Beckman DU/Toshniwal spectrophotometer. A modified Hammett acidity scale[114] and yagil basicity scale[115] were used for the measurement of pK$_a$ of the compounds having values outside the 1-13 pH range. The definitions of these functions ensure that they become identical with pH in dilute solutions. Due to the poor solubility of some of the compounds in water, 5-20% methanol solutions were used and the solvent system used for each compound is listed in Table 6.1.

Three equilibria in AI (Dication $\rightleftharpoons$ Monocation $\rightleftharpoons$ Neutral $\rightleftharpoons$ Monoanion), two equilibria in DPP, MPP, PI and AMP (Cation $\rightleftharpoons$ Neutral $\rightleftharpoons$ Anion) and one equilibrium in the rest of the compounds were studied. All these equilibria except that between AMP and its anion were indicated by an isosbestic point in their absorption spectra taken before carrying out the absorptiometric titration. In the case of AMP, when the pH is increased above 14, the absorption maximum changes but the isosbestic point is constant only for solutions upto pH 15. On a further increase in pH ($>$15) the isosbestic point changes without change in the maximum for each solution. Due to this irregular dependence of the absorption spectrum (fig. 6.1) on pH and a very small range of H_- over which one type of equilibrium is present, the pK_a value for this equilibrium could not be determined. This could be due to the formation of dianion. An unusual behaviour was also observed in the fluorescence spectrum in this range of H_- as discussed below in section 6.2.3.

The pK_a values determined in this work and the isosbestic points observed are given in Table 6.1 along with the pK_a values taken from the literature. They are in accord with the theory that the presence of an electron donating group like $-CH_3$, $-NH_2$, etc., increases the basicity of the compound while the presence of electron withdrawing group like $-C_6H_5$ decreases.[147] These
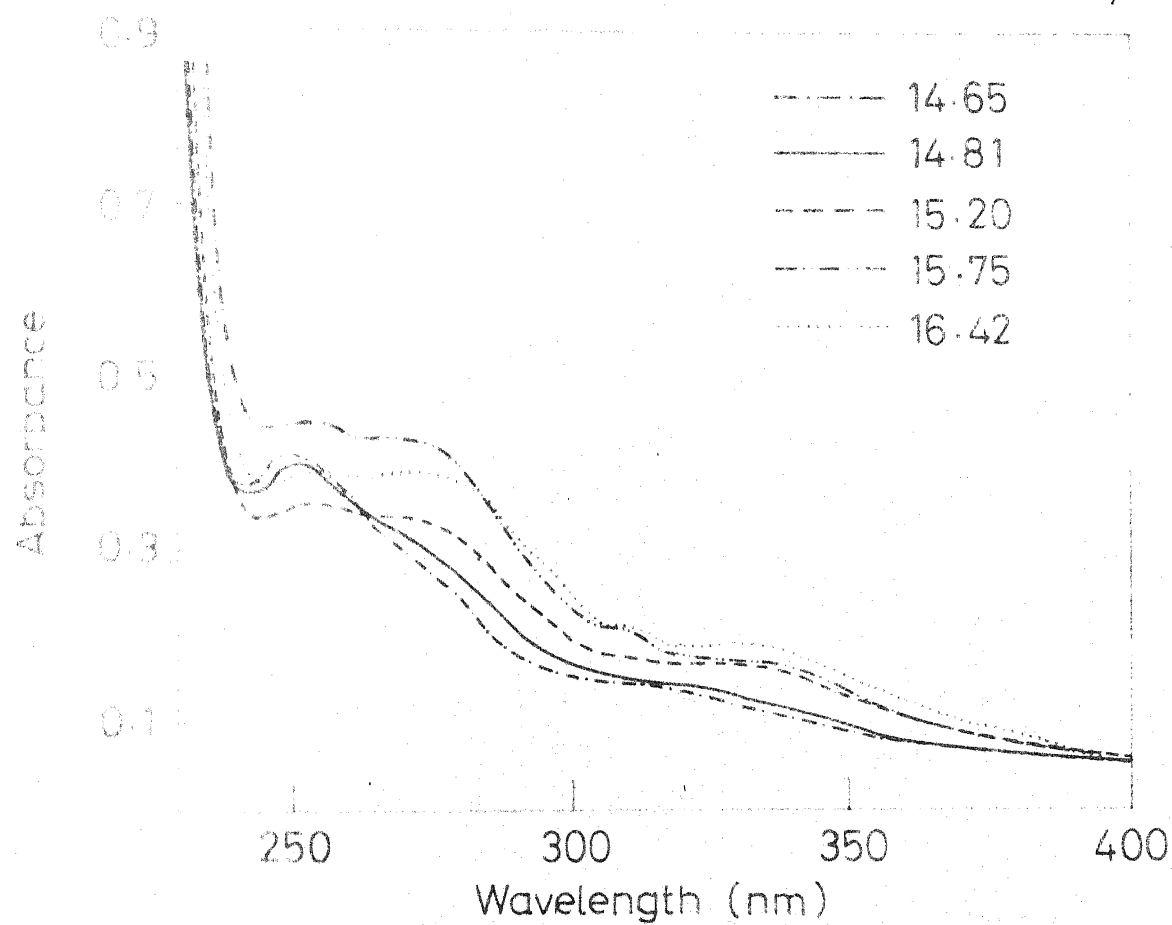
Fig. 6.1 Absorption spectra of 9-Aminophenanthrene in different H-scale.

Table 6.1

Ground state acidity constants

Compound	Eq (DM)		Eq(MN)		Eq(NA)		% MeOH
	pK_a	Isosbestic point(nm)	pK_a	Isosbestic point(nm)	pK_a	Isosbestic point(nm)	
Pyrazole			2.48^a				
3,5-Dime-thylpyra-zole(DMP)			4.38^a				
PDP			2.27	238			5
DPMP			1.48	236			10
TPP			-0.39	265			20
DPP			1.43	262	12.94	260	5
MPP			2.61	223	14.31	256	5
DPI			5.90	^70	12.8	292	5
PI			4.65	283	11.86	278	5
HP					9.05	316	5
AMP			3.5^b		⟩14.00		5
AI	-0.094	270	5.27	297	14.59	295	5

a. From Ref. 146, b. From Ref. 129

Eq(DM) = Equilibrium between dication and monocation.

Eq(MN) = Equilibrium between monocation and neutral form.

Eq(NA) = Equilibrium between neutral form and anion.

pK_a values were used in the calculation of pK_a^* values by Förster cycle methods.

6.2. Excited singlet state acidity constants

Various methods used for the calculation of the excited state acidity constants were discussed in chapter 3. Pyrazoles and DPI are grouped together since these compounds have more or less similar behaviour as far as pK_a^* values are concerned. Results and discussion for other compounds are presented individually.

6.2.1. Pyrazoles and 4,5-diphenylimidazole

a. From absorption spectra

The Förster cycle is applicable only to the 0-0 transition of either absorption or emission spectra. Since the absorption spectra of all the compounds and their cations or anions are structureless and broad, the position of the 0-0 band is unknown. Assuming the maxima of absorption bands of the species involved in each equilibrium occur at equal amounts above the 0-0 transition, absorption maxima were used in the calculation of the pK_a^* values. Results for all the compounds are summarized in Table 6.2 wherein, $\bar{\nu}_m$, $\bar{\nu}_n$, $\bar{\nu}_a$ are the long-wavelength absorption maxima of the mono-cation, neutral form and the anion respectively. Although pyrazole and 3,5-dimethylpyrazole can undergo deprotonation, the

Table –6.2

Excited singlet state acidity constants
determined from absorption spectra

Compound		pK_a	$\bar{\nu}_m(cm^{-1})$	$\bar{\nu}_n(cm^{-1})$	$\bar{\nu}_a(cm^{-1})$	ΔpK_a	pK_a^*
Pyrazole		2.48	46729	47619		−1.89	4.37
DMP		4.38	45662	46512		−1.79	6.13
PDP		2.27	42735	40816		4.03	−1.76
DPMP		1.48	40322	40160		0.34	1.14
TPP		−0.39	36496	39841		−7.03	6.64
DPP	Eq(MN)	1.43	37313	39526		−4.65	6.08
	Eq(NA)	12.94		39526	37879	3.46	9.48
MPP	Eq(MN)	2.61	39370	40322		−2.00	4.61
	Eq(NA)	14.31		40322	37593	5.73	8.58
DPI	Eq(MN)	5.9	39840	36101		7.85	−1.95
	Eq(NA)	12.8		36101	33333	5.8	7.00

excited state equilibrium constant for this reaction could not
be determined due to the interference of high absorbance of OH⁻
ions below 235 nm.

b. From fluorescence spectra

Since fluorescence spectra of all the compounds are
broad, a similar assumption is made as in absorption spectra, i.e.,
the maxima of the fluorescence bands of the species involved in
an equilibrium occur at equal amounts above the 0-0 transition.
The pK_a^* values for the Eq(MN) for DPMP, TPP and DPI were calculated
by using the fluorescence maxima of the respective species at 77K
in Förster cycle equation (3.8). As stated in the previous
chapter the cations of these compounds either do not emit at
room temperature or undergo chemical reaction immediately after
excitation. pK_a^* values for the rest of the compounds were
calculated using fluorescence data at 298K and the results are
given in Table 6.3. $\bar{\nu}'_m$ $\bar{\nu}'_n$ $\bar{\nu}'_a$ are the wavenumbers of short
wavelength fluorescence maxima of the monocation, neutral molecule
and the anion respectively.

c. From an average of the absorption and fluorescence spectra

Bartok and Lucchessi[38] suggested that a more accurate
value for the 0-0 transition energy could be determined by
taking an average of the energy values obtained from absorption
and fluorescence. This method is based on the assumption that

Table-6.3

Excited singlet state acidity constants determined from fluorescence spectra

Compound		pK_a	$\bar{\nu}'_m$	$\bar{\nu}'_n$	$\bar{\nu}'_a$	ΔpK_a	pK_a^*
PDP		2.27	32051	32414		-0.76	3.03
DPMP		1.48	22471[a]	28409[a]		-12.47	13.95[a]
TPP		-0.39	23640[a]	27972[a]		-9.09	9.48[a]
DPP	Eq(MN)	1.43	28901	29498		-1.25	2.68
	Eq(NA)	12.94		29498	27027	5.19	7.75
MPP	Eq(MN)	2.61	32051	33057		-2.11	4.72
	Eq(NA)	14.31		33057	27027	12.67	1.64
DPI	Eq(MN)	5.9	28985[a]	28129[a]		1.8	4.1[a]
	Eq(NA)	12.8		26881	24813	4.34	8.46

a. Measurements at 77K

the solvent relaxation is identical for both members of the conjugate pair. Table 6.4 presents results for those compounds whose pK_a^* were calculated by this method at 298K. $(\bar{\nu}_{ma} + \bar{\nu}_{mf})/2$ is the average value of the wavenumbers of the long wavelehgth maxima of absorption and short wavelength maxima of fluorescence of cation, and $(\bar{\nu}_{na} + \bar{\nu}_{nf})/2$, $(\bar{\nu}_{aa} + \bar{\nu}_{af})/2$ are the respective terms for the neutral and the anionic forms.

Table - 6.4

Excited singletstate acidity constants determined from
the average of absorption and fluorescence spectra

Compound		pK_a	$\dfrac{\bar{\nu}_{ma} + \bar{\nu}_{mf}}{2}$	$\dfrac{\bar{\nu}_{na} + \bar{\nu}_{nf}}{2}$	$\dfrac{\bar{\nu}_{aa} + \bar{\nu}_{af}}{2}$	ΔpK_a	pK_a^*
PDP		2.27	37393	36615		1.63	0.64
DPP	Eq(MN)	1.43	33107	34512		−2.95	4.38
	Eq(NA)	12.94		34512	32453	4.32	8.62
MPP	Eq(MN)	2.61	35711	36690		−2.06	4.66
	Eq(NA)	14.31		36690	32310	9.2	5.11
DPI	Eq(NA)	12.8		31491	29073	5.08	7.72

d. Fluorescence intensity as a function of acidity

The method of determining the pK_a^* values from the pH/H$_o$/H$_-$ dependence of fluorescence intensity is called fluorimetric titration.[46] Even if one member of the acid-base pair is fluorescent this method can be used. Unlike Förster cycle methods, it is free of assumptions but the excited state equilibrium should be established within the life time of the singlet state. This is because the proton transfer reaction has to compete with radiative and non-radiative processes of the excited state. If the rate of the former reaction is slower than that of the latter processes, the molecule gets deactivated immediately after excitation and the emission is governed by the ground state equilibrium conditions. Under these circumstances this technique gives the ground state pK_a value but at the same time it also gives a qualitative idea about the life time of the species involved.

Since the fluorescence intensities are taken as a direct measure of the concentration of the species, other factors like intensity of excitation light, absorbance at the excitation wavelength and total concentration are to be kept constant for all pH solutions. This was ensured by taking the same concentration of the compound and exciting it at the isosbestic point, mentioned in Table 6.1.

The intensity of fluorescence was measured and a plot of I/I_o against acidity of the solution gave a sigmoid curve for each species. If one species is fluorescent the point of inflection or if both are fluorescent then the point of intersection of the two sigmoid curves gives the dissociation constant. The fluorimetric titration curves thus obtained are reported in figs. 6.2-6.6. The dissociation constants determined from these curves are given in Table 6.5 along with the pK_a^* values obtained from other methods. For DPI, care has been taken to measure the fluorescence intensity immediately after excitation to avoid the complications which may arise due to the formation of the photoproduct.

e. Summary of excited singlet state acidity constants

Results obtained by the four methods are compared in Table 6.5; pK_a^*(abs), pK_a^*(flu), pK_a^*(ave) are the excited singlet state acidity constants obtained from absorption, fluorescence spectra and from their average; pK_a(FT) is the dissociation constant obtained from the fluorimetric titration.

Discussion

The pK_a^* values, as expected, differ very much from the pK_a values. In addition, the pK_a^* values calculated by four different methods do not agree among themselves (Table 6.5).
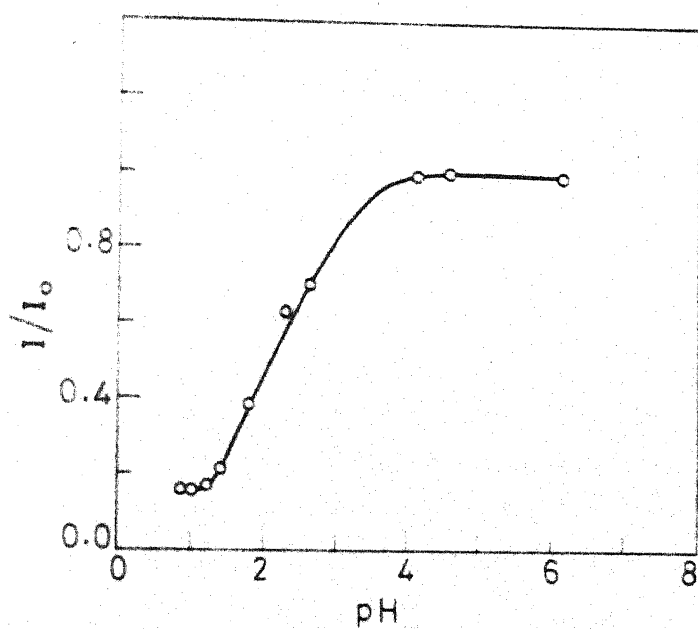
Fig. 6·2 Plot of relative fluorescence intensities
of N-Phenyl-3,5-dimethylpyrazole Vs pH.
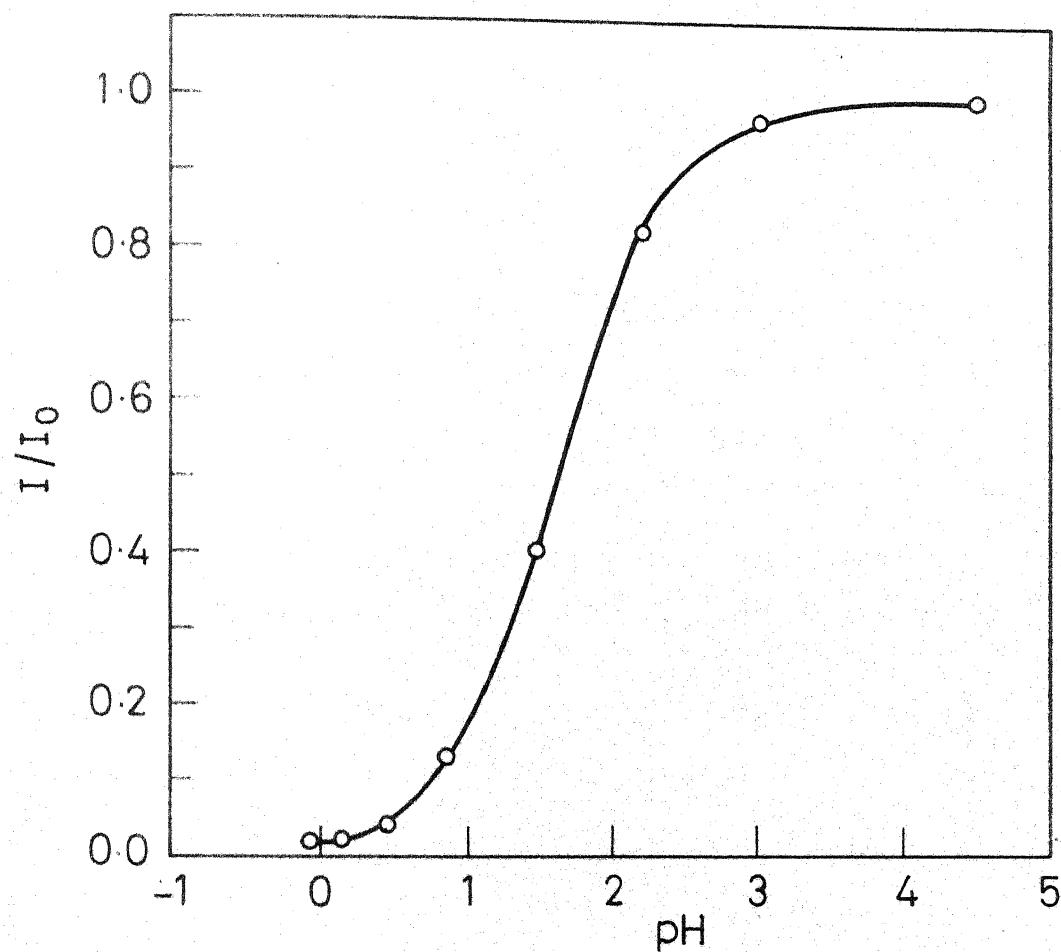
Fig. 6·3 Plot of relative fluorescence intensities of
1,5-Diphenyl-3-methylpyrazole Vs pH
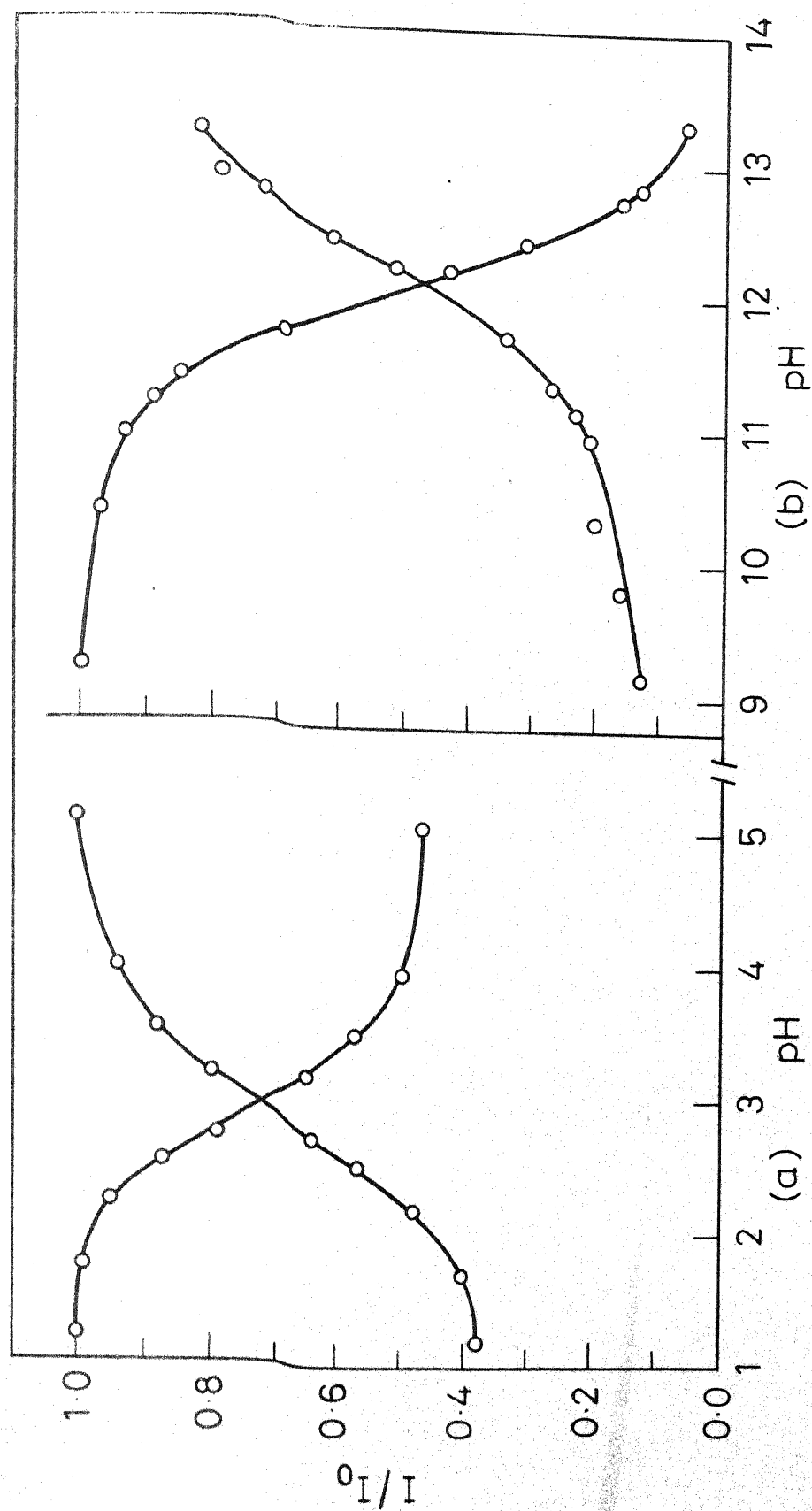
Fig. 6.5 Plot of relative fluorescence intensities of 3-Methyl-5-phenylpyrazole Vs pH (a) cation and neutral form (b) neutral form and anion.
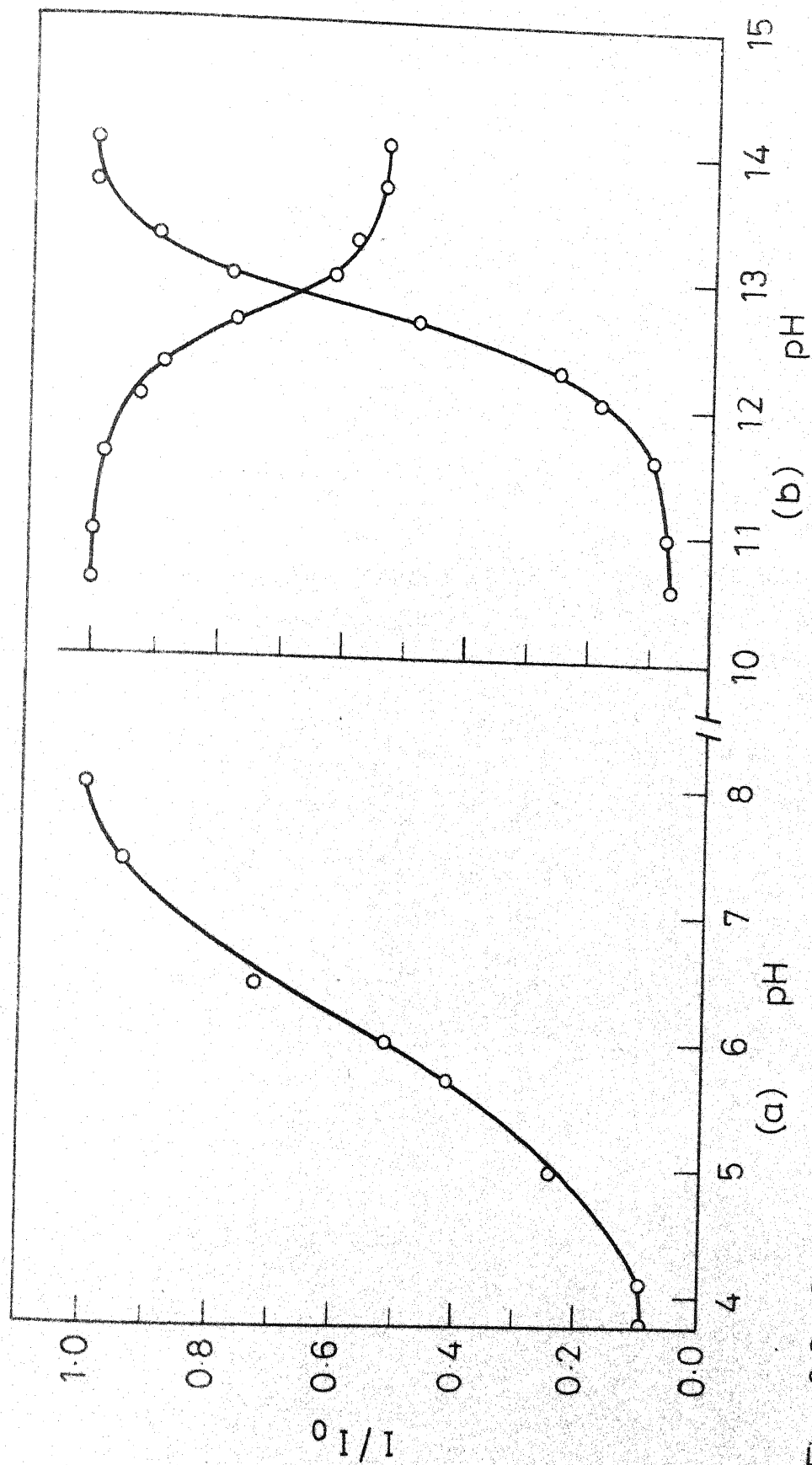
Fig. 6.6 Plot of relative fluorescence intensities of 4,5-Diphenylimidazole
Vs pH   (a) Neutral form (b) Neutral form and anion

Table-6.5

Summary of excited singlet state acidity constants

Compound		pK_a	pK_a^*(abs)	pK_a^*(flu)	pK_a^*(ave)	pK_a(FT)
Pyrazole		2.48	4.37			
DMP		4.38	6.13			
PDP		2.27	-1.76	3.03	0.64	2.3
DPMP		1.48	0.64			1.55
TPP		-0.39	6.64			
DPP	Eq(MN)	1.43	6.08	2.68	4.38	1.7
	Eq(NA)	12.94	9.48	7.75	8.62	12.64
MPP	Eq(MN)	2.61	4.61	4.72	4.67	2.91
	Eq(NA)	14.31	8.58	1.64	5.11	12.04
DPI	Eq(MN)	5.90	-1.95			6.00
	Eq(NA)	12.8	7.00	8.46	7.73	12.9

Of the four, three methods are based on the Förster cycle.
Though the merits and shortcomings of these methods have been
reviewed in detail by many authors,[41,50,54,86] a brief description
is given below to explain our results.

The accuracy of pK_a^* values by Förster cycle is based on
the validity of the following assumptions.

$\bar{\nu}$ and $\bar{\nu}'$ used in Förster cycle calculation (Eq. 3.8)
represent the transitions from the ground to the excited state
for an acid and conjugate base respectively. This means that
the conformational (conjugation) and the angular momentum
quantum numbers of the excited states of the acid and the base
are generally the same. There are a few cases for which there
is a change in going from the former to the latter. In such
cases, the electronic transition is to be accompained by a
chemical reaction. This process usually introduces a large
entropy error, associated with configurational change, in the
Förster cycle calculations.[34] For example 3,4-benzocinnoline,[148]
fluoresces from its $n-\pi^*$ singlet state but the cation fluoresces
from the $\pi-\pi^*$ singlet state. Similarly ^1L_b is the lowest
singlet state in neutral benzimidazole and ^1L_a is for the
cation.[131] In these cases, the results obtained from the
Förster cycle are meaningless and can not be compared with the
results obtained by other techniques.

That the entropy of protonation must be equal in the ground and excited electronic states seems to be a reasonable assumption. In aromatic molecules where there is not much change in molecular electronic structures subsequent to excitation, the change in the entropies of protonation in the excited and the ground states would be very small. For example in case of protolytic dissociation of β-naphthylammonium ion it has been shown that the maximum error caused by the assumption is not more than $\pm$ 0.2 units in the ΔpK_a.[149] By calculating pK_a^*s at different temperatures, Weller[37] showed that there was practically no difference in ΔS^* for the ionization of β-naphthol in the S_o and S_1 states, despite a large change in pK_a and obvious differences in solvation between the acid and its base. Similarly in aromatic acids it was found that $T \Delta S^*$ do not contribute more than 1 pK_a unit.[151]

Förster cycle is applicable only to 0-0 vibrational bands of either absorption or emission spectra (if both species are emitting) and should not include the contribution of the vibrational energy. In general, the spectra at room temperature for the species are broad and the 0-0 band can not be located easily. Instead of the 0-0 band, either the average of absorption and emission bands or band maxima can be used. It has been shown by Levshin[150] that if the vibrational spacings in the ground and excited states are the same, there exists a mirror image

relationship between the fluorescence band and the long wave-
length absorption band. From this mirror image relation, the
frequency of the 0-0 transition can be approximated. But this
kind of behaviour is missing in most of the cases and one has
to depend upon the band maxima. It has been assumed that the
vibrational spacing in the ground and the excited states of both
the acid and its base are the same and also the vibrational
energy distribution is identical. If this assumption is valid
absorption data would be sufficient in calculating pK_a^* values,
provided solvent relaxation and geometrical changes are the
same for both species in the excited state.

Besides the error introduced in the Forster cycle method
by vibrational energy difference,there are other sources of error
originating from changes in geometry, electronic configuration
and solvent cage with excitation. These changes arise because the
charge distribution in the excited state is different from the
ground state. Thus the Förster cycle methods can provide better
values of pK_a^* only if the electronic transition energies used in
the calculation also account for all the differences in energy
between thermally equilibrated ground and excited states.

Solvent relaxation,geometry change, and vibrational
effects can be grouped together and called as thermal relaxation.
Then the calculation of reasonable values of pK_a^* from absorption
data is dependent upon how small or how nearly equal thermal

relaxations are for both the acid and its base in the excited state. By taking into account thermal relaxations, which are taking place in the ground as well as in the excited state, Kovi and Schulman[59] proposed a modified thermodynamic cycle and it is shown in fig. 6.7. By assuming again that the dissociation entropies are equal in ground and electronically excited states they derived equations for the equilibrium $A \rightleftharpoons B + H^+$

$$pK_a - pK_a^* = \frac{Nhc}{2.303\ RT} (\tilde{\nu}^A_{abs} - \tilde{\nu}^B_{abs}) + \Delta H^{B^*}_{te} - \Delta H^{A^*}_{te} \quad \cdots 6.1$$

$\Delta H^{A^*}_{te}$, $\Delta H^{B^*}_{te}$ are the enthalpies of thermal relaxation of acid and the conjugate base in the S_1 state subsequent to emission. As per the equation (6.1) if either of the species becomes more polar and/or if it undergoes a geometry change in the excited state then the difference, $\Delta H^{B^*}_{te} - \Delta H^{A^*}_{te}$ will be more and it will lead to a large error in pK_a^*.

Similarly the equation derived for the calculation of pK_a^* from fluorescence data is

$$pK_a - pK_a^* = \frac{Nhc}{2.303\ RT} (\tilde{\nu}^A_{flu} - \tilde{\nu}^B_{flu}) + \Delta H^A_{te} - \Delta H^B_{te} \quad \cdots 6.2$$

where ΔH^A_{te} and ΔH^B_{te} are the respective terms for the ground state. Calculation of reasonable values of pK_a^* from fluorescence data is dependent upon how small or how nearly equal thermal relaxation is for, both species in the ground state. Here it
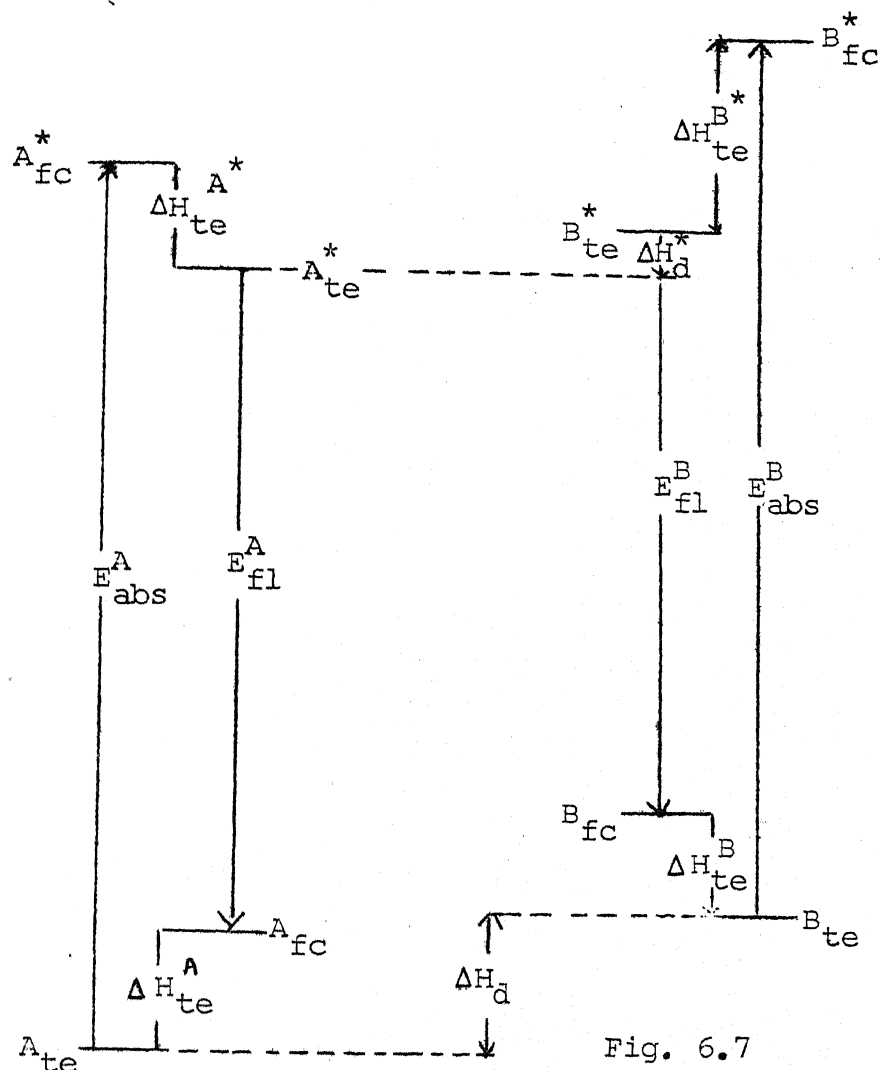
Fig. 6.7

A modified thermodynamic cycle for the calculation of pK_a^*; A_{te}, A_{te}^*, A_{fc} and A_{fc}^* - Thermally equilibrated ground and electronically excited states respy. of the acid B_{te}, B_{te}^*, B_{fc}, B_{fc}^* are the corresponding states of the conjugate base. E_{abs}^A, E_{fl}^A, E_{abs}^B, E_{fl}^B are respectively, the spectroscopically determined absorption and fluorescence energies for acid and conjugate base. ΔH and ΔH_d^* are the enthalpies of protolytic dissociation in ground and electronically excited states (Ref. 116).

is to be expected that for species which are more polar in the
ground state than in the excited state, the solvent relaxation
error will be large.[153] In an acid-base pair, functional groups
which are more extensively conjugated with the aromatic system
in the ground state and have different symmetries in the excited
state, would lead to an appreciable error due to the conformati-
onal relaxation.

The averaging of absorption and fluorescence maxima to
obtain 0-0 bands of the electronic transition in the Förster
cycle (or in modified thermodynamic cycle) is supposed to result
in a cancellation of the energy discrepancies between the conju-
gate species due to unequal thermal relaxations i.e., even if
all ΔH_{te}^{A*}, ΔH_{te}^{B*}, ΔH_{te}^{A}, ΔH_{te}^{B} are different, sometimes the net
change may be zero. This technique often, but not always, yields
accurate results. If the error is large in one method and
negligible in another, the error will be distributed while
averaging. For example in the calculation of pK_a^* for the
equilibrium between o-phenanthroline dication and its monocation,
this method gives a pK_a^* value greater than pK_a, although the
fluorimetric titration indicates that the opposite is true.[25]
This is a result of the averaging of the solvent relaxation error
from the absorption spectra in the calculation. Apparently in
this case, the vibrational error in the fluorescence shift is
less than half of the solvent relaxation error in the absorption
shift.

Above discussion clearly shows that the accuracy of pK_a^*, obtained by Förster cycle depends upon the choice of the method employed which inturn depends upon the validity of the assumptions made. Since fluorimetric titration does not involve any assumption, if it gives excited state pK_a value, a comparison of this pK_a^* value with the pK_a^* values obtained by the three different Förster cycle methods would indicate which of the Förster cycle methods is more accurate.

Analysis of the pK_a^* values obtained by the different Förster cycle methods

Fluorescence of pyrazole and 3,5-dimethylpyrazole could not be detected and therefore pK_a^* were calculated using absorption data and they are 4.37 and 6.13 respectively. This shows that heterocyclic pyridinic nitrogen atom becomes more basic in the excited state than in the ground state. This is in accordance with the usual trend observed in pyridines.[152] Though this is the only method available to calculate the pK_a^* values for these compounds, these values can not be far from the true values as these molecules are simple and rigid. Any error can be only due to solvent relaxation in the excited state and it will be less as was observed in phenanthroimidazole (6.2.2).

As seen in Table 6.5, except in the case of de-protonation of MPP, pK_a(FT) values obtained for other equilibria, are more or less close to the ground state pK_a values. Thus a comparison

of pK_a(FT) with Förster cycle pK_a^* values could not be done for these compounds. Yet, by considering the nature of electronic transitions and the trends observed in similar compounds, a comparison has been made among the pK_a^* values calculated by the Förster cycle method.

In PDP the difference between pK_a^* values obtained from absorption and fluorescence data is 4.79. Absorption shift shows that pyridinic nitrogen in the carbocyclic ring becomes more acidic whereas fluorescence shift shows that the same nitrogen atom becomes more basic in the excited state. In general it has been observed that if $\pi - \pi *$ is the lowest singlet electronic transition in a molecule containing nitrogen atom with the sp^2 hybrid orbital (e.g. pyridine) the electron density increases at the nitrogen atom and thus it becomes more basic in the S_1 state. Since in the conjugate-acid-base pair of pyrazoles the lowest electronic transition is $\pi - \pi *$, the result obtained from fluorescence data will be more accurate than those obtained by any of the two methods.

A similar behaviour is shown by the absorption data in the case of DPMP. Since the cation of this compound is nonfluorescent at room temperature, pK_a^* from fluorescence data could not be obtained and compared. But pK_a^* from absorption data is against the usual trend observed in other pyrazoles. TPP^+ is also non-fluorescent initially at room temperature but starts fluorescing

after some time due to the formation of a photoproduct. So pK_a^* was calculated only from absorption data and the increase in the basicity is in agreement with the expected trend.

But as was pointed out in chapter 5, $DPMP^+$ and TPP^+ are fluorescent at 77K. The pK_a^* values for cation $\rightleftarrows$ neutral form were calculated from the low temperature fluorescent maxima of these species and are given in Table 6.3. In rigid media i.e. at 77K these molecules have ground state conformation and the solvent relaxation subsequent to excitation is not taken into account. It is known in some cases the solvent relaxation can overweigh the effect of polarization of the electronic transition in determining the value of pK_a^* relative to pK_a. So pK_a^* calculated by this method will be only qualitatively accurate. On seeing the trend of other pyrazoles studied, these values do not seem to be far from true values and atleast tell qualitatively that the pyridinic nitrogen atom, as expected becomes more basic in the excited state and not as predicted by absorption data of DPMP. For DPP, pK_a^* calculated by absorption and fluorescence data for the equilibrium between the cation and the neutral form shows that the pyridinic nitrogen atom becomes more basic in the excited state but the difference between pK_a^*(abs) and pK_a^*(flu) is quite large. Generally a maximum difference of 2 in pK_a^* occurs due to unequal vibrational and solvent relaxations of both species.[50] A difference of 3.4 here

could be due to unequal relaxation due to geometry change (section 5.2.1.c), in addition to the solvent relaxation.

The difference between $pK_a^*(abs)$ and $pK_a^*(flu)$ for the equilibrium between the neutral form and the anion is less than 2 which is mainly due to the unequal solvent, vibrational relaxations in both the species. In this equilibrium $pK_a^*(ave)$ will be more accurate than other pK_a^* values.

The pK_a^* values obtained from absorption and fluorescence data for the equilibrium between the cation and neutral forms of MPP are 4.61 and 4.72 respectively. These values are nearly the same and thus show that the thermal relaxations (vibrational, solvent, geometrical) for both species in ground and excited states are nearly same. This can be seen from the tables 4.1 and 5.1 that solvent relaxations in absorption and emission for the two extreme cases (in n-hexane and water) are only 322 cm^{-1} and 643 cm^{-1} respectively. For the equilibrium between the neutral form and the anion, fluorimetric titration gives the pK_a^* value. This is the only pyrazole for which proton transfer equilibrium is attained in the excited state. A comparison of Förster cycle pK_a^* values with the $pK_a(FT)$ which is supposed to be the most accurate value,[25] shows that $pK_a^*(abs)$ is closer to $pK_a(FT)$ than the $pK_a^*(flu)$ value. The difference of 3.4 between $pK_a^*(abs)$ and $pK_a(FT)$ can be explained by the difference in thermal relaxations. But the difference of 10.4 between $pK_a^*(flu)$ and $pK_a^*(FT)$ is quite large. This large difference suggests that

some other process is taking place in the excited state. Compared to the neutral form, the fluorescence of the anion is largely red shifted and it is broad. This indicates that there may be stoichiometric complex formation between the solute and the solvent in the excited state. Low temperature fluorescence spectra of neutral and anionic forms are shown in fig. 6.8. The small red shift (2517 cm^{-1}) observed for neutral and anionic species at low temperature (77K) when compared to the redshift at room temperature (6085 cm^{-1}) for the same species also supports the conclusion of excited state complex formation.

Fluorescence of DPI^+ was not observed at room temperature due to the formation of 9,10-phenanthroimidazole. So the pK_a^* for the equilibrium between the cationic and the neutral forms was calculated only from absorption data. The resulting pK_a^* shows the pyridinic nitrogen atom to be more acidic in the excited state than in the ground state and the pK_a^* calculated from low temperature fluorescence shift also shows the same trend.

For the equilibrium between the neutral form and the anion, the difference, $pK_a^*(abs) - pK_a^*(flu) < 2$. This is due to the differences in the vibrational and solvent relaxations of both species. So in this case $pK_a^*(ave)$ (7.73) gives a better value.

pK_a values from fluorimetric titration

From the fluorescence titration curves (figs. 6.2 - 6.6) it is seen that in all the cases except for the equilibrium
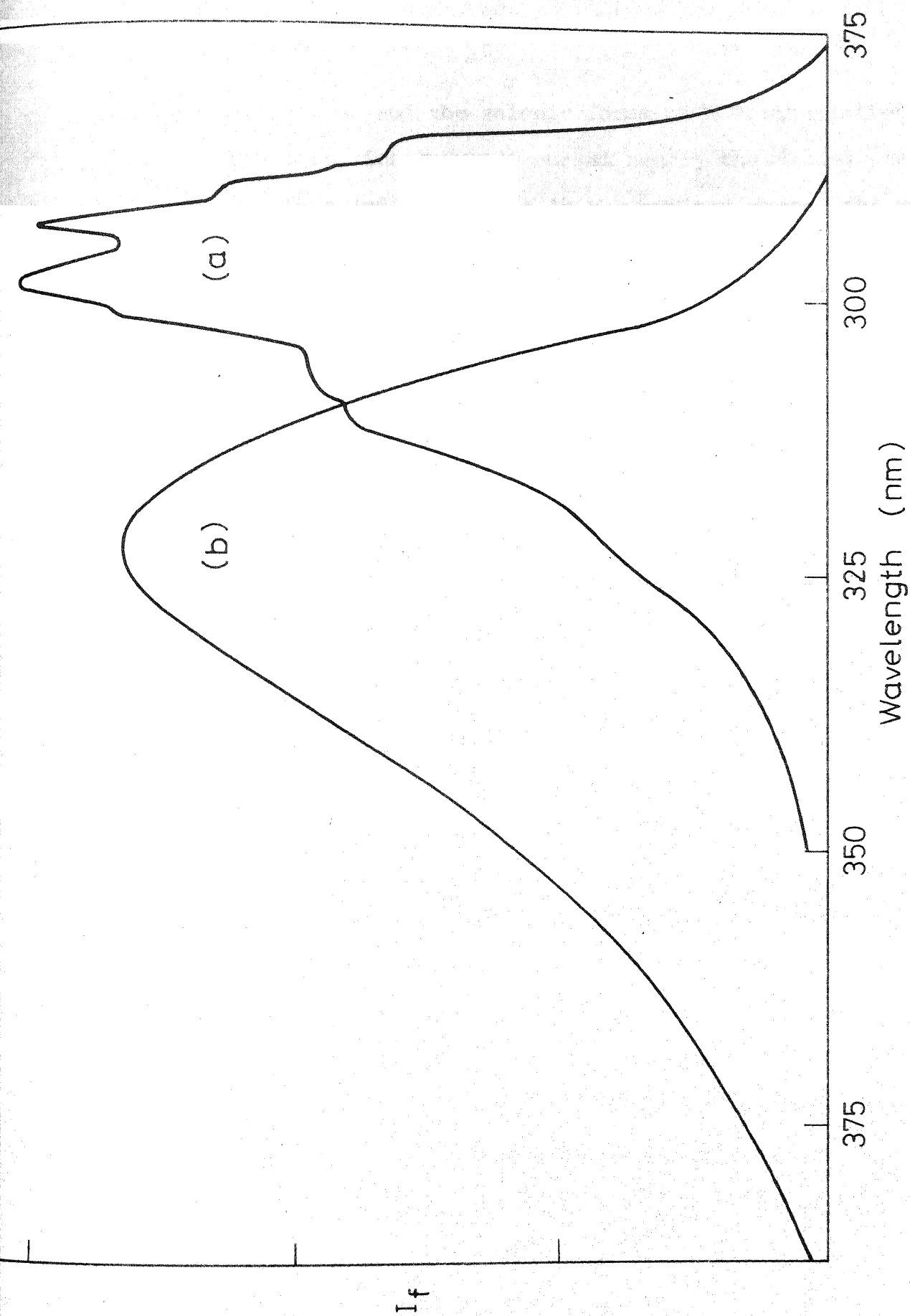
Fig. 6.8 Fluorescence spectra of 3-Methyl – 5-phenylpyrazole and its anion at 77 K
(a) Neutral form (~ pH 7) , (b) Anion (~ H_16).

between the neutral and the anionic forms of MPP, the inflection points in the titration curves occur at nearly the ground state pK_a values. This indicates that in the excited state, the rate of fluorescence is so fast that the molecule, before proton exchange, loses its energy by radiation. So the fluorescence emission is governed by the ground state prototropic equilibrium. Such a static protonation has been observed for most of the heterocyclic compounds whose pK_a^*s fall in the mid pH region[25,26,45,153] i.e. between 3 and 10. This may be either due to a short life time of the excited state or due to a lower concentration of protons in the mid-pH region, which makes the rate of proton exchange slower. Since a high concentration of a buffer has no effect on the fluorimetric titration, it appears that the static protonation is due to short life time of the species involved.

When there is static protonation for sparingly soluble substances in water the fluorimetric titration gives accurate ground state pK_a value.[154] For absorption measurements, 10^{-4}M solutions have to be prepared using mixed organic solvents where as for fluorescence measurements $\sim 10^{-6}$M solutions in water are sufficient due to its high sensitivity. In the cases of DPP and DPI, the saturated solutions are of 10^{-6}M concentrations. So the ground state dissociation constants of DPP and DPI in water obtained by fluoremetric titration are more meaningful than the

dissociation constants in mixed solvents, obtained by
absorptiometric titration for these compounds.

6.2.2. 9,10-Phenanthroimidazole

The pK_a values for both equilibria Eq(MN) and Eq(NA)
were determined spectrophotometrically. The values obtained
(4.65 and 11.86) are lower than those of benzimidazole (5.52 and
13.2). This is because of the presence of more electron with-
drawing groups (three fused phenyl rings) which lowers the
basicity and increases the acidity of the molecule.

The absorption and fluorescence maxima of PI, its anion
and the cation have been listed in Tables 4.2 and 5.2 respecti-
vely. The long wavelength absorption maxima and fluorescence
maxima which were used for the calculation of pK_a^* are given in
Table 6.6.

Table - 6.6

Long wavelength absorption maxima and fluorescence maxima
of the three forms of 9,10-Phenanthroimidazole

Species	Absorption maxima(cm^{-1})	Fluorescence maxima(cm^{-1})
Cation	29585	28090
Neutral	28735	26560
Anion	27322	24360

The pK_a^* values calculated for both equilibria from absorption and fluorescence data by using Förster cycle are given in Table 6.7 along with the pK_a values. Fluorimetric titrations were carried out by exciting the species at isosbestic points and the titration curves for Eq(MN) and Eq(NA) are shown in fig. 6.9. The resulting pK_a(FT) values 'are also given in Table 6.7.

Table - 6.7

Excited singlet state acidity constants of 9,10-Phenanthroimidazole

Equilibrium	pK_a	pK_a^*(abs)	pK_a^*(flu)	pK_a^*(ave)	pK_a(FT)
Eq(MN)	4.65	2.87	1.44	2.16	2.2
Eq(NA)	11.86	8.89	7.24	8.07	11.82

Comparing the pK_a^* values for the equilibrium between the cation and the neutral species, the difference between pK_a^*(abs) and pK_a^*(flu) is 1.43. This small difference is only due to an unequal solvent relaxation for the conjugate species in their ground and excited states. In neutral molecule the solvent relaxation for two extreme solvents (n-hexane and water) is only 500 cm^{-1}. Similarly a small difference of 0.8 between pK_a^*(flu) and pK_a(FT) is because of the use of band maxima instead of the
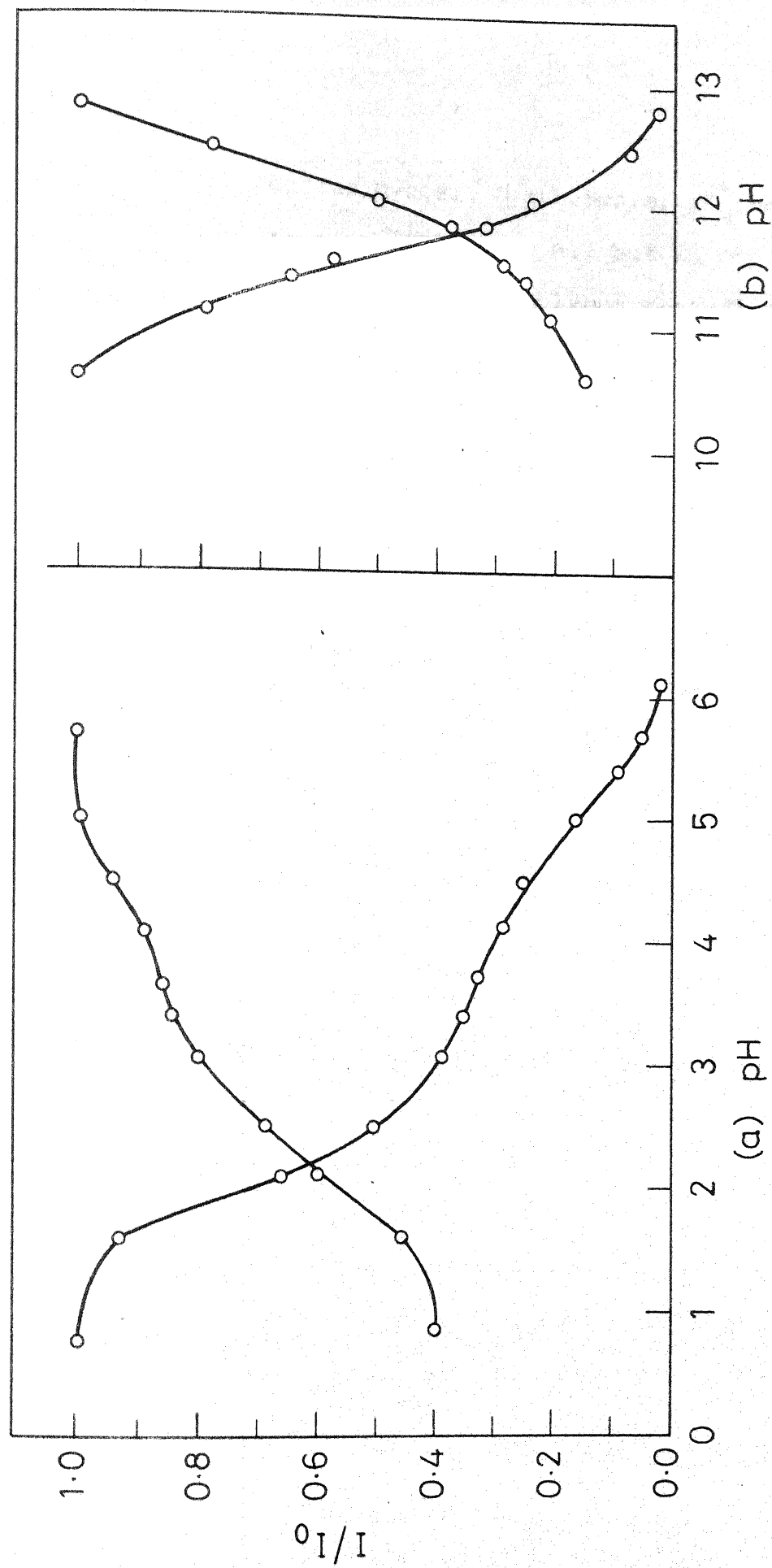
Fig. 6.9 Plot of relative fluorescence intensities of 9,10-Phenanthroimidazole Vs pH. (a) Cation and neutral form (b) Neutral form and anion.

0-0 band in the Förster cycle. Furthermore, pK_a^*(abs) and pK_a^*(flu) deviate from pK_a(FT) by $\sim$ 0.7 but in opposite directions confirming the unequal solvent relaxation. The pK_a^*(ave) of 2.16 is in excellent agreement with pK_a^* obtained from the fluorimetric titration. Under these circumstances the pK_a^* obtained by the method of averaging absorption and fluorescence maxima gives the best accurate value.

The difference between pK_a^*(abs) and pK_a^*(flu) for Eq(NA) is also not much and it can be explained as has been done for Eq(MN). Accordingly the pK_a^*(ave) of 8.07 is more accurate than pK_a^*(abs) or pK_a^*(flu). Since the fluorimetric titration yields only the pK_a, a comparison of pK_a^* values from the Förster method could not be made. The pK_a obtained by fluorimetric titration shows that excited state prototropic equilibrium is not attained during the life times of excited species. This behaviour is generally observed for the compounds whose pK_a^*s fall in the mid pH region. So in this case because of the low concentration of protons at a pH of 8.07, the rate of proton transfer is slower than that of fluorescence, although the rate constant for the former is supposed to be large. This conclusion is also supported by the displacement of the excited state equilibrium with an increase in the concentration of buffers. The effect of buffers on this equilibrium will be discussed in the next chapter.

An unusual behaviour observed in this compound is the decrease in the basicity of pyridinic nitrogen atom in the excited state. The pK_a^* values obtained by all the four methods show this behaviour, which is contrary to the usual trend observed in pyridine,[152] pyrazoles (sec. 6.2.1) etc., indicating that the lone pair which is supposed to be in one of the sp^2 orbitals is more involved in the π cloud interaction of the molecule. This kind of behaviour was observed to some extent in benzimidazoles[128] also but not in indazole (sec. 7.3.1). Thus the pyridinic nitrogen in this molecule behaves more or less like amino nitrogen. These results support the conclusion made earlier on the solvent effects on absorption and fluorescence of PI.

The fluorimetric titration for the equilibrium between the monocation and the neutral form gives a stretched sigmoid curve (fig. 6.9.a) covering both ground and excited state pK_a regions. This indicates that in the excited state the rate of the reaction is comparable to that of fluorescence. This kind of behaviour will be discussed in detail using excited state kinetics in the case of HP (sec. 6.2.4). The large flat region between the ground and the excited state pK_a observed in the fluorimetric titration curves of β -naphthol[155] and HP is absent here because in this compound both ground and excited state pK_as are close to each other.

6.2.3. <u>9-Aminophenanthrene</u>

The pK_a^* value for the Eq(MN) was determined by Tsutsumi et.al.,[129] from Förster cycle using the average of absorption and fluorescence maxima. We have carried out a study of the pH dependence of fluorescence of this compound inorder to find out whether the equilibrium of this reaction is established in the excited state or not and to determine the pK_a^* value for the equilibrium between the neutral molecule and the anion. The fluorimetric titration curves for both equilibria are shown in fig. 6.10. The pK_a^* value reported in the literature and the pK_a^* values determined in this work by fluorimetric titration are given in Table 6.8. The pK_a value for the Eq(NA) is not reported since it could not be determined due to the reasons discussed in the section 6.1.

<u>Table - 6.8</u>

Excited singlet state acidity constants of 9-Aminophenanthrene

Equilibrium	pK_a	pK_a^*(ave)	pK_a(FT)
Eq(MN)	3.5^a	-3.2^a	-3.6
Eq(NA)	>14.00		12.18

a. From ref. 129.

The effect of acidity on the fluorescence intensity of 9-aminophenanthrene (fig. 6.10·a) shows that fluorescence is quenched with a decrease in pH/H_o. The middle of quenching occurs at pH 1.1. But phenanthrylammonium ion starts fluorescing only from $H_o \leqslant$ -1 and its intensity increases with an increase in the acidity. The point of inflection of this fluorimetric titration curve occurs at H_o -3.6. The value of H_o -3.6 is the excited state pK_a and it is in good agreement with the value (H_o -3.2) obtained by the Förster cycle method. The small difference of 0.4 in pK_a^* calculated by two methods can be explained on the same lines as has been done for PI. The initial quenching of fluorescence of the neutral form before the formation of the cation is also observed in α and β -naphthylamines.[149] As suggested by Schulman et.al.,[156] the fluorescence quenching may be due to the formation of a non fluorescent solvent-solute cation complex in the ground state. This complex loses its energy before the formation of the neutral form by its decomposition in the excited state.

The fluorescence of the neutral form is again quenched when pH is increased above 10.5 due to the formation of the imino anion. The middle of quenching occurs at a pH of 12.8 which is the pK_a^* for the equilibrium between the neutral form and the anion. When the pH is increased beyond 14 a new fluorescence peak which is blue shifted relative to the neutral form appears. Fig.6.11 represents the fluorescence spectrum
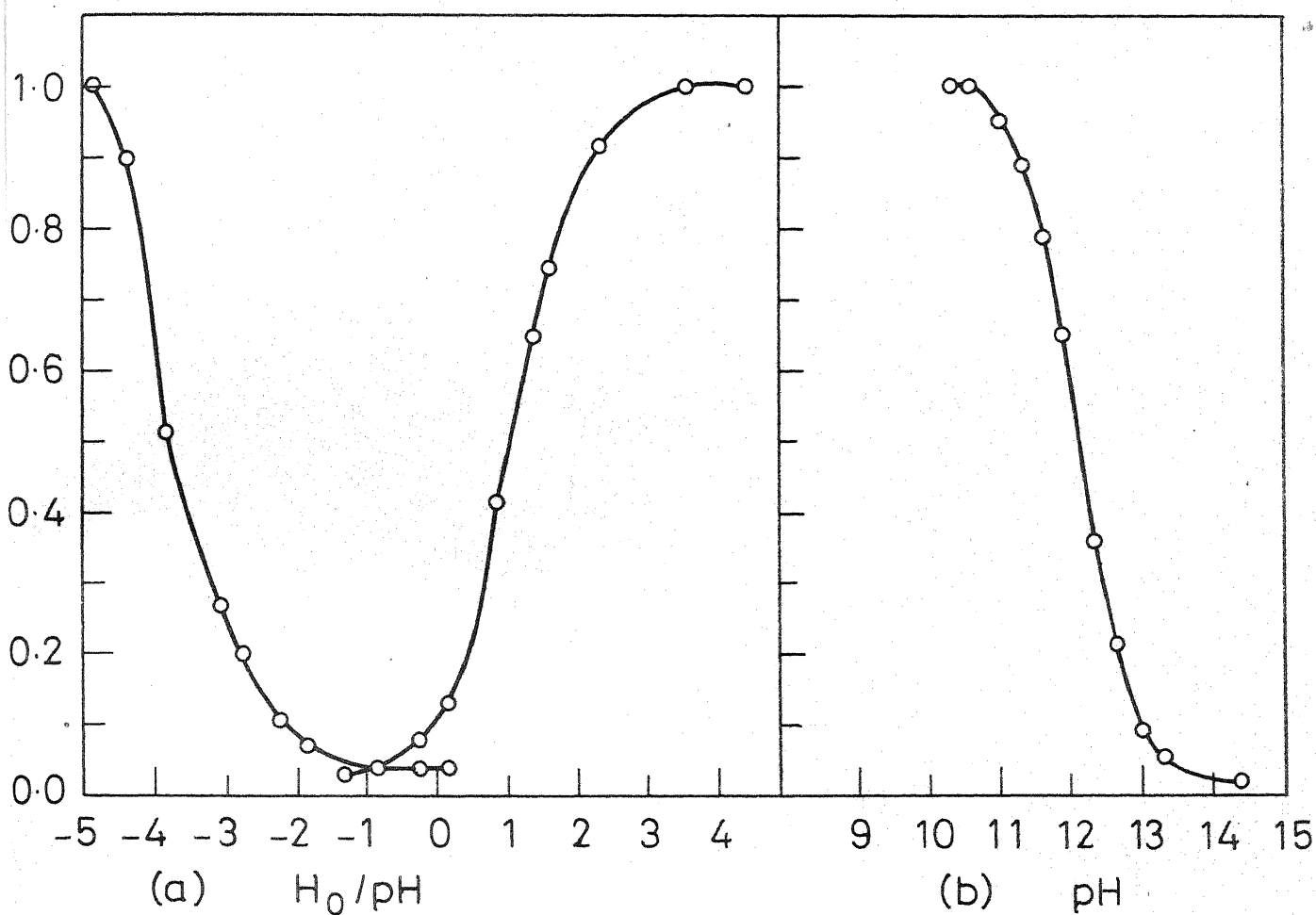
6·10 Plot of relative fluorescence intensities of 9 Amino-
phenanthrene Vs pH/H$_0$ (a) Cation and neutral form
(b) Neutral form.
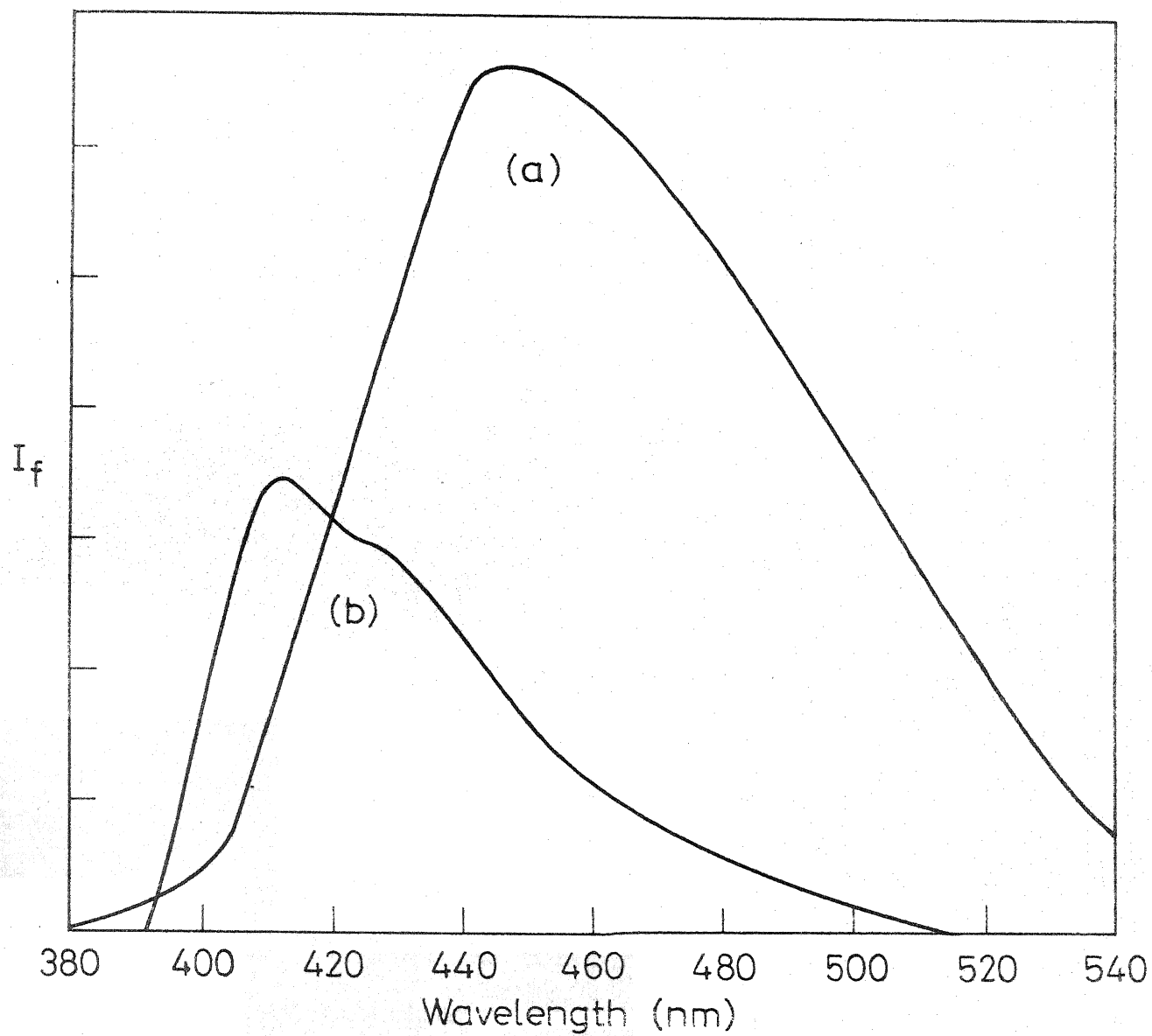
Fig. 6·11 Fluorescence spectra of 9-Aminophenanthrene
(a) Neutral form (pH~7), (b) Dianion (H_ 15·2)

at pH 7 and at H_- 16. The intensity of this peak increases upto H_- 16.75 ($\sim$ 8 M NaOH) but it decreases with further increase in the concentration of NaOH. α and β -naphthylamines[128] were also found to behave in a similar way. This may be due to the formation of a dianion in the excited state. Fluorimetric titration could not be used to calculate the pK_a^* value for the equilibrium between the mono- and the dianions because the isosbestic point in this region is not constant. But a blue shift in the band maxima when compared to the neutral form indicates qualitatively that NH^- is a very weak acid compared to the amino group.

6.2.4. 9-Hydroxyphenanthrene

The pK_a value for 9-hydroxyphenanthrene was determined spectrophotometrically. The absorption spectrum of its anion is so broad that its maxima could not be correlated with the corresponding band maxima in the absorption spectrum of the neutral form as the latter is structured. Hence the pK_a^* value was calculated by the Förster cycle, only using the fluorescence shift. A fluorimetric titration was done from H_o -1 to pH 13, and the titration curve is shown in fig. 6.12. The pK_a^* values determined by these methods are listed in Table 6.9 along with the fluorescence maxima of both forms.
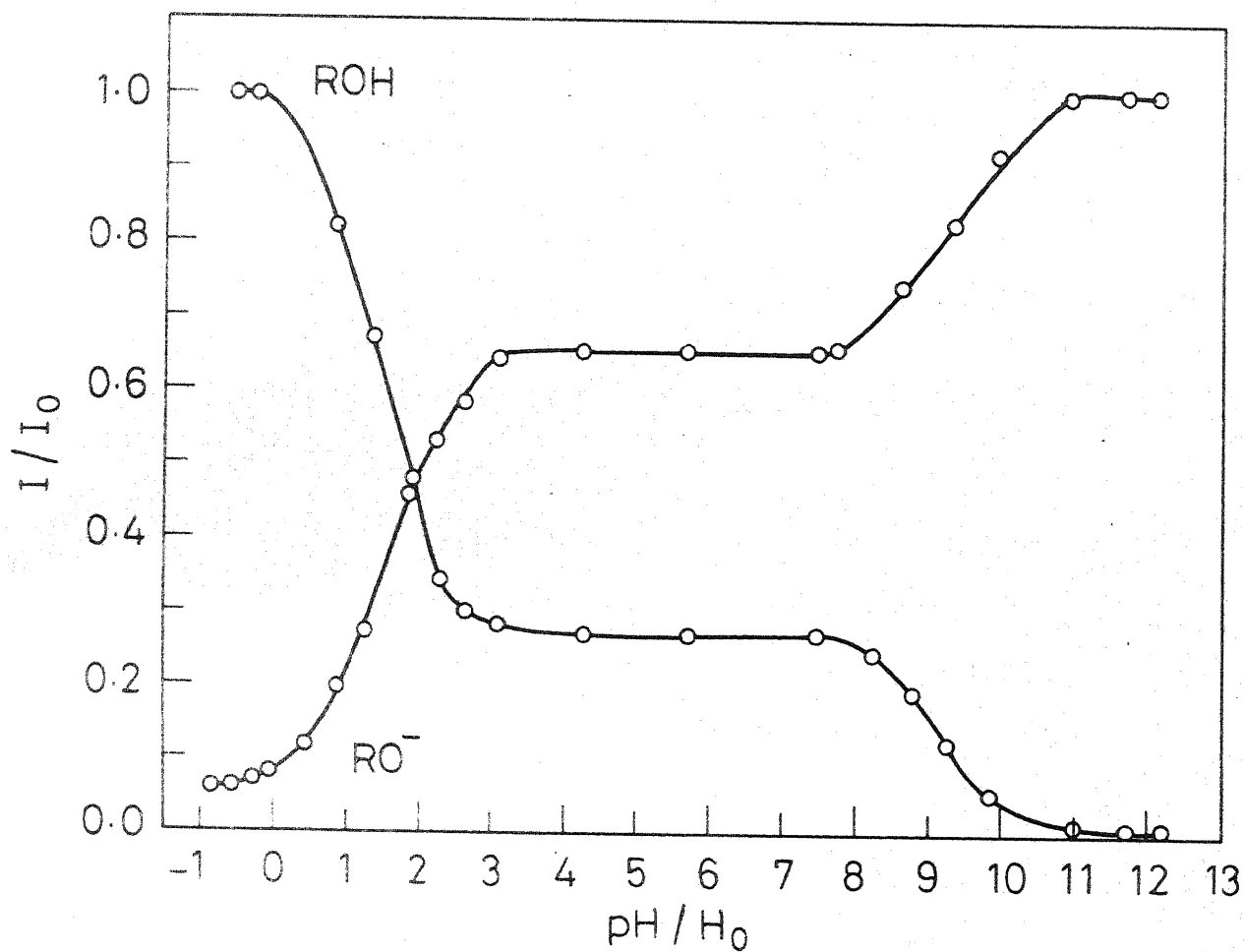
Fig. 6·12 Plot of relative fluorescence intensities of
9-Hydroxyphenanthrene and its anion Vs pH/H_0.

Table - 6.9

Excited singlet state acidity constants of 9-Hydroxyphenanthrene

Equilibrium	$\bar{\nu}_{BH}(cm^{-1})$	$\bar{\nu}_{B^-}(cm^{-1})$	$pK_a^*(flu)$	$pK_a(FT)$
Eq(NA)	25974	20833	-1.75	1.9

Fluorimetric titration always yields an accurate pK_a^* value. The difference of 3.65 between $pK_a^*(flu)$ and $pK_a(FT)$ must be due to the increased charge transfer interaction at the anion in the excited state resulting in a larger solvent relaxation error.

The fluorimetric titration curves are stretched sigmoid curves with two inflection points, one of which corresponds to pK_a and the other to pK_a^*. Even though the point with $I/I_0 = I'/I_0' \approx 0.5$, occurs at pK_a^*, the extension of the curve upto pH 12 shows that the equilibrium in the excited state is not completly attained. This type of curve indicates that the rate of proton transfer in the excited state is comparable to the rate of fluorescence. The shape of the fluorimetric titration curve obtained can be explained on the basis of kinetics of excited state proton exchange taking place in HP.

At pH ≈ 1 the excited molecule dissociates forming the anion. In this pH range H_2O is the only proton acceptor and so

the excited state proton transfer reaction can be written as

$$ROH + H_2O \underset{k_{-a}}{\overset{k_a}{\rightleftharpoons}} RO^- + H_3O^+ \qquad \ldots 6.3$$
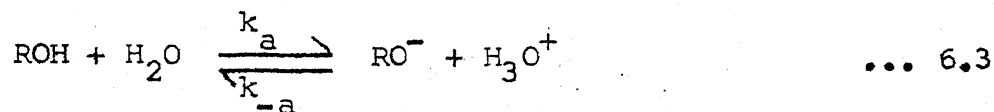
If the equations derived by Weller,[5,37] using simple steady state kinetics are applied, then relative quantum yields of $ROH(\emptyset/\emptyset_o)$ and $RO^-(\emptyset'/\emptyset_o')$ are given by,

$$\emptyset/\emptyset_o = \frac{1 + k_{-a}\,\tau'_o\,[H_3O^+]}{1 + k_a\tau_o + k_{-a}\,\tau'_o[H_3O^+]} \qquad \ldots 6.4$$

and

$$\emptyset'/\emptyset_o' = \frac{k_a\,\tau_o}{1 + k_a\,\tau_o + k_{-a}\,\tau'_o[H_3O^+]} \qquad \ldots 6.5$$

where τ_o and τ'_o are the life times of ROH and RO^- respectively.

If the rate of reaction with the solvent in eq.(6.3), that is , $ROH + H_2O \longrightarrow RO^- + H_3O^+$ is comparable to or greater than the rate of fluorescence of ROH, and the rate of the second order protonation of RO^- is much less than the rate of fluorescence, the eq. (6.4) and (6.5) become

$$\emptyset/\emptyset_o = \frac{1}{1 + k_a\tau_o} \qquad \ldots 6.6$$

$$\emptyset'/\emptyset_o' = \frac{k_a\,\tau_o}{1 + k_a\,\tau_o} \qquad \ldots 6.7$$

They show that $\emptyset/\emptyset_o$ and $\emptyset'/\emptyset'_o$ are independent of $[H^+]$ or $[OH^-]$. A plot of $\emptyset/\emptyset_o$ or $\emptyset'/\emptyset'_o$ Vs $[H^+]$ or $[OH^-]$ should give a flat horizontal line for each species as we see for the neutral and anionic forms of 9-phenanthrol in the pH range 3.2 - 7.7. The independence of $\emptyset/\emptyset_o$ and $\emptyset'/\emptyset'_o$ on pH may be due to small values of k_{-a} relative to $1/\tau'_o$ or due to low concentration of protons since at low pH (about 0.1) the excited 9-phenanthrolate ion from excited 9-phenthrol gets reprotonated quickly. As the pH increases the reprotonation rate becomes smaller and at pH >3, the rate becomes negligible. So $\emptyset/\emptyset_o$ settles down to the plateau value of $\frac{1}{1+k_a\tau_o}$ and $\emptyset'/\emptyset'_o$ to $k_a\tau_o/1+k_a\tau_o$. At 25°C the following values were obtained for the flat region of the curves i.e.
$\emptyset/\emptyset_o = 0.265, \emptyset'/\emptyset'_o = 0.75$. Thus knowing $\emptyset/\emptyset_o$ and $\emptyset'/\emptyset'_o$ and the lifetimes of both species the rate constants k_a and k_{-a} can be determined.

A similar behaviour was observed for β-naphthol by Weller[155] and the $\emptyset/\emptyset_o$, $\emptyset'/\emptyset'_o$ values obtained for the flat region of the curve were 0.73 and 0.28 respectively. The difference between these two molecules is in the extent of the proton transfer reaction in the excited state. In β-naphthol only 28% of the molecules undergo dissociation (deprotonation) at the pK_a^* whereas in 9-phenanthrol 75% of the molecules get deprotonated in the excited state. This could be due to the longer lifetime of 9-phenanthrol relative to β-naphthol.

6.2.5. 5-Aminoindazole

Absorption spectra of 5-aminoindazole have been studied in the basicity/acidity range from H_- 16 to H_o -4. Four ground state prototropic species (fig. 6.14), the neutral molecule(III), a monocation(II), a dication(I), and an anion(IV) have been observed. The absorption spectra of these compounds are shown in fig. 6.13. The blue shift observed in the absorption spectrum of the monocation and its resemblence with absorption spectrum of indazole[142] shows that the first protonation in the ground state occurs at the amino group. The absorption spectrum of the dication is red shifted to the monocation and it is due to the protonation at the ring nitrogen atom.

The absorption spectra of the anion is red shifted as compared to the neutral form and the pK_a for the equilibrium between the neutral molecule and the anion is found to be 14.59 which is slightly greater than the pK_a of indazole. These results indicate that the anion involved in the equilibrium is the one deprotonated at the ring nitrogen atom. From the absorption spectra of these species the ground state equilibrium reactions can be written as shown in fig. 6.14.

The fluorescence spectrum of this compound have been studied in the range H_- 16 to H_o -10. The neutral species shows a fluorescence maxima at 408 nm. When the pH is lowered below 4.5, the fluorescence intensity at 408 nm. starts
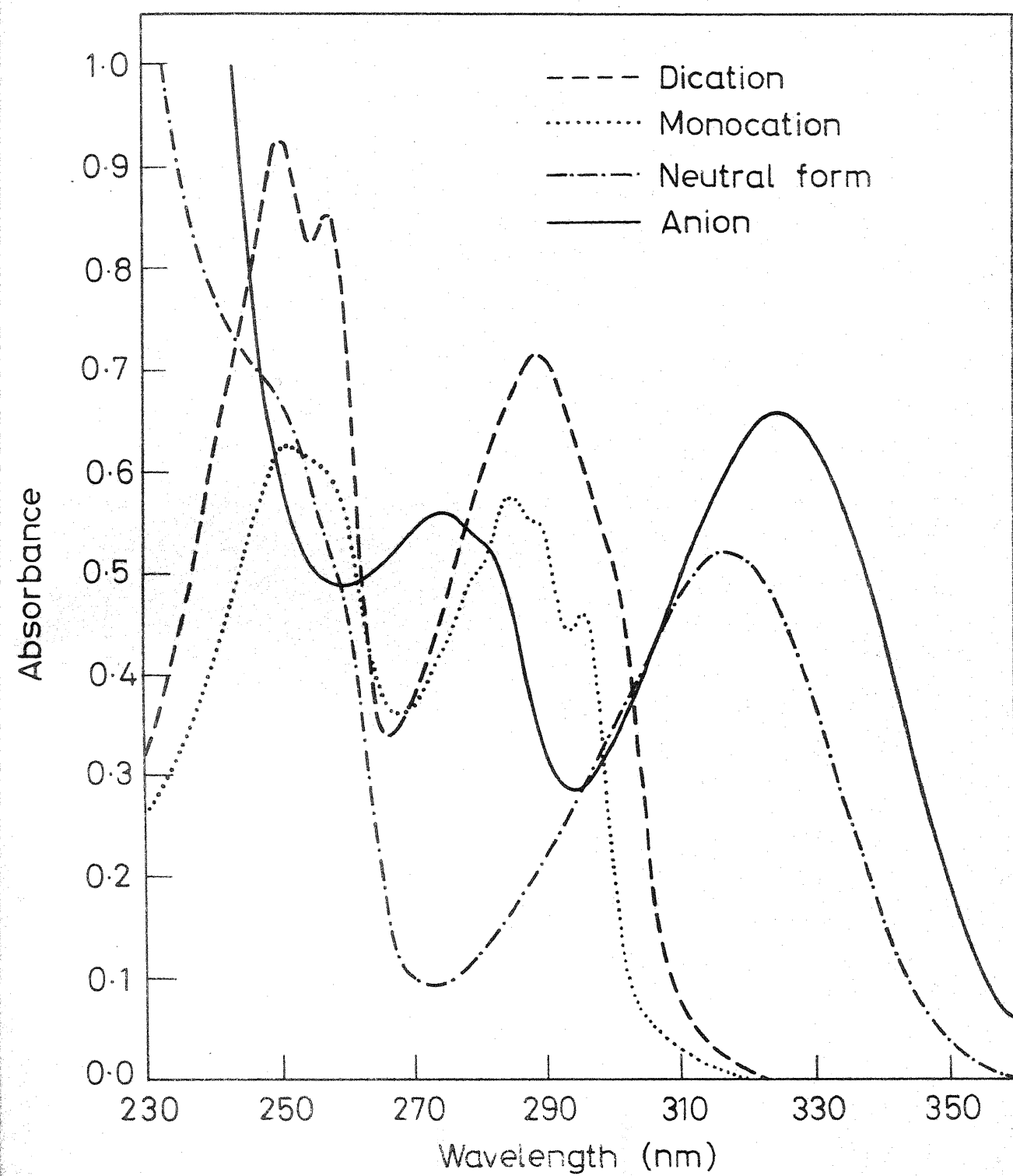
Fig. 6·13 Absorption spectra of 5-Aminoindazole.
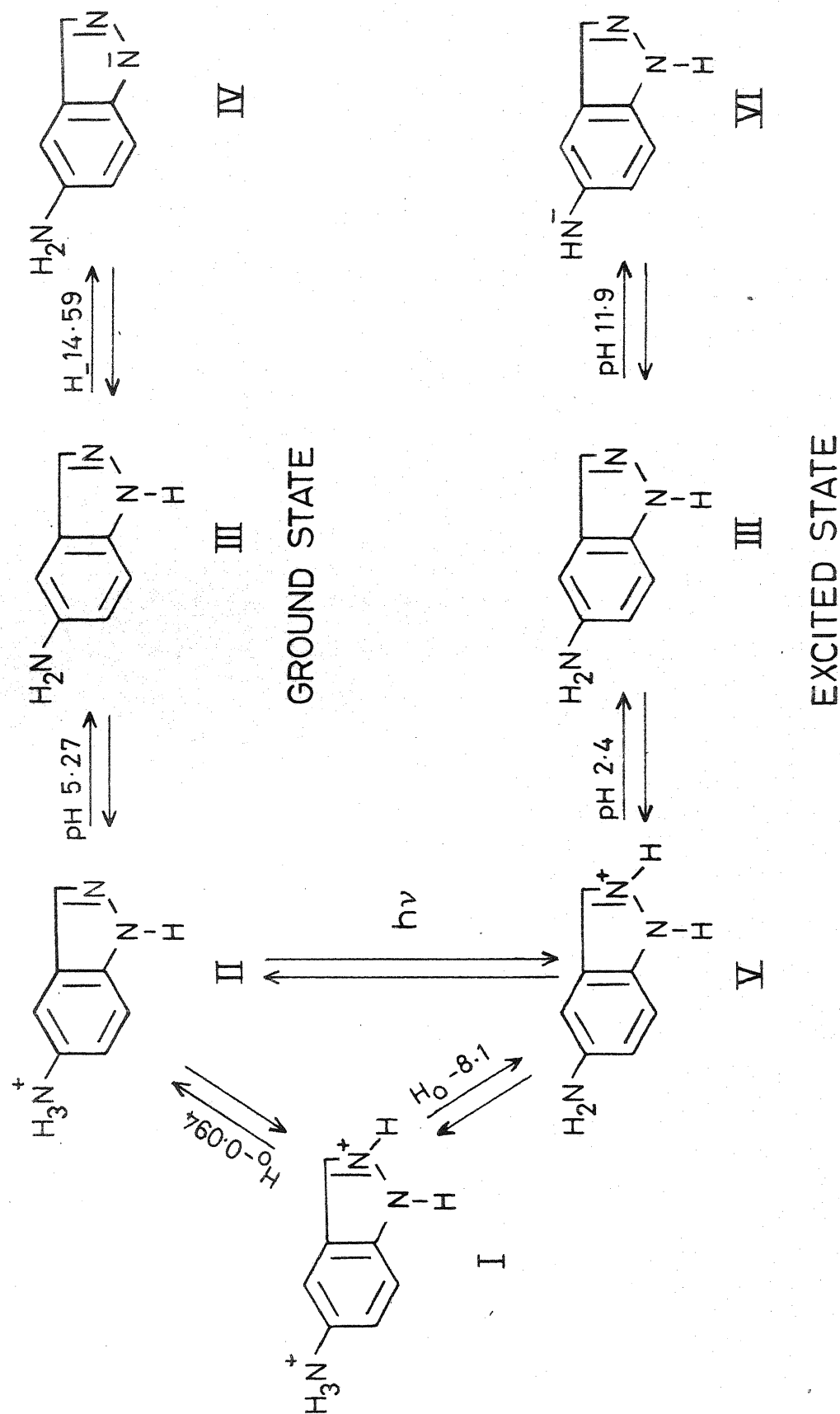
Fig. 6.14 Scheme of Ground and Excited state equilibria of 5-Aminoindazole at different $H_0/pH/H_-$ I. Dication II. Indazolammonium ion III. Neutral form IV. 5-Aminoindazole anion V. 5-Aminoindazole cation VI. Imino anion.

decreasing and a new band with very low intensity starts appearing at 505 nm. The intensity of the new band is relatively so weak (even at H_O -1.12 its intensity is 30 times less than that of the neutral form at 408 nm) that its appearence could be detected only below pH 1.2. This band is due to the formation of the monocation and its formation is complete at pH 0.2.

A further decrease of H_O results in the quenching of the fluorescence at 505 nm and it is nearly complete at H_O -5. At this stage another new band with a λ_{max} at 363 nm starts appearing and this band is found to be due to the formation of the dication. On the other hand when the pH is increased from 7 to 10, the fluorescence of the neutral form at 408 nm gets quenched and the quenching is complete at pH 14 without the appearance of any other fluorescence band. Above pH 14, upto H_- 16, no fluorescence is observed at room temperature. Fluorescence spectra of different excited state species are shown in fig. 6.15. The absorption and fluorescence maxima of different forms of 5-aminoindazole are given in Table 6.10 and the $pH/H_O/H_-$ at which the spectra were recorded are given in brackets.
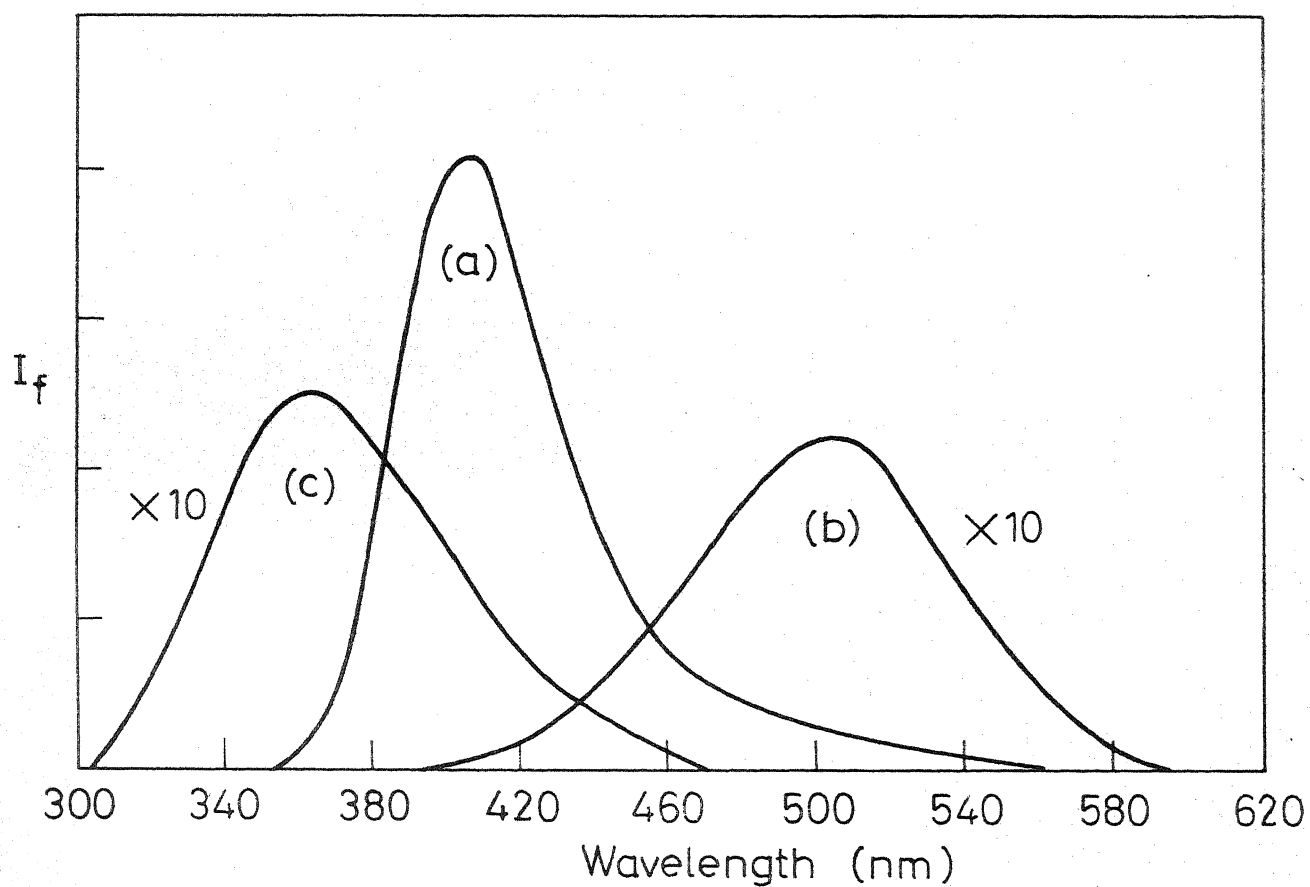
Fig. 6·15 Fluorescence spectra of 5-Aminoindazole (a) Neutral form (~pH 7), (b) Monocation (Ho -0·5), (c) Dication (~ Ho -9)

Table - 6.10

Absorption and fluorescence maxima (cm^{-1}) of various forms
of 5-Aminoindazole

Species	Absorption maxima at 298K	Fluorescence maxima at 298K	Fluorescence maxima at 77K
Dication	40160		
	38910 (H_o -2.5)	27548 (H_o -9.0)	
	34722(m)		
Mono-cation	39840		
	38910		
	35211(m)(pH 2.5)	19801 (H_o -1)	
	34722(s)		
	33898		
Neutral form	31645 (pH 8.5)	24509 (pH 3)	
Anion	30864 (H_- 16)		26007 (H_- 16)

a. **Excited state equilibrium between the Monocation and the Neutral form**

The monocation fluorescence is largely red shifted in comparision to the neutral form and the monocation formed may be due to the protonation either at the ring nitrogen atom or at the amino group. If the protonation had occured at the

latter position, the fluorescence maxima should have been blue shifted, as observed for other amino compounds.[129] Also the fluorescence spectrum of the monocation should have resembled the indazole fluorescence spectrum as did the absorption spectrum and also as noticed in other aromatic amines,where the fluorescence spectra of the protonated forms resemble those of the parent molecules.

To prove further that the protonation at the amino group should result in a blue shift in fluorescence, we prepared the salt indazolammonium chloride. The structure was confirmed by the absorption spectra of the salt in acetonitrile, methanol and water solutions. Due to its very poor solubility, the spectra could not be recorded in nonpolar solvents. Fluorescence spectra of the salt recorded in different solvents at room temperature and in methanol at low temperature are shown in fig. 6.16. The absorption and fluorescence maxima are reported in Table 6.11.
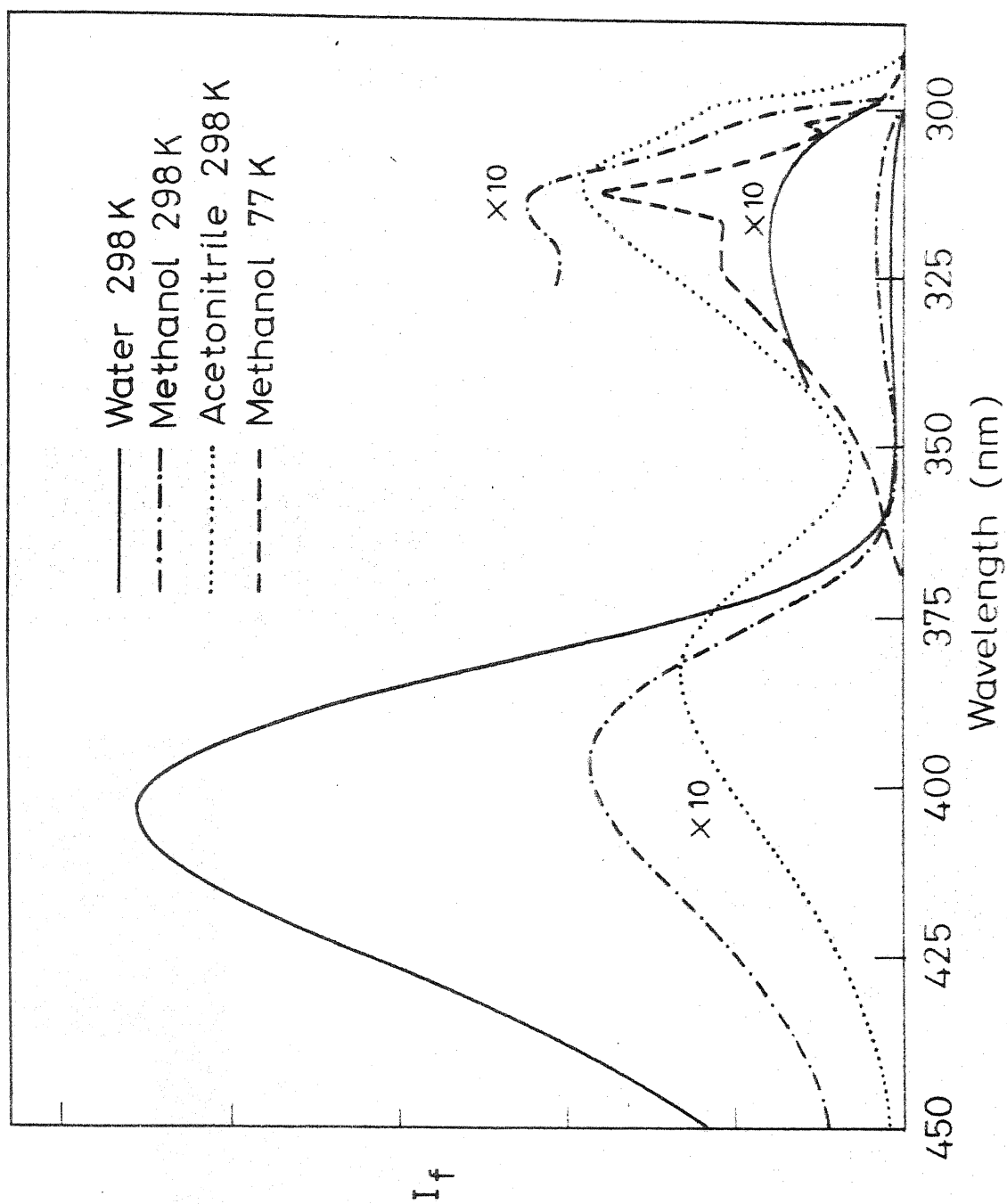
Fig. 6.16 Fluorescence spectra of Indazolammonium chloride in different solvents.

Table - 6.11

The absorption and fluorescence maxima (cm^{-1}) of indazola-
mmonium chloride in different solvents

Solvent	Absorption maxima	Fluorescence maxima
Acetonitrile	39682	33333
	34843	32514,25940
Methanol	39525	31796
	38910	25094
	34843	
	34482	
	33613	
Water	39682	31250
	39062	24539
	35087	
	34602	
	33783	

In all solvents at room temperature two fluorescence bands
appear, one near 310 nm, corresponding to the indazolammonium
ion (close to the indazole fluorescence) and another at a
longer wavelength, corresponding to the neutral form. This
shows that indazolammonium ion, being unstable in the excited
state dissociates to the neutral form and the dissociation
increases as the solvent is changed from acetonitrile to water.

But at the low temperature (77K), due to the rigidity of the medium, the dissociation can not occur. Hence the fluorescence in methanol at 77K has no band corresponding to the neutral form and the shape of the spectrum matches with the fluorescence of indazole. These results again confirm that a blue shift should have been observed if the protonation in the excited state had occured at the amino group. So from the red shift obtained by decreasing the pH, we conclude that the protonation in the excited state occurs only at the ring nitrogen atom.

Fluorimetric titration was carried out for this equilibrium by measuring the variation of fluorescence intensity of the neutral form with pH and the titration curve is shown in fig. 6.18. The variation of the fluorescence intensity of the monocation at 505 nm with pH/H_o could not be measured due to its weak emission relative to the emission of the neutral form. The middle of the quenching of the neutral form occurs at pH 2.58 and this is the pK_a^* between the neutral form and the ring nitrogen protonated monocation (5-aminoindazole cation).

b. The equilibrium between the mono- and the dication

The 5-aminoindazole cation fluorescence has a maximum at 505 nm whereas the dication has a maximum at 363 nm. The blue shift shows that the protonation has occured now at the amino group and thus reiterates our earlier conclusion that the first protonation occurs at the ring nitrogen atom. Fluorimetric
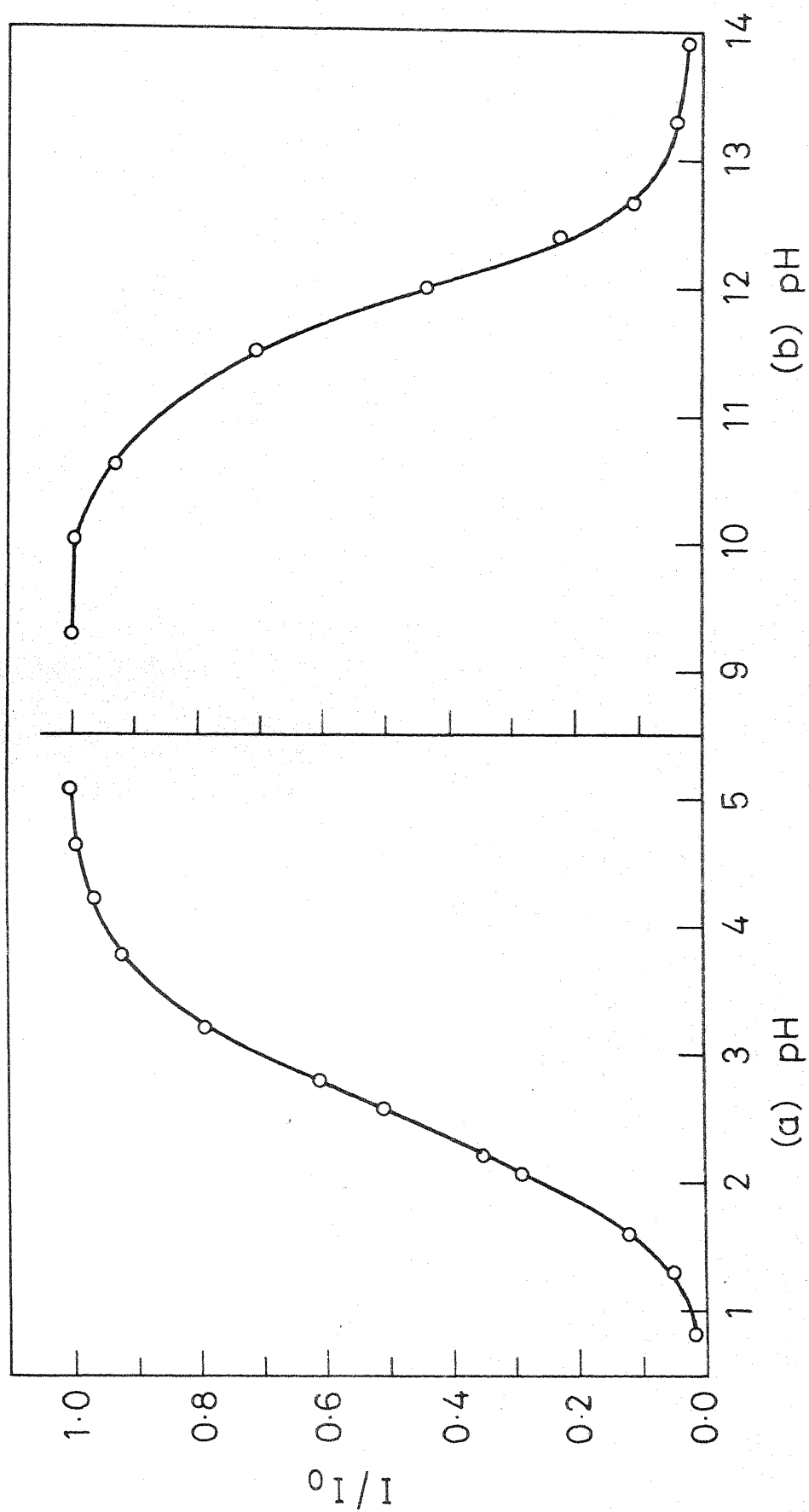
Fig. 6.17 Plot of relative fluorescence intensities of 5-Aminoindazole Vs pH.
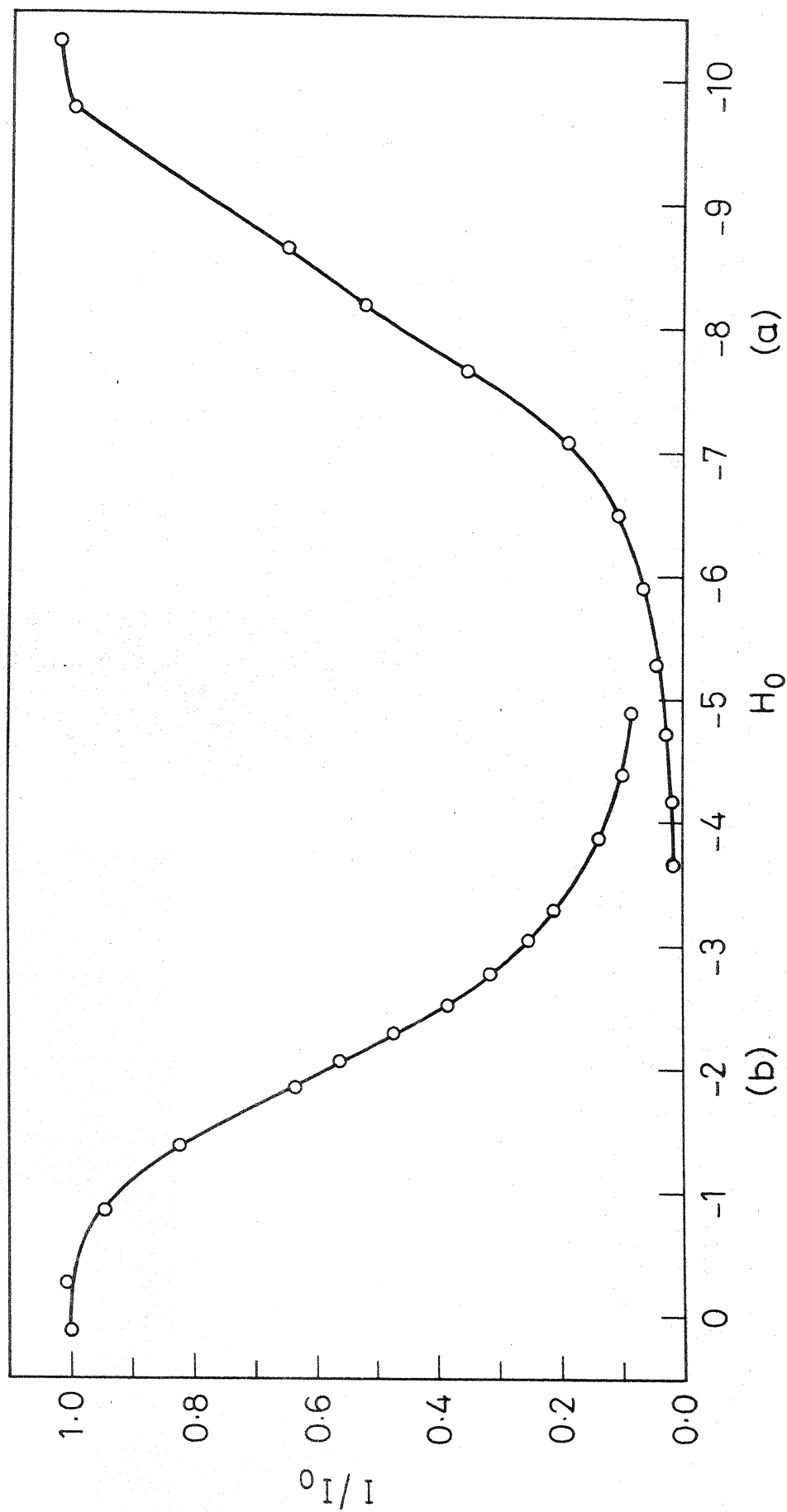
Fig. 6.18 Plot of relative fluorescence intensities of 5-Aminoindazole Vs H_0
(a) Dication   (b) Monocation

titration was carried out for both species and the titration curves are shown in fig. 6.17. The fluorescence of 5-amino-indazole cation is quenched and the middle of quenching occurs at H_O -2.1 but the mid point of dication formation occurs at H_O -8.1. This kind of quenching behaviour before the attainment of equilibrium in the excited state is quite common in amino compounds such as α, β -naphthylamines,[149] and phenanthrylamine (sec. 6.2.3). As explained in 9-aminophenanthrene, the initial quenching observed for the monocation may be due to the formation of a non fluorescent ground state complex and not to the forma-tion of a dication. Hence the mid point of inflection in the formation curve gives the pK_a^* value for the equilibrium between the mono- and the dication.

c. Equilibrium between the Neutral form and the Anion

Fluorescence quenching of the neutral form without the appearance of a new band above pH 10 is due to the formation of the iminoanion and not the 5-aminoindazole anion. A similar behaviour has been observed in amino compounds[13] where there can be only the formation of an iminoanion. Moreover if 5-amino-indazole anion is formed the fluorescence of the ion might have been observed as in indazole anion.[128] To substantiate this further, the fluorescence spectrum of 5-aminoindazole anion at H_- 16 and at 77 K was recorded and shown in fig. 6.19. At this
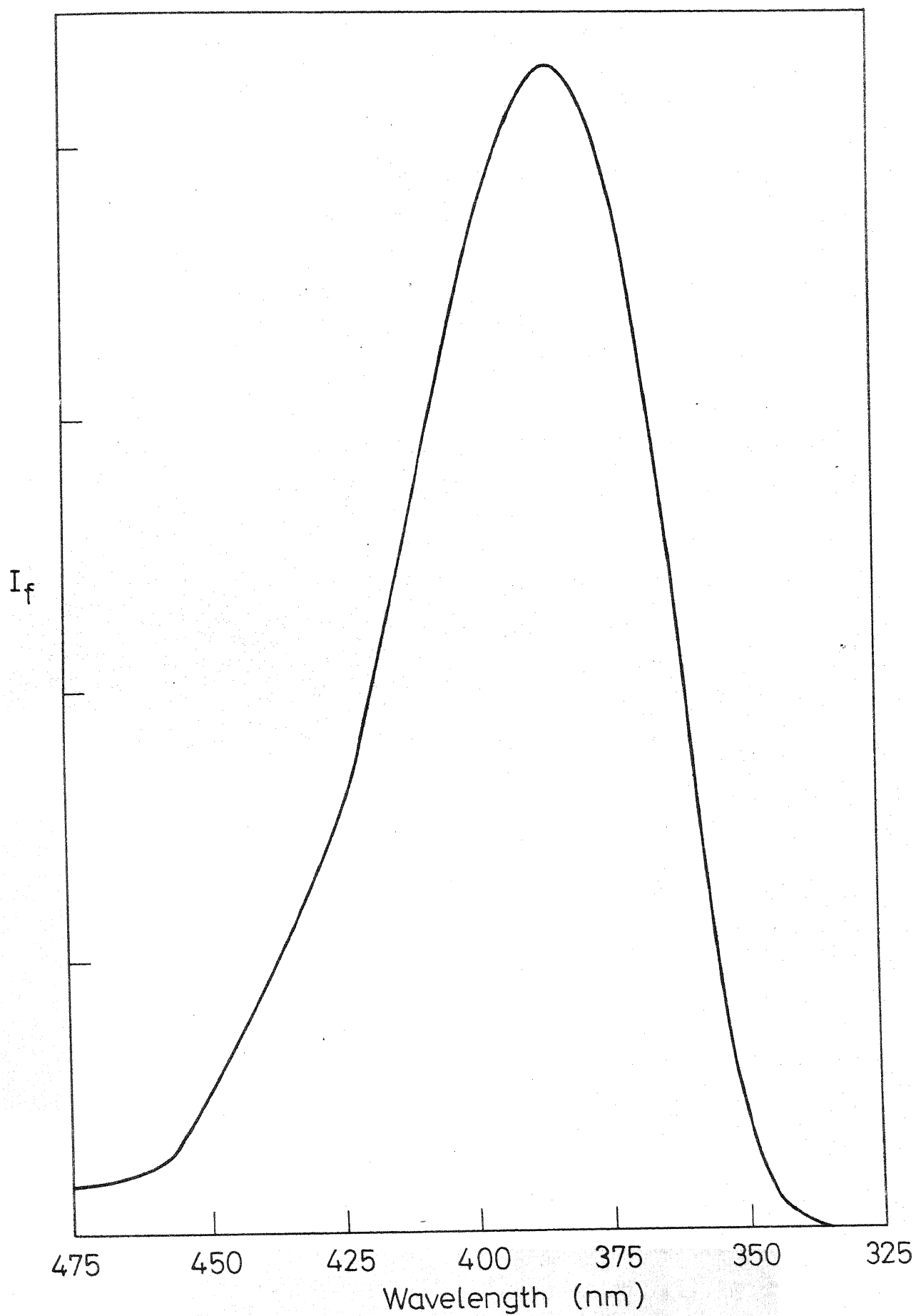
Fig. 6.19 Fluorescence spectrum of 5-Aminoindazole anion at 77 K (H_16).

low temperature only the ground state species i.e. 5-aminoindazole anion can exist as confirmed by its fluorescence. These results demonstrate that the quenching behaviour is due to the formation of the iminoanion in the excited state. Fluorimetric titration was carried out and the titration curve is shown in fig. 6.18. The mid point of quenching occurs at 11.9 which is the pK_a^* for the equilibrium between the neutral form and the iminoanion. Further increase in pH does not give rise to any fluorescence as in other aromatic amines, indicating that there is no formation of a dianion in this case.

In all the three equilibria discussed so far it has been found that any of the the species involved in the ground state equilibria is different from those involved in the excited state equilibria. Since Förster cycle is applicable only when pK_a and pK_a^* in the equation (3.8) correspond to the same equilibrium in the ground and the excited state, calculation of pK_a^* values by using Förster cycle methods has no meaning in these cases.

d. Biprotonic Phototautomerism

Biprotonic phototautomerism generally occurs when the proton donor and acceptor groups in a molecule are well separated.[157] 5-Aminoindazole is such a molecule where the proton donor group ($-NH_2$) is present in the homocyclic ring and the proton acceptor group (pyridine type nitrogen atom) is present in the heterocyclic ring. At pH 1.4, in the ground state,

the monocation that exists is indazolammonium ion . When it is excited, it decomposes and the protonation occurs at the ring nitrogen atom. This is found out by the absorption and emission spectra of 5-aminoindazole at pH 1.4 (fig. 6.20). The absorption spectrum corresponds to the indazolammonium ion whereas the fluorescence spectrum shows the presence of the neutral and the ring nitrogen protonated monocation, indicating that at this pH 5-aminoindazole and its cation are in equilibrium in the excited state.

Deprotonation at one site and protonation at another in the excited state would be assisted by a suitable solvent such as methanol or water. It is clear from the spectra of indazolammonium chloride in methanol and water at room temperature and in methanol at low temperature (fig. 6.16) that dissociation takes place in the excited state at room temperature. But the fluorescence maxima of the 5-aminoindazole cation at 505 nm could not be detected in aqueous solution since at this pH ($\sim$3) the protonation of the ring nitrogen atom can not occur. At low temperature, indazolammonium cation does not decompose during the life time of the species.

From the above results, a scheme of ground and excited state equilibria taking place in the whole range of H_o/pH/H_- is proposed as shown in fig. 6.14.
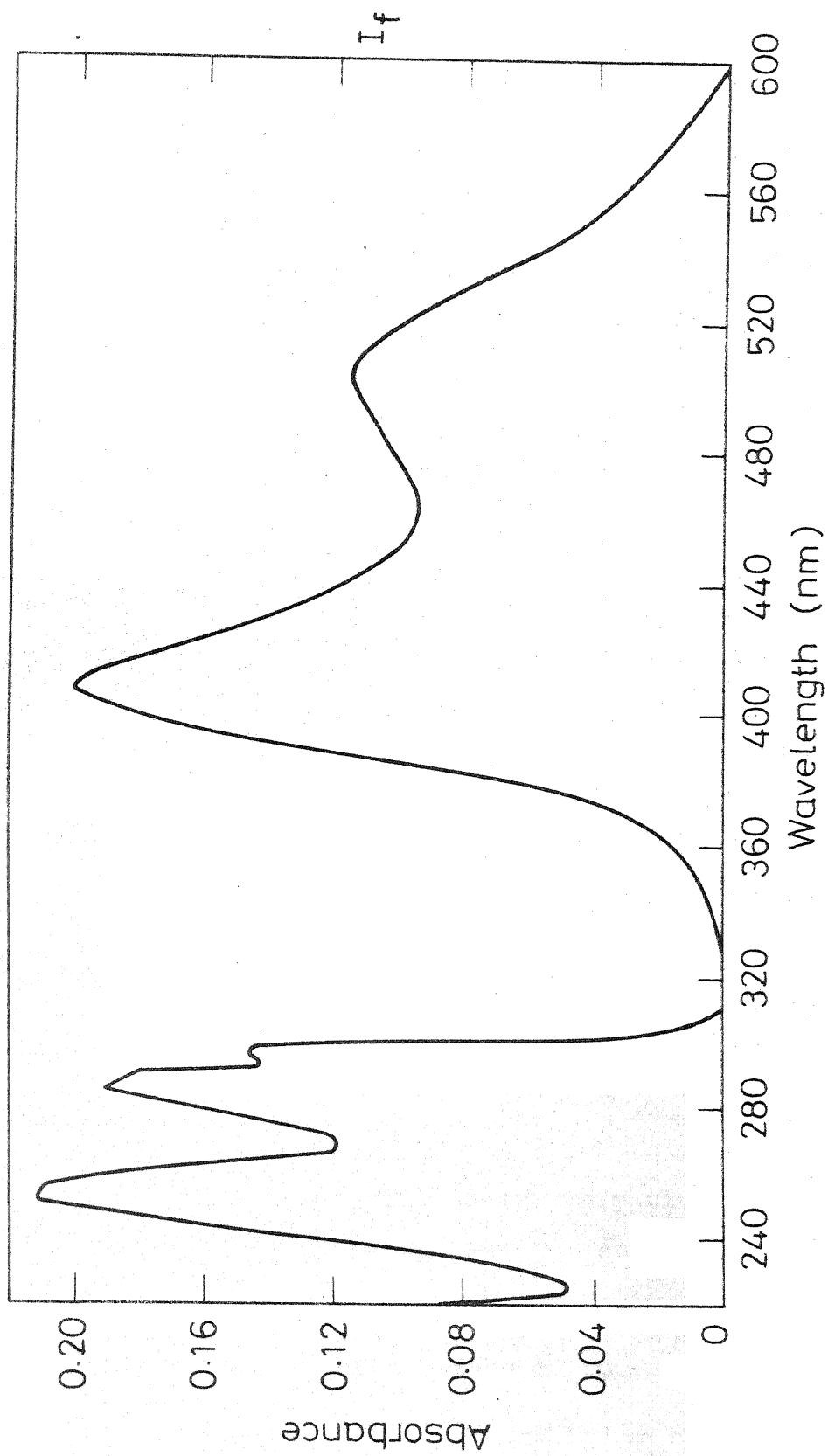
Fig. 6.20 Absorption and fluorescence spectra of 5-Aminoindazole at pH 1.4

6.3. Excited triplet state acidity constants

Acidity constants in the lowest triplet state have been determined from the phosphorescence data using the Förster cycle. Since the 0-0 transitions could not be located for both the acid and its conjugate base in some compounds, the phosphorescence maxima were used for those compounds in the calculation of the pK_T^* values. For the low temperature spectra, fairly high concentration of the solute is required and so methanol-water mixtures containing 20 to 50% methanol were used for the preparation of the solutions. Furthermore methanol-water solutions form a better glass than the pure aqueous solutions at .77K. Sulphuric acid and sodium hydroxide were used to prepare acidic and alkaline methanol solutions.

Phosphorescence spectra of different forms of all the compounds studied, are shown in figs. 5.19-5.26. The band maxima used in the calculation of pK_T^* values and the resultant pK_T^* values are listed in Table 6.12. $\bar{\nu}_m$, $\bar{\nu}_n$, $\bar{\nu}_a$ are the phosphorescence maxima of monocation, neutral and anionic forms respectively.

The pK_T^* values obtained are very close to the pK_a value and in most of the cases the change in pK_a occurs in the same direction as in pK_a^*. In a few compounds the pK_a change in the triplet state is either zero or opposite to the trend observed in the singlet state. But this opposite change is very little

Table - 6.12

Low - temperature phosphorescence maxima and pK_T^* values

Compound	$\bar{\nu}_n$	$\bar{\nu}_m$	$\bar{\nu}_a$	$pK_{a(T)}^*$ Eq(MN)	$pK_a^*(T)$ Eq(NA)	pK_a Eq(MN)	pK_a Eq(NA)
PDP	24691	24390		2.9		2.27	
DPMP	22883	23530		0.12		1.48	
TPP	24096	23530		1.58		0.39	
DPP	23809	23809	24067	1.43	13.44	1.43	12.94
MPP	24630	24390	23951	3.11	12.88	2.61	14.31
DPI	20000	19900	19801	6.11	12.38	5.90	12.8
PI	23530	23530	23537	4.65	11.86	4.65	11.86
HP	20408		20513		9.27		9.05

and may be due to the error involved in the location of the 0-0 band. In all other compounds the pK_T^* values obtained are in good agreement with the results obtained by other workers.[60,158]

CHAPTER - 7

EFFECT OF BUFFERS ON EXCITED STATE EQUILIBRIUM

7.1. Introduction

Most analytical measurements on biological or model biological systems are carried out in solutions containing buffers, often in high concentrations to maintain a constant pH. The buffers consist of proton donors and acceptors and therefore they can enter into proton-transfer reactions with excited potentially fluorescent molecules. Rate constants for the reaction of many common buffer ions, for example acetates and phosphates, with several fluorescent species have been shown to be comparable to the rate constants for the interaction of H_3O^+, OH^- and H_2O with these species.[5] Because the concentration of buffer ions are considerably greater than that of H_3O^+ and OH^- in a buffered solution, especially in the mid pH region where the concentrations of H_3O^+ and OH^- are very low, the probability of reaction of excited species with buffer ions is high. Hence a

study on the effect of buffers on fluorescence reveals their
(potential) interference in the excited state equilibrium. In
some cases, where life times of the fluorescent species are
sufficiently long, the study also helps in determining the
excited state dissociation constants which otherwise may not be
possible.

7.2. Theory

Weller[5,51,117] used steady state kinetics and derived
equations for the calculation of relative quantum yields of
fluorescent species in the presence of buffers. Schulman and
Capomacchia[56] used the same principle but modified the equations
to incorporate the conditions in the mid pH region. Later, the
theory of the effect of buffers on the acid-base equilibria was
reviewed by Schulman.[86]

For a general acid-base reaction in aqueous solutions
the equilibria can be written as

$$HA + H_2O \underset{k_{-a}}{\overset{k_a}{\rightleftharpoons}} A^- + H_3O^+ \qquad \ldots 7.1$$

$$B + H_2O \underset{k_{-b}}{\overset{k_b}{\rightleftharpoons}} BH^+ + OH^- \qquad \ldots 7.2$$
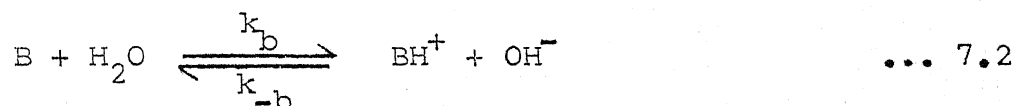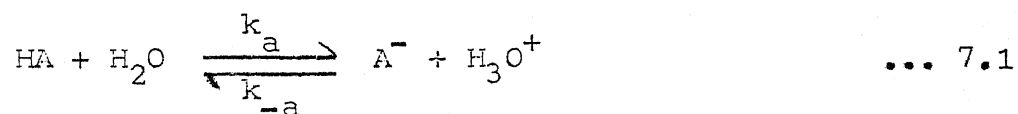
In the presence of a buffer system DH^+/D the reaction

$$HA + D \underset{k_{-D}}{\overset{k_D}{\rightleftharpoons}} A^- + DH^+ \qquad \ldots 7.3$$
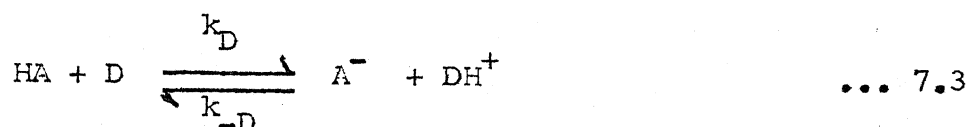
can accompany the reaction (7.1) while the reaction

$$B + DH^+ \underset{k_{-D}}{\overset{k_{DH^+}}{\rightleftharpoons}} BH^+ + D \qquad \ldots 7.4$$
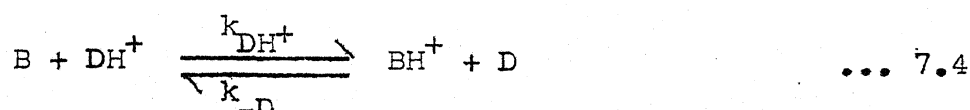
can accompany the reaction (7.2) in the excited state. Weller[5] has derived equations for the relative quantum yields of HA and A^- when the reactions (7.1) and (7.3) are simultaneously operative and for the relative quantum yields of B and BH^+ when (7.2) and (7.4) are operative simultaneously.

However if the solutions under consideration have pH between 3 and 11, and if the reaction of the excited HA or B with H_2O is too slow to occur within the lifetime, the k_a, k_{-a}, k_b, k_{-b} become negligible.

Weller's equations reduce to

$$\phi/\phi_0 = \frac{1 + k_{DH^+}[DH^+]\,\tau'_0}{1 + k_{DH^+}[DH^+]\,\tau'_0 + k_D[D]\,\tau_0} \qquad \ldots 7.5$$

$$\phi'/\phi'_0 = \frac{k_D[D]\,\tau_0}{1 + k_{DH^+}[DH^+]\,\tau'_0 + k_D[D]\,\tau_0} \qquad \ldots 7.6$$

for the equilibrium (7.3) and

$$\phi/\phi_0 = \frac{1 + k_D[D]\,\tau_0}{1 + k_D[D]\,\tau_0 + k_{DH^+}[DH^+]\,\tau'_0} \qquad \ldots 7.7$$

and $\quad \phi'/\phi'_o = \dfrac{k_{DH}+ [DH^+] \, \tau'_o}{1 + k_D [D] \, \tau_o + k_{DH}+ [DH^+] \, \tau'_o}$ ... 7.8

for the equation (7.4)

ϕ/ϕ_o is the relative quantum yield and τ_o is the lifetime of either HA or B and ϕ'/ϕ'_o, τ'_o are the corresponding variables for A^- or BH^+. These equations indicate that in the presence of sufficiently high buffer concentrations, with sufficiently high k_D and $k_{DH}+$, excited state proton transfer is possible even if the reaction with the solvent species is not taking place. If the concentration of the buffer species is high enough, excited state equilibrium corresponding to reaction (7.3) and (7.4) may occur. The pK_a^* in the presence of the buffer i.e. pK_{D-HA}^* and pK_{D-B}^* for these reactions have been shown[5] to be related to pK_a^* and pK_b^* by the following equations

$$pK_{D-HA}^* + pK_D = pK_a^* \qquad \text{... 7.9}$$

$$pK_{D-B}^* + pK_W - pK_D = pK_b^* \qquad \text{... 7.10}$$

Where k_W is the autoprotolysis constant of water and k_D is the equilibrium constant of the buffer. The equilibria character- ized by pK_a^* and pK_b^* are coupled to the equilibria characterized by pK_{D-HA}^* and pK_{D-B}^* and the excited state equilibrium in reactions (7.3) or (7.4) is a sufficient condition for excited state equilibrium in reactions (7.1) or (7.2). However, HA^* and A^{-*} are the only fluorescent species in reaction (7.3) while

B^* and BH^* are the only fluorescent species in reaction (7.4).

Consequently, at any buffer concentration high enough to

sustain the excited state equilibria corresponding to equations

(7.3) and (7.4), variations in the relative fluorescence quantum

yield of HA^* and A^{-*} and of B^* and BH^{+*} with pH would reflect

the equilibrium fluorimetric titration curves corresponding to

equations (7.1) and (7.2). Hence buffer systems are useful in

forcing to attain the excited state equilibrium in acid-base

pairs, which by themselves in water can not be studied under

excited state equilibrium conditions.

In this chapter, results from a study of the effect of

phosphate buffers on the protonation and deprotonation of

indazole, benzimidazole and 9,10-phenanthroimidazole are

presented.

7.3. Results and discussion

A careful selection of buffers is essential for this

study and few of the necessary characteristics are stated below.

A buffer system should have a pH range to cover the range

of excited state pK_a ($pK_a^* \pm 2$). It should not have absorbance

at the excitation wavelength used for the fluorimetric titration.

The total analytical concentration of the buffer ions should be

kept constant in all solutions.

For all the compounds studied by us only phosphate buffer was found to be suitable. Acetate buffer was found to quench the fluorescence of benzimidazole and indazole. Buffer solutions were prepared by taking a fixed amount of orthophosphoric acid and adding sodium hydroxide of suitable strength to attain the required pH. Then all solutions were made upto a fixed volume so as to keep the total analytical concentration of $[H_2PO_4^- + HPO_4^=]$ equal. The exact pH of the solution was again measured after the addition of the compound to be analysed i.e., just before taking the fluorescence measurements.

7.3.1. Indazole

Longworth et.al.,[142] have calculated ΔpK_a ($pK_a - pK_a^*$) by using Förster cycle method of averaging absorption and emission maxima for the equilibrium between monocation and neutral form. We have carried out a fluorimetric titration for indazole in aqueous solution and the titration curves are shown in fig.7.2(a). The crossing of the two curves gives a pK_a^* value of 1.8 which is slightly different from the pK_a value of 1.22. The fluorescence spectra of indazole in aqueous, 0.1 M and 1 M phosphate buffer solutions ($\sim$ pH 3.3) were recorded to test the effect of the buffer. The fluorescence spectra in aqueous solution and in 0.1 M buffer are exactly same where as in 1 M buffer it is displaced, as shown fig. 7.1. Fluorimetric titrations were also done with 0.1 M and 1 M buffer solutions. Once again, the
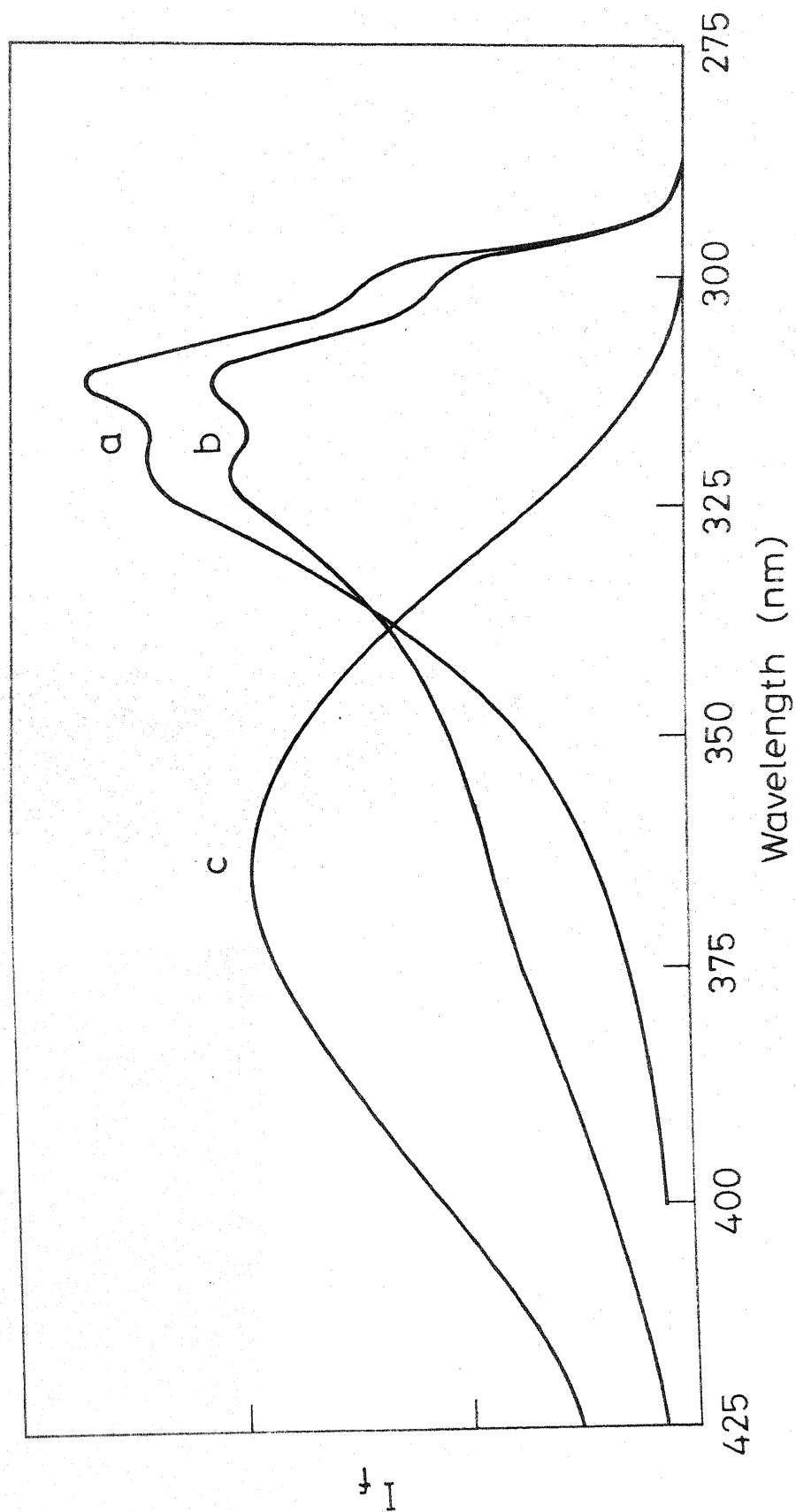
Fig. 7.1 Fluorescence spectra of Indazole at (a) pH=3.3 (without buffer)
(b) pH=3.36 (1M phosphate buffer) (c) pH<1 (without buffer)

excited state equilibrium is not affected by the 0.1 M buffer solution but the 1 M buffer displaces the equilibrium constant to 2.8 (fig. 7.2.a).

For the deprotonation equilibrium between indazole and its anion the pK_a value was determined spectrophotometrically. The pK_a^* values, determined by using Förster cycle methods and fluorimetric titration with and without buffers, are given in Table 7.1. The fluorimetric titration curves for this equilibrium are shown in fig. 7.2(b).

<u>Table - 7.1</u>

Excited singlet state acidity constants determined by different methods and at different buffer concentrations

Equilibrium	pK_a	pK_a^*(abs)	pK_a^*(flu)	pK_a^*(ave)	pK_a(FT) C=0.0M	pK_a(FT) C=0.1M	pK_a(FT) C=0.5M	pK_a(FT) C=1M
Eq(MN)	1.22	2.99	11.83	7.41 6.22[a]	1.8	1.8		2.8
Eq(NA)	13.79	10.11	2.57	6.34	12.2		11.2	

a. From ref. 142

In the deprotonation equilibrium, a levelling effect of buffers on pK_a^* could not be achieved because phosphate buffers get precipitated if the concentration exceeds 0.5 M.
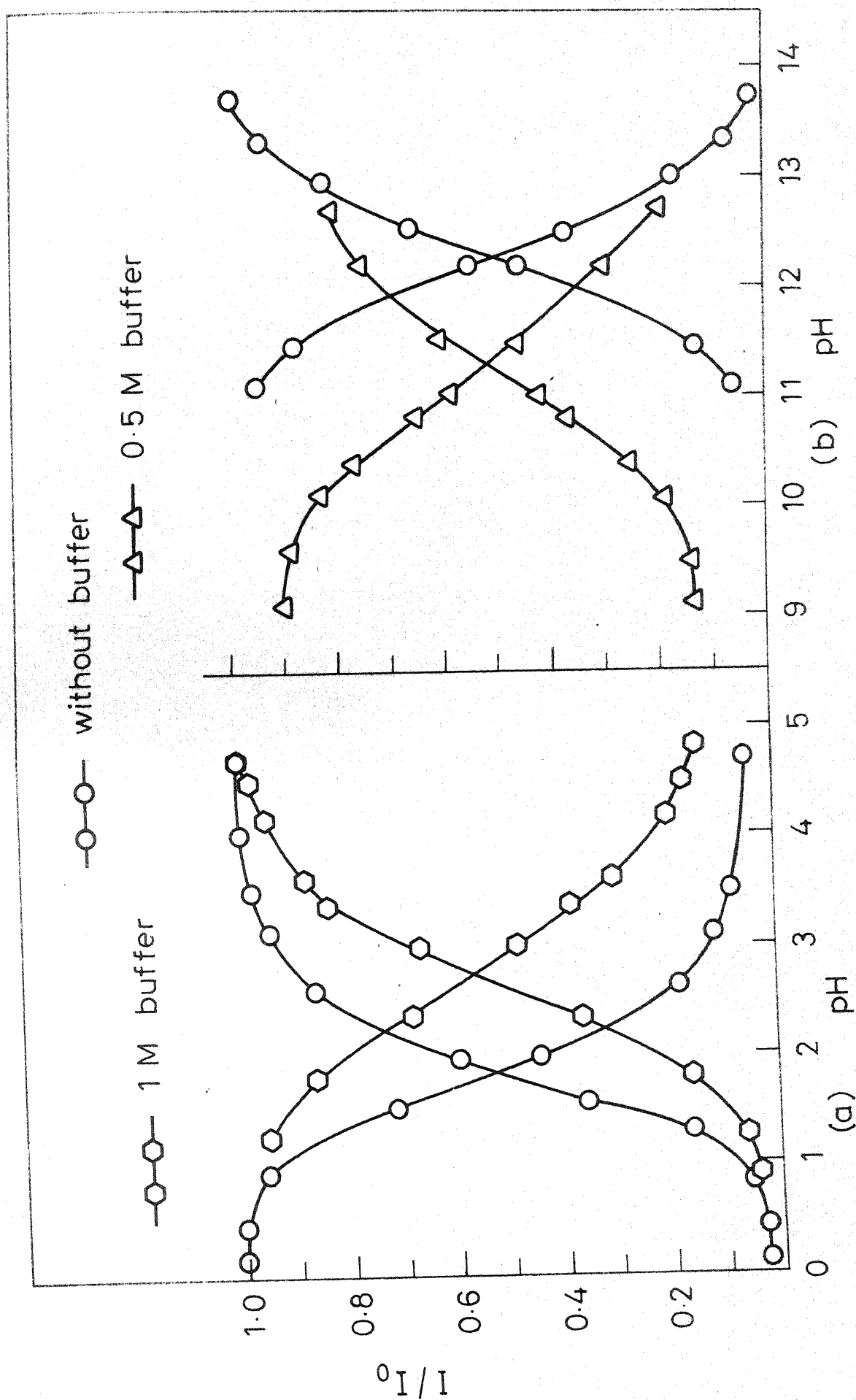
Fig. 7.2 Plot of relative fluorescence intensities of (a) indazole and its cation (b) indazole and its anion Vs pH.

In the Eq(MN) the pK_a^* value obtained by fluorimetric titration is greater than pK_a by about 1.6 but the ΔpK_a reported by Longworth et.al. is 5 . The **reported value** seems to be inaccurate because of the discrepancy in the method used for the calculation of pK_a^*. In indazole, on protonation, the red shift observed in the fluorescence spectrum, is quite large compared to the red shift observed in its absorption spectrum. This broad and largely red shifted fluorescence spectrum of the monocation shows that these changes may be due to either an excited state solute-solvent complex formation or due to the mixing of ^1L_a and ^1L_b bands as was reported for benzimidazole.[131] Therefore, the fluorescence shift for indazole can not give a reliable pK_a^* value. Consequently the method of averaging also becomes unsuitable. Among the three Förster cycle pK_a^* values, pK_{abs}^* is found to be the most accurate for this compound. The pK_a^* of 2.8, obtained by fluorimetric titration in the presence of a buffer is closer to the $pK_{a(abs)}^*$ value, showing that equilibrium is attained in the excited state.

Similar behaviour is also observed in the deprotonation equilibrium of indazole. Based on the same reasons, it is concluded that $pK_{a(abs)}^*$ is relatively more accurate than $pK_{a(flu)}^*$ and $pK_{a(ave)}^*$ values. Fluorimetric titration without a buffer gives a pK_a^* value of 12.22 which is displaced in the presence of buffer. This indicates that even though fluorimetric

titration gives a pK_a^* different from pK_a, it corresponds to a non-equilibrium condition[86] in the S_1 state due to its displacement in the presence of buffers.

7.3.2. Benzimidazole

Acid-base properties of this compound in the ground and excited states were studied by several authors,[131,142,160-162] but there has been no agreement between their results for the acid-base equilibria. A blue shift in absorption and a large red shift in fluorescence of the benzimidazole cation relative to the absorption and fluorescence maxima of the neutral form were observed by Adler.[159] This large red shift in fluorescence has been shown to be due to the reversal of states ^1L_a and ^1L_b in the cation.[131] Consequently in benzimidazole,cation fluorescence origenates from ^1L_a state,instead of ^1L_b state. So fluorescence data can not be used in the Förster cycle calculation of pK_a^* for this species. Blue shift in absorption on protonation shows that pyridinic nitrogen becomes less basic in the excited state, against the usual trend. Recently Svejda et.al.[162] have shown from an ODMR (optical detection of magnetic resonance) study that benzimidazole cation is present at pH 7 in the presence of buffer possibly due to an increased basicity of the molecule. Fluorimetric titration in the absence of buffer has given only the ground state pK_a value.[160]

Hence our study was carried out mainly to find out the effect of buffers on the benzimidazole equilibria. In the study of the protonation equilibrium, fluorescence spectra recorded at a pH of 6.5 with and without a buffer (fig. 7.3) shows the formation of benzimidazole cation in the presence of the buffer. The fluorimetric titration curves in aqueous solution and in buffer solutions are shown in fig. 7.4. Table 7.2 gives the pK_a^* values obtained by fluorimetric titration at different buffer concentrations.

The deprotonation equilibrium is not significantly affected by the buffer concentration.

Table - 7.2

Excited singlet state acidity constants of Benzimidazole at different buffer concentrations

Equilibrium	pK_a	$pK_a(FT)$ C = 0 M	$pK_a(FT)$ C = 0.1 M	$pK_a(FT)$ C = 1 M
Eq(MN)	5.53	5.6	5.8	6.45

These results show that benzimidazole becomes more basic in the excited state. The equilibrium is continuously displaced with the increase in concentration of buffers upto 1 M.
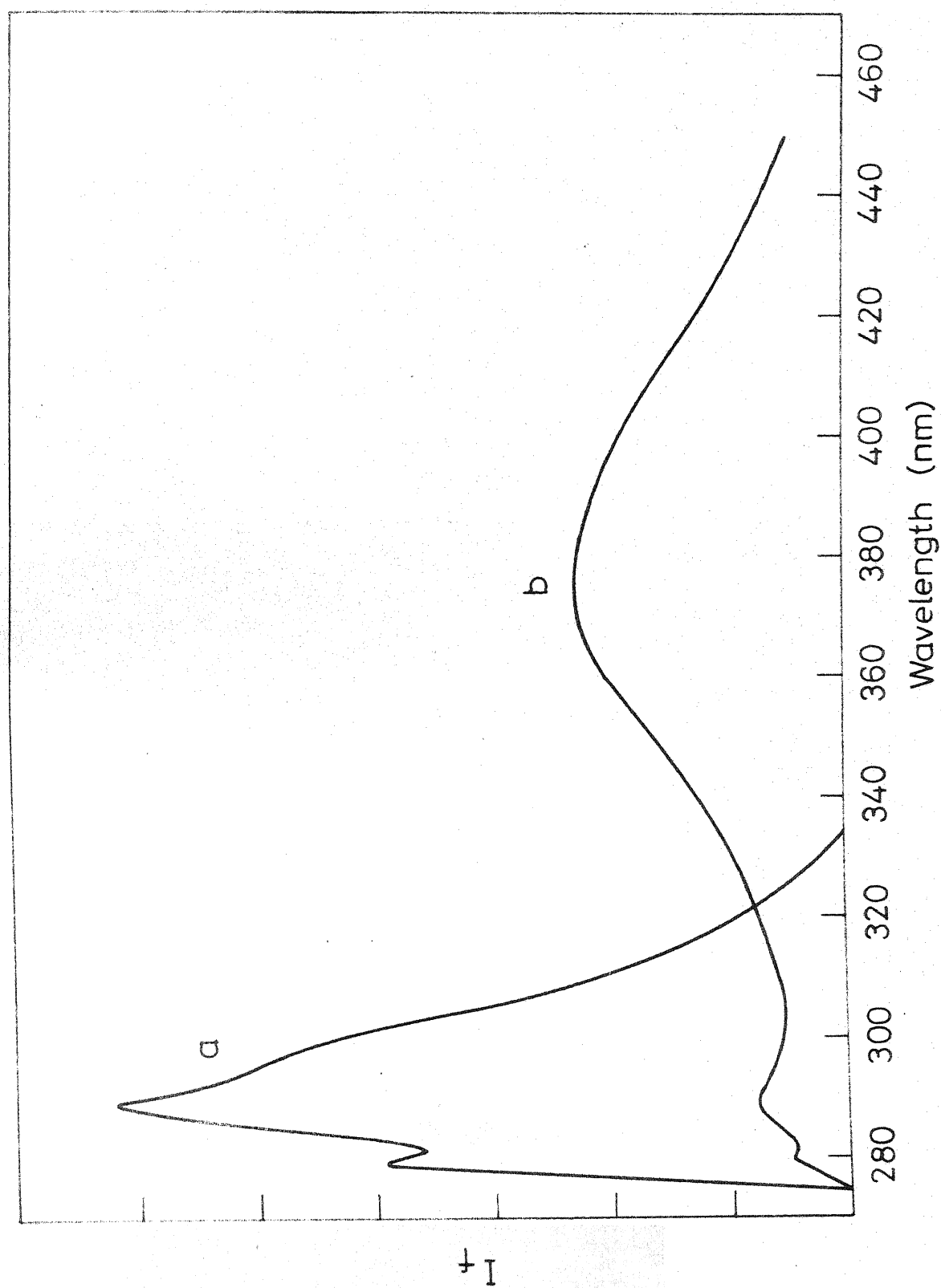
Fig. 7·3 Fluorescence spectra of Benzimidazole (a) pH 6·5 (without buffer)
(b) pH 6·3 (with 1 M buffer)

Fig. 7·4 Plot of relative fluorescence intensities of Benzimida-
zole Vs pH (a) without buffer (b) with 0·1 M
buffer (c) with 1 M buffer

A levelling effect could not be achieved as the preparation of buffers above 1 M was not possible. But the pK_a^* of 6.45 in 1 M buffer may be close to the true pK_a^* value because ODMR studies have indicated the existence of the cation at pH 7 in the presence of the buffer.

7.3.3. 9,10-Phenanthroimidazole

The pK_a^* values determined by different methods for both equilibria were analysed and discussed already in chapter 6.2.2. The effect of buffers for these equilibria have been studied and the pK_a^* values obtained are given in Table 7.3. The buffer concentration has no effect on the protonation equilibrium since the pK_a^* obtained by all the methods agree well. This shows that excited state equilibrium is established. Moreover the pK_a^* of 2.2 falls in the high pH region.

In contrast, the deprotonation equilibrium is displaced in the presence of a buffer as shown by fluorescence spectra recorded in aqueous and in buffer solutions at pH 10.3 (fig. 7.5). The fluorimetric titration curves for this equilibrium in aqueous, 0.1 M and 1 M buffer solutions are shown in fig. 7.6. The pK_a^* values obtained at different concentration of buffers [pK_a(FT)] for both equilibria are given in Table 7.3.
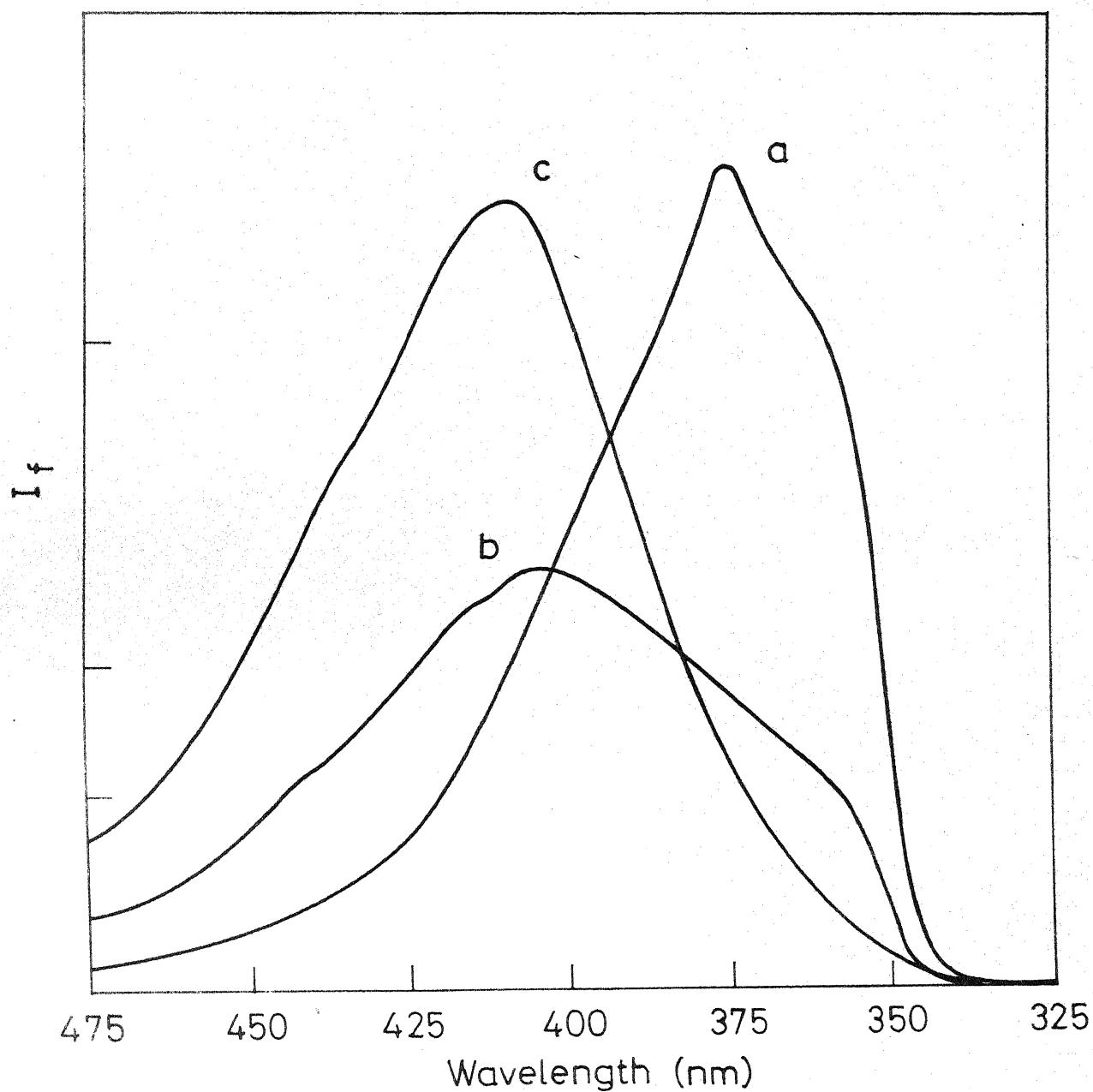
Fig. 7·5 Fluorescence spectra of 9,10-Phenanthroimidazole
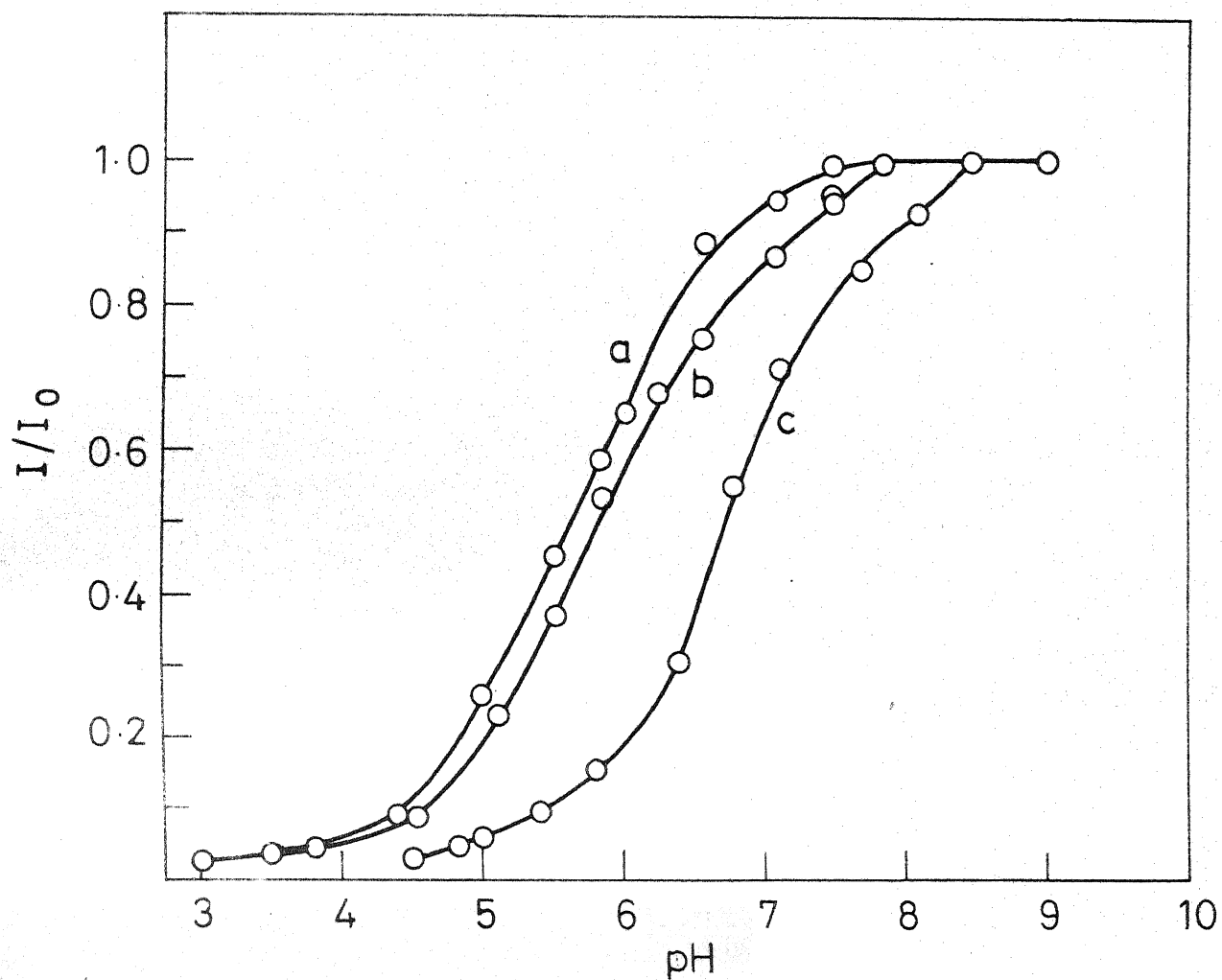(a) pH 10·2 (without buffer) (b) pH 10·55 (0·5 M buffer)
(c) pH 12·3 (without buffer)
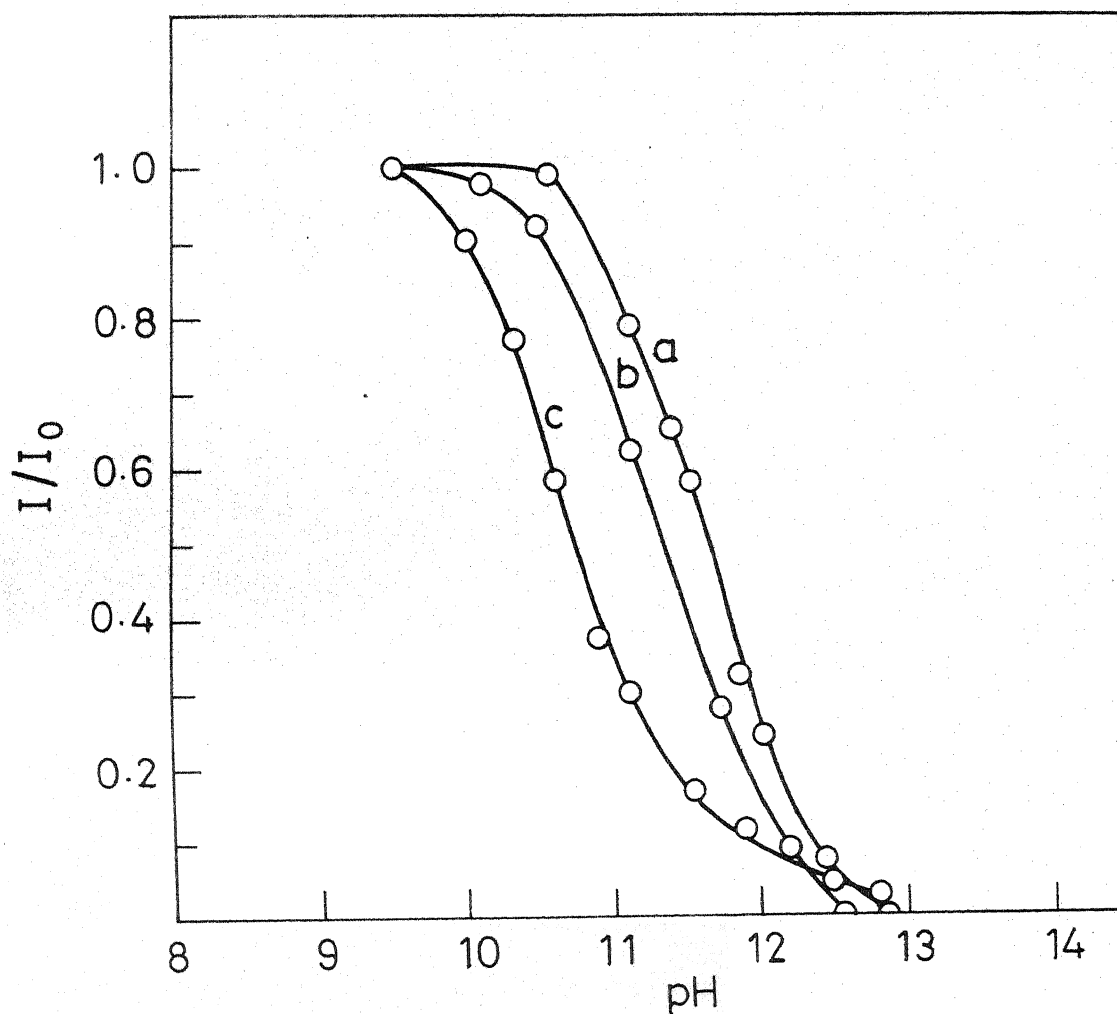
Fig. 7.6 Plot of relative fluorescence intensities of 9,10-Phenanthroimidazole Vs pH. (a) without buffer (b) with 0.1 M buffer (c) 0.5 M buffer

Table - 7.3

Excited singlet state acidity constants of 9,10-Phenanthro-imidazole at different buffer concentrations

Equilibrium	pK_a	pK_a(FT) $C = 0\,M$	pK_a(FT) $C = 0.1\,M$	pK_a(FT) $C = 1\,M$
Eq(MN)	4.65	2.2	2.2	2.2
Eq(NA)	11.86	11.66	11.3	10.72

This compound is an example to show that buffer has a significant effect on the equilibrium only when the pK_a^* falls in the mid pH region. The pK_a^* value for Eq(NA) in the presence of buffers shifts towards the pK_a^* value obtained by Forster cycle methods. The pK_a^* value of 10.72 obtained in 1 M buffer solution may not represent the true equilibrium but the change of pK_a^* value with the concentration of buffers shows the interference of the buffer in the excited state equilibrium.

Since the buffer affects the equilibrium in the excited state, one should be aware of their effect at different concentrations on the equilibrium. If the equilibrium obtained in the absence of buffers is displaced with increase in concentration of buffers and if it can be established that buffer ions do not quench the fluorescence of the excited state species, the

fluorimetric titration curve without buffer can be safely

assumed to correspond to a non-equilibrium condition in the

lowest excited singlet state. So in some cases, for example,

in the deprotonation equilibrium of indazole, the effect of

buffer concentration helps in ascertaining the non-equilibrium

condition in the lowest excited singlet state.

CONCLUSIONS AND SOME FURTHER PROSPECTS

Absorption and emission characteristics of a series of pyrazoles, imidazoles and phenanthrenes in different solvents and at different pH have been investigated.

The unusual solvent shifts in the $\pi - \pi^*$ transition of pyrazoles and 4,5-diphenylimidazole have been explained with the help of steric effect caused by the solvent interactions. The hydrogen bonding interactions are predominant in other compounds, and hydrogen donor and acceptor interactions are distinguished to a certain extent using solvent shifts.

The peculiar behaviour of TPP in acid medium, i.e. TPP^+, is due to a reversible chemical reaction taking place in the excited state. The fluorescence quenching of MPP^+ by chloride ion is found to be dynamic in nature. An interesting observation from the solvent effect on absorption and fluorescence is the change in nuclear conformation of 3,5-diphenyl-pyrazole, being non-planar in the ground state, becomes planar in the excited state. In 9-aminophenanthrene and 5-aminoindazole the site of hydrogen bonding interactions changes from the ground state to the excited state. 5-Aminoindazole forms a solute-solvent exciplex in ethanol.

The molecular vibrational frequencies are obtained from the analysis of low temperature fluorescence and phosphorescence spectra of a few compounds.

Ground and excited state pK_a values have been determined from the pH effects on absorption and fluorescence for the protonation/deprotonation equilibria of all the compounds and are compared.

The two nitrogen atoms in pyrazoles behave in a similar way as they were in pyridine or pyrrole i.e. pyridinic nitrogen becomes more basic and pyrrolic nitrogen becomes more acidic in the excited state. But in 1-phenyl-3,5-dimethylpyrazole, the pK_a^* calculated from absorption data has indicated that pyridinic nitrogen atom becomes less basic on excitation. The discrepancy in this method is found to be due to steric effect. Because of the short excited state life times of pyrazoles the pK_a^* values could not be found out from fluorimetric titration method except in 3-methyl-5-phenylpyrazole. A stoichiometric complex formation between 3-methyl-5-phenylpyrazole anion and solvent, in the excited state is inferred from the pK_a^* value calculated using Förster cycle and fluorescence data. A large difference in pK_a^*(abs) and pK_a^*(flu) in the Eq(MN) of 3,5-diphenylpyrazole also confirms its change in geometry upon excitation.

The pyridinic nitrogen atom in 9,10-phenanthroimidazole, where both nitrogen atoms are (separated by a carbon atom) apart, behaves in a different way, i.e. it becomes less basic in the excited state. This is against the usual behaviour observed in pyridine, pyrazole and other related compounds. This peculiar

behaviour is found to be due to the greater perturbation of the lone pair in the sp^2 orbital with the π cloud of the molecule.

The excited state proton transfer rate is comparable to the rate of fluorescence in 9-phenanthrol above pH 3, as in β-naphthol. But in 9-phenanthrol, below pH 3, 75% of the reaction takes place in the excited state leading almost to the attainment of the equilibrium where as in β-naphthol only 28% of the reaction takes place in the excited state. This shows the longer life time of 9-phenanthrol relative to β-naphthol.

The proton transfer reactions of 5-aminoindazole in the excited state follows a path which is entirely different from the ground state. Two different schemes for the ground and excited state equilibria are proposed. Indazolammonium ion undergoes a biprotonic phototautomerism. So pK_a and pK_a^* values could be obtained only by absorptiometric and fluorimetric titrations and, Förster cycle methods should not be used to calculate pK_a^* for this compound.

The effect of the high concentration of buffers on the excited state equilibrium of indazole, benzimidazole and 9,10-phenanthroimidazole has been investigated. The pK_a^* for the Eq(MN) of indazole has been realized in practice by the fluorimetric titration with 1M phosphate buffer. The phosphate buffers are found to displace the excited state equilibrium of benzimidazole $\left[Eq(MN)\right]$ and phenanthroimidazole $\left[Eq(NA)\right]$, but not to the attainment of true excited state equilibrium.

The excited state properties (pK_a and emission characteristics) of pyrazoles presented here are not complete but have opened a new field to study these above properties in the five membered diaza systems.

The following properties of pyrazoles and other compounds can be investigated in greater detail to gain a complete understanding about the excited state processes.

Only relative fluorescence intensities of the molecules have been studied. Hence quantum yields can be calculated to understand the primary photophysical and photochemical processes.

Fluorimetric titrations have qualitatively indicated the excited state lifetimes of all the molecules relative to their reaction lifetimes. But the exact lifetimes of the species can be determined only from time dependent fluorimetry. Since these lifetimes can be used in the determination of rate constants for the protonation/deprotonation reactions, it is proposed to extend our study on these molecules by using the above technique.

Preliminary study has indicated that Cl^- can quench the fluorescence of the cation of some of the molecules. This study can be extended to other inorganic anions and the respective quenching rate constants can be evaluated. Similarly using time dependent fluorimeter, the quenching of the fluorescence of the compounds by other molecules can be investigated and proper mechanism can be elucidated.

BIBLIOGRAPHY

1. N.S. Bayliss and E.G. McRae, J. Phys. Chem., 58, 1002 (1954).

2. G.J. Brealey and M. Kasha, J. Amer. Chem. Soc., 77, 4462 (1955).

3. E. Lippert, Z. Electrochem., 61, 962 (1957).

4. V.G. Krishna and L. Goodman, J. Amer. Chem. Soc., 83, 2042 (1961).

5. A. Weller in "Progress in Reaction Kinetics", Vol. I, Ed. G. Porter, Pergamon Press, New York, p. 187 (1961).

6. H.H. Jaffe and M. Orchin, "Theory and applications of ultraviolet spectroscopy", John Wiley, New York, p. 186 (1962).

7. H. Suzuki, "Electronic absorption spectra and geometry of organic molecules", Academic press, New York, p. 94 (1967).

8. N. Mataga, Y. Kaifu and M. Koizumi, Bull. Chem. Soc. Japan, 29, 465 (1956).

9. E.G. McRae, J. Phys. Chem., 61, 562 (1957).

10. P. Suppan and C. Tsiamis, Spectrochim. Acta, 36A, 971 (1950).

11. L.P. Hammett and A.J. Deyrup, J. Amer. Chem. Soc., 54, 2721 (1932).

12. S.G. Schulman, J. Pharm. Sci., 60, 371 (1971).

13. S.G. Schulman and A.C. Capomacchia, Anal. Chim. Acta., 58, 91 (1972).

14. S.B. Costa, A.L. Maccanita and M.J. Prieto, J. Photochem., 11, 109 (1979).

15. P. Pringshein, "Fluorescence and Phosphorescence", Interscience publishers, Inc., New York (1949).

16. Th. Förster, "Fluoreszenz Organisher Verbindungen", Vanden hoeck and Rupreht, Gottingen (1951).

17. B.L. Van Duuren, Chem. Rev., 63, 325 (1963).

18. N. Mataga and S. Tsuno, Bull. Chem. Soc. Japan, 30, 711 (1957).

19. N. Mataga and Y. Kaifu, Mol. Phys., $\underline{7}$, 137 (1964).

20. N. Mataga, Bull. Chem. Soc. Japan, $\underline{31}$, 487 (1958).

21. N. Mataga, Bull. Chem. Soc. Japan, $\underline{36(6)}$, 654 (1963).

22. T.C. Werner and D.M. Hercules, J. Phys. Chem., $\underline{73}$, 2005 (1969).

23. G. Bartocci, P. Bortolus and U. Mazzucato, J. Phys. Chem., $\underline{77}$, 605 (1973).

24. I.B. Berlman, J. Phys. Chem., $\underline{74}$, 3085 (1970).

25. S.G. Schulman, P.T. Tidwell, J.J. Cetorelli and J.D. Winefordner, J. Amer. Chem. Soc., $\underline{93}$, 3179 (1971).

26. S.G. Schulman and L.B. Sanders, Anal. Chim. Acta., $\underline{56}$, 91 (1971).

27. P.J. Kovi, A.C. Capomacchia and S.G. Schulman, Anal. Chem., $\underline{44}$, 1611 (1972).

28. S.G. Schulman, K. Abate, P.J. Kovi, A.C. Capomacchia and D. Jackman, Anal. Chim. Acta, $\underline{65}$, 59 (1973).

29. A.C. Capomacchia, J. Casper and S.G. Schulman, J. Pharm. Sci., $\underline{63}$, 1272 (1974).

30. P.J. Kovi, C.L. Miller and S.G. Schulman, Anal. Chim. Acta., $\underline{61}$, 7 (1972).

31. S.G. Schulman and K. Abate, J. Pharm. Sci., $\underline{61}$, 1576 (1972).

32. R.J. Sturgeon and S.G. Schulman, J. Pharm. Sci., $\underline{65}$, 1833 (1976).

33. K. Weber, Z. Phys. Chem. (Leipzig), $\underline{B15}$, 18 (1931).

34. Th. Förster, Z. Electrochem., $\underline{54}$, 42 (1950).

35. Th. Förster, Z. Electrochem., $\underline{54}$, 531 (1950).

36. Th. Förster in "Photochemistry in the liquid and solid states", Ed. F. Daniels, John Wiley & Sons, Inc., New York (1960).

37. A. Weller, Z. Electrochem., $\underline{56}$, 662 (1952).

38. W. Bartok, P.J. Lucchesi and N.S. Snider, J. Amer. Chem. Soc., $\underline{84}$, 1842 (1962).

39. J.C. Haylock, S.F. Mason and B.E. Smith, J. Chem. Soc., 4897 (1963).

40. S.F. Mason, J. Philip and B.E. Smith, J. Chem. Soc., 3051 (1968).

41. H.H. Jaffe and H. Lloyd Jones, J. Org. Chem., $\underline{30}$, 964 (1964).

42. H.H. Jaffe, D.L. Beveridge and L. Jones, J. Amer. Chem. Soc., $\underline{86}$, 2962 (1964).

43. R.H. Ellerhorst, H.H. Jaffe and A.L. Miller, J. Amer. Chem. Soc., $\underline{88}$, 5342 (1966).

44. E.L. Wehry and L.B. Rogers, J. Amer. Chem. Soc., $\underline{87}$, 4235 (1965).

45. R.E. Ballard and J. Edwards, J. Chem. Soc., 4868 (1964).

46. S.G. Schulman and Q. Fernando, J. Phys. Chem., $\underline{71}$, 2668 (1967).

47. S.G. Schulman and Q. Fernando, Tetrahedron, $\underline{24}$, 1777 (1968).

48. M. Goldman and E.L. Wehry, Anal. Chem., $\underline{42}$, 1178 (1970).

49. S.G. Schulman, Anal. Chem., $\underline{43}$, 285 (1971).

50. E. Vander Donckt in "Progress in Reaction Kinetics", Ed. G. Porter, Pergamon Press, New York, $\underline{Vol.\ 5}$, p.273 (1970).

51. A. Weller, Z. Electrochem., $\underline{58}$, 849 (1954).

52. S.G. Schulman, Rev. in Anal. Chem., $\underline{1}$, 85 (1971).

53. J.F. Ireland and P.A.H. Wyatt, in "Adv. in Phys. Org. Chem." $\underline{Vol.\ 12}$, ed.AR.Katritzky,Academic Press,New York,p.131(1976).

54. S.G. Schulman in "Physical methods in Heterocyclic Chemistry", Academic Press, New York, $\underline{Vol.\ VI}$, p. 147 (1974).

55. S.G. Schulman, R.M. Threatte, A.C. Capomacchia and W.L. Paul, J. Pharm. Sci, $\underline{63}$, 876 (1974).

56. S.G. Schulman and A.C. Capomacchia, J. Phys. Chem., $\underline{79}$, 1337 (1975).

57. A.C. Capomacchia and S.G. Schulman, J. Pharm. Sci., $\underline{64}$, 1256 (1975).

58. S.G. Schulman, D.V. Naik, A.C. Capomacchia and Timothy Roy, J. Pharm. Sci., 64, 982 (1975).

59. P.J. Kovi and S.G. Schulman, Anal. Chim. Acta., 63, 39 (1973).

60. G. Jackson and G. Porter, Proc. Roy. Soc., (London), A260, 13 (1961).

61. B.R. Fitch, Ph.D. Thesis, Rensselair Polytechnique Institute, Troy, New York (1972).

62. T.S. Godfrey, G. Porter and P. Suppan, Disc. Faraday. Soc., 39, 194 (1965).

63. J.F. Ireland and P.A.H. Wyatt, J. Chem. Soc. Faraday I, 69, 161 (1973).

64. S. Kato, M. Monto and M. Koizumi (1964), Bull. Chem. Soc. Japan, 37, 117 (1964).

65. D.N. Bailey, D.K. Roe and D.M. Hercules, J. Amer. Chem. Soc., 90, 6291 (1968).

66. K.E. Hine and R.F. Childs, J. Amer. Chem. Soc., 95, 6116 (1973).

67. J. Woolridge and T.D. Roberts, Tetrahedron Lett., 4007 (1973).

68. T.D. Roberts, L. Ardemagni and H. Shechter, J. Amer. Chem. Soc., 91, 6185 (1969).

69. J.G. Burr, E.H. Park and A. Chen, J. Amer. Chem. Soc., 94, 5886 (1972).

70. C.D. Gutsche and B.A.M. Oude-Alink, J. Amer. Chem. Soc., 90, 5855 (1968).

71. O. Kysel, Kinet. Mech. Polyreactions, Int. Symp. Macromol. Chem. Prepar. 5, 263 (1969).

72. D.L. Williams and A. Heller, J. Phys. Chem., 74, 4473 (1970).

73. W.J. McCarthy and J.D. Winefordner in "Fluorescence Theory, Instrumentation and Practice", Ed. C.G. Guilbault, Dekker, New York (1967).

74. R. Argauer and C.E. White, "Fluorescence Analysis", Dekker, New York (1970).

75. S.G. Schulman and J.D. Winefordner, Talanta, 17, 607 (1970).

76. G.J. Yakatan and S.G. Schulman, J. Phys. Chem., 76, 508 (1972).

77. S. Udenfriend, Fluorescence, 359 (1967).

78. R.F. Chen, Fluorescence, 443 (1967).

79. R.A. Morton, T.A. Hopkins and H.H. Seliger, Biochem., 8, 1598 (1969).

80. N. Lasser and J. Feitelson, J. Phys. Chem., 77, 1011 (1973).

81. L. Brand and J.R. Gohlke, J. Biol. Chem., 246, 2317 (1971).

82. M.R. Loken, J.W. Hayes, J.R. Gohlke and L. Brand, Biochem., 11, 4779 (1972).

83. M. DeLuca, L. Brand, T.A. Cebula, H.H. Seliger and A.F. Makula, J. Biol. Chem., 246, 6702 (1971).

84. L.J. Bowie, R. Irwin and M. DeLuca, Fed. Pro., Fed. Amer. Soc. Biol., 31, 42 Abstr. (1972).

85. L.J. Bowie, R. Irwin, M. Loken, M. DeLuca and L. Brand, Biochem., 12, 1852 (1973).

86. S.G. Schulman in, "Mod. Flu. Spect.", Vol 2, Ed. E.L. Wehry, Plenum Press, New York, p. 239 (1976).

87. S.G. Schulman in "Phy. Meth. in Het. Chem", Vol VI, Ed. AR. Katritzky, Academic Press, New York, p. 193 (1974).

88. S.G. Schulman, Anal. Chem., 44, 400 (1972).

89. A.C. Capomacchia and S.G. Schulman, Anal. Chim. Acta., 59, 471 (1972).

90. J. Bridges and R.T. Williams, Biochem. J., 107, 225 (1968).

91. R.F. Chen, Proc. Nat. Acad. Sci. US. 60, 598 (1968).

92. H. Boaz and G. Rollefson, J. Amer. Chem. Soc., 72, 3435(1950).

93. A. Weisstuch and A.C. Testa, J. Phys. Chem., 72, 1982 (1968).

94. S.G. Schulman, A.C. Capomacchia and M.S. Reitta, Anal. Chim. Acta., 56, 91 (1971).

95. S.G. Schulman in "Fluorescence and Phosphorescence spectroscopy: Physicochemical principles and practice", Pergamon Press, New York (1977).

96. I.I. Grandberg, S.V. Tabak and A.N. Kost, J. Gen. Chem. (USSR), 33, 517 (1973).

97. C.A. Parker, Nature, 182, 1002 (1958).

98. C.E. White, MayHo and E.Q. Weimer, Anal. Chem., 32, 438 (1960).

99. C.A. Parker and W.T. Rees, Analyst, 85, 587 (1960).

100. W.H. Melhuish, J. Opt. Soc. Amer., 52, 1256 (1962).

101. R.F. Chen, Anal. Biochem., 20, 339 (1967).

102. C.A. Parker "Photoluminescence of Solutions", Elsevier Publications, New York (1968).

103. J.U. White, Anal. Chem. 48, 2089 (1976).

104. C.R.C. Handbook of Chemistry and Physics, 60th edition (1979-80) p.E 392.

105. A.O. Fitton and R.K. Smalley, "Practical Heterocyclic Chemistry", Academic Press, New York, p. 21 (1968).

106. I.I. Grandberg and A.N. Kost, Zh. Obsch. Khim., 30, 203-8 (1960), CA 54, 22583.

107. O. Widman, Ber., 49, 477 (1916).

108. Emil Fisher and Caal Bülow, Ber., 18, 2131 (1885).

109. V.N.R. Pillai and E. Purushothaman, Curr. Sci., 47(7), 627 (1978).

110. B.B. Lohary, Research Assistant, compound prepared in this laboratory.

111. R. Ragunathan, Research Assistant, compound prepared in this laboratory.

112. J.A. Riddick and W.B. Bunger, "Organic Solvents", Wiley Interscience, New York (1970).

113. M.A. Paul and F.A. Long, Chem. Rev., 57, 1 (1957).

114. M.J. Jorgenson and D.R. Hartter, J. Amer. Chem. Soc., 85, 878 (1963).

115. G. Yagil, J. Phys. Chem., 71(4), 1034 (1967).

116. S.G. Schulman in, "Modern Fluorescence Spectroscopy", Vol 2, Ed. E.L. Wehry, Plenum Press, New York, p.266-275 (1976).

117. A. Weller, Z. Physik. Chem., 17, 224 (1958).

118. R.N. Hazeldine, J. Chem. Soc., 69 (1954).

119. I.L. Finar, J. Chem. Soc. B, 725 (1968).

120. A.K. Mishra and S.K. Dogra, unpublished results.

121. M. Kasha, Disc. Farad. Soc., 9, 14 (1950).

122. B.M. Burness, J. Org. Chem., 21, 97 (1956).

123. I.I. Grandberg, J. Gen. Chem. (USSR), 33, 511 (1963).

124. A.V. Blackburn and C.J. Timmons, Quart. Rev. Chem. Soc., 23, 480 (1969).

125. D. Dal Monte, A. Mangini and R. Passerini, Gazz. Chim. Ital., 86, 797 (1956).

126. S. Tabak, I.I. Grandberg and A.N. Kost, Tetrahedron, 22, 2703 (1966).

127. R.A. Friedel and M. Orchin, "Ultraviolet spectrum of aromatic compounds", John Wiley & Sons, New York (1951).

128. M. Swaminathan and S.K. Dogra, unpublished results.

129. K. Tsutsumi, K. Aoki, H. Shizuka and T. Morita, Bull. Chem. Soc. Jap., 44, 3245 (1971).

130. D.M. Hercules, "Fluorescence and Phosphorescence analysis", John Wiley & Sons, New York, p. 135 (1966).

131. M. Kondo and H. Kuwano, Bull. Chem. Soc. Jap., 42, 1433-5 (1969).

132. T.C. Werner in "Modern Fluorescence Spectroscopy" Vol 2, Ed. E.L. Wehry, Plenum Press, New York, p. 277 (1976).

133. P. Bortolus, G. Bartocci and U. Mazzucato, J. Phys. Chem., 79, 21 (1975).

134. I.B. Berlman, "Hand Book of Fluorescence Spectra of Aromatic molecules, 2nd Ed., Academic Press, New York (1971).

135. R. Srinivasan and J.N.C. Husu, J. Amer. Chem. Soc., 93, 2816 (1971).

136. J. Hennessy and A.C. Testa, J. Phys. Chem., 76, 3362 (1972) and other references mentioned therein.

137. E.L. Wehry, Fluorescence News, 61, 1 (1971).

138. R.A. Passwater, Fluorescence News, 5(5), 4 (1971).

139. D.M. Hercules and L.B. Rogers, J. Phys. Chem., 64, 397 (1960).

140. E.V. Shpolskii, Soviet. Phys. Usp., 2, 378 (1959).

141. M.L. Bhaumik and R. Hardwick, J. Chem. Phys., 39, 1595 (1963).

142. J.W. Longworth, R.O. Rahn and R.G. Schulman, J. Chem. Phys., 45, 2930 (1966).

143. J. Charette and P. Teyssie, Spectrochim. Acta , 15, 70 (1959).

144. C.S. Rondestvedt and P.K. Change, J. Amer. Chem. Soc., 77, 6532 (1955).

145. C.R. Hansen and C.E. Cain, J. Org. Chem., 23, 1142 (1958).

146. 'Dissociation constants of organic bases in aqueous solution' by D.D. Perrin, Butterworths, London (1964).

147. C.A. Matuszak and A.J. Matuszak, J. Chem. Educ., 53, 280 (1976).

148. R.E. Ballard and J.W. Edwards, spectrochim. Acta, 20, 1275 (1964).

149. S.G. Schulman and A.C. Capomacchia, Spectrochim. Acta., 28A, 1 (1972).

150. W.L. Levshin, Z. Phys., 43, 230 (1931).

151. R.P. Bell, "The Proton in Chemistry", Methuen, London (1959).

152. E. Bauwhuis and J.M. Janssen, Tetrahedron Lett., 233 (1972).

153. S.G. Schulman, A.C. Capomacchia and B. Tussy, Photochem. Photobiol. 14, 733 (1971).

154. L.S. Rosenberg, G. Lam, C. Grow and S.G. Schulman, Anal. Chim. Acta, 106, 81 (1971).

155.   A. Weller, Z. Physik. Chem., <u>3</u>, 238 (1955).

156.   S.G. Schulman and P. Liedke, Z. Physik. Chem., <u>N.F.84</u>, 317 (1973).

157.   B. Zalis, A.C. Capomacchia, D. Jackman and S.G. Schulman, Talanta, <u>22</u>, 30 (1973).

158.   S.G. Schulman, L.B. Sanders and J.D. Winefordner, Photochem. Photobiol., <u>13</u>, 381 (1971).

159.   T.K. Adler, Anal. Chem., <u>34</u>, 685 (1962).

160.   H.C. Borreson, Acta chem. Scand., <u>17</u>, 921 (1963).

161.   K.S. Rogers and C.C. Clayton, Anal. Biochem., <u>48(1)</u>, 199 (1972).

162.   P. Svejda , R.R. Anderson and A.H. Maki, J. Amer. Chem. Soc., <u>100</u>, 7131 (1978).

VITAE

Born on April 4, 1950 at Kandavarayanpatti (Tamilnadu), the author had his early education at De Britto High School, Devakottai. He obtained his B.Sc. degree in 1969 from Thiagarajar College, Madurai and M.Sc. degree in 1972 from Annamalai University, Chidambaram. He was working as a Junior Lecturer in Chemistry from 1972 to 1975 at A.P.S.A. College, Tiruppattur (R.D) and later he joined as Assistant Professor in Chemistry at Government College, Kumbakonam (known as Southern Cambridge). In 1979 he was selected for the award of teacher fellowship under the Faculty Improvement Programme of U.G.C. for research at Indian Institute of Technology, Kanpur.

LIST OF PUBLICATIONS

1. A Modification in the Cell for Increased Sensitivity in Fluorescence Measurements, M. Swaminathan and S.K. Dogra, ~~Ind. J Chem. (Communicated)~~, under preparation

2. A Study of Nuclear Conformation and Proton-Transfer Reaction of 3-5,Diphenylpyrazole in the Excited state, M. Swaminathan and S.K. Dogra, J. Photochem. ~~(communicated)~~, 21 ,245 ,1983

3. Solvent Effect and Excited State Proton Transfer Studies of 4,5-Diphenylimidazole, M. Swaminathan and S.K. Dogra, ~~J. Physical Chem. (Communicated)~~. Ind. J. Chem., in press

4. Effects of Solvents and pH on the Absorption and Fluorescence Spectra of Pyrazoles, M. Swaminathan and S.K. Dogra, ~~Physical Chem. (Communicated)~~. under preparation

5. Effect of Buffers on the Excited State Prototropic Equilibria-I. Benzimidazole, M. Swaminathan and S.K. Dogra, ~~(Manuscript under preparation)~~. Ind. J. Chem., in press

6. Effect of Buffers on the Excited State Prototropic Equilibria-II. Indazole, M. Swaminathan and S.K. Dogra, (Manuscript under preparation).

7. An Unusual Behaviour and Acid-Base Kinetics of 9,10-Phenan-throimidazole in the excited singlet state; Effect of Buffer on the Excited State Prototropic Equilibria, M. Swaminathan and S.K. Dogra ~~(Manuscript under preparation)~~. J. Chem. Soc. Perkin Transaction II, in press.

8. A Study of Solvent Dependence and Kinetics of Proton Transfer Reaction of 9-Phenanthrol in the Excited Singlet State, M. Swaminathan and S.K. Dogra (Manuscript under preparation).

9. A Study of Proton Transfer Reactions and Hydrogen bonding
   Interactions of 5-Aminoindazole in the Ground and Excited
   Singlet State; Biprotonic Phototautomerism of Singly
   Protonated Species, M. Swaminathan and S.K. Dogra
   (Manuscript under preparation). communicated, J. Am. Chem.
   Soc

10. A Study on the Phosphorescence Spectra of Pyrazoles at 77K,
    M. Swaminathan and S.K. Dogra (Manuscript under preparation).
    communicated, Spectrochim Acta.

11. Solvent and pH Effect on the fluorescence spectra
    of 9-phenanthrylamine. Can. J. Chem., in press.